藥學博士學位論文

오리나무의 화학성분 및 지방세포형성 억제활성

Chemical constituents of *Alnus japonica* and their anti-adipogenic activities

2012 年 8 月

서울大學校 大學院

藥學科 生藥學專攻

李 旻 兒

Abstract

Obesity causes many health problems and is known to be associated with an excessive growth of adipocyte mass tissue by increasing the number and size of adipocytes differentiated from preadipocytes. The inhibition of adipogenesis has been considered as an effective treatment for obesity. In the course of searching for anti-adipogenic drug condidates from nature sources using 3T3-L1 cells, it was found that the 80 % MeOH extract of *Alnus japonica* Steud. fruits, *Alnus hirsuta* Turcz. var. *sibirica* (Spach) H. Ohba leaves, *Alnus firma* Sieb. et Zucc. barks (Betulaceae) showed significant inhibitory activity on adipocyte differentiation. These *Alnus* species has been used for hemorrhage, burn injuries, anti-pyretic fever, diarrhea, and alcoholism in traditional Korean medicine. The various types of plant secondary metabolites such as flavonoids, triterpenoids, tannin, phenols, steroids, and diarylheptanoids have been reported from *Alnus* species. In the present study, thirty five diarylheptanoids, ten flavonoids, nine tannins, seven triterpenoids, five phenolic compounds and two sterols were isolated by the bioactivity-guided isolation over three *Alnus* species. Among the compounds **AJ1**, **AJ2**, **AJ12**, **AJ37**, **AJ41**, **AH2**, and **AF19** were newly reported from the nature.

Among these compounds, diarylheptanoids showed the most significant anti-differentiation effect than other on 3T3-L1 cells. These results showed that the presence of carbonyl group at C-3 in heptane chain is an important structural determinant for the activity, and additions of hydroxyl group in benzene ring and

substitution of glucosyl moiety, α,β-unsaturated ketone moiety also affect their biological activity. Compounds **AJ9**, **AJ10**, and **AJ13** showed much better potent activity than other diarylheptanoids and induced the down-regulation of adipocyte fatty acid binding protein (aP2), lipoprotein lipase (LPL), and leptin gene as well as the peroxisome proliferator-activated receptors gamma (PPARγ) and CCAAT/enhancer-binding protein alpha (C/EBPα) genes. Compounds **AJ9** and **AJ10** also inhibited the expression of sterol regulatory element binding protein 1 (SREBP1), steroyl-coenzyme A desaturase 1 (SCD-1), and fatty acid synthase (FAS), target gene of lipogenesis, while compound **AJ13** slightly affected these genes. In addition, compounds **AJ9**, **AJ10**, and **AJ13** promoted lipolysis on mature adipocyte. The measurement of cell proliferation on 3T3-L1 cells revealed that compounds which showed potent anti-differentiation activity effectively decreased preadipocytes proliferation. Among them, compounds **AF17-19**, lupane type triterpenoids, showed the most anti-proliferative activity in concentration-dependent manner and decreased cell viability through inducing apoptosis.

Consequently, the present study suggests that various constituents isolated from three *Alnus* species prove beneficial for decreasing adipose tissue volume, targeting different stages of the adipocyte life cycle.

Keywords: *Alnus japonica* Steud., *Alnus hirsuta* Turcz. var. *sibirica* (Spach) H. Ohba, *Alnus firma* Sieb. et Zucc., Betulaceae, 3T3-L1 cells, preadipocyte, adipocyte, obesity, anti-adipogenic activity

Student number: 2009-30470

Contents

List of schemes

List of tables

List of figures

List of abbreviations

AcCN: acetonitrile

ACC: acetyl-CoA carboxylase

AMPK: AMP-activated protein kinase

aP2: adipocyte fatty acid binding protein

CC: column chromatography

C/EBPα: CCAAT/enhancer-binding protein alpha

C/EBPβ: CCAAT/enhancer-binding protein beta

C/EBPδ: CCAAT/enhancer-binding protein delta

COSY: correlation spectroscopy

CPT 1: carnitine palmitoyl transferase 1

CS: newborn calf serum

DM: differentiation medium

DMSO: dimethyl sulfoxide

DMEM: Dulbecco's modified Eagle's media

DTT: Dithiothreitol

ECL: enhanced chemiluminescence

EDTA: Ethylenediaminetetraacetic acid

EGCG: (-)-epigallocatechin-3-gallate

EIMS: electron impact mass spectroscopy

ESIMS: electrospray ionization mass spectroscopy

FAB: fast atomic bombardment

FAS: fatty acid synthase

FBS: Fetal bovine serum

GAPDH: glyceraldehyde 3-phosphate dehydrogenase

G$i\alpha_1$: GTP binding protein

Glc: glucose

GPDH: Glycerol-e-phosphate dehydrogenase

HILIC: hydrophilic interaction liquid chromatography

HMBC: heteronuclear multiple bond correlation

HSL: hormone sensitive lipase

HPLC: high performance liquid chromatography

HRFAB: high resolution fast atomic bombardment

Hz: hertz

IC_{50}: the half maximal inhibitory concentration

IBMX: 3-isobutyl-1-methylxanthine

IgG: immunoglobulin G

IR: infrared radiation

LPL: lipoprotein lipase

m: multiplet

MeOH: methanol

mp: melting point

MTT: 3-(4,5-dimethylthiazol-2-yl)-2,5-diphenyltetrazolium

NMR: nuclear magnetic resonance

NOE: nuclear overhauser effect

NOESY: nuclear overhauser effect spectroscopy

ODS: octadeca silica gel

ORO: Oil Red O

PBS: phosphate-buffered saline

PDE3B: phosphodiesterase 3B

PMSF: phenylmethanesulfonylfluoride or phenylmethylsulfonyl fluoride

PPARγ: peroxisome proliferator-activated receptors gamma

RP: reverse phase

R_t: retention time

RXR: retinoid X receptor

SCD-1: steroyl-coenzyme A desaturase 1

SREBP1: sterol regulatory element binding protein 1

TLC: thin layer chromatography

TNFα: tumor necrosis factor α

UV: ultraviolet

I. Introduction

Obesity

Obesity is now so common within the world's population that it is beginning to replace undernutrition and infectious diseases as the most significant contributor to ill health. Obesity causes or aggravates many health problems, both independently and in association with several pathological disorders, including Type II diabetes, hypertension, coronary heart disease, atherosclerosis, and cancer (Kopelman, 2000). Obesity condition is determined by the interaction between genetic, environmental and psychosocial factors acting through the physiological mediators of energy intake and expenditure. Obesity has become a prevalent health risk in industrialized countries. Therefore, obesity is no longer considered to be a cosmetic problem affecting certain individuals. Although weight loss and weight control drugs are becoming extremely common in today's society, the remedies provided by the diet industry have failed in the long-term maintenance of weight loss in obese patients (Wadden et al, 1993). Moreover, it has been estimated that more than 90% of the people who lose weight by dieting return to their original weight within 2−5 years (Stern et al., 1995). Adipose tissue growth involves formation of new adipocytes from precursor cells, further leading to an increase in adipocyte size. The transition from undifferentiated fibroblast-like preadipocytes into mature adipocytes constitutes the adipocyte life cycle, and treatments that regulate both size and number of adipocytes may provide a better therapeutic approach for treating obesity (Rayalam et al., 2008).

Adipogenesis and adipocyte life cycle

Adipose tissues are critical integrators of organismal energy balance, through the regulation of both food intake and energy expenditure. This adipose tissue mass results from both increased fat cell number and increased fat cell size (Yang et al., 2008; Rosen et al., 2006). The amount of adipose tissue mass can be regulated by the suppression of adipogenesis from fibroblastic preadipocytes to mature adipocytes (Roncari et al., 1981). Adipocytes play a pivotal role in regulating adipose mass and lipid homeostasis. Predipocytes are derived from mesenchymal stem cells, which have the potential to differentiate into myoblasts, chondroblasts, osteoblasts or adipocytes. The adipocyte life cycle includes alteration of cell shape and growth arrest, clonal expansion and a complex sequence of changes in gene expression leading to storage of lipid and finally cell death (Figure 1) (Rayalam et al., 2008). Preadipocytes can proliferate throughout life to increase fat mass. Once preadipocytes are triggered to mature, they begin to change shape and undergo a round of cell division known as clonal expansion, followed by initiation of the genetic program that allows them to synthesize and store triglycerides. Mature adipocytes can continue storing lipid when energy intake exceeds output, and they can mobilize and oxidize lipid when energy output exceeds input. The first hallmark of the adipogenesis process is alteration in cell shape, paralleled by changes in the type and the expression levels of extracellular matrix components and cytoskeletal components. These events further promote the expression of adipogenic transcription factors, including peroxisome proliferator-activated receptors gamma (PPARγ) and CCAAT/enhancer-binding protein alpha (C/EBPα). Mature adipocytes can also undergo lipolysis and apoptotic cell death under certain conditions.

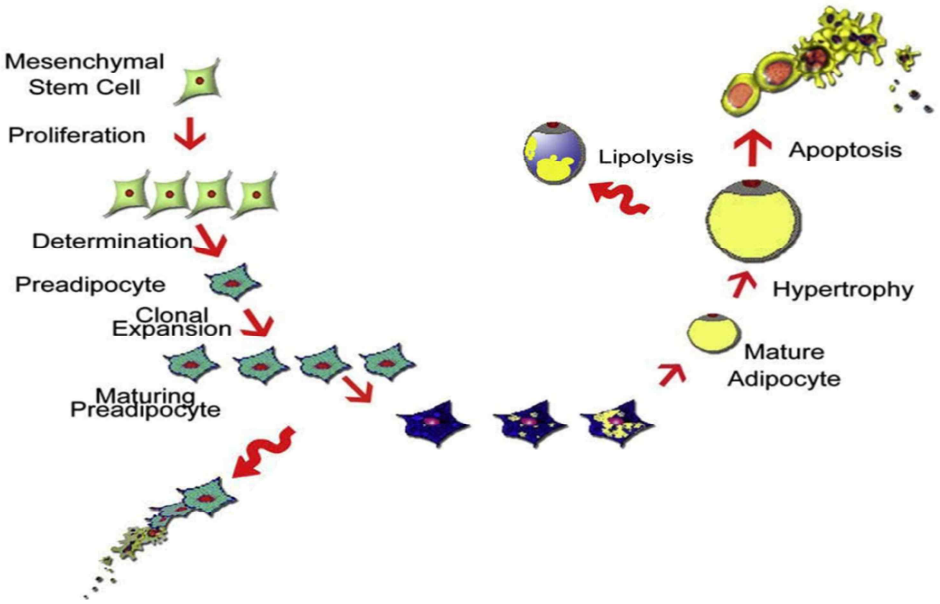

Figure 1. Adipocyte life cycle. The adipocyte life cycle includes alteration of cell shape and growth arrest, clonal expansion and a complex sequence of changes in gene expression leading to storage of lipid and finally cell death (Rayalam et al., 2008).

3T3-L1 cell

3T3-L1 cells have been served as well established *in vitro* assay system to assess adipogenesis and adipocyte differentiation (Kong et al., 2009). The 3T3-L1 preadipocyte cell lines originally established by Green and associates have greatly facilitated our knowledge of the molecular mechanisms controlling adipogenesis (Green et al., 1975). Although committed to the adipocyte lineage, proliferating 3T3-L1 preadipocytes exert characteristics similar to those of other 3T3 fibroblasts. Confluent 3T3-L1 preadipocytes differentiate upon exposure to the adipogenic inducers fetal bovine serum (FBS), dexamethasone, isobutylmethylxanthine, and insulin. This cocktail activates an adipogenesis, which occurs in two well-defined phases. The

stimulated cells immediately reenter the cell cycle and progress through at least two cell-cycle divisions, a phase often referred to as clonal expansion (Farmer, 2006). During this stage, the cells express specific adipogenic transcription factors as well as cell cycle regulators that together assist expression of PPARγ and C/EBPα. Following this incident, the committed cells undergo terminal differentiation manifested by production of lipid droplets as well as expression of multiple metabolic programs characteristic of mature fat cells.

Adipocyte differentiation

The differentiation of preadipocytes into adipocytes is modulated by a complex network of transcription factors that organize the expression of proteins responsible for establishing the mature adipocyte phenotype. The PPARγ and C/EBPα are the master regulator of adipogenesis, and oversee the entire terminal differentiation process (Farmer, 2006). In particular, PPARγ is considered the master regulator of adipogenesis; without it, precursor cells are incapable of expressing any known aspect of the adipocyte phenotype (Rosen et al., 2002). The PPARγ is a member of the nuclear hormone receptor superfamily. The PPARγ must heterodimerize with another nuclear hormone receptor, retinoid X receptor (RXR), to bind DNA and be transcriptionally active (

Figure 2) (Rosen et al., 2000; Vazquez-Vela et al., 2008). PPARγ exists as two protein isoforms generated by alternative promoter usage and alternative splicing. PPARγ2 is 30 amino acids longer at the amino terminus than PPARγ1, and is the dominant isoform found in fat cells (Tontonoz et al., 1995). PPARγ can be activated by thiazolidinediones (TZDs), in which treatment with this in preadipocytes increases both the extent and rate of adipogenesis (Rosen et al., 2000). The C/EBPs belong to the basic-leucine zipper class of transcription factors and can

be regulated at many levels, including transcriptionally, as measured by mRNA levels in cells. The cAMP, a well-known inducer of adipogenesis in vitro and a component of most prodifferentiative regimens, can enhance expression of both C/EBPα and CCAAT/enhancer-binding protein beta (C/EBPβ) (Tang et al., 1999). The expression of mRNA and protein levels of C/EBPβ and transiently enhanced in preadipocyte, which induce differentiation. The cAMP regulatory element binding (CREB) protein, which is activated on initial stage of adipogenesis in 3T3-L1 cells, contributes in the induction of C/EBPβ expression (Zhang et al., 2004). This observation is consistent with earlier study showing a role for cAMP signaling in controlling C/EBPβ expression (Cao et al., 1991). It is likely that additional factors of parallel pathways are induced early and converge on PPARγ at a stage downstream of C/EBPβ and CCAAT/enhancer-binding protein delta (C/EBPδ), such as the sterol regulatory element binding protein 1c/ adipocyte determination and differentiation dependent factor-1 (SREBP1c/ADD-1) (Rosen et al., 2006). A potential role for SREBP1c in regulating adipogenesis derives from studies showing that its expression is significantly enhanced in 3T3-L1 adipocytes in response to insulin (Kim et al., 1998). Ectopic expression of dominant-negative SREBP1c was shown to inhibit preadipocyte differentiation, while overexpression of this HLH protein significantly enhances the adipogenic activity of PPARγ (Kim and Spiegelman, 1996). Expression of SREBP1c alone, however, is only capable of inducing adipogenesis to a modest extent (Kim et al., 1998). SREBP1c, which is involved in the production of an endogenous PPARγ ligand, regulates the expression of genes related to the metabolism of lipids and cholesterol and the enzymes involved in lipogenesis and desaturation of fatty acid, and then, a series of activation promotes the expression of fatty acid synthase (FAS) (Rosen et al., 2000; Chen et al., 2011). The FAS is a

critical metabolic enzyme for lipogenesis, and is highly expressed in the liver and adipose tissue. It catalyzes the synthesis of saturated fatty acids in cells (Smith et al., 1994). Steroyl-coenzyme A desaturase 1 (SCD-1), highly expressed by adipose tissue, is a key rate-limiting enzyme in the desaturation of cellular lipids into monounsaturated fatty acids (Yao-Borengasser et al., 2008). The cellular deprivation of the product for the enzymatic activity of SCD-1 led to the down-regulation of SREBP1 and PPARγ, resulting in a decrease in lipogenesis. PPARγ, C/EBPα, and SREBP1c are induced prior to the transcriptional activation of most adipocyte specific genes in the early stage of adipocyte differentiation, while the adipocyte fatty acid binding protein (aP2) and FAS have been known as terminal markers of adipocyte differentiation (Chen et al., 2011; Ericsson et al., 1997). Leptin, a hormone secreted exclusively in adipose tissue, plays a central role in the regulation of energy expenditure and food intake (Kim et al., 2007).

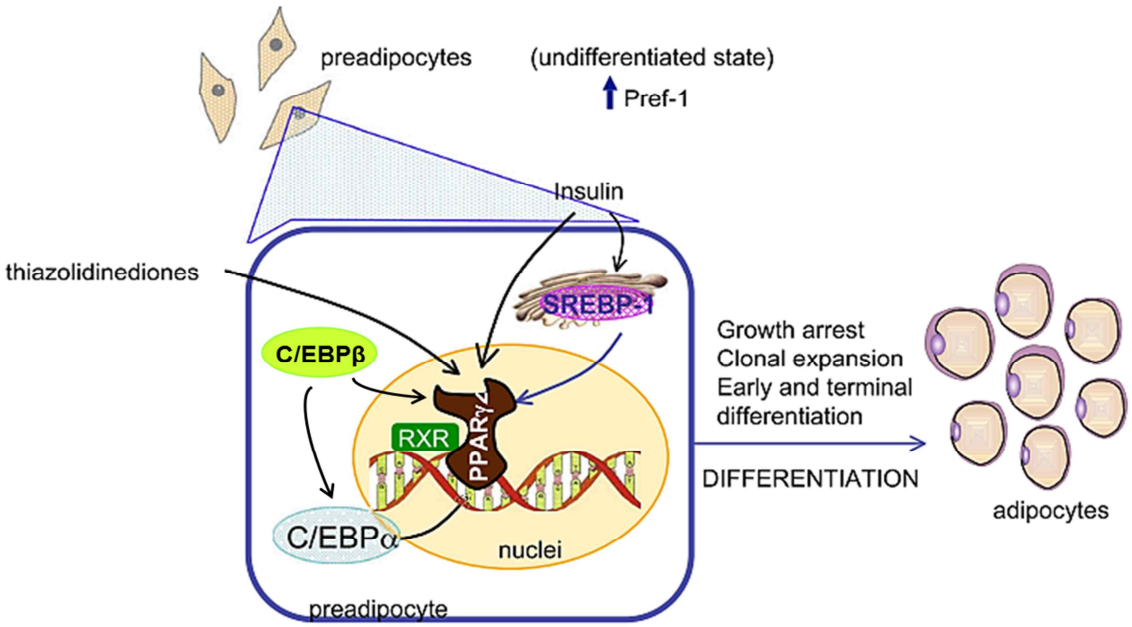

Figure 2. Adipogenesis by regulation of PPARγ, C/EBPα, SREBP1(Vazquez-Vela et al., 2008).

AMP-activated protein kinase (AMPK) is a metabolic-stress-sensing protein kinase that regulates metabolism in response to energy homeostasis by directly phosphorylating rate-limiting enzymes in metabolic pathways as well as controlling gene expression, and is recognized as a target for metabolic disorders including obesity, diabetes, and cancer (Kemp et al., 2003; Luo et al., 2005). Activation of AMPK induces the phosphorylation and regulation of downstream target genes, which are involved in diverse pathways in various tissues such as adipose tissue, liver, muscles, and hypothalamus (Moon et al., 2009). AMPK cascades have emerged as novel targets for the treatment of obesity (Luo et al., 2005). The activation of AMPK by muscle contraction and hypoxia has been shown to phosphorylate acetyl-CoA carboxylase beta (ACC-β), which leads to the inhibition of ACC activity and a consequent reduction in the malonyl-CoA content, thereby decreasing carnitine palmitoyl transferase 1 (CPT 1) activity and increasing fatty-acid oxidation (Yamauchi et al., 2002) (Figure 3). Inactivation of ACC in hepatocytes also decreases the concentration of malonyl-CoA, product of ACC, which has marked effects on fatty acid oxidation. Malonyl-CoA is a potent inhibitor of CPT-1, the ‘‘gatekeeper’’ for entry of fatty acids into the mitochondria (Winder and Hardie, 1999). CPT 1 is subject to regulation at the transcriptional level and to acute control by malonyl-CoA (Kerner et al., 2000). Overall effects of AMPK activation in the liver is decreases in fatty acid, triglyceride, and sterol synthesis and increases in fatty acid oxidation, lipogenesis, and ketogenesis. Recent data implicate AMPK as being important in control of fatty acid oxidation and glucose uptake in skeletal muscle, and possibly in modulating insulin secretion by the pancreatic β-cell.

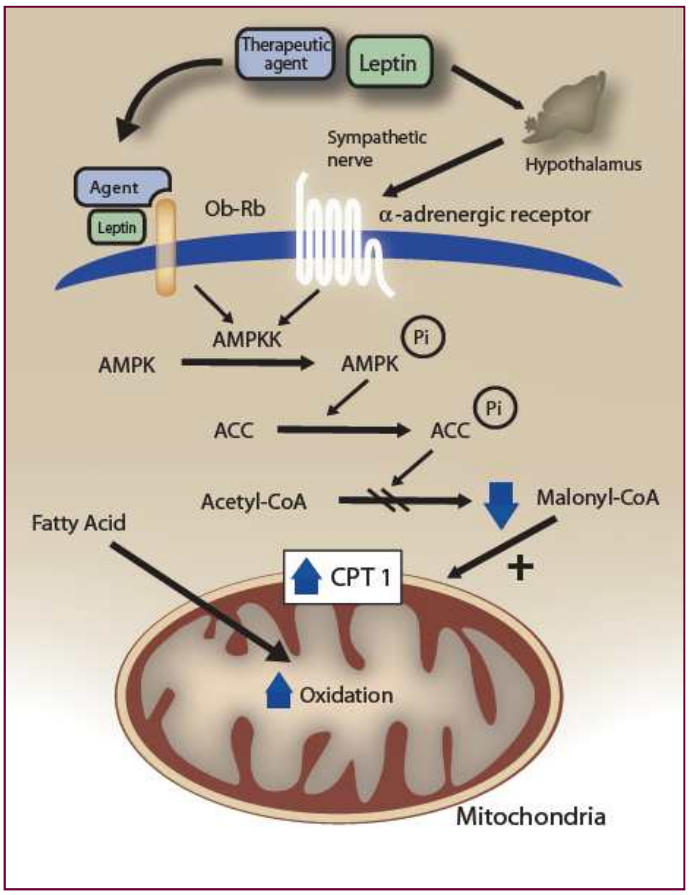

Figure 3. Activation of AMPK-CPT-1 cascade.

Malonyl CoA synthase is inhibited through the action of AMPK resulting in activation of CPT-1, thereby increasing mitochondrial import and fatty acid oxidation (Wasan and Looije, 2005)

Lipolysis

Breakdown of triglycerides in adipocytes and the release of glycerol and fatty acids are important for the regulation of energy homeostasis (Frayn et al., 2003). Hormone sensitive lipase (HSL) is the most important lipase that catalyses the process of lipolysis, and HSL is subject to hormonal regulation (Holm et al., 2003). Perilipin, which is not detectable but is increased during adipocyte differentiation, has been postulated to modulate HSL activity (Martinez-Botas et al., 2000). The phosphorylation of HSL and perilipin translocation into lipid droplets is critical processes of lipolysis and regulate (Ardevol et al., 2000) (Figure 4). Therefore, the expression levels of perilipin and HSL were determined as the lipolytic response. Tumor necrosis factor alpha (TNFα) has been shown to increase the lipolysis rate in humans *in vivo* (Starnes et al., 1988). The TNFα stimulates adipocyte lipolysis and down-regulates the expression of the lipid droplet-associated protein perilipin which is thought to modulate the accession of HSL to the surface of the fat droplet (Ryden et al., 2004). TNFα can suppress expression and function of PPARγ which is known to promote phosphorylation and down-regulation of perilipin (Xing et al., 1997; Arimura et al., 2004). TNFα induced lipolysis is also known to down-regulate anti-lipolytic genes PDE3B and G*i*α1 (Rahn Landstrom et al., 2000; Gasic et al., 1999). PDE3B, expressed in insulin sensitive cells such as adipocytes, plays a important role in regulating anti-glycogenosis, anti-lipolysis and insulin secretion (Degerman et al., 1997). The reduction in cAMP/protein kinase A activity along with PDE3B activation results in net dephosphorylation and decreased activity of HSL, and then leads to decreased hydrolysis of stored triglyceride (Degerman et al., 1997).

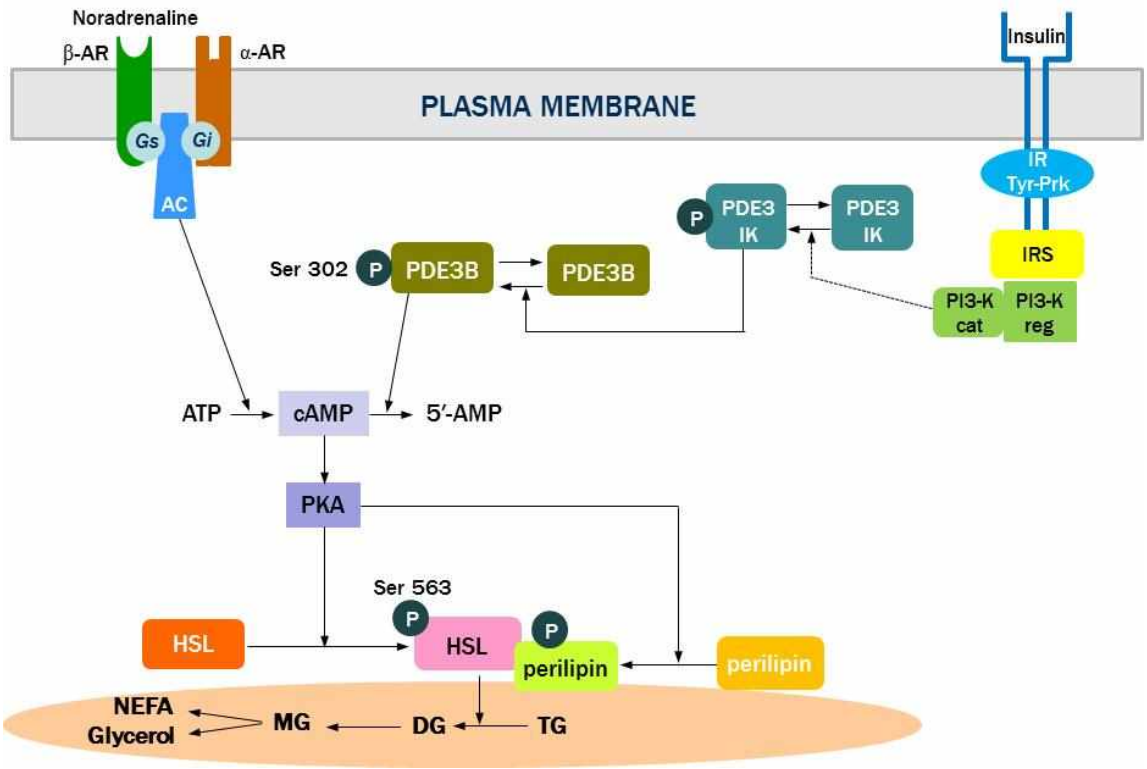

Figure 4. Mechanism for hormonal regulation of the rat fat cell lipolysis. HSL phosphorylation promotes its translocation from the cytosol to the surface of the lipid droplet. Perilipin phosphorylation induces an important physical alteration of the droplet surface that facilitates the action of HSL and the initiation of lipolysis. Insulin, via stimulation of fat cell insulin receptors and PDE3B stimulation promotes cAMP degradation and antilipolytic effects. AC, adenylyl cyclase; Gi, inhibitory GTP-binding protein; Gs, stimulatory GTP-binding protein; NEFA, nonesterified fatty acid; PDE3-IK, insulin-stimulated protein serine kinase (Lafontan et al., 2009).

Preadipocyte proliferation and apoptosis

The preadipocytes can proliferate throughout life to increase fat mass and play a central role by differentiating into mature adipocytes. Obesity is characterized at the cell biological level by an increase in the number and size of adipocytes differentiated from fibroblastic preadipocytes in adipose tissue (Furuyashiki et al., 2004). Therefore, inhibition of preadipocyte proliferation will be a strategy for development of anti-adipogenic agents and decreases in adipocyte number occur via preadipocyte apoptosis (Prins et al., 1997). Preadipocyte apoptosis is important for destruction of undesired cells during development and homeostasis of multicellular organisms and is characterized by distinct morphological changes such as plasma membrane blebbing, cell shrinkage, depolarization of mitochondria, chromatin condensation, and DNA fragmentation (Vermeulen et al., 2005). Two major apoptosis pathways have been defined in mammalian cells, the Fas/TNF-R1 death receptor pathway and the mitochondria pathway (Yin et al., 2000). In the latter pathway, the Bcl-2 family proteins consist of both anti-apoptosis and pro-apoptosis members that regulate apoptosis, mainly by controlling the release of cytochrome c and other mitochondrial apoptotic events (Yin et al., 2000). However, death signals mediated by Fas/TNF-R1 receptors can usually activate caspases directly, bypassing the need for mitochondria and escaping the regulation by Bcl-2 family proteins. In turn, induction of cytochrome c release activates downstream caspases (Green and Reed, 1998). Caspase are a family of cysteine proteases that are activated during the execution phase of the cell apoptotic process (*Woo et al., 2004*). Caspase-9 initiated cytochrome c activates effector Caspase-3 and -7, eventually leading to cell death (Riedl and Shi, 2004).

Anti-obesity agents from natural products

Herbal preparation from single or multiple plants represent the oldest and most widespread form of medication. Dissatisfaction with the high costs and potentially harmful side effects of pharmaceuticals have resulted in a larger percentage of people purchasing and exploring the applications of medicinal plants than before (Kessler et al., 2001). Several plants like willow, poppy, foxglove, cinchona, aloe and garlic have been verified as medicinally beneficial through repeated clinical testing and laboratory analyses, and a number of plant extracts like green tea, garlic compounds and conjugated linoleic acid (CLA) were shown to possess either anti-diabetic effects or have direct effects on adipose tissue (Rayalam et al., 2008). Several pharmacological agents from natural products have been reported to treat obesity (Table 1). Natural products have potential effect for decreasing inducing apoptosis, lipid accumulation, and stimulating lipolysis in preadipocyte and/or adipocytes. A number of studies have been carried out to investigate the anti-obesity effects of polyphenols like apigenin and luteolin, kaempferol, quercetin, genistein, grape seed proanthocyanidin extract (GSPE), and (-)-epigallocatechin (EGCG), and the effects on lipid metabolism have been carried out with coumarin derivatives like esculetin and phytoalexins like resveratrol (Rayalam, et al., 2008). Based on many studies searching for effects of various components of extracts from natural products on adipogenesis, it is expected the development of the therapeutic agents derived from natural products providing alternative options for obesity.

On the basis of above background, the present study was conducted to evaluate anti-adiogenic effects of constituents isolated from *A. japonica* Steud. fruits, *A. hirsuta* Turcz. var. *sibirica* (Spach) H. Ohba leaves, *A. firma* Sieb. et Zucc. barks which were selected from

screening of natural products having anti-adipogenic activity in response to adipocyte differentiation in 3T3-L1 cells. In this regard, inhibitory effects of constituents on adipocyte differentiation and preadiocyte proliferation were investigated. Furthermore, the expression of transcription factors regulating adipogenesis such as PPARγ and C/EBPα, and involvement of AMPK signaling were examined to reveal the anti-adipogenic mechanism.

Table 1. Potential natural products for anti-obesity

Compound	**Source**	**Target of Action**	**Reference**
EGCG	Green tea	Apoptosis, inhibition of adipocyte differentiation by activating AMPK,	Kao et al., 2000; Lin et al., 2005; Hwang et al., 2005
Quercetin	Fruits and vegetable	Apoptosis, lipolysis	Harmon et al., 2001; Kuppusamy et al., 1992
Genistein	Fruits and vegetable	Apoptosis, inhibition of adipocyte differentiation, lipolysis	Harmon et al., 2001; Hwang, et al., 2005
Resveratrol	Fruits and vegetable	Inhibition of proliferation in preadipocyte, inhibition of adipocyte differentiation	Harmon et al., 2001
Capsaicin	Red pepper	Apoptosis, inhibition of adipocyte differentiation,	Hsu et al., 2007; Hwang, et al., 2005
Esculetin	Fruits and vegetable	Apoptosis, inhibition of adipocyte differentiation	Yang et al., 2006
CLA	Soy oil	Apoptosis, inhibition of adipocyte differentiation	Hargrave et al., 2002; Tsuboyama-Kasaok et al., 2000
Docosahexa enoic aicd	Fish oil	Apoptosis, inhibition of adipocyte differentiation, lipolysis	Kim et al., 2006
Berberine	*Cortidis japonica*	Inhibition of adipocyte differentiation	Huang et al., 2006
Baicalin	*Scutellaria baicalensis*	Inhibition of adipocyte differentiation	Cha et al., 2006

Three *Alnus* species

Betulaceae consists of six genera of deciduous nut-bearing trees and shrubs, including the birches, alders, hazels, hornbeams, and hop-hornbeams, numbering about 130 species (Sati et al., 2011). *Alnus*, called alders, is main genus belonging to Betulaceae which comprises 30 species worldwide (Mitchell et al., 1982). According to Korea Food and Drug Administration (KFDA), it is reported that fifteen *Alnus* species were indigenous in Korea (http://fse.foodnara.go.kr/origin). The *Alnus* species are well known for their traditional medicinal values. These have been used for the treatment of various diseases including cancer and as an astringent, cathartic, emetic, febrifuge, galactogogue, hemostatic, parasiticide, skin tonic, vermifuge, etc (Sati et al., 2011). *A. japonica* is one of the indigenous *Alnus* species growing in damp areas of mountain valleys of Korea and the barks of these species have been used in Asian traditional medicine as remedies for fever, hemorrhage, diarrhea and alcoholism. Also, *A. japonica* is a popular folk medicine in Korea for cancer and hepatitis (Kim et al., 2004). *A. hirsuta* var. *sibirica*, an indigenous *Alnus* species found in Korea, is a deciduous broad-leaved tree growing in the damp areas of mountain valleys. In Korean traditional medicine, the bark of this plant been used for antipyretic and as a health tea for alcoholism (Lee et al., 2000a). The barks of *A. firma* have been used as a tonic in Korean folk medicine. The various types of plant secondary metabolites such as flavonoids, triterpenoids, tannin, phenols, steroids, and diarylheptanoids have been reported from three *Alnus* species (Figure 5-7).

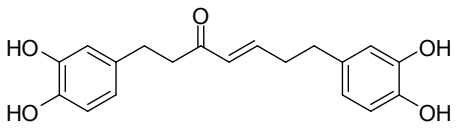

hirsutenone

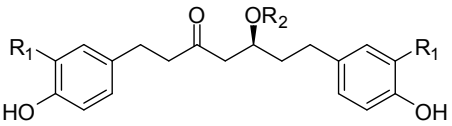

R_1=H, R_2=*β*-D-glucopyranoside: **platyphylloside**
R_1=H, R_2= *β*-D-apiofuranosyl-(1→6)-*β*-D-glucopyranoside: **(5*S*)-5-hydroxy-1,7-bis-(4-hydroxyphenyl)-3-heptanone-5-*O*-*β*-D-apiofuranosyl-(1→6)-*β*-D-glucopyranoside**
R_1=OH, R_2=*β*-D-xylopyranoside: **oregonin**
R_1=OH, R_2=OCH_3: **1,7-bis-(3,4-dihydroxyphenyl)-5-methoxy-3-heptanone**
R_1=OH, R_2=OH: **hirsutanonol**

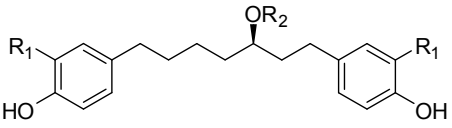

R_1=H, R_2= *β*-D-apiofuranosyl-(1→6)-*β*-D-glucopyranoside: **aceroside VIII**
R_1=H, R_2= *β*-D-glucopyranosyl-(1→3)-*β*-D-xylopyranoside: **(3*R*)-1,7-bis-(3,4-dihydroxyphenyl)-3-heptanol-3-*O*-*β*-D-glucopyranosyl-(1→3)-*β*-D-xylopyranoside**
R_1=H, R_2=OH: **(3*R*)-1,7-bis-(3,4-dihydroxyphenyl)-3-hydroxyheptane**
R_1=OH, R_2= *β*-D-glucopyranoside: **(3*R*)-1,7-bis-(3,4-dihydroxyphenyl)-3-heptanol-3-*O*-*β*-D-glucoopyranoside**
R_1=OH, R_2=6-*O*-galloyl-*β*-D-glucopyranoside: **hirsutanonol-5-*O*-(6-*O*-galloyl)-*β*-D-glucopyranoside**
R_1=OH, R_2=*β*-D-xylopyranoside: **(3*R*)-1,7-bis-(3,4-dihydroxyphenyl)-3-heptanol-3-*O*-*β*-D-xylopyranoside**

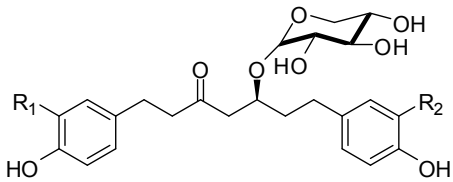

R_1=H, R_2=OH: **7-(3,4-dihydroxyphenyl)-5-hydroxy-1-(4-hydroxyphenyl)-3-heptanone-5-*O*-*β*-D-xylopyranoside**
R_1=OH, R_2=H: **1-(3,4-dihydroxyphenyl)-5-hydroxy-7-(4-hydroxyphenyl)-3-heptanone-5-*O*-β-D-xylopyranoside**

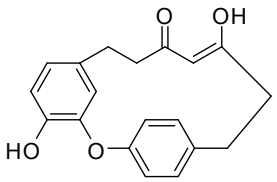

garugamblin-3

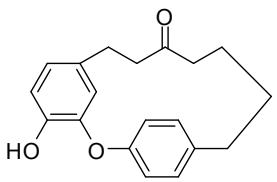

acerogenin L

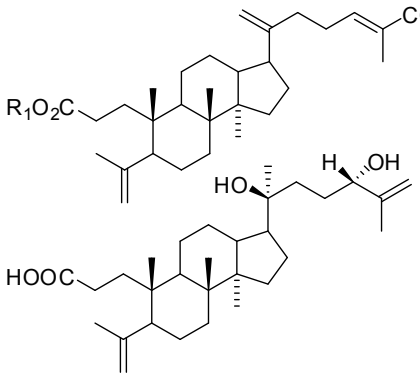

R_1=Me, R_2=H
: **methyl (24*E*)-3,4-secodammara-4(28),20,24-trien-26-oic-acid-3-oate**
R_1=R_2=H
: **(24*E*)-3,4-secodammara-4(28),20,24-trien-3,26-dioic-acid**

(20*S*,24*S*)-20,24-dihydroxy-3,4-secodammara-4(28),23-dien-3-oic-acid

Figure 5. Structures of chemical constituents known in *A. japonica*

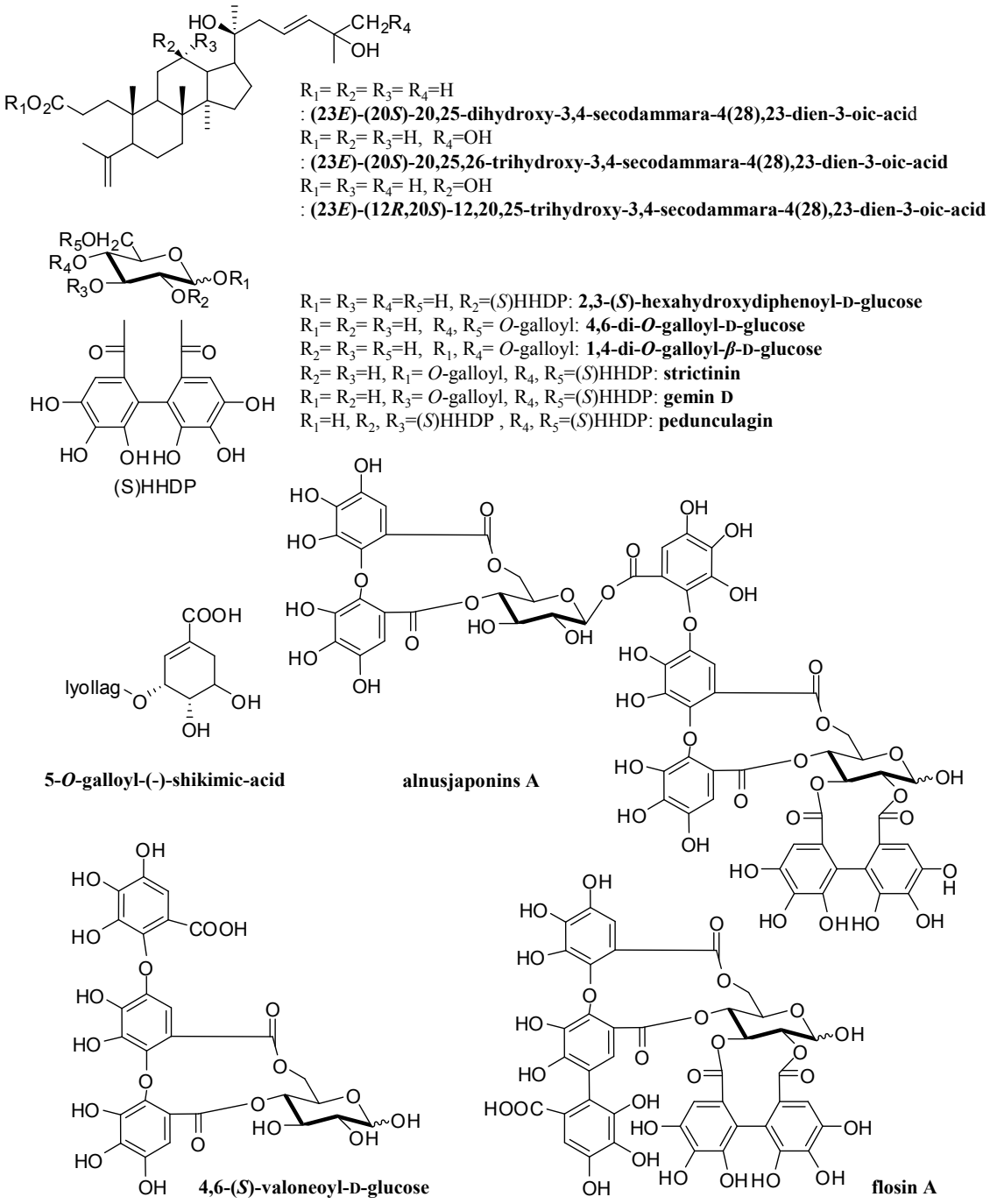

Figure 5. Structures of chemical constituents known in *A. japonica* (Continued)

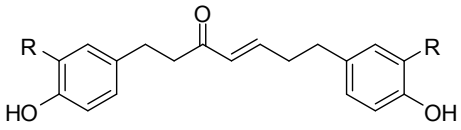

R=H: **1,7-bis-(4-hydroxyphenyl)-5-hepten-3-one**
R=OH: **hirsutenone**

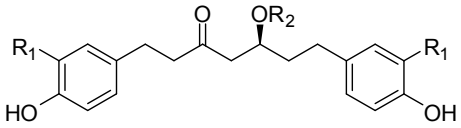

R_1=H, R_2=*β*-D-glucopyranoside: **platyphylloside**
R_1=H, R_2= *β*-D-apiofuranosyl-(1→6)-*β*-D-glucopyranoside: **(5*S*)-5-hydroxy-1,7-bis-(4-hydroxyphenyl)-3-heptanone-5-*O*-*β*-D-apiofuranosyl-(1→6)-*β*-D-glucopyranoside**
R_1=OH, R_2=*β*-D-xylopyranoside: **oregonin**

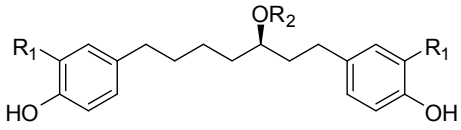

R_1=H, R_2= *β*-D-apiofuranosyl-(1→6)-*β*-D-glucopyranoside: **aceroside VIII**
R_1=OH, R_2= *β*-D-glucopyranoside: **(3*R*)-1,7-bis-(3,4-dihydroxyphenyl)-3-heptanol-3-*O*-*β*-D-glucoopyranoside**
R_1=H, R_2= *β*-D-glucopyranosyl-(1→3)-*β*-D-xylopyranoside: **(3*R*)-1,7-bis-(3,4-dihydroxyphenyl)-3-heptanol-3-*O*-*β*-D-glucopyranosyl-(1→3)-*β*-D-xylopyranoside**
R_1=OH, R_2=*β*-D-xylopyranoside: **(3*R*)-1,7-bis-(3,4-dihydroxyphenyl)-3-heptanol-3-*O*-*β*-D-xylopyranoside**

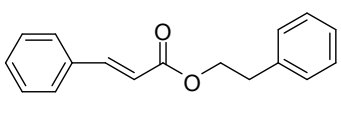

***β*-pheylethyl cinnamate**

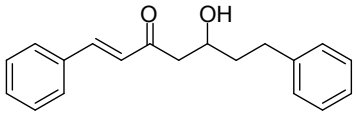

yashabushiketol

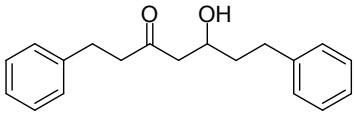

dihydroyashabushiketol

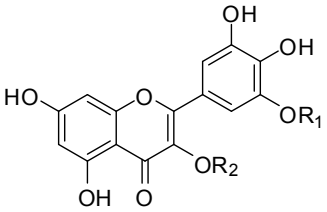

R_1=H, R_2=*α*-L-arbinofuranoside: **quercetrin-3-*O*-*α*-L-arbinofuranoside**
R_1=H, R_2=*β*-D-glucopyranoside: **isoquercetrin**
R_1=OH, R_2= *α*-L-rhamnopynoside: **quercetrin**

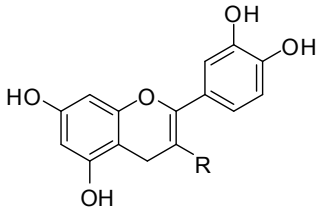

R= ▬OH: **(+)-catechin**
R= ⋯OH: **(-)-epicatechin**

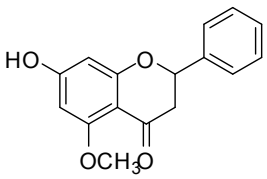

apinetin

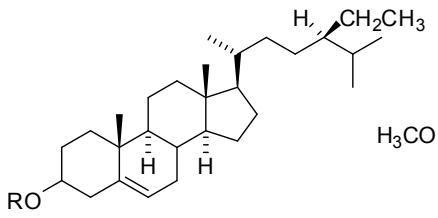

R=H: ***β*-sitosterol**
R=*β*-D-glucopyranoside: ***β*-sitosterol-3-*O*-*β*-D-glucoside**

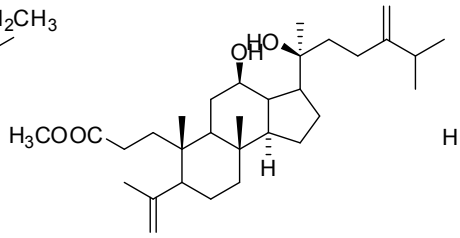

alnustic acid methyl ester

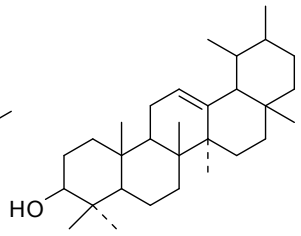

β-amyrin

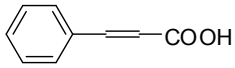

cinnamic acid

Figure 6. Structures of chemical constituents known in *A. firma*

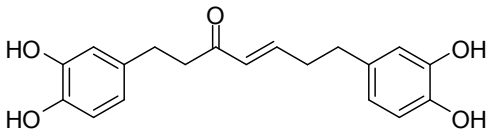

hirsutenone

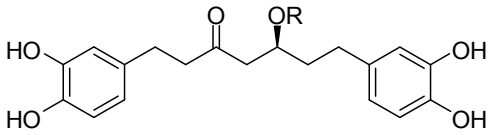

R=H: **hirsutanone**
R=*β*-D-xylopyranoside: **oregonin**

Figure 7. Structures of chemical constituents known in *A. hirsuta* var. *sibirica*

Recently, there is a growing interest in searching for genus *Alnus* related to the chemistry and pharmacology (Table 2-4). Diarylheptanoids, which are classified into linear and cyclic types, are the dominant constituents within the genus *Alnus*, few of them exhibited antioxidant effects and inhibitory activity against nuclear factor kappaB activation, nitric oxide (NO), protein kinase C (PKC), cyclooxygenase 2 (COX2) and tumor necrosis factor-α production, human umbilical vein endothelial cells, farnesyl protein transferase, cell-mediated low-density lipoprotein oxidation, HIF-1 in AGS cells, and the HIV-1-induced cytopathic effect in MT-4 cells (Sati et al., 2011; Lee et al., 2005). Some tannins showed hepato-protective activity even in a dose of 1 mg/kg which is ten-fold smaller compared with the dose of traditional flavonoid-based drugs (Sati et al., 2011).

Table 2. Pharmacological studies reported in *A. japonica*

Therapeutic Target	***In vitro*/*vivo* Assay**	**Plants/their Constituents**	**Reference**
Antioxidative activity	ABTS1 radical scavenging assay	*Alnus japonica* stems/ hirsutanonol 5-*O*-*β*-D-glucopyranoside, 3-deoxohirsutenonol 5-*O*-*β*-D-glucopyranoside, and hirsutenone	Lim et al., 2011
Atopic dermatitis	NC/Nga mice	*Alnus japonica* barks	Choi et al., 2011
Anti-influenza activity	Anti-viral assay: egg-bit assay	*Alnus japonica* barks/ betulinic aldehyde	Tung et al., 2010a
Anti-influenza activity	Anti-viral assay: egg-bit assay	*Alnus japonica* barks/ platyphyllone, platyphyllonol-5-xylopyranoside	Tung et al., 2010b
Anti-oxidative and Hepatoprotective activity	TOSC assay- evaluate the ROS scavenging capacity	*Alnus japonica* barks/ hirsutenone, hirsutanonol, oregonin, alnuside A, alnuside B, platyphyllonol-5-xylose, platyphyllone, latyphylloside, rubranoside B, rubranoside C	Tung et al., 2010c
Atopic dermatitis	Mouse splenocytes and RBL-2H3 mast cells	*Alnus japonica* barks/ hirsutenone	Joo et al., 2009
Cytotoxic activities	Murine B16 melanoma cells and human SNU-C1 gastric cancer cell	*Alnus japonica* barks/1,7-bis-(3,4-dihydroxyphenyl)-heptane-3-one-5-*O*-*β*-D-glucopyranoside, oregonin, hirsutanonol, hirsutenone, 1,7-bis-(3,4-dihydroxyphenyl)-5-hydroxyheptzane-3-*O*-*β*-D-xylopyranoside, platyphylloside	Choi et al., 2008

Anti-inflammatory activity	RAW264.7 cells	*Alnus japonica* leaves/ Methylhirsutanonol	Han et al., 2008
Anti-inflammatory activity	Human umbilical vein endothelial cells (HUVECs)	*Alnus japonica* leaves/ 5-O-methylhirsutanonol, oregonin	Han et al., 2007
Antioxidative activity	1,1-Diphenyl-2-picrylhydrazyl (DPPH) radical scavenging assay	*Alnus japonica* leaves/ oregonin	Kuroyanagi et al., 2005
Inhibition of human low-density lipoprotein oxidation	THP1 cells/ low-density lipoprotein receptor-null (B6, 129-Ldlrtml Icr-/-) mice	*Alnus japonica* fruits/ garugamblin-3, acerogenin L	Kang et al., 2006
Low-density lipoprotein - antioxidant activity	Human monocytic THP-1cell/ TBARS assay	*Alnus japonica* leaves/ oregonin, hirsutanone	Lee et al., 2005
Nitric oxide and prostaglandin E2 synthesis inhibitory activity	RAW 264.7 cells	*Alnus japonica* barks/ oregonin, hirsutanonol, hirsutenone, platyphylloside	Kim et al., 2005
Hepatoprotective and antioxidant activity	Rat hepatocyte	*Alnus japonica* barks	Kim et al., 2004
Inhibitory activity of farnesyl protein transferase	Farnesyl protein transferase assay	Garugamblin-3, acerogenin L	Kang et al., 2004

Table 3. Pharmacological studies reported in *A. hirsuta* var. s*ibirica*

Therapeutic Target	***In vitro*/*vivo* Assay**	**Plants/their Constituents**	**Reference**
Inhibition of TPA-induced upregulation of COX-2 and MMP-9	human breast epithelial MCF10A cells	*A. hirsuta* var. *sibirica* bark/ hirsutenone	Kim et al., 2006
Inhibition of COX-2 expression	human breast epithelial MCF10A cells	*A. hirsuta* var. *sibirica* bark/ oregonin and hirsutanonol	Lee et al., 2000

Table 4. Pharmacological studies reported in *A. firma*

Therapeutic Target	***In vitro*/*vivo* Assay**	**Plants/their Constituents**	**Reference**
Inhibit HIV-1 virus replication and controlled its essential enzymes	human breast epithelial MCF10A cells	*Alnus firma* leaves/ alnustic acid methyl ester, quercetin and myricetin 3-*O*-*β*-D-galactopyranoside	Yu et al., 2007
Inhibitory activity on lipopolysaccharide-induced nitric oxide production in BV2 microglia	BV microglial cell	*Alnus firma* barks/ dehydrohirsutanonol, 5-hydroxy-3-platyphyllone, platyphylloside, (5*S*)-5-hydroxy-7-(3,4-dihydroxyphenyl)-1-(4-hydroxyphenyl)-3-heptanone-5-*O*-*β*-D-xylopyranoside, (5*R*)-5-methoxy-1,7-bis-(3,4-dihydroxyphenyl)-3-heptanone, oregonin	Lee et al., 2010
Anti-fibrotic activity	hepatic stellate cell (HSC-T6 cell)	*Alnus firma* barks/ hirsutanone and lup-20(29) en-2,28-diol-3-yl caffeate	Lee et al., 2011

II. Materials and methods

1. Isolation of bioactive constituents from three *Alnus* species

1.1. Material

1.1.1. Plant

The *A. japonica* fruits (Figure 8A) and *A. hirsuta* var. *sibirica* leaves (Figure 8B) were collected in Nambu forest of Seoul, Beagwoon Mountain, Gwangyang city, Jeollanam-do, Korea. The *A. firma* barks (Figure 8C) were obtained from SK forest, Chungju, Korea in March 2008. These *Alnus* species authenticated by Dr. Jong Hee Park, professor of Pusan National University (Pusan, Korea). The voucher specimens (*A. japonica*: SNU 752, *A. hirsuta* var. *sibirica*: SNU 753, and *A. firma*: SNU 751) has been deposited at the Herbarium of the Medicinal Plant Garden, College of Pharmacy, Seoul National University, Koyang, Korea.

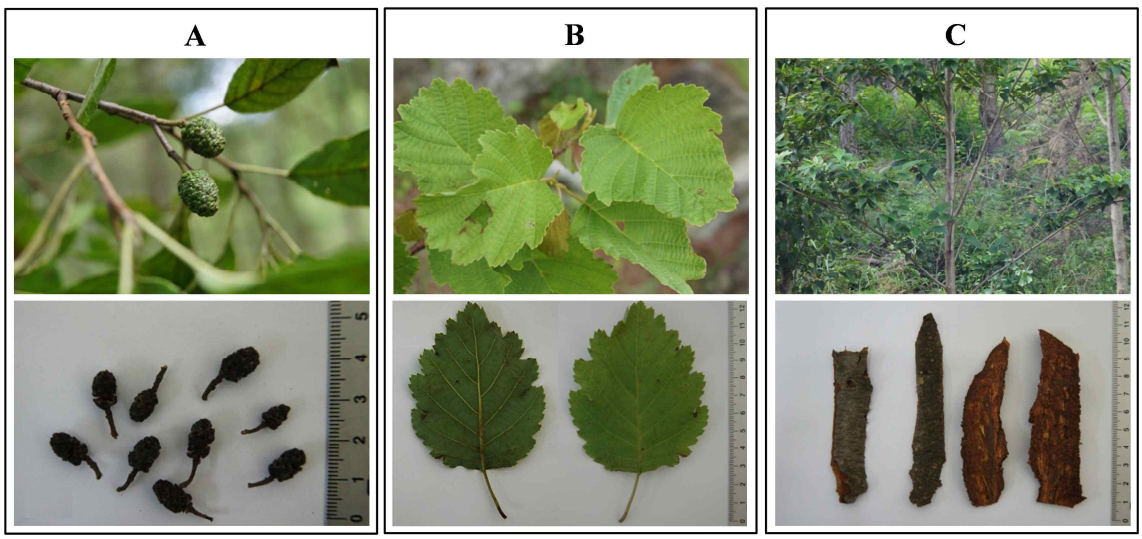

Figure 8. *A. japonica* fruits (A), *A. hirsuta* var. *sibirica* leaves (B), and *A. firma* barks (C)

1.1.2. Reagents for isolation and purification

First grade solvents (Duksan chemical Co., Korea) were used for extraction, fractionation and isolation. HPLC grade solvents were purchased from Fisher Scientific (Pittsburgh, PA, USA). Column chromatography was purchased from Merck & Co., Inc. (Whitehouse station, NJ, USA) (9025) silica gel 60 (0.04-0.063 mm). Analytical TLC was performed on precoated Merck F_{254} silica gel plates and visualized by spraying with anisaldehyde-H_2SO_4. An HPLC system (Hitachi L-6200, Japan) equipped with a UV-visible detector and C_{18} semi-preparative column was used for isolation.

1.2. Equipments

Analytical balance: Mettler AE 50, Switzerland and EK-1200A, Japan

Applied Biosystems 7300 Real-Time PCR System: Life Technologies Co., USA

Autoclave: Sanyo MLS 3000, Japan

Centrifuge: Eppendorff, Germany

Drying oven: CO-2D-1S, Wooju Sci. Co., Korea

Elisa reader: Molecular Devices E_{max}, USA

ESI-MS: Finnigan LCQ ion-trap mass, USA

Fluorometer: Gemini XS, Molecular device, USA

Freeze-dryer: DURA-DRY, Fts system Inc., USA

FT-IR: Perkin Elmer 1710 spectrophotometer, UK

Gel Doc EQ Gel Documentation System: Bio-Rad Laboratories Inc., USA

HPLC pump: Hitachi L-6200, Japan

HPLC UV detector: Hitachi L-4000, Japan

HPLC column: YMC-Pack ODS-a, A-323, AA12S05-2510WT, Japan

Luminescent Image Analyzer (LAS): LAS 1000, FUJIFILM Co., Japan

Mass: VG Trio-2 spectrometer, UK

VG 70-VSEQ mass spectrometer

Hewlet-Packard 5890-JMS AX 505-WA spectrometer, USA

Melting Point apparatus: Buchi 535, Germany

Microplate reader: SPECTRAFlour, Austria

NMR: JEOL LA 300 spectrometer, Japan

JEOL GSX 400 spectrometer, Japan

Brucker AMX 500 spectrometer, Germany

Brucker Avance 600 spectrometer, Germany

Optical rotation: Jasco DIP-1000 digital polarimeter, Japan

pH meter: phoenix PMS-500, USA

Phase contrast inverted microscope: Olympus CK2- Japan

Real-time PCR: Applied Biosystems 7300 Real-Time PCR System, Life Technologies Co., USA

Rotary evaporator: Eyela Tokyo Rikakikai Co., Japan

Sonicator: Branson 5200, 5210, UK

UV lamp: UVP UV GL 58, VP Inc., USA

UV spectrometer: Shimadzu 2101 Spectrophotometer, Japan

Water-jacked CO_2 incubator: Forma Scientific Co., USA

1.3. Methods

1.3.1. Extraction and fractionation of *A. japonica*

The dried fruits of *A. japonica* (1500 g) was pulverized and then extracted with 80% methanol (4 L, 3 h x 5) by ultrasonication at room temperature. The methanolic extract was concentrated *in vacuo* to give a crude extract (419.1 g). This methanolic extract was suspended in H_2O and partitioned successively with *n*-hexane (4 L), $CHCl_3$ (4 L), *n*-BuOH (4 L) and H_2O, giving solid residue of 29.5 g, 47.6 g, 251.6 g, and 62.7 g, respectively (Scheme 1). Of these fractions, the $CHCl_3$ and *n*-BuOH fractions with significantly inhibitory effect on adipocyte differentiation (67.7±5.9% and 31.4±6.8% at a concentration 50 μg/mL, respectively) were used for follow-up isolation work.

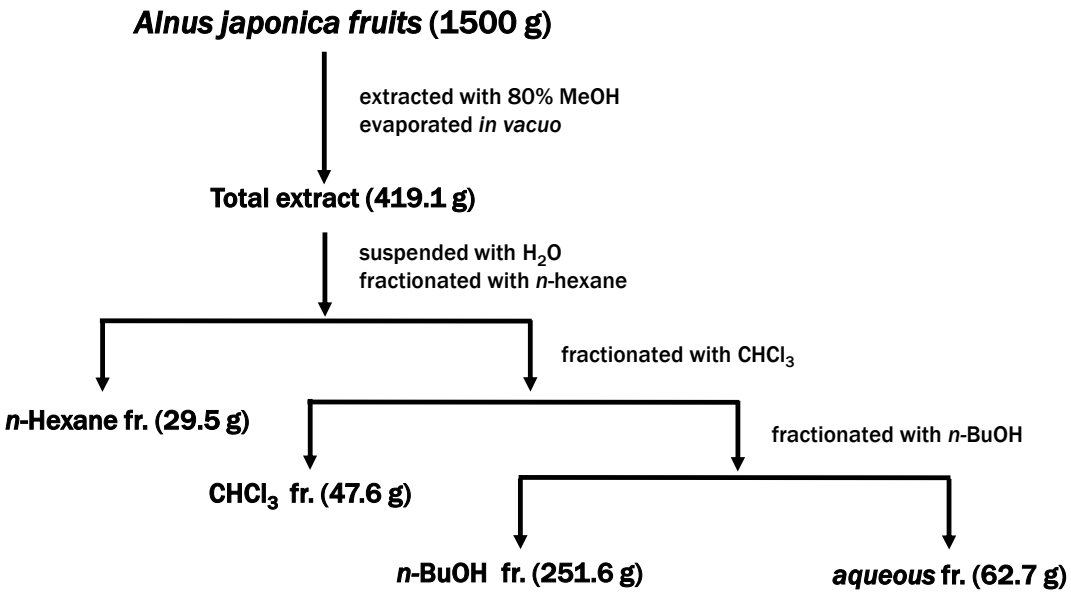

Scheme 2. Extraction and fractionation of *A. japonica* fruits

1.3.2. Isolation of compounds from $CHCl_3$ and *n*-BuOH fractions

The $CHCl_3$ fraction was subjected to silica gel column chromatography and eluted by $CHCl_3$-MeOH-water gradient to yield fifteen fractions (C1~C7) (Scheme 2). C4 was subjected to MPLC (RediSep silica gel; $CHCl_3$-MeOH, 15:1→MeOH, 30 mL/min) to yield six fractions (C4-1~C4-6). Compounds **AJ43** (5.1 mg) and compound **AJ 44** (20.4 mg) yielded from C4-2 and C5, respectively, by recrystallization. Compound **AJ39** (4.1 mg) was obtained from C4-3 by column chromatography on Sephadex LH-20 ($CHCl_3$-MeOH, 1:1). C4-5 was subjected to MPLC (RediSep silica gel; $CHCl_3$→MeOH; 22 mL/min) to yield seven fractions (C4-5-1~C4-5-7). Compound **AJ1** (6.7 mg, t_R 279.26 min), compound **AJ2** (8.1 mg, t_R 302.60 min), compound **AJ4** (3.1 mg, t_R 292.46 min), compound **AJ23** (2.7 mg, t_R 306.58 min), compound **AJ27** (2.0 mg, t_R 372.11 min), compound **AJ28** (3.2 mg, t_R 360.22 min), compound **AJ29** (2.9 mg, t_R 401.28 min), and compound **AJ35** (1.9 mg, t_R 387.64 min) obtained from C4-5-4 through preparative HPLC (polymeric gel filtration, 500 x 20 mm, Hexane: EtOAc 3:1→1:1, 4 mL/min). C4-5-6 was subjected to preparative HPLC (polymeric gel filtration, 500 x 20 mm, *n*-hexane: EtOAc 3:1→1:1, 4 mL/min) to yield thirty fractions (C4-5-6-1~C4-5-6-30). Compounds **AJ40**-**AJ42** yielded by recrystallization from C4-5-6-7, C4-5-6-9, and C4-5-6-10, respectively. Compound **AJ3** was obtained from C4-5-6-27 by column chromatography on Sephadex LH-20 ($CHCl_3$-MeOH, 1:1). The *n*-BuOH fraction (251.6 g) was eluted from Diaion HP-20 resin using H_2O-MeOH gradient as a mobile phase to afford six fractions (B1~B6) (Scheme 2). The B3 was subjected to silica gel CC and eluted by $CHCl_3$-MeOH-water gradient to yield eleven fractions (B3-1~B3-11). Compound **AJ5** (6.7 mg, t_R 68.14 min), compound **AJ7** (1.5 mg, t_R 346.12 min), compound **AJ9** (2.4 mg, t_R 138.14 min), compound **AJ10** (5.2 mg, t_R 255.16 min), and

compound **AJ11** (3.4 mg, t_R 240.00 min) obtained from B3-5 through preparative HPLC (C_{18}, 500 x 20 mm, MeOH-H_2O, 30:70, 4 mL/min). Compound **AJ12** (2.9 mg, t_R 68.64 min), compound **AJ13** (126 mg, t_R 45.12 min), compound **AJ14** (2.4 mg, t_R 80.98 min), compound **AJ20** (2.9 mg, t_R 165.54 min), and compound **AJ21** (4.1 mg, t_R 130.88 min) yielded from B3-6 through preparative (C_{18}, 500 x 20 mm, MeOH-H_2O, 30:70, 4 mL/min). B3-7 was divided into two fraction by Sep-Pak (C_{18}, H_2O→MeOH) (B3-7-1~B3-7-2). B3-7-1 yielded compound **AJ31** (1.1 mg, t_R 150.88 min) by preparative HPLC (C_{18}, 500 x 20 mm, CH_3CN-H_2O, 10:90, 4 mL/min). Compound **AJ32** (3.6 mg, t_R 75.66 min) was purified from B3-7-2 through preparative HPLC (C_{18}, 500 x 20 mm, CH_3CN-H_2O, 10:90, 4 mL/min). Compound **AJ30** (1.7 mg, t_R 262.14 min), compound **AJ33** (5.6 mg, t_R 67.64 min), compound **AJ37** (7.5 mg, t_R 77.20 min), and compound **AJ38** (12.9 mg, t_R 252.98 min) obtained from B3-8 through preparative HPLC (Polymeric Gel filtration, 500 x 20 mm, CH_3CN-H_2O, 10:90→30:70, 4 mL/min). B4 yielded compound **AJ6** (1.9 mg, t_R 182.12 min) and **AJ18** (10.5 mg, t_R 90.48 min) by preparative HPLC (C_{18}, 500 x 20 mm, CH_3CN-H_2O, 10:90, 4 mL/min). B5 was subjected to RP C_{18} column chromatography and eluted by H_2O-MeOH gradient to yield sixty five subfractions (B5-1~B5-65). Compound **AJ26** (14.2 mg) and **AJ24** (9.6 mg) was refined from B5-21 and B5-34, respectively, by recrystallization. Compound **AJ17** (5.1 mg) and **AJ16** (2.6 mg) was refined from B5-32 and B5-40, respectively, by column chromatography on Sephadex LH-20 (MeOH). Compound **AJ22** (1.7 mg, t_R 123.88 min), compound **AJ25** (2.8 mg, t_R 102.46 min), compound **AJ34** (7.9 mg, t_R 77.64 min), and compound **AJ36** (2.2 mg, t_R 35.34 min) obtained from B6 through preparative HPLC (Polymeric Gel filtration, 500 x 20 mm, $CHCl_3$-MeOH-H_2O, 50:4:1→6:5:1, 4 mL/min).

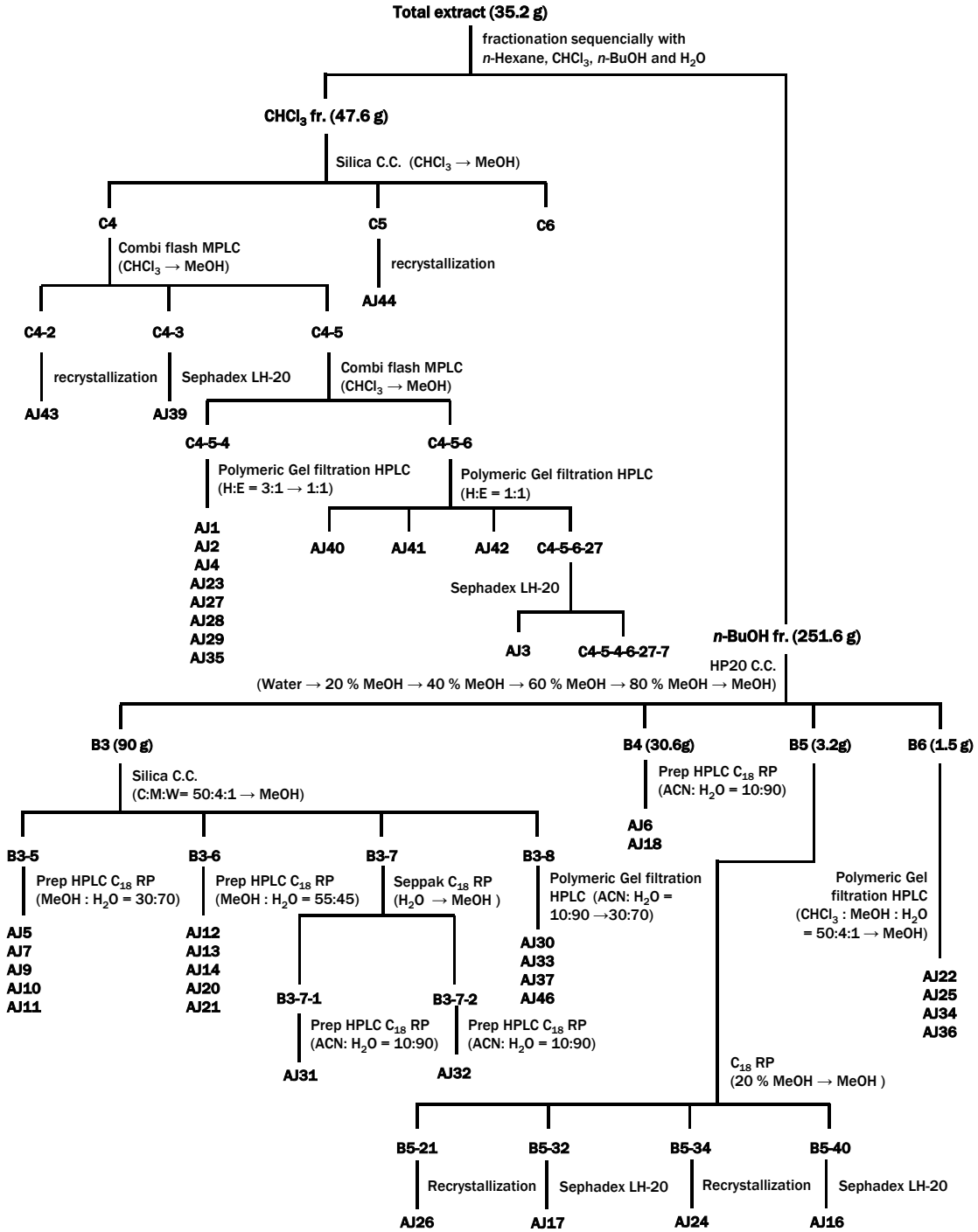

Scheme 2. Isolation of compounds from *A. japonica* fruits

1.3.3. Extraction and fractionation of *A. hirsuta* var. *sibirica*

The dried leaves of *A. hirsuta* var. *sibirica* (119 g) was pulverized and then extracted with 80% methanol (2 L, 3 h x 3) by ultrasonication at room temperature. The methanolic extract was concentrated *in vacuo* to give a crude extract (35 g). This methanolic extract was suspended in H_2O and partitioned successively with $CHCl_3$ (2 L), EtOAc (2 L) and *n*-BuOH (2 L), giving solid residue of 2.8 g, 8.7 g, and 9.9 g, respectively (Scheme 3). Of these fractions, the EtOAc and *n*-BuOH extracts with significantly inhibitory effect on adipocyte differentiation (17.7±3.6% and 56.9±7.5% at a concentration 100 μg/mL, respectively) were used for follow-up isolation work.

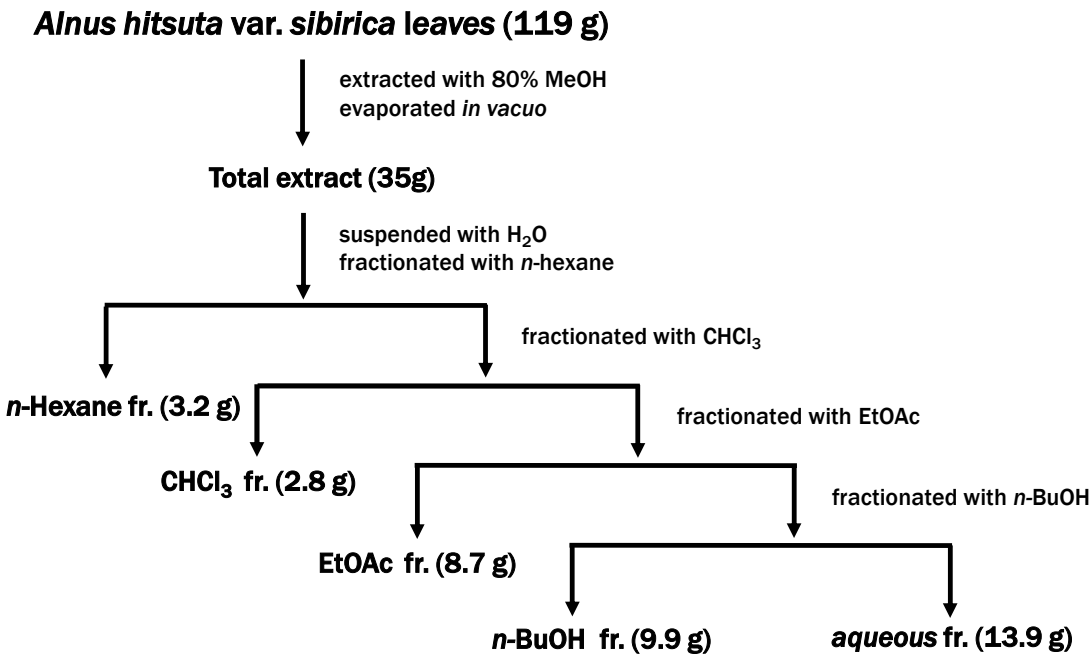

Scheme 3. Extraction and fractionation of *A. hirsuta* var. *sibirica* leaves

1.3.4. Isolation of compounds from EtOAc and *n*-BuOH fractions

The EtOAc fraction was subjected to silica gel column chromatography and eluted by $CHCl_3$-MeOH-water gradient to yield fifteen fractions (E1~E13). E3 was subjected to preparative HPLC (C_{18}, 500 x 20 mm, CH_3CN-H_2O, 38:62, 7 mL/min) to yield two fractions. Compound **AH9** (3.4 mg, t_R 37.64 min), obtained from E3-1 (t_R 25.4 min) and was purified through semi-preparative HPLC (YMC J'Sphere, C_{18}, 250 x 10 mm, MeOH-H_2O, 45:55, 2 mL/min). E4 yielded compound **AH3** (4.3 mg, t_R 72.36 min), compound **AH1** (3.0 mg, t_R 98.88 min) and compound **AH21** (6.9 mg, t_R 103.28 min) through preparative HPLC (C_{18}, 500 x 20 mm, MeOH-H_2O, 45:55, 6 mL/min), respectively. Compound **AH2** (2.3 mg, t_R 58.24 min) from E5, and Compound **AH17** (4 mg, t_R 31.18 min) and compound **AH11** (34.5 mg, t_R 45.13 min) from E6 were isolated using preparative HPLC (C_{18}, 500 x 20 mm, MeOH-H_2O, 55:45, 6 mL/min). E7 was further subjected to preparative HPLC (C_{18}, 500 x 20 mm, MeOH-H_2O, 48:52, 6 mL/min) to yield six fractions. Compound **AH7** (6 mg, t_R 22.75 min) and compound **AH24** (3.4 mg, t_R 12.75 min) was purified from E7-2 and E7-5, respectively, through semi-preparative HPLC (YMC J'Sphere, C_{18}, 250 x 10 mm, MeOH-H_2O, 50:50, 2 mL/min). Compound **AH22** (2.1 mg) was obtained from E13 by column chromatography on Sephadex LH-20 (MeOH). The *n*-BuOH fraction was chromatographed on a silica gel column eluting with a gradient of $CHCl_3$-MeOH-H_2O to yield nine fractions (B1~B9). B4 afforded compound **AH10** (14.5 mg, t_R 13.05 min) and compound **AH14** (10.6 mg, t_R 20.01 min) through semi-preparative HPLC (YMC J'Sphere, C_{18}, 250 x 10 mm, MeOH-H_2O, 50:50, 2 mL/min). Compound **AH12** (126.5 mg, t_R 73.92 min), compound **AH13** (10.5 mg, t_R 98.99 min), compound **AH19** (6.7 mg, t_R 127.68 min), compound **AH18** (5.9 mg, t_R 152.92 min), compound **AH5** (3.4 mg, t_R 202.56 min) and

compound **AH4** (3.8 mg, t_R 232.32 min) were isolated from B7 through preparative HPLC (C_{18}, 500 x 20 mm, MeOH-H_2O, 60:40, 4 mL/min). B8 yield compound **AH23** (5.2 mg) by recrystallization. Compound **AH16** (3.9 mg), compound **AH15** (4.9 mg) and compound **AH20** (3.0 mg) were obtained from B9 by column chromatography on Sephadex LH-20 (MeOH). The overall procedures of isolation of other constituents were summarized in Scheme 4.

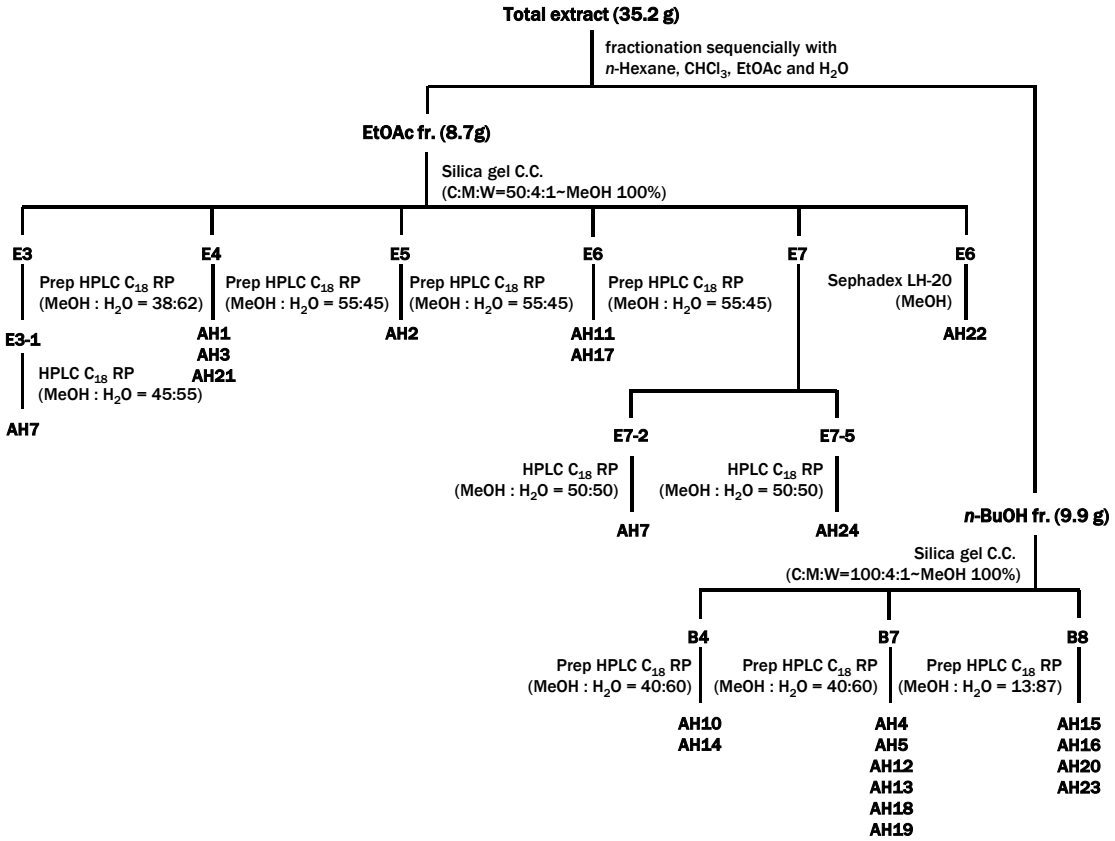

Scheme 4. Isolation of compounds from *A. hirsuta* var. *sibirica* leaves

1.3.5. Extraction and fractionation of *A. firma*

The dried barks of *A. firma* (5.7 kg) was pulverized and then extracted with 80% MeOH (10 L, 3 h x 4) by ultrasonication at room temperature. The methanolic extract was concentrated *in vacuo* to give a crude extract (1.1 kg). This methanolic extract was suspended in H_2O and successively partitioned with $CHCl_3$ (4 L), EtOAc (4 L) and *n*-BuOH (4 L), giving solid residue of 204.6 g, 494.7 g, and 225.5 g, respectively (Scheme 5). The CH_2Cl_2 layer was suspended in 90% MeOH and then partitioned with *n*-hexane, giving solid residue of 108.4 g, and 83.2 g, respectively. Of these fractions, the 90% MeOH and EtOAc fractions with significant inhibitory effect on adipocyte differentiation (49.7±2.6% and 40.8±8.8% at a concentration 100 μg/mL, respectively) were used for follow-up isolation work.

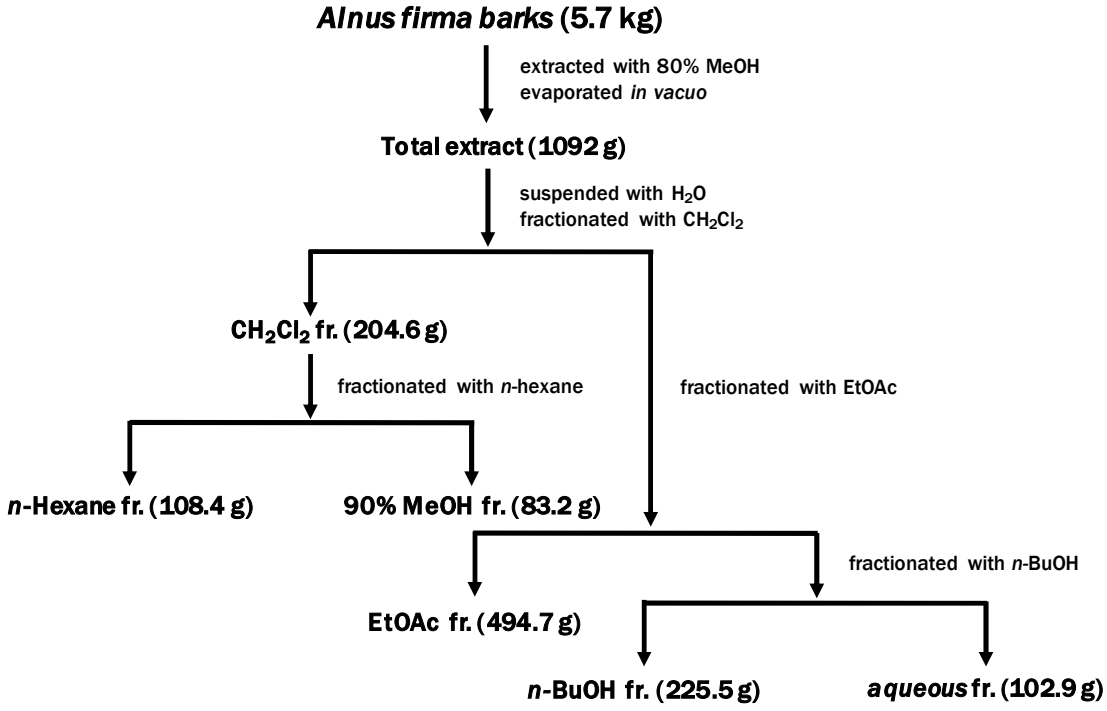

Scheme 5. Extraction and fractionation of *A. firma* barks

1.3.6. Isolation of compounds from 90% MeOH and EtOAc fractions

The EtOAc fraction (494 g) was subjected to column chromatography over silica gel, eluted with ($CHCl_3$-MeOH, 10:1→1:1) to give eight subfractions (E1~E8) (Scheme 6). Among these subfractions, E3 yielded compound **AF13** (7.1 mg, t_R 20.2 min), compound **AF14** (7.4 mg, t_R 21.9 min), compound **AF15** (9.2 mg, t_R 27.1 min) and compound **AF16** (8.7 mg, t_R 29.1 min) by semi-preparative HPLC (YMC Hydrosphere, C_{18}, 250 x 10 mm, CH_3CN-H_2O, 15:85, 2 mL/min). Compound **AF2** was isolated from E2 by MPLC (RediSep C_{18}, H_2O→MeOH, 20 mL/min). E5 was chromatographed on RP C_{18} column chromatography (H_2O→MeOH) to yield seven subfractions (E5-1~E5-7) and afforded compound **AF8** from E5-5. Compound **AF5** (8.7 mg, t_R 225.76 min), **AF9** (165 mg, t_R 183.79 min), **AF10** (301 mg, t_R 138.40 min), **AF11** (219 mg, t_R 100.11 min), and **AF12** (122mg, t_R 128.56 min) were isolated from E5-7 (AcCN-H_2O, 13:87) through preparative HPLC (C_{18}, 500 x 20 mm, CH_3CN-H_2O, 13:87, 7 mL/min). Compound **AF4** (15.2 mg, t_R 172.57) and **AF6** (9.2 mg, t_R 165.79 min) were isolated from E5-2 on the preparative HPLC (C_{18}, 500 x 20 mm, MeOH-H_2O, 32:68, 7 mL/min). Silica gel column chromatography of 90% MeOH fraction (68.2 g) was subjected with ($CHCl_3$→MeOH) and yielded nine fractions (MC1 ~ MC9) (Scheme 6). **AF17** yielded from MC1 by recrystallization. MC2 was subjected to silica gel CC ($CHCl_3$-MeOH, 25:1→0:100) to give four subfractions (MC2-1 ~ MC2-4). MC2-3 was divided into six fractions (MC2-3-1 ~ MC2-3-6) by MPLC (RediSep silica gel, $CHCl_3$-MeOH, 25:1→0:100, 30 mL/min). MC2-3-2 was chromatographed on MPLC (RediSep silica gel, $CHCl_3$-MeOH, 15:1→0:100, 30 mL/min) to yield eight subfraction (MC2-3-2-1– MC2-3-2-8) and afforded compound **AF1** (3.5 mg) from MC2-3-2-5. Compound **AF3** (4.8 mg, t_R 21.4 min) and **AF19** (202 mg) were isolated from MC2-3-4 by

semi-preparative HPLC (YMC Hydrosphere H80 C_{18}; 250 x 10 mm, CH_3CN-H_2O, 45:55; 2 mL/min) and from MC2-3-3 by recrystallization, respectively. Compound **AF18** (5.4 mg, t_R 67.34 min) were isolated from MC2-3-5 through preparative HPLC (C_{18}, 500 x 20 mm, MeOH-H_2O, 60:40, 4 mL/min). MC4 was subjected to MPLC (RediSep silica gel; $CHCl_3$-MeOH, 10:1→0:100, 30 mL/min) to yield ten fractions (MC4-1 ~ MC4-10). MC4-3 was fractioned by MPLC (RediSep RP_{18}, H_2O→MeOH, 20 mL/min) (MC4-3-1 ~ MC4-3-5). Compound **AF7** (22 mg, t_R 8.5 min) were isolated from MC4-3 on the semi-preparative HPLC (YMC Hydrosphere, C_{18}, 250 x 10 mm, CH_3CN-H_2O, 34:66, 2 mL/min).

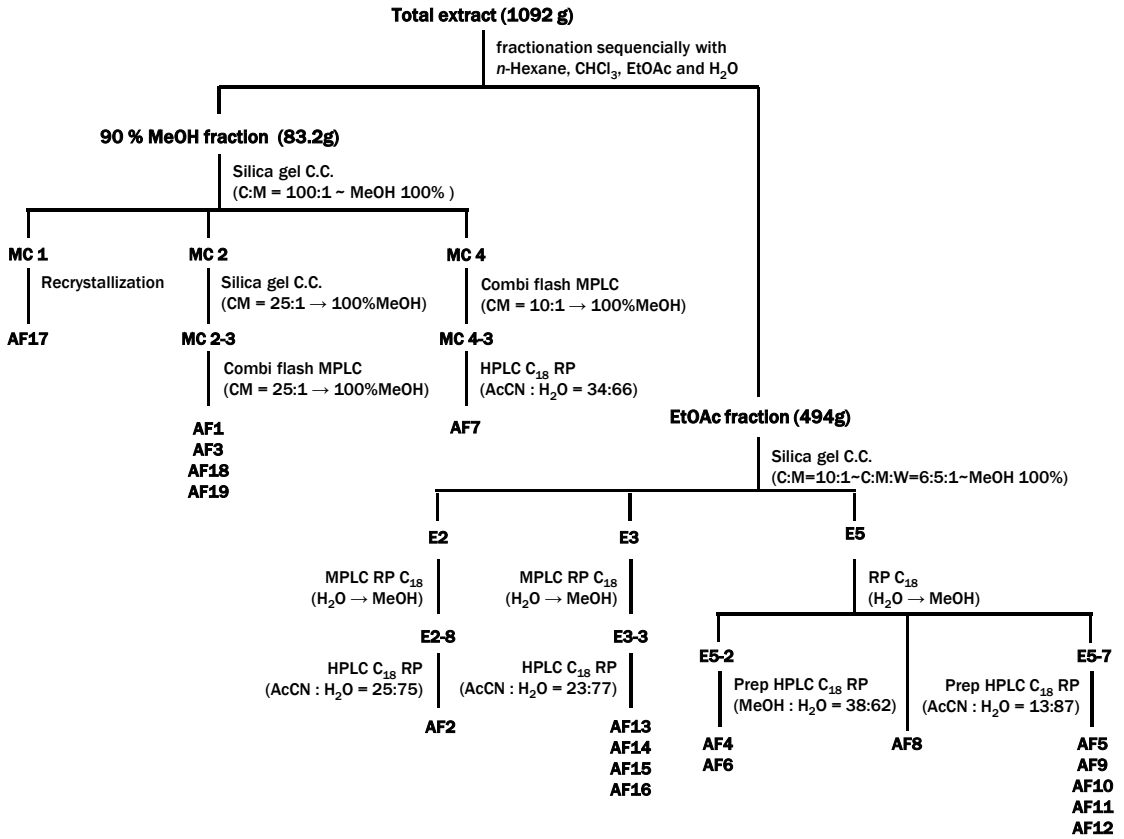

Scheme 6. Isolation of compounds from *A. firma* barks

Compound **AJ1**

brownish syrup

$C_{20}H_{20}O_4$

$[\alpha]_D^{25}$: -2.3 (*c* 1.0 $CHCl_3$:MeOH=1:1)

UV λ_{max} (MeOH) (log ε) (nm): 228 (3.87), 287 (3.47)

IR (KBr) ν_{max} (cm^{-1}): 3382, 2939, 1710, 1594, 1503, 1207, 1166, 1033 cm^{-1}

EIMS: *m/z* 325 $[M+H]^+$ (23), 324 $[M]^+$ (100), 306 $[M-H_2O]^+$ (29)

FABMS (positive mode): *m/z* 324 $[M]^+$

HRFABMS (positive mode): *m/z* 324.1358 $[M]^+$ (calcd. for $C_{20}H_{20}O_4$, 324.1362)

^1H NMR (500 MHz, $CDCl_3$): see Table 5

^{13}C NMR (125 MHz, $CDCl_3$): see Table 6

Compound **AJ2**

brownish syrup

$C_{19}H_{18}O_5$

$[\alpha]_D^{25}$: -0.5 (*c* 1.0 MeOH)

UV λ_{max} (MeOH) (log ε) (nm): 251 (3.55), 289 (3.43)

IR (KBr) ν_{max} (cm^{-1}): 3024, 2916, 1700, 1588, 1508, 1430, 1410, 1238, 1011, 951, 816

FABMS (positive mode): *m/z* 326 $[M]^+$

HRFABMS (positive mode): *m/z* 326.1152 $[M]^+$ (calcd. for $C_{19}H_{18}O_5$, 326.1154)

^1H NMR (400 MHz, $CDCl_3$): see Table 5

^{13}C NMR (100 MHz, $CDCl_3$): see Table 6

Compound **AJ3**

yellowish syrup

$C_{19}H_{20}O_3$

$[\alpha]_D^{25}$: -0.8 (*c* 1.0 MeOH)

UV λ_{max} (MeOH) (log ε) (nm): 298 (2.15)

IR (KBr) ν_{max} (cm^{-1}): 3341, 2929, 1702, 1608, 1505, 1430, 1411, 1237, 1211, 817

ESIMS (negative mode): *m/z* 295.23 $[M-H]^-$

^1H NMR (500 MHz, DMSO-d_6): see Table 5

^{13}C NMR (125 MHz, DMSO-d_6): see Table 6

Compound **AJ4**

yellowish syrup

$C_{19}H_{20}O_4$

$[\alpha]_D^{25}$: +4.6 (*c* 1.0 MeOH)

UV λ_{max} (MeOH) (log ε) (nm): 231 (3.77), 295 (3.65)

IR (KBr) ν_{max} (cm^{-1}): 3335, 2928, 1735, 1509, 1417, 1363, 1206

ESIMS (negative mode): *m/z* 311.10 $[M-H]^-$

^1H NMR (500 MHz, $CDCl_3$:CD_3OD=1:3): see Table 5

^{13}C NMR (125 MHz, $CDCl_3$:CD_3OD=1:3): see Table 6

Compound **AJ5**

yellowish syrup

$C_{19}H_{18}O_3$

$[\alpha]_D^{25}$: -12.8 (*c* 0.3 MeOH)

UV λ_{max} (5% DMSO in MeOH) (log ε) (nm): 267 (3.78)

IR (KBr) ν_{max} (cm^{-1}): 3349, 2930, 1735, 1607, 1362, 1230, 1033

ESIMS (negative mode): *m/z* 293.15 $[M-H]^-$

^1H NMR (400 MHz, DMSO-d_6): see Table 5

^{13}C NMR (100 MHz, DMSO-d_6): see Table 6

Compound **AJ6**

yellowish syrup

$C_{19}H_{22}O_6$

$[\alpha]_D^{25}$: +1.8 (*c* 1.0 $CHCl_3$:MeOH=1:1)

UV λ_{max} (MeOH) (log ε) (nm): 300 (2.91)

IR (KBr) ν_{max} (cm^{-1}): 3373, 2927, 1596, 1245, 1098, 1024, 998

ESIMS (negative mode): *m/z* 345.12 $[M-H]^-$

^1H NMR (500 MHz, DMSO-d_6): see Table 5

^{13}C NMR (125 MHz, DMSO-d_6): see Table 6

Compound **AH1**

brownish syrup

$C_{19}H_{18}O_5$

$[\alpha]_D^{25}$: -7.6 (*c* 0.6 MeOH)

UV λ_{max} (MeOH) (log ε) (nm): 223 (4.60), 259 (4.30), 279 (4.33), 338 (4.30)

IR (KBr) ν_{max} (cm^{-1}): 3249, 2928, 1715, 1594, 1516, 1445, 1286, 984

ESIMS (negative mode): *m/z* 325.00 $[M-H]^-$

HRFABMS (negative mode): *m/z* 325.1078 $[M-H]^-$ (calcd. for $C_{19}H_{17}O_5$, 325.1076)

^1H NMR (400 MHz, DMSO-d_6): see Table 7

^{13}C NMR (100 MHz, DMSO-d_6): see Table 8

Compound **AH2**

yellowish syrup

$C_{19}H_{20}O_5$

$[\alpha]_D^{25}$: -13.7 (*c* 0.2 MeOH)

UV λ_{max} (MeOH) (log ε) (nm): 280 (3.63), 345 (3.50)

IR (KBr) ν_{max} (cm^{-1}): 3266, 2932, 1710, 1514, 1286, 1267, 1024

ESIMS (negative mode): *m/z* 327.03 $[M-H]^-$

HRFABMS (negative mode): *m/z* 327.1225 $[M-H]^-$ (calcd. for $C_{19}H_{19}O_5$, 327.1232)

^1H NMR (300 MHz, DMSO-d_6): see Table 7

^{13}C NMR (75 MHz, DMSO-d_6): see Table 8

Compound **AH3**

yellowish syrup

$C_{19}H_{18}O_5$

$[\alpha]_D^{25}$: +3.8 (*c* 1.0 MeOH)

UV λ_{max} (MeOH) (log ε) (nm): 274 (3.40), 365 (3.64)

IR (KBr) ν_{max} (cm^{-1}): 3294, 2928, 1716, 1597, 1515, 1450, 1364, 1277, 1231, 1108

ESIMS (negative mode): *m/z* 324.97 $[M-H]^-$

^1H NMR (300 MHz, CD_3OD): see Table 7

^{13}C NMR (75 MHz, CD_3OD): see Table 8

Compound **AH4**

yellowish syrup

$C_{19}H_{20}O_3$

$[\alpha]_D^{25}$: -15.9 (*c* 1.0 MeOH)

UV λ_{max} (5% DMSO in MeOH) (log ε) (nm): 278 (3.41)

IR (KBr) ν_{max} (cm^{-1}): 3414, 3013, 2934, 1715, 1660, 1516, 1437, 1405, 1364, 1018, 951,

ESIMS (negative mode): *m/z* 295.03 $[M-H]^-$

^1H NMR (400 MHz, CD_3OD): see Table 7

^{13}C NMR (100 MHz, CD_3OD): see Table 8

Compound **AH5**

yellowish syrup

$C_{19}H_{20}O_5$

$[\alpha]_D^{25}$: -6.9 (*c* 0.1 MeOH)

UV λ_{max} (MeOH) (log ε) (nm): 282 (3.55)

IR (KBr) ν_{max} (cm^{-1}): 3365, 2927, 1650, 1608, 1520, 1445, 1364, 1282, 1195, 954, 868

ESIMS (negative mode): *m/z* 327.06 $[M-H]^-$

^1H NMR (300 MHz, CD_3OD): see Table 7

^{13}C NMR (75 MHz, CD_3OD): see Table 8

Compound **AH6**

yellowish syrup

$C_{19}H_{22}O_4$

$[\alpha]_D^{25}$: -4.2 (*c* 1.0 MeOH)

UV λ_{max} (MeOH) (log ε) (nm): 278 (3.49)

IR (KBr) ν_{max} (cm^{-1}): 3348, 2927, 1650, 1608, 1520, 1445, 1364, 1282, 1195, 1112, 954, 868

ESIMS (negative mode): *m/z* 313.13 $[M-H]^-$

^1H NMR (500 MHz, C_5D_6N): see Table 9

^{13}C NMR (125 MHz, C_5D_6N) see Table 10

Compound **AJ9**

yellowish syrup

$C_{24}H_{30}O_8$

$[\alpha]_D^{25}$: -10.3 (*c* 0.5 MeOH)

UV λ_{max} (MeOH) (log ε) (nm): 229 (3.88), 278 (3.47)

IR (KBr) ν_{max} (cm^{-1}): 3329, 2926, 1708, 1610, 1517, 1445, 1268, 1024,

ESIMS (negative mode): *m/z* 444.85 $[M-H]^-$

^1H NMR (300 MHz, CD_3OD): see Table 9

^{13}C NMR (75 MHz, CD_3OD): see Table 10

Compound **AJ10**

brownish syrup

$C_{25}H_{32}O_9$

$[\alpha]_D^{25}$: -5.3 (*c* 1.0 MeOH)

UV λ_{max} (MeOH) (log ε) (nm): 225 (3.77), 278 (3.49)

IR (KBr) ν_{max} (cm^{-1}): 3347, 2926, 1707, 1613, 1515, 1449, 1265, 1045, 1024, 824, 762

ESIMS (negative mode): *m/z* 475.02 $[M-H]^-$

^1H NMR (500 MHz, CD_3OD): see Table 9

^{13}C NMR (125 MHz, CD_3OD): see Table 10

Compound **AF5**

brownish syrup

$C_{30}H_{40}O_{13}$

$[\alpha]_D^{25}$: -55.9 (*c* 0.1 MeOH)

UV λ_{max} (MeOH) (log ε) (nm): 279 (3.43)

IR (KBr) ν_{max} (cm^{-1}): 3377, 2927, 1704, 1613, 1516, 1449, 1368, 1263, 1059, 826

ESIMS (negative mode): *m/z* 607.07 $[M-H]^-$

^1H NMR (500 MHz, CD_3OD): see Table 9

^{13}C NMR (125 MHz, CD_3OD): see Table 10

Compound **AH9**

yellowish syrup

$C_{19}H_{22}O_5$

$[\alpha]_D^{25}$: -1.8 (*c* 1.0 MeOH)

UV λ_{max} (MeOH) (log ε) (nm): 281 (3.41)

IR (KBr) ν_{max} (cm^{-1}): 3345, 2926, 1710, 1615, 1512, 1367, 1024

ESIMS (negative mode): *m/z* 328.95 $[M-H]^-$

^1H NMR (300 MHz, C_5D_6N): see Table 11

^{13}C NMR (75 MHz, C_5D_6N): see Table 12

Compound **AJ11**

yellowish syrup

$C_{24}H_{30}O_9$

$[\alpha]_D^{25}$: -14.7 (*c* 1.0 MeOH)

UV λ_{max} (MeOH) (log ε) (nm): 225 (3.86), 281 (3.47)

IR (KBr) ν_{max} (cm^{-1}): 3347, 2926, 1706, 1612, 1515, 1446, 1369, 1024, 823

ESIMS (negative mode): *m/z* 461.10 $[M-H]^-$

^{1}H NMR (500 MHz, DMSO-d_6): see Table 11

^{13}C NMR (125 MHz, DMSO-d_6): see Table 12

Compound **AJ12**

brownish syrup

$C_{25}H_{32}O_{10}$

$[\alpha]_D^{25}$: -3.5 (*c* 1.0 MeOH)

UV λ_{max} (MeOH) (log ε) (nm): 281 (3.51)

IR (KBr) ν_{max} (cm^{-1}): 3373, 2927, 1715, 1293, 1152, 1045, 1024, 820

ESIMS (negative mode): *m/z* 491.02 $[M-H]^-$

HRFABMS (negative mode): *m/z* 491.1916 $[M-H]^-$ (calcd. for $C_{25}H_{31}O_{10}$, 491.1917)

^{1}H NMR (500 MHz, DMSO-d_6): see Table 11

^{13}C NMR (125 MHz, DMSO-d_6): see Table 12

Compound **AH11**

yellowish syrup

$C_{19}H_{22}O_6$

$[\alpha]_D^{25}$: -2.6 (*c* 1.0 MeOH)

UV λ_{max} (MeOH) (log ε) (nm): 280 (3.49)

IR (KBr) ν_{max} (cm^{-1}): 3339, 2924, 1710, 1517, 1372, 1290, 1024, 764

ESIMS (negative mode): *m/z* 344.99 $[M-H]^-$

^{1}H NMR (300 MHz, DMSO-d_6): see Table 13

^{13}C NMR (75 MHz, DMSO-d_6): see Table 14

Compound **AJ13**

yellowish syrup

$C_{24}H_{30}O_{10}$

$[\alpha]_D^{25}$: -21.1 (*c* 0.1 MeOH)

UV λ_{max} (MeOH) (log ε) (nm): 275 (3.60)

IR (KBr) ν_{max} (cm^{-1}): 3348, 2926, 1708, 1604, 1517, 1445, 1370, 1285, 1024, 823, 764

ESIMS (negative mode): *m/z* 477.02 $[M-H]^-$

^{1}H NMR (300 MHz, DMSO-d_6): see Table 13

^{13}C NMR (75 MHz, DMSO-d_6): see Table 14

Compound **AJ14**

brownish syrup

$C_{25}H_{32}O_{11}$

UV λ_{max} (MeOH) (log ε) (nm): 281 (3.60)

IR (KBr) ν_{max} (cm^{-1}): 3350, 2924, 1711, 1523, 1445, 1285, 1025, 823

ESIMS (negative mode): *m/z* 507.10 $[M-H]^-$

^{1}H NMR (300 MHz, CD_3OD): see Table 13

^{13}C NMR (75 MHz, CD_3OD): see Table 14

Compound **AJ15**

brownish syrup

$C_{20}H_{24}O_6$

$[\alpha]_D^{25}$: +2.1 (*c* 1.0 MeOH)

UV λ_{max} (MeOH) (log ε) (nm): 282 (3.43)

IR (KBr) ν_{max} (cm^{-1}): 3329, 2939, 1707, 1605, 1519, 1445, 1365, 1285, 1199, 1023, 986

FABMS (negative mode): *m/z* 359 $[M-H]^-$

^1H NMR (400 MHz, DMSO-d_6): see Table 13

^{13}C NMR (100 MHz, DMSO-d_6): see Table 14

Compound **AF7**

brownish syrup

$C_{20}H_{24}O_6$

$[\alpha]_D^{25}$: -11.8 (*c* 0.5 MeOH)

UV λ_{max} (MeOH) (log ε) (nm): 282 (3.48)

IR (KBr) ν_{max} (cm^{-1}): 3439, 2924, 2851, 1733, 1598, 1437, 1366, 1241, 1084

FABMS (negative mode): *m/z* 359 $[M-H]^-$

^1H NMR (400 MHz, DMSO-d_6): see Table 13

^{13}C NMR (100 MHz, DMSO-d_6): see Table 14

Compound **AJ16**

brownish syrup

$C_{33}H_{36}O_{11}$

$[\alpha]_D^{25}$: -2.6 (*c* 1.0 MeOH)

UV λ_{max} (MeOH) (log ε) (nm): 281 (3.59)

IR (KBr) ν_{max} (cm^{-1}): 3381, 2931, 1707, 1283, 1185, 1073, 1040

ESIMS (negative mode): *m/z* 607.08 $[M-H]^-$

^1H NMR (500 MHz, CD_3OD): see Table 15

^{13}C NMR (125 MHz, CD_3OD): see Table 16

Compound **AJ17**

brownish syrup

$C_{33}H_{36}O_{12}$

$[\alpha]_D^{25}$: -2.0 (*c* 1.0 MeOH)

UV λ_{max} (MeOH) (log ε) (nm): 289 (4.10), 316 (4.08)

IR (KBr) ν_{max} (cm^{-1}): 3370, 2939, 1708, 1603, 1515, 1448, 1368, 1283, 1170, 1044, 1024, 991

ESIMS (negative mode): *m/z* 623.10 $[M-H]^-$

^1H NMR (400 MHz, DMSO-d_6): see Table 15

^{13}C NMR (100 MHz, DMSO-d_6): see Table 16

Compound **AJ18**

brownish syrup

$C_{33}H_{38}O_{13}$

$[\alpha]_D^{25}$: -1.6 (*c* 1.0 MeOH)

UV λ_{max} (MeOH) (log ε) (nm): 290 (4.00), 313 (3.96)

IR (KBr) ν_{max} (cm^{-1}): 3268, 2959, 1712, 1606, 1515, 1447, 1353, 1284, 1202, 1043, 1023, 990

ESIMS (negative mode): *m/z* 653.08 $[M-H]^-$

^1H NMR (500 MHz, DMSO-d_6): see Table 15

^{13}C NMR (125 MHz, DMSO-d_6): see Table 16

Compound **AH14**

yellowish syrup

$C_{19}H_{24}O_3$

$[\alpha]_D^{25}$: -8.3 (*c* 1.0 MeOH)

IR (KBr) ν_{max} (cm^{-1}): 3394, 2939, 1611, 1512, 1236, 1048, 1024

FABMS (negative mode): *m/z* 299 $[M-H]^-$

^1H NMR (500 MHz, CD_3OD): see Table 17

^{13}C NMR (125 MHz, CD_3OD): see Table 18

Compound **AH15**

yellowish syrup

$C_{24}H_{30}O_8$

$[\alpha]_D^{25}$: -25.6 (*c* 1.0 MeOH)

FABMS (negative mode): *m/z* 461 $[M-H]^-$

^{1}H NMR (300 MHz, CD_3OD): see Table 17

^{13}C NMR (75 MHz, CD_3OD): see Table 18

Compound **AJ19**

yellowish syrup

$C_{25}H_{34}O_8$

$[\alpha]_D^{25}$: -37.6 (*c* 1.0 MeOH)

UV λ_{max} (MeOH) (log ε) (nm): 278 (3.56)

IR (KBr) ν_{max} (cm^{-1}): 3370, 2931, 1707, 1611, 1514, 1236, 1041, 1024, 827

ESIMS (negative mode): *m/z* 462.02 $[M-H]^-$

^{1}H NMR (300 MHz, CD_3OD): see Table 17

^{13}C NMR (75 MHz, CD_3OD): see Table 18

Compound **AH16**

dark brownish syrup

$C_{30}H_{42}O_{12}$

$[\alpha]_D^{25}$: -4.9 (*c* 1.0 MeOH)

IR (KBr) ν_{max} (cm^{-1}): 3348, 2931, 1613, 1516, 1454, 1237, 1047, 1024, 826, 765

ESIMS (negative mode): *m/z* 593.24 $[M-H]^-$

^{1}H NMR (500 MHz, DMSO-d_6): see Table 17

^{13}C NMR (125 MHz, DMSO-d_6): see Table 18

Compound **AH17**

yellowish syrup

$C_{19}H_{24}O_5$

$[\alpha]_D^{25}$: -10.3 (*c* 1.0 MeOH)

UV λ_{max} (MeOH) (log ε) (nm): 279 (3.50)

IR (KBr) ν_{max} (cm^{-1}): 3345, 2926, 1516, 1454, 1241, 1049, 1024, 826

ESIMS (negative mode): *m/z* 331.18 $[M-H]^-$

^1H NMR (300 MHz, CD_3OD): see Table 19

^{13}C NMR (75 MHz, CD_3OD): see Table 20

Compound **AF10**

dark brownish syrup

$C_{24}H_{32}O_9$

$[\alpha]_D^{25}$: -41.5 (*c* 0.1 MeOH)

UV λ_{max} (MeOH) (log ε) (nm): 280 (3.61)

IR (KBr) ν_{max} (cm^{-1}): 3334, 2931, 1604, 1365, 1284, 1024, 823, 764

ESIMS (negative mode): *m/z* 463.24 $[M-H]^-$

^1H NMR (500 MHz, CD_3OD): see Table 19

^{13}C NMR (125 MHz, CD_3OD): see Table 20

Compound **AF11**

dark brownish syrup

$C_{25}H_{33}O_{10}$

$[\alpha]_D^{25}$: -14.2 (*c* 0.1 MeOH)

UV λ_{max} (MeOH) (log ε) (nm): 2.77 (3.45)

IR (KBr) ν_{max} (cm^{-1}): 3348, 2932, 1605, 1519, 1445, 1366, 1285, 1078, 823

ESIMS (negative mode): *m/z* 493.24 $[M-H]^-$

^1H NMR (300 MHz, CD_3OD): see Table 19

^{13}C NMR (75 MHz, CD_3OD): see Table 20

Compound **AF12**

dark brownish syrup

$C_{30}H_{42}O_{14}$

$[\alpha]_D^{25}$: -23.6 (*c* 0.1 MeOH)

UV λ_{max} (MeOH) (log ε) (nm): 278 (3.56)

IR (KBr) ν_{max} (cm^{-1}): 3348, 2930, 1613, 1516, 1454, 1363, 1237, 1047, 824, 765

ESIMS (negative mode): *m/z* 625.24 $[M-H]^-$

^1H NMR (500 MHz, CD_3OD): see Table 19

^{13}C NMR (125 MHz, CD_3OD): see Table 20

Compound **AH21**

brownish syrup

$C_{19}H_{24}O_4$

$[\alpha]_D^{25}$: +7.4 (*c* 0.1 MeOH)

UV λ_{max} (MeOH) (log ε) (nm): 277 (3.49)

IR (KBr) ν_{max} (cm^{-1}): 3373, 2938, 1613, 1514, 1451, 1239, 990, 827

ESIMS (negative mode): *m/z* 315.06 $[M-H]^-$

^1H NMR (300 MHz, CD_3OD): δ 7.12 (4H, d, *J* = 8.6 Hz, H-2', 2", 6', 6"), 6.67 (4H, d, *J* = 8.6 Hz, H-3', 3", 5', 5"), 3.80 (2H, m, H-3, 5), 2.62 (2H, m, H-1a, 7a), 2.53 (2H, m H-1b, 7b), 1.70 (4H, m, H-2, 6), 1.59 (2H, t, *J* = 6.6 Hz, H-4)

^{13}C NMR (75 MHz, CD_3OD): δ 157.1 (C-4', 4"), 135.3 (C-1', 1"), 131.1 (C-2', 2", 6', 6"), 116.9 (C-3', 3", 5', 5"), 69.7 (C-3, 5), 46.4 (C-4), 42.1 (C-2, 6), 32.9 (C-1, 7)

Compound **AJ30**

whitish amorphous powder

$C_{14}H_6O_8$

$[\alpha]_D^{25}$: -1.1 (*c* 1.0 5% DMSO in MeOH)

UV λ_{max} (5% DMSO in MeOH) (log ε) (nm): 254 (4.80), 368 (4.20)

IR (KBr) ν_{max} (cm^{-1}): 3270, 1716, 1609, 1327, 1200, 1047, 1024, 988

ESIMS (negative mode): *m/z* 301.17 $[M-H]^-$

^1H NMR (300 MHz, DMSO-d_6): δ 7.50 (2H, s, H-5, 5')

Compound **AJ31**

whitish amorphous powder

$C_{15}H_8O_8$

$[\alpha]_D^{25}$: -2.0 (*c* 1.0 5% DMSO in MeOH)

UV λ_{max} (5% DMSO in MeOH) (log ε) (nm): 257 (4.41), 368 (4.14)

IR (KBr) ν_{max} (cm^{-1}): 3247, 1722, 1606, 1493, 1433, 1364, 1062, 981

ESIMS (negative mode): *m/z* 315.04 $[M-H]^-$

^1H NMR (400 MHz, DMSO-d_6): see Table 21

^{13}C NMR (100 MHz, DMSO-d_6): see Table 22

Compound **AJ32**

whitish amorphous powder

$C_{20}H_{16}O_{12}$

mp (°C): 275.0-278.5

$[\alpha]_D^{25}$: -2.9 (*c* 1.0 5% DMSO in MeOH)

UV λ_{max} (5% DMSO in MeOH) (log ε) (nm): 251 (4.59), 362 (4.32)

IR (KBr) ν_{max} (cm^{-1}): 3284, 1740, 1611, 1489, 1348, 1106, 1051, 981

ESIMS (negative mode): *m/z* 446.99 $[M-H]^-$

^1H NMR (500 MHz, DMSO-d_6): see Table 21

^{13}C NMR (125 MHz, DMSO-d_6): see Table 22

Compound **AJ33**

whitish amorphous powder

$C_{21}H_{18}O_{13}$

mp (°C): 268.0-270.5

$[\alpha]_D^{25}$: -5.8 (*c* 1.0 5% DMSO in MeOH)

UV λ_{max} (5% DMSO in MeOH) (log ε) (nm): 249 (4.37), 365 (4.24)

IR (KBr) ν_{max} (cm^{-1}): 3361, 1747, 1715, 1509, 1364, 1217, 1030

ESIMS (negative mode): *m/z* 477.00 $[M-H]^-$

^1H NMR (300 MHz, DMSO-d_6): see Table 21

^{13}C NMR (75 MHz, DMSO-d_6): see Table 22

Compound **AJ34**

whitish amorphous powder

$C_{15}H_8O_9$

$[\alpha]_D^{25}$: -3.5 (*c* 1.0 5% DMSO in MeOH)

UV λ_{max} (5% DMSO in MeOH) (log ε) (nm): 246 (4.62), 375 (4.19)

IR (KBr) ν_{max} (cm^{-1}): 3297, 2934, 1715, 1653, 1602, 1507, 1438, 1361, 1240, 1090, 1023, 821

ESIMS (negative mode): *m/z* 328.96 $[M-H]^-$

^1H NMR (300 MHz, DMSO-d_6): see Table 21

^{13}C NMR (75 MHz, DMSO-d_6): see Table 22

Compound **AJ35**

whitish amorphous powder

$C_{17}H_{12}O_8$

$[\alpha]_D^{25}$: -6.4 (*c* 1.0 5% DMSO in MeOH)

UV λ_{max} (5% DMSO in MeOH) (log ε) (nm): 251 (4.49), 365 (4.08)

IR (KBr) ν_{max} (cm^{-1}): 3394, 2933, 1719, 1457, 1375, 1208, 1163, 1025

FABMS (negative mode): *m/z* 343 $[M-H]^-$

^1H NMR (300 MHz, DMSO-d_6): see Table 21

^{13}C NMR (75 MHz, DMSO-d_6): see Table 22

Compound **AJ36**

whitish amorphous powder

$C_{22}H_{20}O_{12}$

$[\alpha]_D^{25}$: -12.2 (*c* 1.0 5% DMSO in MeOH)

UV λ_{max} (5% DMSO in MeOH) (log ε) (nm): 246 (4.67), 270 (4.71), 353 (4.41), 365 (4.44)

IR (KBr) ν_{max} (cm^{-1}): 3370, 2928, 1720, 1606, 1355, 1074, 1051

FABMS (negative mode): *m/z* 475 $[M-H]^-$

^1H NMR (600 MHz, DMSO-d_6): see Table 21

^{13}C NMR (150 MHz, DMSO-d_6): see Table 22

Compound **AJ37**

brownish syrup

$C_{20}H_{20}O_{13}$

$[\alpha]_D^{25}$: -2.1 (*c* 1.0 MeOH)

UV λ_{max} (MeOH) (log ε) (nm): 277 (3.45)

IR (KBr) ν_{max} (cm^{-1}): 3327, 2931, 1707, 1488, 1445, 1350, 1242, 1221, 1044, 1024

LRFABMS (negative mode): *m/z* 467.06 $[M-H]^-$

HRFABMS (negative mode): *m/z* 467.0828 $[M-H]^-$ (calcd. for $C_{20}H_{19}O_{13}$, 467.0826)

^1H NMR (500 MHz, DMSO-d_6): δ 7.69 (1H, d, *J*= 3.1 Hz, H-2'), 6.89 (1H, dd, *J* = 8.7, 3.1 Hz, H-6'), 6.61 (1H, d, *J* = 8.7 Hz, H-5'), 7.24 (2H, s, H-2", 6"), 4.73 (1H, d, *J* = 7.8, H-1), 3.24 (1H, m, H-2), 3.30 (1H, m, H-3), 3.10 (1H, m, H-4), 3.67 (1H, m, H-5), 4.75 (1H, d, *J* = 4.6 Hz, H-6a), 3.84 (1H, dd, *J* = 11.8, 4.6 Hz, H-6b)

^{13}C NMR (125 MHz, DMSO-d_6): δ 172.3 (C-7'), 166.1 (C-7"), 157.2 (C-4'), 148.9 (C-3'), 148.9 (C-3", 5"), 138.4 (C-4"), 121.9 (C-6'), 118.7 (C-1'), 118.6 (C-1"), 116.1 (C-5'), 115.5 (C-2'), 108.5 (C-2", 6"), 101.9 (C-1), 75.9 (C-3), 74.7 (C-5), 73.2 (C-2), 70.1 (C-4), 64.7 (C-6)

Compound **AJ38**

whitish amorphous powder

$C_{27}H_{24}O_{18}$

mp (°C): 206.5-209.0

$[\alpha]_D^{25}$: -22.2 (*c* 1.0 MeOH)

UV λ_{max} (MeOH) (log ε) (nm): 278 (3.50)

IR (KBr) ν_{max} (cm^{-1}): 3370, 1702, 1613, 1449, 1343, 1224, 1037, 766

ESIMS (negative mode): *m/z* 635.08 $[M-H]^-$

^1H NMR (500 MHz, DMSO-d_6): δ 6.97, 6.92, 6.88 (each 2H, s, galloyl H, H-2',2",2",6',6",6'"), 5.89 (1H, d, *J* = 8.4 Hz, H-1), 5.03 (1H, t, *J* = 9.3, 9.1 Hz, H-2), 4.44 (1H, br d, *J* = 12 Hz, H-6a), 4.31 (1H, t, *J* = 12, 4.6 Hz, H-6b), 3.81 (1H, m, H-5), 3.70 (1H, t, *J* = 9.3 Hz, H-3), 3.50

(1H, t, J = 9.1 Hz, H-4)

^{13}C NMR (125 MHz, DMSO-d_6): δ 165.7, 164.8, 164.1 (C-7', 7", 7'"), 145.53, 145.51, 145.39 (C-3', 3", 3'", 5', 5", 5'"), 139.2, 138.6, 138.5 (C-4', 4", 4'"), 119.2, 119.0, 117.7 (C-1', 1", 1'"), 108.9, 108.8, 108.6 (C-2', 2", 2'", 6', 6", 6'"), 92.1 (C-1), 74.8 (C-5), 73.6 (C-3), 72.7 (C-2), 69.6 (C-4), 62.9 (C-6)

Compound **AJ39**

whitish amorphous powder

$C_{30}H_{48}O_3$

mp (°C): 209.5-212.5

$[\alpha]_D^{25}$: +5.0 (*c* 1.0 $CHCl_3$:MeOH=1:1)

FABMS (negative mode): *m/z* 455 $[M-H]^-$

^{1}H NMR (600 MHz, C_5D_6N): see Table 23

^{13}C NMR (150 MHz, C_5D_6N): see Table 24

Compound **AJ40**

whitish amorphous powder

$C_{30}H_{52}O_3$

mp (°C): 200.5-202.5

$[\alpha]_D^{25}$: +24.4 (*c* 1.0 $CHCl_3$:MeOH=1:1)

FABMS (negative mode): *m/z* 459 $[M-H]^-$

^{1}H NMR (500 MHz, C_5D_6N): see Table 23

^{13}C NMR (125 MHz, Pyridine-d_5): see Table 24

Compound **AJ41**

whitish amorphous powder

$C_{30}H_{50}O_3$

mp (°C): 203.5-205.5

$[\alpha]_D^{25}$: +40.3 (*c* 1.0 $CHCl_3$:MeOH=1:1)

IR (KBr) ν_{max} (cm^{-1}): 3402, 2938, 1714, 1456, 1375, 1045

FABMS (negative mode): *m/z* 457 $[M-H]^-$

HRFABMS (negative mode): *m/z* 457.0828 $[M-H]^-$ (calcd. for $C_{30}H_{49}O_3$, 457.0826)

^{1}H NMR (500 MHz, C_5D_6N): see Table 23

^{13}C NMR (125 MHz, C_5D_6N): see Table 24

Compound **AJ42**

whitish amorphous powder

$C_{30}H_{52}O_3$

mp (°C): 195.5-197.0

$[\alpha]_D^{25}$: +51.0 (*c* 1.0 $CHCl_3$:MeOH=1:1)

FABMS (negative mode): *m/z* 459 $[M-H]^-$

^{1}H NMR (500 MHz, C_5D_6N): see Table 23

^{13}C NMR (125 MHz, C_5D_6N): see Table 24

Compound **AJ43**

whitish amorphous powder

$C_{29}H_{50}O$

FABMS (positive mode): *m/z* 414 $[M]^+$

^{13}C NMR (75 MHz, C_5D_6N): δ 141.7 (C-5), 120.4 (C-6), 70.9 (C-3), 56.5 (C-14), 56.1 (C-17), 49.8 (C-9), 44.5 (C-24), 41.3 (C-13), 42.2 (C-4), 39.4 (C-12), 37.1 (C-1), 36.0 (C-20), 35.9 (C-10), 33.8 (C-22), 31.7 (C-7), 31.6 (C-2), 29.2 (C-25), 28.0 (C-16), 26.0 (C-23), 24.1 (C-15), 23.4 (C-28), 20.8 (C-11), 19.7 (C-26), 19.0 (C-19), 18.8 (C-27), 18.7 (C-21), 12.5 (C-18), 10.9 (C-29)

Compound **AJ44**

whitish amorphous powder

$C_{35}H_{60}O_6$

ESIMS (positive mode): *m/z* 576 $[M]^+$

^{13}C NMR (75 MHz, C_5D_6N): δ 140.9 (C-5), 121.9 (C-6), 102.6 (C-1'), 78.6 (C-5'), 78.5 (C-3'), 78.1 (C-3), 75.3 (C-2'), 71.7 (C-4'), 62.8 (C-6'), 56.8 (C-14), 56.2 (C-17), 50.3 (C-9), 46.0 (C-24), 42.5 (C-13), 39.9 (C-12), 39.3 (C-4), 37.5 (C-10), 36.9 (C-1), 36.4 (C-20), 34.2 (C-22), 32.2 (C-7), 32.0 (C-8), 30.3 (C-2), 29.4 (C-25), 28.6 (C-16), 26.4 (C-23), 24.5 (C-15), 23.4 (C-28), 21.3 (C-11), 20.0 (C-26), 19.4 (C-19), 19.2 (C-21), 19.0 (C-27), 12.2 (C-29), 12.0 (C-18)

Compound **AF13**

Pale brownish syrup

$C_{23}H_{28}O_{13}$

$[\alpha]_D^{20}$: -28.0 (*c* 0.5 MeOH)

UV λ_{max} (MeOH) (log ε) (nm): 273 (3.42), 229 (3.54)

IR (KBr) ν_{max} (cm^{-1}): 3376, 2922, 1684, 1610, 1514, 1458, 1337, 1217, 1123, 1065

FABMS (negative mode): *m/z* 511 $[M-H]^-$

^1H NMR (500 MHz, CD_3OD): see Table 25

^{13}C NMR (500 MHz, CD_3OD): see Table 26

Compound **AF14**

Pale brownish syrup

$C_{22}H_{26}O_{12}$

$[\alpha]_D^{20}$: -40.7 (*c* 0.6 MeOH)

UV λ_{max} (MeOH) (log ε) (nm): 236 (3.55)

IR (KBr) ν_{max} (cm^{-1}): 3436, 2904, 1716, 1685, 1602, 1513, 1457, 1288, 1218, 1130, 1062

FABMS (negative mode): *m/z* 481 $[M-H]^-$

^1H NMR (500 MHz, CD_3OD): see Table 25

^{13}C NMR (500 MHz, CD_3OD): see Table 26

Compound **AF15**

Pale brownish syrup

$C_{22}H_{26}O_{12}$

$[\alpha]_D^{20}$: -35.0 (*c* 1.0 MeOH)

IR (KBr) ν_{max} (cm^{-1}): 3398, 1704, 1609, 1514, 1460, 1335, 1282, 1217, 1116, 1072, 765

UV λ_{max} (MeOH) (log ε) (nm): 272 (3.47), 230 (3.59)

ESIMS (negative mode): *m/z* 481.07 $[M-H]^-$

^1H NMR (500 MHz, CD_3OD): see Table 25

^{13}C NMR (500 MHz, CD_3OD): see Table 26

Compound **AF16**

Pale brownish syrup

$C_{21}H_{24}O_{11}$

$[\alpha]_D^{20}$: -19.0 (*c* 0.5 MeOH)

IR (KBr) ν_{max} (cm^{-1}): 3398, 2923, 1698, 1604, 1514, 1455, 1430, 1286, 1218, 1031, 764

UV λ_{max} (MeOH) (log ε) (nm): 273 (3.46)

ESIMS (negative mode): *m/z* 451.08 $[M-H]^-$

^1H NMR (500 MHz, CD_3OD): see Table 25

^{13}C NMR (500 MHz, CD_3OD): see Table 26

Compound **AF17**

whitish amorphous powder

$C_{30}H_{48}O_3$

mp (°C): 225.5-227.8

$[\alpha]_D^{20}$: +3.3 (*c* 1.0 $CHCl_3$:MeOH 1:1)

IR (KBr) ν_{max} (cm^{-1}): 3443, 2940, 1638, 1107, 1033

FABMS (negative mode): *m/z* 455 $[M-H]^-$

^{13}C NMR (150 MHz, C_5D_6N): δ 178.9 (C-28), 151.3 (C-20), 109.9 (C-29), 78.1 (C-3), 56.6 (C-17), 55.9 (C-5), 50.8 (C-9), 49.8 (C-18), 48.9 (C-19), 42.9 (C-14), 41.1 (C-8), 39.5 (C-4), 39.3 (C-13), 37.6 (C-1), 37.5 (C-10), 37.4 (C-22), 34.9 (C-7), 32.9 (C-16), 30.3 (C-15), 30.0 (C-21), 28.7 (C-2), 28.7 (C-23), 28.3 (C-12), 26.1 (C-11), 21.2 (C-30), 19.5 (C-6), 18.8 (C-25), 16.4 (C-26), 16.3 (C-24), 14.9 (C-27)

Compound **AF18**

whitish amorphous powder

$C_{39}H_{54}O_7$

mp (°C): 200.0-202.5

$[\alpha]_D^{25}$: +3.2 (*c* 1.0 $CHCl_3$:MeOH=1:1)

UV λ_{max} ($CHCl_3$:MeOH=1:1) (log ε) (nm): 245 (3.08), 328 (2.97)

ESIMS (negative mode): *m/z* 633.28 $[M-H]^-$

^1H NMR (500 MHz, C_5D_6N): see Table 27

^{13}C NMR (125 MHz, C_5D_6N): see Table 27

Compound **AF19**

whitish amorphous powder

$C_{39}H_{56}O_6$

mp (°C): 199.5-200.9

$[\alpha]_D^{20}$: +5 (*c* 0.75 $CHCl_3$:MeOH=1:1)

UV λ_{max} ($CHCl_3$:CH_3OH=1:1) (log ε) (nm): 291 (3.89), 326 (3.88)

IR (KBr) ν_{max} (cm^{-1}): 3364, 2941, 1685, 1604, 1516, 1454, 1374, 1269, 1177, 1022

FABMS (negative mode): *m/z* 619 $[M-H]^-$

HRFABMS (negative mode): *m/z* 619.3997 $[M-H]^-$ (calcd. for $C_{22}H_{26}O_{12}$, 619.3999)

^1H NMR (600 MHz, C_5D_6N): see Table 27

^{13}C NMR (150 MHz, C_5D_6N): see Table 27

Table 5. ^{1}H NMR data of compounds **AJ1-6**

	AJ [a]	**AJ2** [b]	**AJ3** [c]	**AJ4** [d]	**AJ5** [e]	**AJ6** [d]
position			δ_H (*J* in Hz)			
1	6.10, d (11.4)	3.36, t (13.2) 2.77, m	2.86, m	2.98, m	2.83, m	2.79, m
2	5.91, dd (11.4, 9.2)	2.46, t (13.2) 2.69, m	2.71, m	3.12, 2.83, m	3.02, m	4.15, m
3	5.64, m					3.86, m
4	5.63, m	5.88, s	2.83, m	3.00, 2.73, m	6.63, d (15.6)	2.02, m
5	4.09, m		1.83, m	3.61, m	6.93, dt, (15.6, 7.6)	3.86, m
6	2.07, 1.66, m	2.46, t (13.2) 2.69, m	1.63, m	2.36, 1.81, m	2.67, m	4.15, m
7	3.01, dt (13, 3.5) 2.68, td (13, 3.5)	3.36, t (13.2) 2.77, m	2.67, m	2.83, m	2.76, m	2.79, m
2'	5.49, d (1.9)	7.13, d (2.0)	6.58, d (2.2)	6.59, d (1.9)	6.68, br s	6.72, br s
5'		6.83, d (8.1)	6.78, d (8.2)	6.78, d (8.2)	7.00, d (8.0)	6.70, d (8.2)
6'	6.36, d (1.9)	6.98, dd (8.1, 2.0)	7.02, dd (8.2, 2.2)	7.02, d (8.2)	6.79, d (8.0)	6.91, d (8.2)
2"	7.32, dd (8.2, 2.1)	7.13, d (2.0)	6.81, d (2.2)	6.78, d (1.9)	6.76, br s	6.72, br s
3"	7.14, dd (8.2, 2.5)					
5"	7.25, dd (8.2, 2.1)	6.83, d (8.1)	6.78, d (8.2)	6.79, d (8.2)	7.00, d (8.0)	6.70, d (8.2)
6"	6.98, dd (8.2, 2.5)	6.98, dd (8.1, 2.0)	6.98, dd (8.2, 2.2)	7.02, d (8.2)	6.72, d (8.0)	6.91, d (8.2)
-OCH_3	4.11, s					

^{1}H NMR data were measured at [a] 500 ($CDCl_3$), [b] 400 ($CDCl_3$), [c] 500 (DMSO-d_6), [d] 500 ($CDCl_3$:CD_3OD=1:3), [e] 400 (DMSO-d_6) MHz, respectively.

Table 6. ^{13}C NMR data of compounds **AJ1-6**

position	**AJ1**[a]	**AJ2**[b]	**AJ3**[c]	**AJ4**[d]	**AJ5**[e]	**AJ6**[d]
1	129.4	28.3	27.4	28.2	29.4	28.9
2	127.8	38.1	44.1	43.7	42.6	69.3
3	126.3	193.7	212.9	213	203.3	65.8
4	138.7	107	41.4	54.8	128.9	41.4
5	73.3	193.7	25.4	68	144.3	65.8
6	40.9	38.1	21.6	36.2	35.3	69.3
7	33.9	28.3	30.8	31.2	35.1	28.9
1'	132.3	132.3	131.5	132.9	131.9	127.8
2'	110.5	133.7	133.2	135.1	128.9	133.4
3'	153.3	126.2	125.7	126.7	128.1	126.4
4'	134.7	151.2	151.3	152.9	153.3	153.2
5'	149.3	116.3	115.8	117.6	116.3	116.1
6'	108.8	128.6	128.3	130.1	130.9	128.7
1''	139.8	132.3	130.8	132.7	131.9	127.8
2''	131.9	133.7	133.2	135.1	128.9	133.4
3''	125.3	126.2	126	126.7	128.1	126.4
4''	154.8	151.2	151.3	152.7	153.3	153.2
5''	122.1	116.3	116	117.6	116.1	116.1
6''	129.8	128.6	129.2	131.2	130.8	128.7
OCH_3	61.4					

^{13}C NMR data were measured at [a] 125 ($CDCl_3$), [b] 100 ($CDCl_3$), [c] 125 (DMSO-d_6), [d] 125 ($CDCl_3$:CD_3OD=1:3), [e] 100 (DMSO- d_6) MHz, respectively.

Table 7. ^{1}H NMR data of compounds **AH1-5**

	AH1[a]	**AH2**[b]	**AH3**[c]	**AH4**[d]	**AH5**[c]
position			δ_H (*J* in Hz)		
1	7.46, d (15.9)	7.50, d (16.0)	2.77, t (7.0)	2.77, m	2.79, t (7.0)
2	6.85, d (15.9)	6.60, d (16.0)	2.85, t (7.0)	2.77, m	2.69, t (7.0)
4	6.51, d (15.7)	2.86, 2.67, m	6.23, d (15.3)	6.04, d (15.9)	6.05, d (15.9)
5	6.94, dt (15.7, 8.4)	4.06, m	7.37, dd (15.3 10.4)	6.86, dt (15.9, 7.0)	6.86, dt (15.9, 7.5)
6	2.62, m	1.75, m	6.76, dd (15.3, 10.4)	2.65, t (7.8)	2.45, m
7	2.46, m	2.55, m	6.89, d (15.3)	2.46, m	2.60, t (7.6)
2'	7.10, d (1.4)	7.07, d (2.0)	6.63, d (2.2)	6.97, d (8.3)	6.60, d (2.0)
3'				6.67, d (8.4)	
5'	6.77, d (8.2)	6.78, d (8.4)	6.65, d (8.0)	6.67, d (8.4)	6.49, d (8.0)
6'	7.04, dd (8.2, 1.4)	6.98, dd (8.4, 2.0)	6.52, dd (8.0, 2.2)	6.97, d (8.3)	6.46, dd (8.0, 2.0)
2"	6.60, d (1.9)	7.01, d (8.6)	6.98, d (2.0)	6.98, d (8.3)	6.60, d (2.0)
3"		6.68, d (8.6)		6.68, d (8.3)	
5"	6.63, d (7.9)	6.68, d (8.6)	6.73, d (8.2)	6.68, d (8.3)	6.49, d (8.0)
6"	6.46, dd (7.9, 1.9)	7.01, d (8.6)	6.87, dd (8.2, 2.0)	6.98, d (8.3)	6.46, dd (8.0, 2.0)

^{1}H NMR data were measured at [a] 400 (DMSO-d_6), [b] 300 (DMSO-d_6), [c] 300 (CD_3OD), [d] 400 (CD_3OD) MHz, respectively

Table 8. ^{13}C NMR data of compounds **AH1-5**

position	**AH1**[a]	**AH2**[b]	**AH3**[c]	**AH4**[d]	**AH5**[c]
1	143.3	145.5	30.3	31.5	43.5
2	121.8	125.5	42.7	43.5	36.5
3	188.1	202.4	199.5	203.6	203.7
4	129.3	47.7	129.1	132.4	132.4
5	146.4	69.7	143.89	150.0	150.1
6	33.2	40.5	125.0	35.4	31.7
7	34.0	33.8	142.3	36.5	35.6
1'	126.0	128.8	134.0	133.8	134.6
2'	114.9	116.3	116.2	131.1	117.1
3'	145.6	147.2	145.6	117.0	146.9
4'	148.5	146.9	143.9	157.4	145.2
5'	115.7	117.5	115.9	117.0	117.1
6'	121.7	124.5	120.3	131.1	121.4
1"	131.8	135.0	129.5	134.0	134.8
2"	115.7	131.2	114.3	131.2	117.3
3"	143.3	117.0	146.1	117.0	147.0
4"	145.0	157.4	147.5	157.5	145.3
5"	115.4	117.0	116.3	117.0	117.3
6"	118.8	131.2	121.3	131.2	121.5

^{13}C NMR data were measured at [a] 100 (DMSO-d_6), [b] 75 (DMSO-d_6), [c] 75 (CD_3OD), [d] 100 (CD_3OD) MHz, respectively

Table 9. ^{1}H NMR data of compounds **AH6**, **AJ9**, **AJ12**, and **AF5**

	AH6[a]	**AJ9**[b]	**AJ10**[c]	**AF5**[c]
position		δ_H (*J* in Hz)		
aglycone				
1	2.86, m	2.73, m	2.63, m	2.72, m
2	2.84, m	2.73, m	2.69, m	2.73, m
4	2.82, m	2.80, dd (16.7, 6.8)	2.74, m	2.80, dd (16.6, 6.8)
	2.64, dd (15.2. 3.7)	2.55, dd (16.7, 5.5)	2.56, m	2.55, dd (16.6, 5.5)
5	4.45, m	4.11, m	4.04, m	3.90, m
6	1.94, m	1.72, m	1.65, m	1.75, m
7	2.74, m	2.56, m	2.52, m	2.62, m
2',2"	7.19, d (8.4)	6.97, d (8.6)	6.98, d (8.4)	6.97, d (8.6)
3',3"	7.10, d (8.4)	6.67, d (8.6)	6.67, d (8.4)	6.67, d (8.6)
5',5"	7.10, d (8.4)	6.67, d (8.6)	6.67, d (8.4)	6.67, d (8.6)
6',6"	7.19, d (8.4)	6.97, d (8.6)	6.98, d (8.4)	6.97, d (8.6)
		***β*-D-xylose**	***β*-D-glucose**	***β*-D-glucose**
1"'		4.20, d (7.5)	4.15, d (7.7)	4.26, d (7.8)
2"'		3.08-3.25, m	2.91, m	3.14, m
3"'		3.08-3.25, m	3.00-3.20, m	3.31, m
4"'		3.08-3.25, m	3.00-3.20, m	3.29, m
5"'		3.83, dd (11.3, 5.3)	3.00-3.20, m	3.33, m
		3.11, m		
6"'			3.69, 3.47, m	3.62, dd (10.9, 4.8), 3.48, m
				***β*-D-apiose**
1""				5.00, d, (2.3)
2""				4.14, m
4""				3.92, d, (9.7)
5""				3.54, s

^{1}H NMR data were measured at [a] 500 (C_5D_6N), [b] 300 (CD_3OD) and [c] 500 (CD_3OD) MHz, respectively.

Table 10. ^{13}C NMR data of compounds **AH6**, **AJ9**, **AJ12**, and **AF5**

position	**AH6**	**AJ9**	**AJ10**	**AF5**
1	29.0	30.5	30.6	30.6
2	45.7	47.3	47.2	47.3
3	209.5	212.8	212.7	212.7
4	51.1	49.2	49.5	49.2
5	67.1	76.9	77.0	78.9
6	40.4	39.0	39.3	39.5
7	31.9	32.1	32.2	32.3
1'	132.9	134.0	134.0	134.1
2'	129.7	131.1	131.1	131.3
3'	116.1	116.8	116.8	116.9
4'	156.8	157.1	157.0	157.1
5'	116.1	116.8	116.8	117.0
6'	129.7	131.1	131.1	131.3
1"	133.0	135.1	135.1	135.2
2"	129.8	131.2	131.2	131.3
3"	116.1	117.0	117.0	116.9
4"	156.9	157.3	157.3	157.4
5"	116.1	117.0	117.0	117.0
6"	129.8	131.2	131.2	131.3
		***β*-D-xylose**	***β*-D-glucose**	***β*-D-glucose**
1'''		102.6	104.2	104.4
2'''		73.4	76.0	76.1
3'''		76.7	78.8	78.9
4'''		69.6	72.4	72.4
5'''		65.8	78.6	77.6
6''''			63.5	69.3
				***β*-D-apiose**
1''''				111.7
2''''				77.2
3''''				81.3
4''''				75.9
5''''				66.6

^{13}C NMR data were measured at [a] 100 (C_5D_6N), [b] 75 (CD_3OD) and [c] 125 (CD_3OD) MHz, respectively.

Table 11. ^{1}H NMR data of compounds **AH9**, **AJ11**, and **AJ12**

	AH9[a]	**AJ11**[b]	**AJ12**[b]
position		δ_H (*J* in Hz)	
aglycone			
1	2.63, m	2.64, m	2.63, m
2	2.69, m	2.70, m	2.69, m
4	2.73, m	2.74, m	2.74, m
	2.57, m	2.55, dd (16.4, 5.8)	2.56, m
5	4.03, m	3.99, m	4.04, m
6	1.65, m	1.63, m	1.65, m
7	2.47, m	2.42, m	2.52, m
2'	6.98,d (8.4)	6.96,d (8.4)	6.98, d (8.4)
3'	6.66,d (8.4)	6.64,d (8.4)	6.63, d (8.4)
5'	6.66,d (8.4)	6.64,d (8.4)	6.63, d (8.4)
6'	6.98,d (8.4)	6.96,d (8.4)	6.98, d (8.4)
2"	6.53, (2.0)	6.54, (1.9)	6.54, br s
5"	6.59, d (8.0)	6.60, d (8.0)	6.59, d (8.0)
6"	6.35, dd (8.0, 2.0)	6.39, dd (8.0, 1.9)	6.40, br d (8.0)
		***β*-D-xylose**	***β*-D-glucose**
1'"		4.12, d (7.5)	4.15, d (7.7)
2'"		2.91, m	2.91, m
3'"		3.08, m	3.00-3.20, m
4'"		3.27, m	3.00-3.20, m
5'"		3.70, dd (11.3, 5.3), 3.02, t (11.3)	3.00-3.20, m
6'"			3.69, 3.47, m

^{1}H NMR data were measured at [a] 300 and [b] 500 MHz in DMSO-d_6, respectively.

Table 12. ^{13}C NMR data of compounds **AH9**, **AJ11**, and **AJ12**

position	**AH9**	**AJ11**	**AJ12**
1	28.4	28.2	28.2
2	44.9	44.8	44.7
3	209.5	208.9	208.9
4	51.1	47.2	48.6
5	67.2	74.3	76.7
6	40.3	37.1	37.4
7	31.8	30.2	30.4
1'	131.1	131.2	132.0
2'	129.0	129.1	129.1
3'	115.2	115.0	114.9
4'	155.0	155.4	154.9
5'	115.2	115.0	114.9
6'	129.0	129.1	129.1
1"	131.9	132.9	133.6
2"	115.4	115.7	115.5
3"	145.1	144.9	144.9
4"	143.4	143.1	143.3
5"	115.4	115.4	115.4
6"	118.9	118.8	118.7
		***β*-D-xylose**	***β*-D-glucose**
1"'		102.6	101.9
2"'		73.4	73.5
3"'		76.7	76.8
4"'		69.6	70.1
5"'		65.8	74.2
6""			61.0

^{13}C NMR data were measured at [a] 75 MHz in DMSO-d_6, respectively.

Table 13. ^{1}H NMR data of compounds **AH11**, **AJ13-15**, and **AF7**

	AH11[a]	**AJ13**[a]	**AJ14**[b]	**AJ15**[b]	**AF7**[b]
position			δ_H (*J* in Hz)		
1	2.53, m	2.68, m	2.44	2.58, m	2.54, m
2	2.55, m	2.69, m	2.46m	2.61, m	2.58, m
4	2.74, m	2.81, m	2.95	2.67, m	2.65, m
	2.58, m	2.57, m	2.60m	2.41, m	2.44, m
5	4.00, m	4.08, m	4.10, m	3.57, m	3.56, m
6	1.62, m	1.75, m	1.64, m	1.62, m	1.60, m
7	2.42, m	2.44, m	2.41, m	2.39, m	2.37, m
2'	6.60, d (2.2)	6.60, d (2.0)	6.53, d (2.0)	6.55, d (2.0)	6.55, d (2.0)
5'	6.63, d (8.0)	6.64, d (7.9)	6.59, d (8.0)	6.60, d (8.0)	6.60, d (7.8)
6'	6.47, dd	6.46, dd	6.39, dd	6.42, dd	6.40, dd
	(8.0, 2.2)	(7.9, 2.0)	(8.0, 2.0)	(8.0, 2.0)	(7.8, 2.0)
2''	6.60, d (2.2)	6.60, d (2.0)	6.53, d (2.0)	6.56, d (2.0)	6.55, d (2.0)
5''	6.66, d (8.0)	6.64, d (7.9)	6.58, d (8.0)	6.61, d (8.0)	6.60, d (7.8)
6''	6.47, dd	6.46, dd	6.39, dd	6.43,dd	6.40, dd
	(8.0, 2.2)	(7.9, 2.0)	(8.0, 2.0)	(8.0, 2.0)	(7.8, 2.0)
OCH_3				3.21, s	3.17, s
		***β*-D-xylose**	***β*-D-glucose**		
1'''		4.21, d (7.7)	4.96(7.7)		
2'''		3.14, m	3.38-3.85, m		
3'''		3.28, m	3.38-3.85, m		
4'''		3.49, m	3.38-3.85, m		
5'''		3.18, m	3.38-3.85, m		
6'''			4.50, 4.28, m		

^{1}H NMR data were measured at [a] 300 (DMSO-d_6) and [b] 400 (CD_3OD) MHz, respectively.

Table 14. ^{13}C NMR data of compounds **AH11**, **AJ13-15**, and **AF7**

position	**AH11**[a]	**AJ13**[a]	**AJ14**[b]	**AJ15**[b]	**AF7**[b]
1	28.4	28.5	28.3	28.4	28.4
2	44.7	44.9	44.8	44.6	44.6
3	209.6	209.1	208.9	209.9	208.7
4	49.2	47.3	48.6	46.7	46.6
5	67.2	74.4	76.7	76.2	75.8
6	40.1	37.3	38.7	35.3	35.5
7	31.8	30.4	32.8	29.9	30.1
1'	131.1	132.1	131.9	132.3	131.9
2'	115.4	115.8	115.6	114.6	115.6
3'	145.1	145.1	144.8	144.5	145.0
4'	143.4	143.2	142.9	142.6	143.3
5'	115.4	115.6	115.4	114.8	115.7
6'	118.9	118.9	118.7	118.9	118.8
1''	131.9	133.0	132.9	133.1	132.7
2''	115.4	117.2	115.7	114.6	115.6
3''	145.1	145.1	144.9	144.5	145.0
4''	143.4	143.3	143.1	142.8	143.3
5''	115.4	117.2	115.6	114.8	115.7
6''	118.9	118.9	118.9	118.9	118.8
OCH_3				55.4	55.9
		***β*-D-xylose**	***β*-D-glucose**		
1'''		102.7	101.7		
2'''		73.5	73.5		
3'''		76.8	77.8		
4'''		69.7	70.1		
5'''		65.9	73.7		
6''''			61.2		

^{13}C NMR data were measured at [a] 75 (DMSO-d_6) and [b] 100 (CD_3OD) MHz, respectively.

Table 15. ^{1}H NMR data of compounds **AJ16-18**

	AJ16[a]	**AJ17**[b]	**AJ18**[c]
position		δ_H (*J* in Hz)	
1	2.55, m	2.46, m	2.47, m
2	2.52, m	2.56, m	2.53, m
4	2.63, dd (16.9, 7.8),	2.63, m,	2.63, m,
	2.42, dd (16.9, 4.1)	2.40, m	2.41, m
5	4.07, m	4.00, m	4.00, m
6	1.73, m	1.62, m	1.63, m
7	2.47, t (8.0, 7.4)	2.37, m	2.40, m
2'	6.60, d (1.9)	6.49, br s	6.49, br s
5'	6.63, d (8.0)	6.55, d (7.8)	6.53, d (7.9)
6'	6.45, dd (8.0, 1.9)	6.37, dd (7.8, 1.8)	6.37, dd (7.9, 1.6)
2''	6.50, d (2.0)	6.53, br s	6.53, br s
5''	6.57, d (8.0)	6.58, d (7.8)	6.59, d (7.9)
6''	6.29, dd (8.0, 2.0)	6.26, dd (7.8, 1.8)	6.24, dd (7.9, 1.6)
		***β*-D-xylose**	
1'''	4.48, d (7.9)	4.5, d (7.9)	4.5, d (7.9)
2'''	4.75, dd (9.2, 7.7)	4.58, td (6.5, 3.8)	4.59, t (8.8, 8.4)
3'''	3.52, t (9.2)	3.35, m	3.13-3.39, m
4'''	3.58, m	3.39, m	3.13-3.39, m
5'''	3.92, dd (11.5, 5.3), 3.23, t (11.5)	3.78, 3.13, m	3.13-3.39, m
		Acyl moiety	
2''''	7.52, m	7.47, d (8.6)	7.26, br s
3''''	7.35, m	6.77,d (8.6)	
4''''	7.36, m		
5''''	7.35, m	6.77,d (8.6)	7.07, d (8.1)
6''''	7.52, m	7.47, d (8.6)	6.77, dd (8.1, 2.0)
7''''	7.68, d (16.0)	7.54, d (15.9)	7.54, d (15.9)
8''''	6.58, d (16.0)	6.39, d (15.9)	6.37, d (15.9)
-OCH_3			3.77, s

^{1}H NMR data were measured at [a] 500 (CD_3OD), [b] 400 (DMSO-d_6) and [c] 500 (DMSO-d_6) MHz, respectively.

Table 16. ^{13}C NMR data of compounds **AJ16-18**

position	**AJ16**[a]	**AJ17**[b]	**AJ18**[c]
1	30.9	28.2	28.2
2	47.1	44.5	44.6
3	211.7	207.7	207.8
4	60.6	47.0	47.0
5	77.9	73.6	73.6
6	39.3	36.7	36.8
7	32.4	29.9	30.0
1'	134.6	131.7	131.8
2'	117.4	115.5	115.6
3'	146.9	144.9	144.9
4'	145.2	143.2	143.2
5'	117.3	115.4	115.4
6'	121.5	118.7	118.7
1"	135.9	132.6	132.7
2"	117.2	115.4	115.6
3"	146.9	144.9	144.9
4"	145.0	143.0	143.0
5"	117.1	115.4	115.4
6"	121.3	118.5	118.6
		***β*-D-xylose**	
1"'	103.9	100.7	100.7
2"'	76.3	74.4	74.4
3"'	77.0	74.8	74.8
4"'	72.2	69.7	69.7
5"'	67.8	65.7	65.7

		Acyl moiety	
1""	136.4	125.6	125.6
2""	130.1	130.1	111.1
3""	130.9	115.7	149.2
4""	132.4	159.7	145.6
5""	130.9	115.54	115.6
6""	130.1	128.9	122.9
7""	147.5	147.8	147.9
8""	119.8	114.9	114.7
9""	168.6	165.5	165.6
-OCH_3			55.6

^{13}C NMR data were measured at [a] 125 (CD_3OD), [b] 100 (DMSO-d_6) and [c] 125 (DMSO-d_6) MHz, respectively.

Table 17. ^1H NMR data of compounds **AH14**, **AH15**, **AJ19**, and **AH16**

	AH14[a]	**AH15**[b]	**AJ19**[b]	**AH16**[c]
position		δ_H (*J* in Hz)		
1	2.57, m	2.47 m	2.44, m	2.50, m
2	1.63, m	1.63 m	1.64, m	1.65, m
3	3.49, m	3.15-3.38, m	3.15-3.38, m	3.55, m
4	1.46, m	1.47, m	1.47, m	1.48, m
5	1.32, m	1.34 m	1.35, m	1.32, m
6	1.45, m	1.45, m	1.45, m	1.45, m
7	2.35, m	2.36 m	2.37, m	2.42, t (7.5)
2'	6.98, d (8.5)	6.92, d (8.6)	6.96, d (8.7)	6.95, d (8.6)
3'	6.66, d (8.4)	6.65, d (8.6)	6.67, d (8.4)	6.64, d (8.6)
5'	6.66, d (8.4)	6.65, d (8.6)	6.67, d (8.4)	6.64, d (8.6)
6'	6.98, d (8.5)	6.92, (8.6)	6.96, d (8.7)	6.95, (8.6)

2"	6.96, d (8.5)	6.99, d (8.6)	7.01, d (8.1)	6.97, d (8.6)
3"	6.68, d (8.4)	6.65, d(8.6)	6.67, d (8.4)	6.65, d(8.6)
5"	6.68, d (8.4)	6.65, d(8.6)	6.67, d (8.4)	6.65, d(8.6)
6"	6.96, d (8.5)	6.99, d (8.6)	7.01, d (8.1)	6.97, d (8.6)
		β-D-xylose	**β-D-glucose**	**β-D-glucose**
1‴		4.20, d (7.5)	4.29, d (7.8)	4.14, d (7.6)
2‴		3.08-3.25, m	3.15-3.38, m	3.05, m
3‴		3.08-3.25, m	3.67-3.73, m	3.14, m
4‴		3.08-3.25, m	3.15-3.38, m	2.95, m
5‴		3.83, dd (11.3, 5.3)	3.15-3.38, m	3.26, m
		3.11, m		
6‴			3.67-3.73, m	3.58, d (10.8)
			3.87, dd (11.4, 2.7)	4.10, d (10.8)
				β-D-apiose
1⁗				5.00, d (2.3)
2⁗				3.83, d (2.3)
4⁗				3.84, d (9.5)
				3.76, d (9.5)
5⁗				.3.51, d (11.4)
				3.46, d (11.4)

^{1}H NMR data were measured at [a] 500 (CD_3OD), [b] 300 (CD_3OD) and [c] 500 (DMSO-d_6) MHz, respectively.

Table 18. ^{13}C NMR data of compounds **AH14**, **AH15**, **AJ19**, and **AH16**

position	**AH14**[a]	**AH15**[b]	**AJ19**[b]	**AH16**[c]
1	32.9	32.3	32.4	30.1
2	41.4	38.5	38.8	36.7
3	72.5	78.8	79.0	77.7
4	39.0	35.6	35.5	33.5

5	27.1	25.9	26.4	24.0
6	33.8	33.7	33.9	31.5
7	36.8	36.7	36.7	34.3
1'	135.3	134.0	135.6	132.4
2'	131.1	131.1	131.1	129.0
3'	116.9	116.8	116.8	115.0
4'	157.1	157.0	157.0	155.1
5'	116.9	116.8	116.8	115.0
6'	131.1	131.1	131.1	129.1
1"	135.6	135.1	135.6	132.5
2"	131.1	131.2	131.2	129.0
3"	116.8	117.0	116.8	115.0
4"	157.0	157.3	157.0	155.2
5"	116.8	117.0	116.8	115.0
6"	131.1	131.2	131.2	129.1
		β-D-xylose	**β-D-glucose**	**β-D-glucose**
1"'		102.6	104.2	102.1
2"'		73.4	76.1	73.6
3"'		76.7	80.6	76.8
4"'		69.6	72.6	70.1
5"'		65.8	78.5	75.9
6""			63.7	67.4
				β-D-apiose
1""				109.2
2""				75.3
3""				78.8
4""				73.3
5""				63.5

^{13}C NMR data were measured at [a] 125 (CD_3OD), [b] 75 (CD_3OD) and [c] 125 (DMSO-d_6) MHz, respectively.

Table 19. ^{1}H NMR data of compounds **AH17** and **AF10-12**

	AH17[a]	**AF10**[b]	**AF11**[c]	**AF12**[d]
position		δ_H (*J* in Hz)		
1	2.46, m	2.48, m	2.43, m	2.44, m
2	1.67, m	1.72, m	1.77, m	1.64, m
3	3.49, m	3.64, m	3.46, m	3.30, m
4	1.55, m	1.58, m	1.60, m	1.47, m
5	1.37, m	1.38, m	1.36, m	1.35, m
6	1.42, m	1.52, m	1.54, m	1.45, m
7	2.41, t (7.5)	2.44, t (7.5)	2.35, t (7.5)	2.37, t (7.5)
2'	6.59, d (2.0)	6.60, d (2.0)	6.52, d (2.0)	6.52, d (2.0)
5'	6.63, d (8.0)	6.65, d (7.9)	6.58, d (7.9)	6.58, d (7.9)
6'	6.46, dd (8.0, 2.0)	6.47, dd (7.9, 2.0)	6.38, dd (7.9, 2.0)	6.38, dd (7.9, 2.0)
2"	6.60, d (2.0)	6.61, d (2.0)	6.57, d (2.0)	6.57, d (2.0)
5"	6.64, d (8.0)	6.66, d (7.9)	6.59, d (7.9)	6.59, d (7.9)
6"	6.48, dd (8.0, 2.0)	6.48, dd (7.9, 2.0)	6.38, dd (7.9, 2.0)	6.43, dd (7.9, 2.0)
		***β*-D-xylose**	***β*-D-glucose**	***β*-D-xylose**
1'''		4.21, d (7.7)	4.14, d (7.5)	4.25, d (7.5)
2'''		3.14, dd (9.2, 7.9)	3.07, m	3.03-3.22, m
3'''		3.28, m	3.42, m	3.48, t (8.8)
4'''		3.46, m	3.15, m	3.35-3.42, m
5'''		3.18, m, 3.84, dd (11.3, 5.5)	3.28, m	3.91, dd (11.4, 5.4), 3.03-3.22, m
6'''			3.68, dd (11.9, 2.4), 3.55, m	

	***β*-D-glucose**
1""	4.33, d (7.8)
2""	3.03-3.22, m
3""	3.03-3.22, m
4""	3.03-3.22, m
5""	3.03-3.22, m
6""	3.88, dd (11.8, 2.0), 3.35-3.42, m

^{1}H NMR data were measured at [a] 300 (CD_3OD), [b] 500 (CD_3OD), [c] 300 (DMSO-d_6), and [d] 500 (DMSO-d_6) MHz, respectively.

Table 20. ^{13}C NMR data of compounds **AH17** and **AF10-12**

position	**AH17**[a]	**AF10**[b]	**AF11**[c]	**AF12**[d]
1	32.6	32.0	34.6	30.3
2	33.6	38.3	31.6	36.5
3	77.9	77.4	77.4	78.0
4	33.2	35.0	33.4	33.4
5	24.1	25.8	24.1	24.0
6	35.9	33.1	36.5	31.5
7	30.3	36.2	30.3	34.5
1'	133.5	135.7	133.3	133.1
2'	115.8	116.8	115.7	115.6
3'	144.8	144.2	144.9	144.9
4'	142.7	116.3	142.9	143.0

5'	115.8	120.7	115.5	115.4
6'	118.8	135.7	118.8	118.8
1"	133.4	116.9	133.4	133.2
2"	115.8	146.2	115.8	115.6
3"	144.8	144.2	144.9	144.9
4"	142.7	116.5	143.0	143.0
5"	115.8	120.8	115.7	115.4
6"	118.9		119.0	118.8
		β-D-xylose	**β-D-glucose**	**β-D-xylose**
1'''		104.3	101.9	103.9
2'''		75.2	73.7	72.0
3'''		78.1	76.9	87.7
4'''		71.4	70.2	68.3
5'''		67.0	76.7	64.9
6''''			61.3	
				β-D-glucose
1''''				102.2
2''''				73.8
3''''				76.8
4''''				70.2
5''''				76.1
6''''				61.1

^{13}C NMR data were measured at [a] 75 (CD_3OD), [b] 125 (CD_3OD), [c] 75 (DMSO-d_6), and [d] 125 (DMSO-d_6), respectively.

Table 21. ^{1}H NMR data of compounds **AJ31-36**

	AJ31[a]	**AJ32**[c]	**AJ33**[c]	**AJ34**[c]	**AJ35**[c]	**AJ36**[d]
position			δ_H (*J* in Hz)			
5	7.50, s	7.70, s	7.52, s	7.52, s	7.65, s	7.80, s
5'	7.37, s	7.55, s	7.46, s	7.52, s	7.56, s	7.67, s
3-OCH_3				4.04, s	4.09, s	
4-OCH_3					4.00, s	4.11, s
3'-OCH_3	4.02, s	4.05, s	3.99, s	4.04, s	4.06, s	4.02, s
4'-OCH_3						4.06, s
		***β*-D-xylose**	***β*-D-glucose**			***β*-D-xylose**
1"		5.01, d (7.4)	4.45, d (7.4)			5.18, d (7.4)
2"		3.39, m	3.16, m			3.39, m
3"		3.33, m	3.15, m			3.34, m
4"		3.42, m	3.07, m			3.42, m
5"		3.86, dd (10.6, 4.6), 3.38, d (10.6)	3.19, m			3.83, dd (10.6, 4.6), 3.39, d (10.6)
6"			7.71, dd (11.4, 1.8), 3.48, dd (11.4, 5.5)			

^{1}H NMR data were measured at [a] 400, [b] 500, [c] 300 and [d] 600 MHz in DMSO-d_6, respectively.

Table 22. ^{13}C NMR data of compounds **AJ31-36**

position	**AJ31**[a]	**AJ32b**[c]	**AJ33**[c]	**AJ34**[c]	**AJ35**[c]	**AJ36**[d]
1	112.7	114.6	116.2	112.1	114.3	113.8
2	135.8	135.9	138.1	140.2	140.2	140.9
3	141.7	141.8	142.8	141.2	141.7	141.9
4	151.9	146.9	150.4	152.2	154.3	151.5
5	111.1	111.2	114.2	111.7	111.8	112.0
6	108.9	107.0	110.5	111.5	113.8	113.8
7	159.2	158.5	160.3	158.5	159.3	158.3
1'	112.2	111.5	112.9	112.1	112.8	112.6
2'	141.6	140.5	139.9	140.2	141.3	141.9
3'	140.0	140.1	139.4	141.2	139.1	141.2
4'	151.9	152.7	152.4	152.2	154.5	154.3
5'	112.5	113.0	114.2	111.7	108.0	107.6
6'	112.2	111.5	112.9	111.5	113.1	112.6
7'	158.9	158.5	159.6	158.5	159.2	158.3
3-OCH_3				61.0	61.6	61.6
4-OCH_3						
3'-OCH_3		60.9	61.0	61.0	61.3	61.3
4'-OCH_3					56.6	56.8
		***β*-D-xylose**	***β*-D-glucose**			***β*-D-xylose**
1"		102.7	106.2			101.7
2"		72.9	73.9			72.9
3"		75.4	77.2			76.0
4"		69.2	69.9			69.2
5"		65.8	77.8			65.7
6"			61.2			

^{13}C NMR data were measured at [a] 100, [b] 125, [c] 75 and [d] 150 MHz in DMSO-d_6, respectively.

Table 23. ^{1}H NMR data of compounds **AJ39-42**

	AJ39[a]	**AJ40**[b]	**AJ41**[b]	**AJ42**[b]
position		δ_H (*J* in Hz)		
1	2.14, 1.96, m	1.82, 1.54, m	1.81, 1.52, m	1.54, 1.24, m
2	1.97, 1.91, m	1.95, 1.82, m	1.94, m	1.22, m
3	3.45, dd (11.2, 4.5)	3.44, m	3.43, m	3.43, dd (10.6, 5.4)
4				
5	0.99, m	0.97, m	0.99, m	1.37, m
6	1.73, 1.53, m	1.71, 1.54, m	1.72, 1.54, m	1.54, 1.19, m
7	1.63, 1.19, m	1.62, 1.20, m	1.63, 1.21, m	1.96, 1.19, m
8	2.20, m	2.23, m	2.20, m	
9				1.49, m
10				
11	5.94, br d (6.3)	5.30, d (5.7)	5.27, d (5.5)	1.51, 1.36, m
12	2.07, 1.93, m	2.09, 1.95, m	2.05, 1.89 m	1.96, 1.43, m
13				2.07, m
14				
15	1.30, m	1.32, m	1.40, m	1.38, 1.14, m
16	1.23, 1.19, m	1.24, 1.19, m	1.27, m	1.67, 1.54, m
17	1.65, m	1.71, m	1.65, m	2.15, m
18	0.70, s	0.71, s	0.69, s	1.22, s
19	1.23, s	1.22, s	1.12, s	0.97, s
20	1.47, m	1.52, m	1.54, m	
21	0.97, d (6.4)	0.99, d (6.4)	0.96, d (6.3)	1.42, s
22	1.97, m	2.20, m	2.30, 1.89, m	2.05, 1.95, m
23	2.31, 2.20, m	2.12, m	6.12, td (15.5, 8.1)	2.11, 2.08, m
24	7.21, t (7.3)	3.71, d (9.8)	6.00, d (15.5)	4.43, m
25				
26		1.55, s	3.95, d (10.5)	5.27, 4.95, br s
			3.90, d (10.5)	
27	2.11, s	1.52, s	1.65, s	1.90, s
28	1.09, s	1.23, s	1.29, s	1.03, s
29	1.13, s	1.08, s	1.07, s	0.85, s
30	0``.81, s	0.77, s	0.77, s	0.93, s

^{1}H NMR data were measured at [a] 600 and [b] 500 MHz in C_5D_6N, respectively.

Table 24. ^{13}C NMR data of compounds **AJ39-42**

position	**AJ39**[a]	**AJ40**[b]	**AJ41**[b]	**AJ42**[b]
1	37.4, t	36.8, t	36.8, t	35.7, t
2	28.3, t	28.7, t	28.7, t	28.7, t
3	78.0, d	78.0, d	78.0, d	78.1, d
4	39.9, s	39.7, s	39.7, s	39.6, s
5	53.1, d	53.0, d	53.0, d	50.7, d
6	21.8, t	21.8, t	21.8, t	16.8, t
7	28.6, t	28.5, t	28.5, t	37.4, t
8	42.1, d	42.1, d	42.1, d	40.7, s
9	149.2, s	149.2, s	149.2, s	50.6, d
10	39.7, s	39.8, s	39.8, s	38.1, s
11	115.0, d	115.0, d	115.0, d	21.9, t
12	36.8, t	37.4, t	37.4, t	26.3, t
13	44.6, s	44.6, s	44.6, s	42.6, d
14	47.3, s	47.3, s	47.3, s	56.4, s
15	34.2, t	34.1, t	34.1, t	31.7, t
16	28.6, t	28.3, t	28.3, t	25.4, t
17	51.2, d	51.5, d	51.5, d	51.1, d
18	16.6, q	14.7, q	14.7, q	18.3, q
19	22.6, q	22.6, q	22.6, q	18.8, q
20	36.3, d	37.0, d	36.8, d	74.1, s
21	18.8, q	18.8, q	18.7, q	28.2, q
22	28.8, t	34.6, t	39.7, t	39.5, t
23	26.0, t	29.4, t	127.0, d	30.6, t
24	142.5, d	79.9, d	138.2, d	76.0, d
25	129.0, s	72.7, s	73.2, s	150.0, s
26	170.6, q	26.0, q	71.2, t	110.0, d
27	18.4, q	26.0, q	25.5, s	16.5, q
28	30.0, q	28.9, q	28.9, q	28.3, q
29	12.9, q	16.6, q	16.5, q	15.7, q
30	14.7, q	18.9, q	18.6, q	16.3, q

^{13}C NMR data were measured at at [a] 150 and [b] 125 MHz in C_5D_6N, respectively. Multiplicity was determined by DEPT experiments.

Table 25. ^{1}H NMR data of compounds **AF13-16**

	AF13[a]	**AF14**[a]	**AF15**[a]	**AF16**[a]
position		δ_H (*J* in Hz)		
3	6.02, s	6.04, s	6.41, d (2.7)	6.42, d (2.7)
5	6.02,s	6.04, s	6.05, dd (8.7, 2.7)	6.11, dd (8.7, 2.7)
6			6.89, d (8.7)	6.92, d (8.7)
2"	7.24, s	7.45, d (1.9)	7.30, s	7.52, d (2.9)
5"		6.82, d (8.3)		6.85, d (8.2)
6"	7.24, s	7.43, dd (8.3, 1.9)	7.30, s	7.54, dd (8.2, 2.9)
2-OCH_3	3.66, s	3.67, s	3.80, s	3.77, s
6-OCH_3	3.66, s	3.67, s		
3"-OCH_3	3.82, s	3.80, s	3.67, s	3.85, s
5"-OCH_3	3.82, s		3.67, s	
			***β*-D-glucose**	
1'	4.68, d (7.5)	4.68, d (7.5)	4.76, d (7.5)	4.75, d (7.5)
2'	3.43, m	3.45, m	3.45, m	3.47, m
3'	3.47, m	3.48, m	3.48, m	3.48, m
4'	3.39, m	3.42, m	3.42, m	3.41, m
5'	3.51, m	3.49, m	3.49, m	3.65, m
6'	4.55, dd (11.8, 6.9), 4.38, m	4.56, dd (11.8, 6.9), 4.33, m	4.55, dd (11.8, 6.9), 4.37, m	4.54, dd (11.8, 6.9), 4.35, m

^{1}H NMR data were measured at [a] 500 MHz in DMSO-d_6, respectively.

Table 26. ^{13}C NMR data of compounds **AF13-16**

position	**AF13**[a]	**AF14**[a]	**AF15**[a]	**AF16**[a]
1	130.1	130.0	141.9	141.6
2	95.1	155.8	152.9	152.9
3	155.8	95.1	102.5	102.6
4	156.8	156.8	155.7	155.7
5	155.8	95.1	108.2	108.3
6	95.1	155.8	121.3	121.4
1"	122.0	123.3	122.1	123.2
2"	109.0	114.4	109.0	114.5
3"	149.8	149.5	149.7	149.6
4"	143.1	153.7	142.8	153.8
5"	149.8	116.8	149.7	116.8
6"	109.0	126.1	109.0	126.1
7"	168.8	168.8	168.6	168.7
2-OCH_3	57.5	57.5	57.3	57.2
6-OCH_3	57.5	57.5		
3"-OCH_3	57.6	57.2	57.6	57.3
5"-OCH_3	57.6		57.6	
			***β*-D-glucose**	
1'	106.7	106.5	104.8	105.0
2'	76.4	76.4	75.8	75.8
3'	78.6	78.6	78.5	78.6
4'	72.8	72.8	72.8	72.9
5'	76.5	76.5	76.4	76.4
6'	66.1	65.9	66.0	65.9

^{13}C NMR data were measured at [a] 125 MHz in DMSO-d_6, respectively.

Table 27. ^{1}H and ^{13}C NMR data for compounds **AF18-19**

	AF18[a]		**AF19**[b]	
position	δ_H (J in Hz)			
1	0.97, 1.90, m	45.0	1.34, m, 2.39, dd (12.0, 4.5)	48.8
2	5.59, ddd (10.6,10.6,4.6)	73.7	4.31, td (10.8, 4.5)	66.6
3	3.69, d (9.9)	79.8	5.25, d (9.6)	84.9
4		40.4		39.9
5	0.94,m	55.7		55.5
6	1.58, 1.46, m	18.7	1.46, 1.36, m	18.6
7	1.37, m	34.7	1.39, 1.28, m	34.4
8		41.1		41.2
9	1.41, m	50.8	1.43, m	50.6
10		38.8		38.5
11	1.26, 1.15, m	21.3	1.47, 1.20, d	21.2
12	1.52, 1.27, m	26.0	1.76, 1.14, m	25.6
13	2.71, m	38.6	1.80, m	37.5
14		42.9		43.0
15	1.84, 1.14, m	30.2	1.04, m, 1.91, td (13.2, 3.6)	27.5
16	2.62, 1.51, m	32.9	2.47, 1.35, m	30.3
17		56.6		48.5
18	1.75, m	49.8	1.69, t (12.0, 11.4)	49.1
19	2.73, 2.52 ,m	47.7	2.62, td (10.9, 6.0)	48.4
20		151.3		151.2
21	2.28, 1.58, m	31.1	2.16, 1.52, m	30.3
22	2.23, 1.56, m	37.6	1.22, m, 2.43, t (10.8)	34.9
23	1.26, s	29.0	1.03, s	28.8
24	1.07, s	17.39	1.02, s	18.1
25	0.97, s	17.37	0.96, s	17.6

26	1.00, s	16.3	0.99, s	16.1
27	1.06, s	14.9	1.05, s	14.9
28		178.8	3.68, d (10.8), 4.10, d (10.8)	54.9
29	4.93,4.78,br s	110.0	4.76, 4.89, br s	110.0
30	1.79, s	19.4	1.78, m	19.3
1'		127.0		127.0
2'	7.53, d (1.9)	115.7	7.59, d (1.8)	115.8
3'		145.3		145.4
4'		147.7		147.6
5'	7.17, d (8.1)	116.7	7.24, d (8.0)	116.7
6'	7.12, dd (8.1, 1.9)	121.9	7.15, dd (8.0, 1.8)	121.9
7'	8.02, d (15.8)	145.3	8.03, d (16.2)	145.4
8'	6.60, d (15.8)	115.9	6.69, d (16.2)	115.9
9'		167.5		168.0

^{1}H NMR data were measured at [a] 500 and [b] 600 MHz in C_5D_6N, respectively. ^{13}C NMR data were measured at [a] 125 and [b] 150 MHz in C_5D_6N, respectively.

1.3.7. Preparation of (*S*)-MTPA ester and (*R*)-MTPA ester

Compounds **AH2** and **AJ1** (1 mg) was transferred into a 5 mL glass vial. Dry pyridine (20 μL), $CHCl_3$ (100 μL), and (*R*)-(-)-*α*-Methoxy-*α*-trifluoromethylphenylacetyl (MTPA) chloride (20 μL) were added into the 5 mL glass vial immediately, and it was shaken carefully to mix the sample and MTPA chloride at room temperature. Every 30 min, the reactant was subjected to TLC analysis (*n*-hexane:EtOAc = 1:1) to verify the obtention of the (*S*)–MTPA ester derivative (**AH2s** and **AJ1s**). In the manner described for **AH2s** and **AJ1s**, another portion of compounds **AH2** and **AJ1** (1 mg) was reacted in another 5 mL glass vial with (*S*)-(+)-MTPA chloride at room temperature using dry pyridine (20 μL) and $CHCl_3$ (100 μL) as solvent to afford the (*R*)-

MTPA derivative (**AH2r** and **AJ1r**). The ^{1}H NMR data (600 MHz, C_5D_5N) of the (*S*)-MTPA ester derivative (**AH2s** and **AJ1s**) and (*R*)-MTPA ester derivative (**AH2r** and **AJ1r**) were obtained to clarify the stereochemistry of compound **AH2**.

1.3.8. General acid hydrolysis

Compounds **AJ12** (2 mg) and **AJ37** (2 mg) were dissolved in 6 N HCl (dioxane-H_2O, 1:1, 1 mL) and the solution was heated to 90 ^{o}C for 2 h. After neutralizing acidic solution with silver carbonate, the solvent was evaporated to dryness under N_2. The reaction mixture was extracted with $CHCl_3$ and H_2O, successively, and the aqueous layer was concentrated to dryness. The dried reactant was subjected to HILIC-ESI-MS. The HPLC electrospray ionisation–mass spectrometry (ESI-MS) system consisted of a Finnigan Surveyor HPLC system with a pump, an autosampler and the Finnigan LCQ Advantage with Xcalibur software. Separation was achieved at 30 ^{o}C on a ZIC®-HILIC column (5 mm, 4.6 mm i.d. x 100 mm, SeQuant AB). The mass spectrometer was operated with the ion source voltage set to -3000 V, capillary voltage -30 V, capillary temperature 300 ^{o}C, tube lens offset -60 V, sheath gas 40 (arbitrary units) and auxiliary gas 30 (arbitrary units). The mobile solvent consisted of (A) 0.03 % formic acid in water and (B) 100 % acetonitrile at a flow rate of 1.0 mL/min, with isocratic conditions of 30 % A and 70 % B for 10min. HILIC-MS analysis afforded the retention times (t_R 6.65 min) and mass spectra (m/z 178.69 $[C_6H_{12}O_6\text{-H}]^-$, 224.73 $[C_6H_{12}O_6\text{+HCOOH-H}]^-$) of D-glucose.

2. Evaluation of anti-adipogenic effects in 3T3-L1 cells

2.1. Materials

2.1.1. Reagents for cell cultures

DMEM, penicillin/streptomycin, trypsin, PBS for cultures of 3T3-L1 cells were purchased from Sigma Chemical Co. (St. Louis, MO, USA). MTT, IBMX, dexamethasone, insulin, EGCG, Nonidet P-40, isopropyl alcohol and reagents for ORO 1-[4-(Xylylazo)xylyl]-azo-2-naphthol1-[2,5-Dimethyl-4-(2,5-dimethylphenylazo) phenylazo]-2-naphthol Solvent Red staining assay were also obtained from Sigma Chemical Co (St. Louis, MO, USA). FBS, CS was obtained from Hyclone Co. (Logan, UT, USA), Gibco Co. (Grand Island, NY, USA), respectively. Multi well culture plate and cell culture dishes were purchased from Corning (New York, NY, USA).

2.2. Methods

2.2.1. Cell culture and Adipocyte differentiation

Mouse embryo fibroblasts 3T3-L1 cells were obtained from the American Type Culture Collection (Manassas, VA, U.S.A.) and incubated in DMEM supplemented with 10% bovine calf serum until confluence. Two days after confluence (designated day 0), preadipocytes were stimulated to differentiate with differentiation medium (DM, DMEM with 10% FBS, 0.5 mM 3-isobutyl-1-methyl-xanthine, 10 μg/mL insulin and 1 μM dexamethasone) for 2 day (day 2). Cells were then maintained in DM (DMEM 10% FBS and 10 μg/mL insulin) for another 2 d (day 4), followed by culturing with DM (DMEM with 10% FBS) for an additional 4 day (day 8). All media contained 100 IU/mL penicillin and 100m g/mL streptomycin. Cells were maintained

at 37°C in a humidified atmosphere of 95% air-5% CO_2. The purity of each compound was verified as > 95% by HPLC. Test compounds were dissolved in DMSO (final concentration of 0.1% in media). The cultures were treated with test samples for the whole culture period (day 0-8).

2.2.2. Oil Red O staing

Lipid droplets in cells were stained with Oil Red O (ORO) on day 8. Briefly, culture dishes were washed three times with PBS and fixed with 10% formalin for 1 hour at room temperature. After fixation, cells were washed once with PBS and stained with a filtered ORO solution (6 parts of saturated 0.6% ORO in isopropyl alcohol and 4 parts of water) for 15 minutes at room temperature. Cells were washed twice with water for 15 minutes and visualized. To quantify the intracellular lipids, spectrophotometrical quantification of the stain was performed by dissolving the stained lipid droplets with 4% Nonidet P-40 in isopropyl alcohol for 5 minutes. The absorbance was measured at 544 nm.

Lipid contents (% of control) = A_{540nm}(sample- undifferentiated control)/
A_{540nm}(differentiated control- undifferentiated control) x 100

2.2.3. Determination of GPDH Activity

Sample-treated 3T3-L1 adipocytes were harvested on day 8, washed twice with PBS, and collected with a scraper into 25 mM Tris buffer containing 1 mM EDTA and 1 mM DTT (pH 7.5). The harvested cells were sonicated in 25 ultrasonic bursts of 10 s, after which they were centrifuged at 10000 rpm for 5 min at 4°C. The supernatants were assayed for GPDH activity

using a commercial assay kit (Takara Bio, Shiga, Japan).

2.2.4. Measurement of inhibitory activity on cell proliferation

Compounds to be tested were dissolved in DMSO (final culture concentration, 0.1%). A preliminary study showed that DMSO at a final concentration of 0.1% in media did not affect the cell viability. For the assay, the cells were seeded in 96-well plates at a density of 5×10^3 cells/well and incubated for 24 h. 3T3-L1 cells were treated with vehicle or compounds to be tested for 24, 48 and 72 h. Inhibitory activity of compounds on cell proliferation was assessed by the MTT assay. MTT (0.5 mg/mL) was directly added to cultures, followed by incubation at 37°C for 4 h. The supernatant was then aspirated and 100 μl of DMSO was added to dissolve the formazan. After insoluble crystals were completely dissolved, absorbance (Abs) at 540 nm was measured using a microplate reader. Data were expressed as percent cell viability relative to control cultures.

Cell proliferation (% of control) = A_{540nm}(sample)/A_{540nm}(control) x 100

2.2.5. Evaluation for caspase-3/7 activity

Caspase-3/7 activity was evaluated with Apo-ONE Homogenous Caspase-3/7 assay kit using Z-DEVD-rhodamine 110 as a substrate (Promega, Madison, WI, USA) (Yang et al., 2011). After treatment with compounds for the time indicated, 100 μL of homogeneous Caspase-3/7 reagent (buffer + substrate) was added to each well of the cultured 3T3-L1 cells in 96-well plates. The 96-well plate was incubated at room temperature and measured on a

Cytofluor II multiwell fluorescence spectrophotometer (excitation at 485nm and emission at 535 nm).

Caspase-3/7 activity (% of control) = $A_{sample}/A_{control}$ x 100

2.2.6. Western blot

3T3-L1 cells were lysed in RIPA buffer (Cell Signaling, Beverly, MA) containing 0.5 mM DTT, 1 mM phenylmethylsulfonyl fluoride (PMSF), and 1% protease inhibitor cocktail. Total proteins (40 μg) were separated by 5% or 10% sodium dodecyl sulfate (SDS) polyacrylamide gel electrophoresis, transferred to polyvinylidene difluoride membranes (Millipore, Billerica, MA). After blocking in TBS-T with 5% non-fat dry milk for 30min at room temperature, the membrane was incubated overnight at 4°C with 1:1000 diluted anti-pAMPK, anti-AMPK, anti-pACC, and anti-ACC primary antibodies (Cell Signaling Technology, Beverly, MA, USA), and anti-Cytochrome *c*, anti-Bcl-2, and anti-Bax (Cell Signaling Technology, Beverly, MA, USA). After incubation with 1:1000 diluted horseradish peroxidase-conjugated goat anti-rabbit immunoglobulin G secondary antibody (Santa Cruz Biotechnology, Santa Cruz, CA) for 1 h at room temperature, immunoreactive proteins were visualized by an enhanced chemiluminescent solution (Amersham, Uppsala, Sweden). After normalization to anti-β-actin (Santa Cruz Biotechnology, Santa Cruz, CA), density values for the protein bands of interest were expressed as a percentage of the control using ImageJ software (http://rsweb.nih.gov/ij) (Popivanova et al., 2008).

2.2.7. RT-PCR and quantitative real-time RT-PCR

The total RNA was extracted from the 3T3-L1 cells using RNease Plus Kit (QIAGEN Korea Ltd., Seoul, Korea). cDNA was synthesized with 1 μg of total RNA using QuantiTech Reverse Transcription Kit (QIAGEN Korea Ltd., Seoul, Korea), and then was mixed with QuantiFast SYBR Green PCR master mix (QIAGEN Korea Ltd., Seoul, Korea) and specific primers. The conventional PCR products were generated by AccuPower PCR Premix (Bioneer Corp. Daejeon, Korea) in a total reaction volume of 20 μL. The PCR specific primers used with the QIAGEN kits for SYBR® Green-based real time RT-PCR were PPARγ (NM_01146), C/EBPα (NM_007678), C/EBPβ (NM_009883), C/EBPδ (NM_007679), SREBP1 (NM_011480), SCD-1 (NM_009127), leptin (NM_008493), LPL (NM_008509), aP2 (NM_024406), FAS (NM_007988), TNFα (NM_136393), perilipin (NM_175640), HSL (NM_010719), PDE3B (NM_011055), G*i*α1 (NM_013818) and GAPDH (NM_008084) and were obtained from (QIAGEN Korea Ltd., Seoul, Korea). The amplification cycles were carried out at 95°C for 20 s, 60°C for 20 s, and 72°C for 20 s. The last cycle was followed by a final extension step at 72°C for 5 min. The RT-PCR products were electrophoresed in 1.5% agarose gels under 100 V and stained with diluted 1:20000 SYBR™ Safe DNA Gel Stain in DMSO (Invitrogen Corp., Carlsbad, CA). The gel image was visualized by Gel Doc EQ Gel Documentation System (Bio-Rad Laboratories Inc., CA, USA). After normalization to GAPDH, density values for the protein bands of interest were expressed as percentage of the control using ImageJ software (http://rsweb.nih.gov/ij) (Popivanova et al., 2008). Quantitative SYBR Green real-time PCR was performed with an Applied Biosystems 7300 Real-Time PCR System (Life Technologies Corporation, Carlsbad, CA, USA) and analyzed by means of comparative C_t quantification (Popivanova et al., 2008). GAPDH was amplified as an internal control. The Ct values of

GAPDH were subtracted from the Ct values of the target genes (ΔCt). The ΔCt values of the treated mice were compared with the ΔCt values of the untreated animals.

Table 28. Genes associated with lipid metabolism

name	gene	gene desscription	Gen Bank
Adipoq	Adiponectin	adiponectin	NM_009605
Cebpa	C/EBPα	CCAAT/enhancer-binding protein alpha	NM_007678
Cebpb	C/EBPβ	CCAAT/enhancer-binding protein beta	NM_009883
Cebpd	C/EBPδ	CCAAT/enhancer-binding protein delta	NM_007679
Fabp4	aP2	adipocyte fatty acid binding protein 4	NM_024406
Fasn	FAS	fatty acid syntahse	NM_007988
Gapdh	GAPDH	glyceraldehyde 3-phosphate dehydrogenase	NM_008084
Gtpbp1	G*i*α1	GTP binding protein	NM_013818
Lipe	HSL	hormone sensitive lipase	NM_010719
Lpl	LPL	lipoprotein lipase	NM_008509
Lep	Leptin	leptin	NM_008493
Pde3b	PDE3B	phosphodiesterase 3B	NM_011055
Plin1	perilipin	perilipin	NM_175640
Pparg	PPARγ	peroxisome proliferator-activated receptors gamma	NM_011146
Scd1	SCD-1	stearoyl coenzyme A desaturase 1	NM_009127
Srebf1	SREBP1	sterol regulatory element binding protein 1	NM_011480
Tnf	TNFα	tumor necrosis factorα	NM_013693

2.3. Statistical analysis

Statistical analysis was performed using Student's *t* test. Data were expressed as the means ± standard deviation (SD). Statistical significance was represented with an asterisk for *p* values < 0.05, with two asterisks for *p* values < 0.01 and three asterisks for *p* values < 0.001.

III. Result and discussion

1. Identification of chemical structure of compounds isolated from three *Alnus* species

1.1. Compound AJ1

Compound **AJ1**, brownish syrup, $[\alpha]_D^{25}$ -2.3 (*c* 1.0 $CHCl_3$:MeOH=1:1), was formulated as $C_{20}H_{20}O_4$ from the positive HRFABMS (*m/z* 324.1358 $[M]^+$, calcd. for $C_{20}H_{20}O_4$, 324.1362). The IR spectrum showed absorption bands corresponding to hydroxyl (3382 cm^{-1}), *cis* double bond (1710 cm^{-1}), and aromatic ring (1594, 1503 cm^{-1}) functions. In the UV spectrum, absorption at 287 nm indicated a biphenyl ether-type cyclic diarylheptanoid. The ^1H NMR spectroscopic data showed the presence of a 1,3,4,5-tetrasubstituted aromatic ring [δ_H 6.36 (1H, d, *J* = 1.9 Hz, H-6'), 5.49 (1H, d, *J* = 1.9 Hz, H-2')], a 4-substituted aromatic ring which is restricted free rotation [δ_H 7.32 (1H, dd, *J* = 8.2, 2.1 Hz, H-2"), 7.25 (1H, dd, *J* = 8.2, 2.1 Hz, H-5"), 7.14 (1H, dd, *J* = 8.2, 2.5 Hz, H-3"), and 6.98 (1H, dd, *J* = 8.2, 2.5 Hz, H-6")], an aromatic methoxy moiety [δ_H 4.11 (3H, s)], two conjugated double bond [δ_H 6.10 (1H, d, *J* = 11.4 Hz, H-1), 5.91 (1H, dd, *J* = 11.4, 9.2 Hz, H-2), 5.64 (1H, m, H-3), and 5.63 (1H, m, H-4)], and a secondary hydroxy moiety [δ_H 4.09, (1H, m, H-5)]. The ^{13}C-NMR spectrum also exhibited 20 carbon signals as two benzene ring (δ_C 154.8, 153.3, 149.3, 139.8, 134.7, 132.3, 131.9, 129.8, 125.3, 122.1, 100.5, 108.8), two conjugated double bond (δ_C 138.7, 129.4, 127.8, 126.3), one oxygenated methane (δ_C 73.3), two methylene (δ_C 40.9, 33.9), and methoxy group (δ_C 61.4). The ^1H-^1H COSY correlations of H-2 to H-1/H-2/H-3, H-4 to H-3/H-4/H-5, enabled us to construct structure **AJ1** shown in Figure 11.

The absolute configuration of a hydroxyl group at C-5 was confirmed by application of the modified Mosher′s method (Hoye et al, 2007; Fuchino et al., 1996). Compound **AJ1** was subjected to esterification with (*R*)-(-)-MTPA chloride and (*S*)-(+)-MTPA chloride in dry pyridine to yield the corresponding (*S*)-MTPA ester and (*R*)-MTPA ester, respectively. The $\Delta\delta$ values ($\Delta\delta = \delta_S - \delta_R$) were determined as shown in Figure 10. The signals due to the protons at C-1 and C-4 in the **AJ1s** were observed at lower field in the ^{1}H NMR spectrum than those in the **AJ1r**, while the signals due to the protons at C-6 and C-7 in **AJ1s** were observed at higher field than those in **AJ1r**. Following the MPTA rules, these data indicated an *R* configuration at C-5. With above observed spectroscopic data, compound **AJ1** was determined to be (5*R*)-3,5'-dihydroxy-4'-methoxy-3',4"-oxo-1,7-diphenyl-1,3-diheptene and it was isolated for the first time from nature.

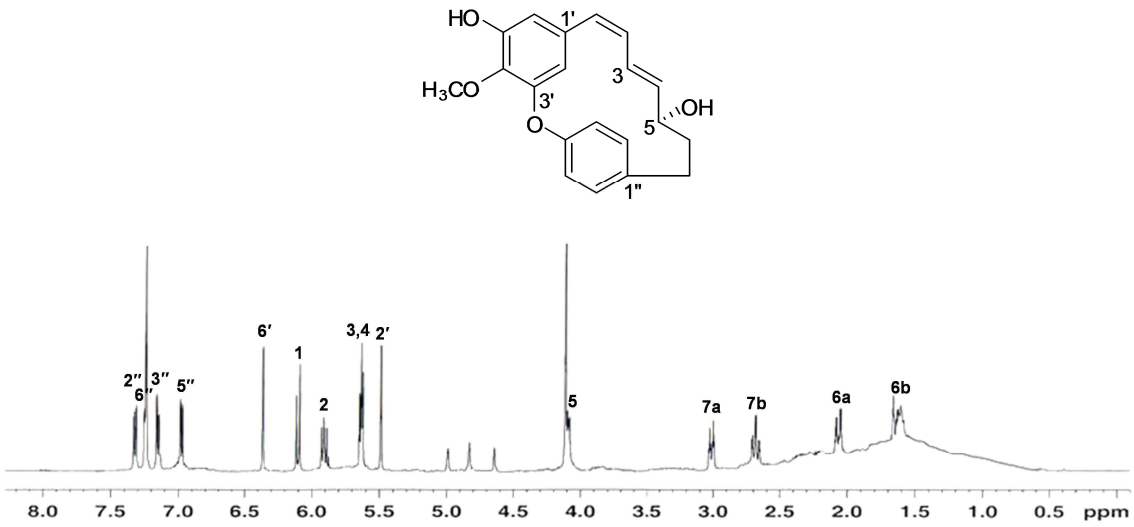

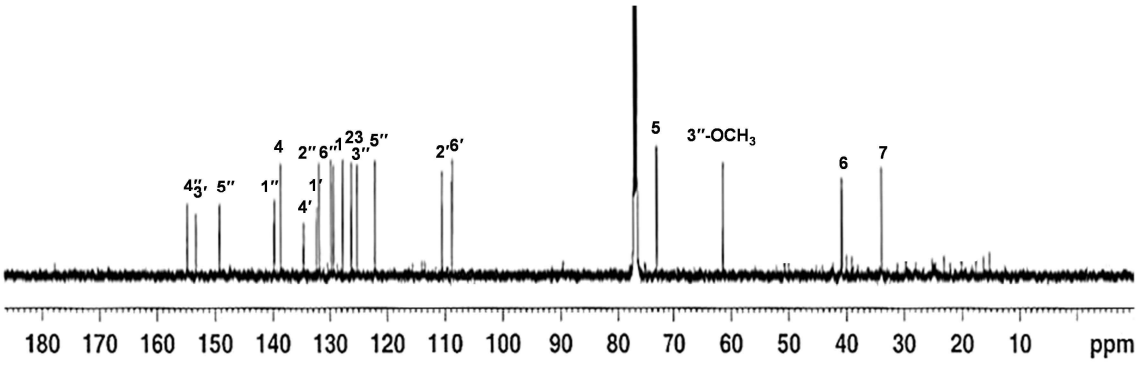

Figure 9. ^{1}H and ^{13}C NMR spectra of compound **AJ1**

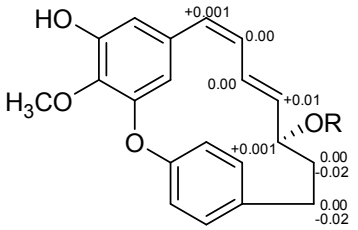

AJ1s R = (*S*)-MTPA ester

AJ1r R = (*R*)-MTPA ester

Figure 10. $\Delta\delta$ (δ_S-δ_R) (ppm) values obtained from MTPA esters for compound **AJ1**

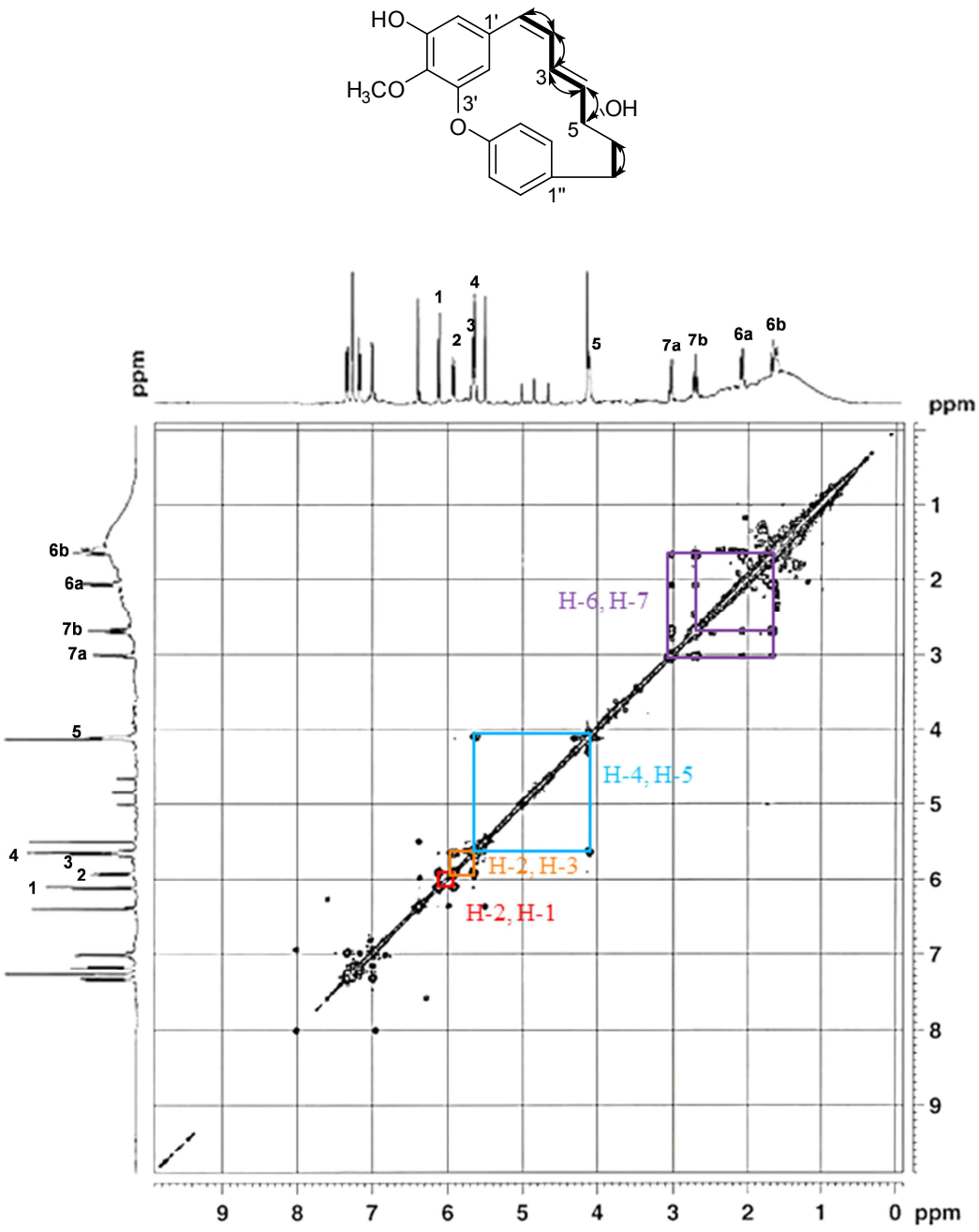

Figure 11. ^{1}H-^{1}H COSY spectrum of compound **AJ1**

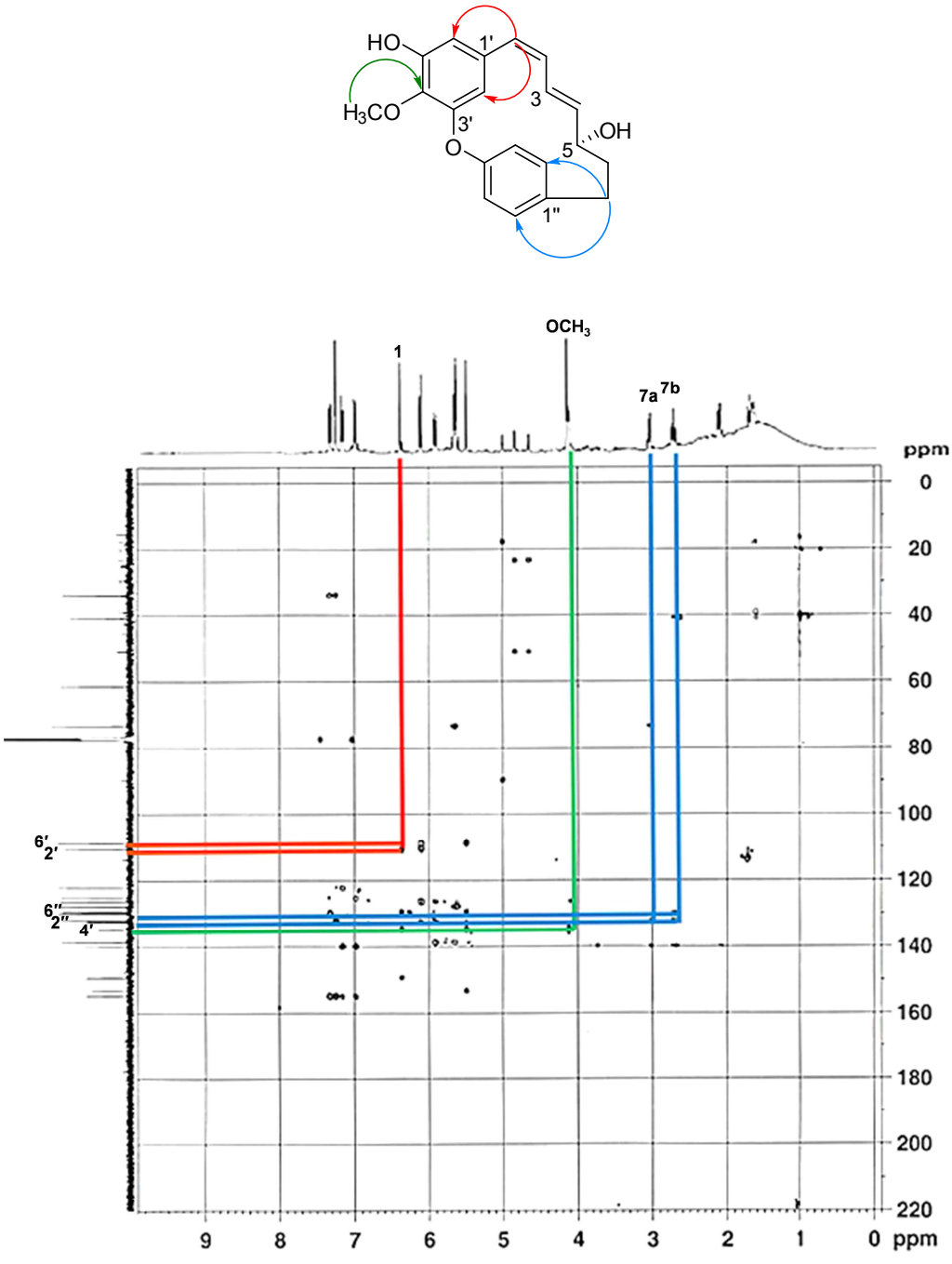

Figure 12.HMBC spectrum of compound **AJ1**

1.2. Compound AJ2

Compound **AJ2** was obtained as brownish syrup and $[\alpha]_D^{25}$ -0.5 (*c* 1.0 MeOH). The IR spectrum revealed the presence of carbonyl (1700 cm^{-1}) and aromatic ring (1588 and 1430 cm^{-1}) functions. The signal in the ^1H and ^{13}C NMR and HSQC experiments indicated that compound **AJ2** showed the existence of carbonyl carbon at δ_C 193.7 (C-3), hydroxy-bearing methane carbon δ_C 107.0 (C-4), methylene carbon δ_C 28.3 (C-1) and δ_C 38.1 (C-2). Furthermore, the ^1H NMR spectroscopic data revealed signals for 1,3,4-trisubstituted aromatic rings [δ_H 7.13 (1H, d, *J* = 2.0 Hz, H-2'), 6.98 (1H, dd, *J* = 8.1, 2.0 Hz, H-6'), and 6.83 (1H, d, *J* = 8.1 Hz, H-5')], signals for two neighboring methylene at δ_H 2.77(2H, m, H-1b, H-7b) and 2.46 (2H, m, H-2b, H-6b) and signal for hydroxy-bearing methane at δ_H 5.88 (1H, s, H-4) (Figure 13). The HMBC analysis showed the correlations of H-2' to C-1' and C-4', H-5' and H-6' to C-4', and H-2 and H-4 to C-3 (Figure 14). Taken into account all of the above described spectroscopic data, compound **AJ2** was considered as arylbutanoid. However, the molecular formula of compound **AJ2** was established as $C_{19}H_{22}O_6$ by the observed pseudo-molecular ion peak at *m/z* 326.1152 $[M]^+$ (calcd. for $C_{19}H_{18}O_5$ 326.1154) in the positive HRFABMS. In the ^1H NMR spectrum, the area ratio of four peaks at δ_H 7.13 (H-2'), 6.98 (H-5'), 6.83 (H-6') and 5.88 (H-4) was 2:2:2:1. On the basis of above information, the structure of compound **AJ2** was considered to be symmetrical. Therefore, compound **AJ2** was determined as 4-hydroxy-alnus-3,5-dione, and newly isolated from nature.

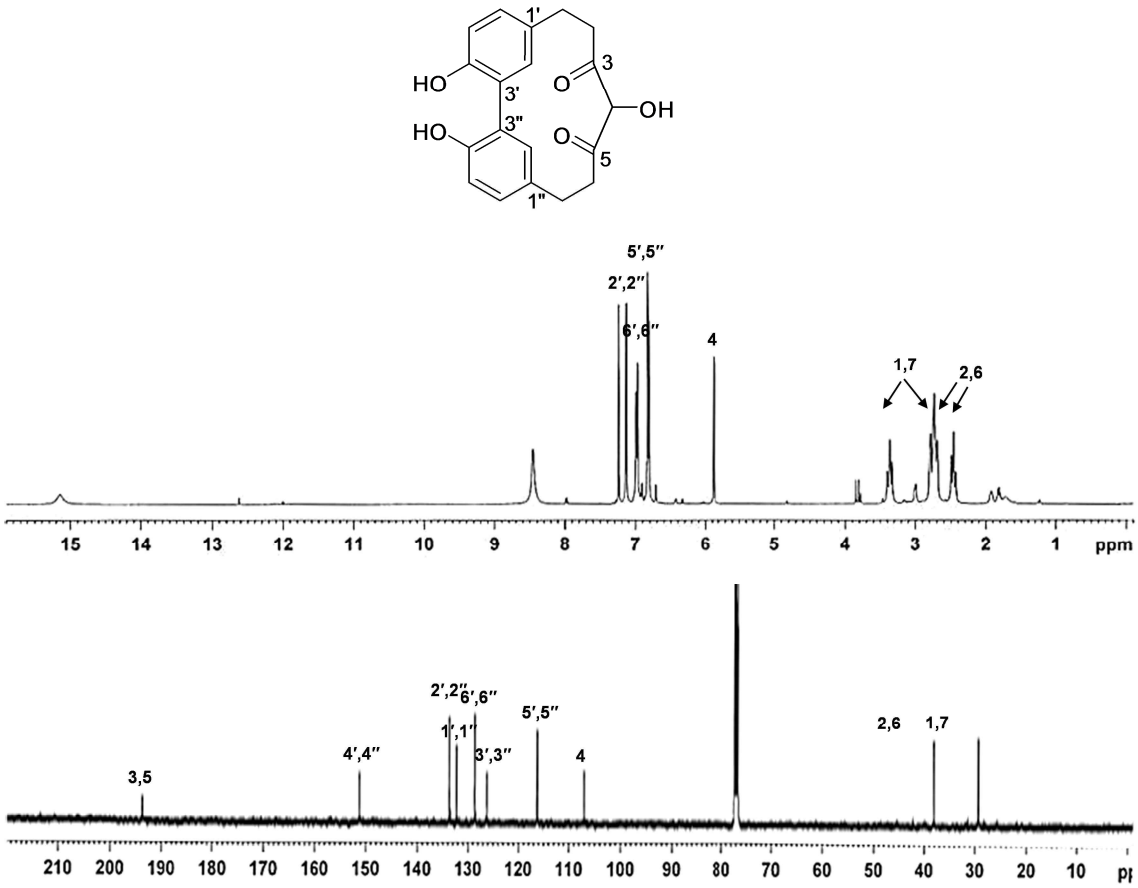

Figure 13. ^{1}H and ^{13}C NMR spectra of compound **AJ2**

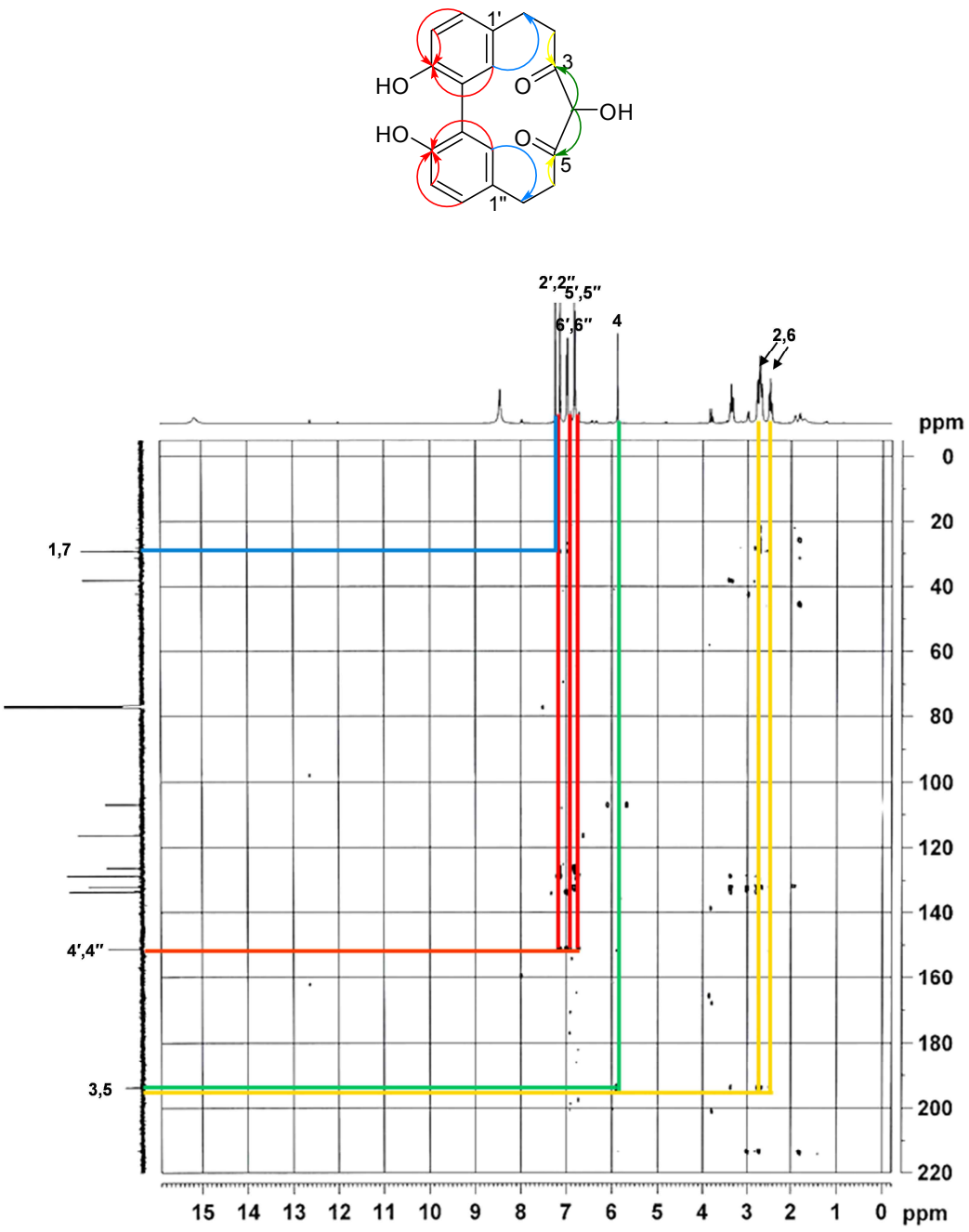

Figure 14. HMBC spectrum of compound **AJ2**

1.3. Compounds AJ3-6

Compound **AJ3** was characterized as a yellowish syrup, and $[\alpha]_D^{25}$ -0.8 (*c* 1.0 MeOH). The ion peak in ESIMS (negative mode) was *m/z* 295.23 $[M-H]^-$ indicating $C_{19}H_{20}O_3$ as its molecular formula. The IR spectrum showed the presence of hydroxyl (3341 cm^{-1}), carbonyl (1702 cm^{-1}), and aromatic ring (1608 and 1430 cm^{-1}) functions. The ^1H and ^{13}C NMR spectroscopic data revealed signals for 1,3,4-trisubstituted aromatic rings [δ_H 6.98 (1H, dd, *J* = 8.2, 2.2 Hz, H-6'), 6.78 (1H, d, *J* = 8.2 Hz, H-5'), and 6.58 (1H, dd, *J* = 2.2 Hz, H-2')] and [δ_H 7.13 (1H, d, *J* = 2.2 Hz, H-2"), 6.98 (1H, dd, *J* = 8.2, 2.2 Hz, H-6"), and 6.83 (1H, d, *J* = 8.2 Hz, H-5")], signals for six methylene at δ_H 2.86, 2.83, 2.71, 2.67, 1.83, and 1.63 and signal for carbonyl group at δ_C 212.9 (Figure 15). With above observed spectroscopic data, compound **AJ3** was confirmed as dihydroalnusone (Nomura et al., 1981)

Compound **AJ4** was obtained as a yellowish syrup, and $[\alpha]_D^{25}$ +4.6 (*c* 1.0 MeOH). The negative ESIMS exhibited molecular ion peak at *m/z* 311.10 $[M-H]^-$ indicating $C_{19}H_{20}O_4$ as its molecular formula. The IR spectrum revealed absorption bands corresponding to hydroxyl (3335 cm^{-1}) and carbonyl (1735 cm^{-1}) functions. The ^1H and ^{13}C NMR spectra of compound **AJ4** were similar to those of compound **AJ3** except for the substitution of hydroxyl group at C-5 [δ_H 3.61 (1H, m, H-5), δ_C 68.0] (Figure 16). The absolute configuration of a hydroxyl group at C-5 was confirmed by application of the modified Mosher's method (Hoye et al, 2007). (*S*)-MTPA ester (**AJ4s**) and (*R*)-MTPA ester (**AJ4r**) were prepared. As shown in Figure 17, the signals due to the protons at C-2 and C-4 in the **AJ4s** were observed at higher field in the ^1H NMR spectrum than those in the **AJ4r**, while the signals due to the protons at C-6 and C-7 in

AJ4s were observed at lower field than those in **AJ4r**. Thus, these data indicated an *S* configuration at C-5.Thus, compound **AJ4** was confirmed as alnusonol (Nomura et al., 1981).

Compound **AJ5** was yellowish syrup, and $[\alpha]_D^{25}$ -12.8 (*c* 0.3 MeOH). Its molecular formula was identified as $C_{19}H_{18}O_3$ by ESIMS (negative mode, 293.15 $[M-H]^-$). The IR spectrum revealed absorption bands corresponding to hydroxyl (3349 cm^{-1}) and carbonyl (1735 cm^{-1}) functions. The ^1H and ^{13}C NMR spectra of compound **AJ5** were similar to those of compound **AJ3** except for the apearing one double bond with *trans* configuration at δ_H 6.93 (1H, dt, *J* = 15.5, 7.6 Hz, H-5), and 6.63 (1H, d, *J* = 15.5 Hz, H-4) (Figure 18). Taken together, compound **AJ5** was determined as alnusone (Nomura et al., 1981).

Compound **AJ6** was obtained as yellowish syrup and $[\alpha]_D^{25}$ +1.8 (*c* 1.0 $CHCl_3$:MeOH=1:1). In IR spectrum, the absorption bands at 3373 cm^{-1} indicated the presence of hydroxyl functions, but the absorption band corresponding to carbonyl function was not observed, dissimilar to compounds **AJ3-5**. The ^1H NMR spectroscopic data revealed signals for 1,3,4-trisubstituted aromatic rings [δ_H 7.00 (1H, d, *J* = 8.0 Hz, H-5'), 6.79 (1H, d, *J* = 8.0 Hz, H-6'), and 6.68 (1H, br s, H-2')], signals for methylene at δ_H 2.79, and neighboring two hydroxy-bearing methane at δ_H 4.15 and 4.40, and signal for carbonyl group at δ_C 193.7 (Figure 19). The ^{13}C NMR spectrum showed ten carbon signals. Taken into account all of the above described spectroscopic data, compound **AJ6** was considered as arylbutanoid. However, the molecular formula of compound **AJ6** was established as $C_{19}H_{22}O_6$ by the observed pseudo-molecular ion peak at *m/z* 345.15 $[M-H]^-$ in the negative mode ESIMS. Thus, taking into account the above ^1H and ^{13}C NMR data, the structure of compound **AJ6** was also estimated to be symmetrical like compound **AJ2**. On the basis of these data, compound **AH6** was confirmed as betulatetraol (Lee et al., 1992).

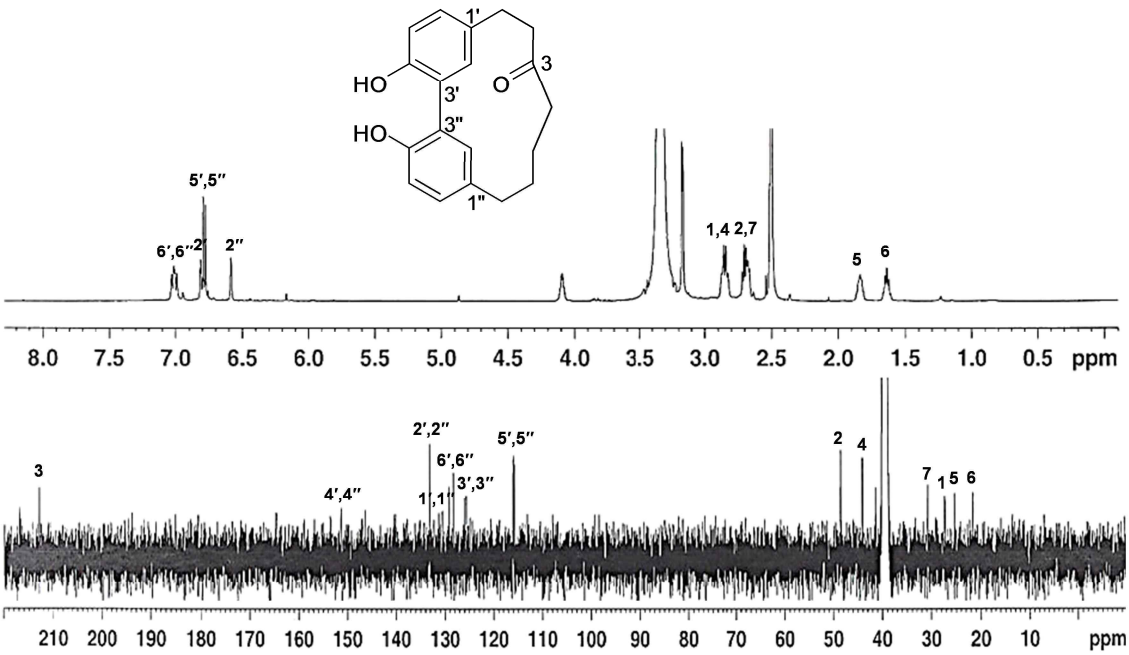

Figure 15. ^{1}H and ^{13}C NMR spectra of compound **AJ3**

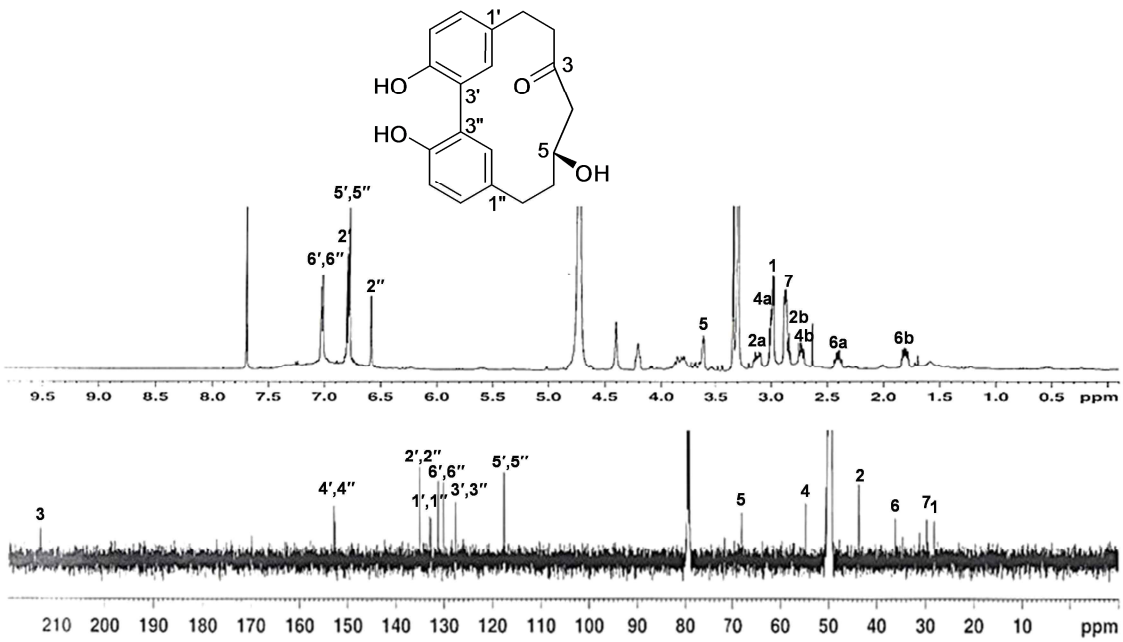

Figure 16. ^{1}H and ^{13}C NMR spectra of compound **AJ4**

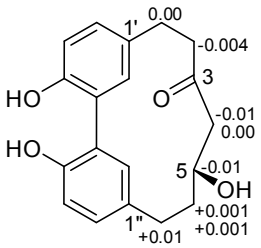

AJ4s R = (*S*)-MTPA ester

AJ4r R = (*R*)-MTPA ester

Figure 17. $\Delta\delta$ (δ_S-δ_R) (ppm) values obtained from MTPA esters for compound **AJ4**

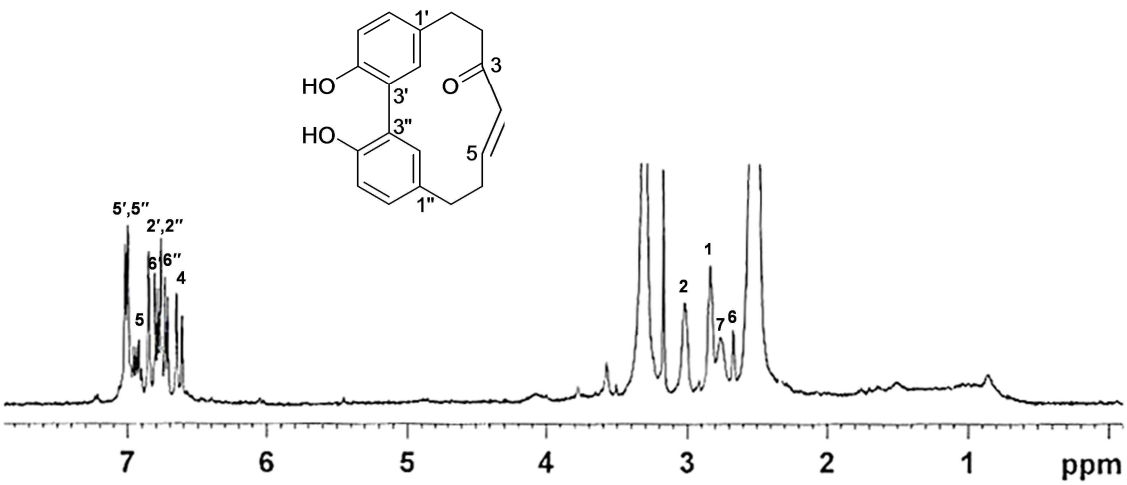

Figure 18. ^{1}H NMR spectrum of compound **AJ5**

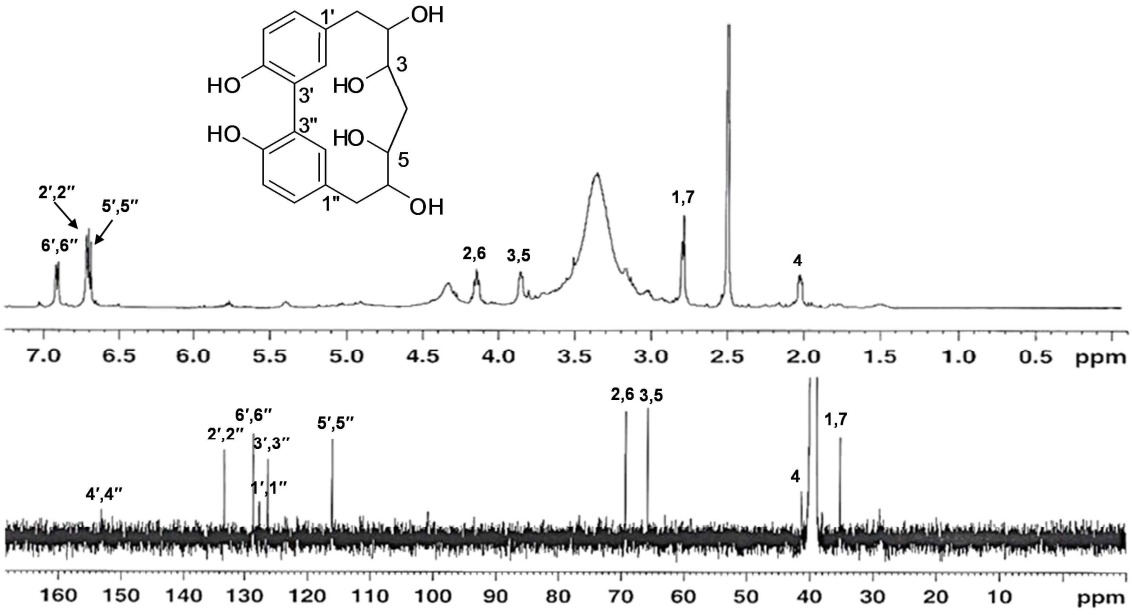

Figure 19. ^{1}H and ^{13}C NMR spectra of compound **AJ6**

1.4. Compound AH1

Compound **AH1** was obtained as a brownish syrup and $[\alpha]_D^{25}$ -7.6 (*c* 0.6 MeOH), and its molecular formula of $C_{19}H_{18}O_5$ was established by the observed pseudo-molecular ion peak at *m/z* 325.1078 $[M-H]^-$ (calcd. for $C_{19}H_{17}O_5$ 325.1076) in the negative HRFABMS. The IR spectrum showed the presence of hydroxyl (3249 cm^{-1}), carbonyl (1715 cm^{-1}) and *trans* double bond (984 cm^{-1}), and aromatic ring (1594, 1445 cm^{-1}) functions. The characteristic UV absorption at 259, 279, and 338 nm also suggested the presence of diarylheptanoid skeleton with *α,β*-unsaturated ketone. The ^{13}C NMR spectrum showed nineteen carbon signals, indicating two aromatic ring (δ_C 148.5, 145.6, 145.0, 143.3, 131.8, 126.0, 121.7, 118.4, 115.73, 115.65, 115.4, 114.9), two double bond (δ_C 146.4, 143.3, 129.3, 121.8), two methylene (δ_C 34.0, 33.2), and carbonyl (δ_C 188.1) carbons. The ^{1}H NMR spectroscopic data revealed signals for two

1,3,4-trisubstituted aromatic rings [δ_H 7.10 (1H, d, *J* = 1.4 Hz, H-2'), 6.77 (1H, d, *J* = 8.2 Hz, H-5'), and 7.04 (1H, dd, *J* = 8.2, 1.4 Hz, H-6')] and [δ_H 6.60 (1H, d, *J* = 1.9 Hz, H-2"), 6.63 (1H, d, *J* = 7.9 Hz, H-5"), and 6.46 (1H, dd, *J* = 7.9, 1.9 Hz, H-6")], signals for an isolated double bond with *trans* configuration at δ_H 7.45 (1H, d, *J* = 15.9 Hz, H-1), and 6.85 (1H, d, *J* = 15.9 Hz, H-2), and signals for two methylenes at δ_H 2.62 and 2.46, and one double bond with *trans* configuration at δ_H 6.94 (1H, dt, *J* = 15.7, 8.4 Hz, H-5) and 6.51 (1H, d, *J* = 15.7 Hz, H-4), similar to compound **AH5** except for an additional double bond (Figure 20). The HMBC correlations of H-1 to C-3, C-1', C-2' and C-6', H-5 to C-3, C-6, and C-7, and H-7 to C-1", C-2" and C-6" enabled us to construct structure **AH1** shown in Figure 20. Thus, compound **AH1** was determined as 1,4-heptadien-3-one-1,7-bis(3,4-dihydroxyphenyl)-(1*E*,4*E*) (Lai et al., 2012).

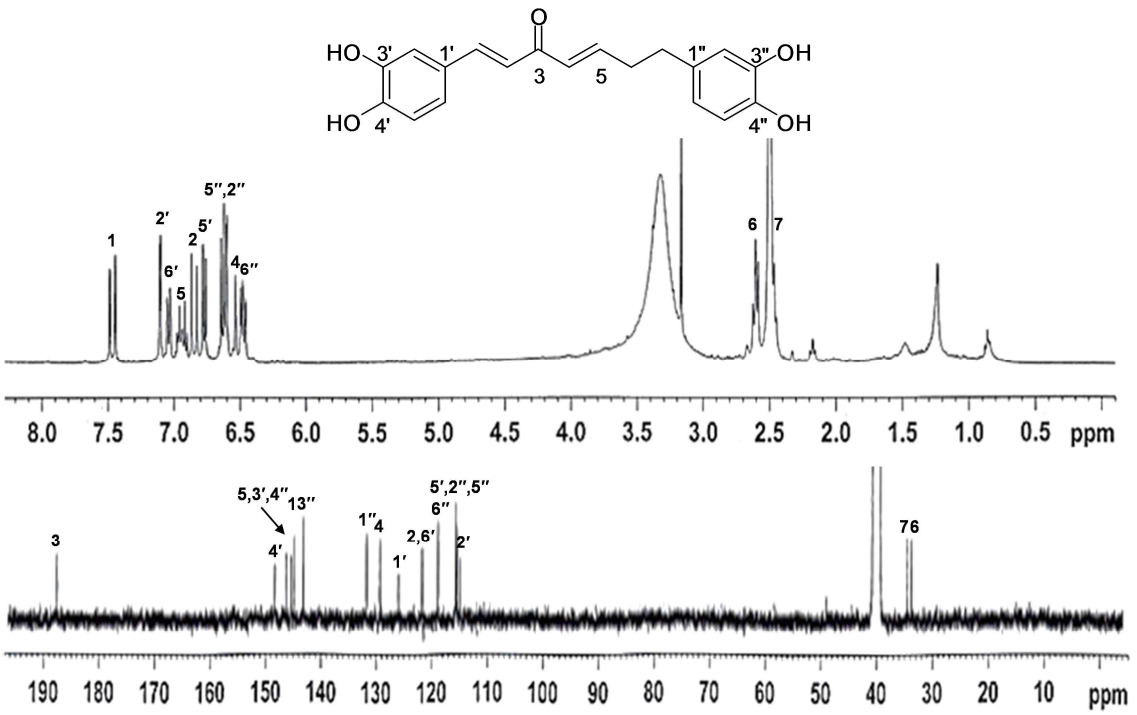

Figure 20. ^{1}H and ^{13}C NMR spectra of compound **AH1**

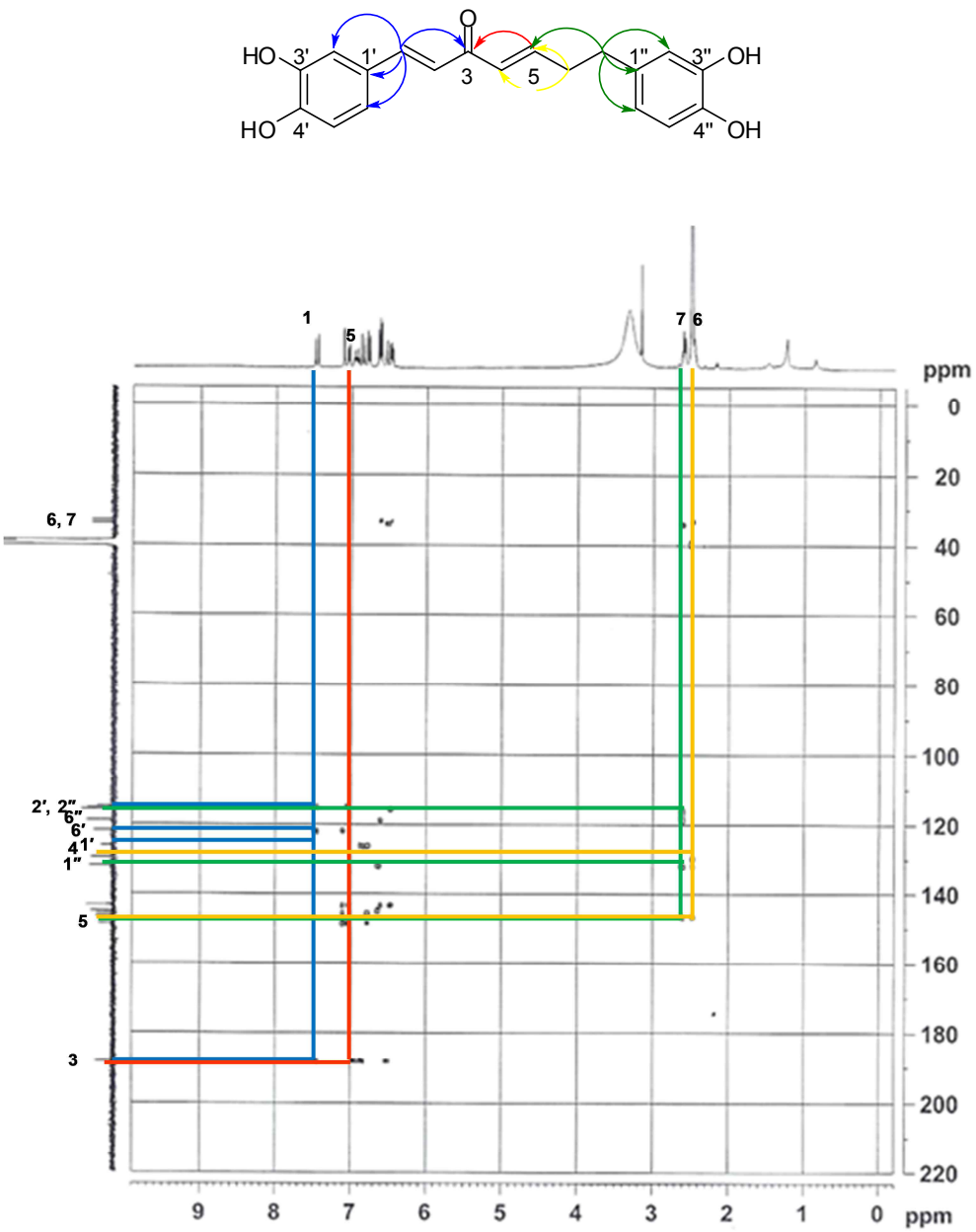

Figure 21. HMBC spectrum of compound **AH1**

1.5. Compound AH2

Compound **AH2** was obtained as brownish syrup and $[\alpha]_D^{25}$ -13.7 (*c* 0.2 MeOH) , and its molecular formula of $C_{19}H_{20}O_5$ was established by the observed pseudo-molecular ion peak at *m/z* 327.1225 $[M-H]^-$ (calcd. for $C_{19}H_{19}O_5$ 327.1232) in the negative HRFABMS. The IR spectrum showed the presence of hydroxyl (3266 cm^{-1}), carbonyl (1710 cm^{-1}), and *trans* double bond (1024 cm^{-1}), functions. The ^{13}C NMR spectrum showed nineteen carbon signals, indicating three methylene (δ_C 47.7, 40.5, 33.8), two aromatic ring [δ_C 157.4, 147.2, 135.0, 131.2 (x 2), 128.8, 124.5, 117.5, 117.0 (x 2), 116.3], *trans* double bond (δ_C 145.5, 125.5), hydroxyl (δ_C 69.7) and carbonyl (δ_C 202.4) carbons. The ^1H NMR spectrum revealed an 1,3,4-trisubstituted aromatic ring [δ_H 7.07 (1H, d, *J* = 2.0 Hz, H-2'), 6.98 (1H, dd, *J* = 8.4, 2.0 Hz, H-6'), and 6.78 (1H, d, *J* = 8.4 Hz, H-5')] and an 1,4-disubstituted aromatic ring [δ_H 7.01 (2H, d, *J* = 8.6 Hz, H-2",6"), 6.68 (2H, d, *J* = 8.6 Hz, H-3",5")], *trans* double bond [δ_H 7.50 (1H, d, *J* = 16.0 Hz, H-1), 6.60 (1H, d, *J* = 16.0 Hz, H-2)], and a secondary hydroxyl group [δ_H 4.06 (1H, m, H-5)]. Taken into account all of ^1H and ^{13}C NMR spectroscopic data, compound **AH2** bore a resemblance to those of compound **AH1** except for one double bond disappearing and instead one methylene carbon and one oxygenated carbon appearing (Figure 22). The location of the oxygenated carbon was established by the observed HMBC correlations of H-5 to C-3 as well as the sequential ^1H-^1H COSY correlations of H-4/H-5/H-6 (Figure 24-25). The absolute configuration of a hydroxyl group at C-5 was confirmed by application of the modified Mosher's method (Hoye et al, 2007). (*S*)-MTPA ester (**AH2s**) and (*R*)-MTPA ester (**AH2r**) were prepared. As shown in Figure 23, the signals due to the protons at C-1, C-2, and C-4 in the

AH2s were observed at higher field in the ^{1}H NMR spectrum than those in the **AH2r**, while the signals due to the protons at C-6 and C-7 in **AH2s** were observed at lower field than those in **AH2r**. Following MTPA rule, these data indicated an *S* configuration at C-5. With above observed spectroscopic data, compound **AH2** was determined to be (5*S*)-3,5'-dihydroxy-4'-methoxy-3',4''-oxo-1,7-diphenyl-1,3-diheptene and it was isolated for the first time from nature (Fuchino et al., 1996).

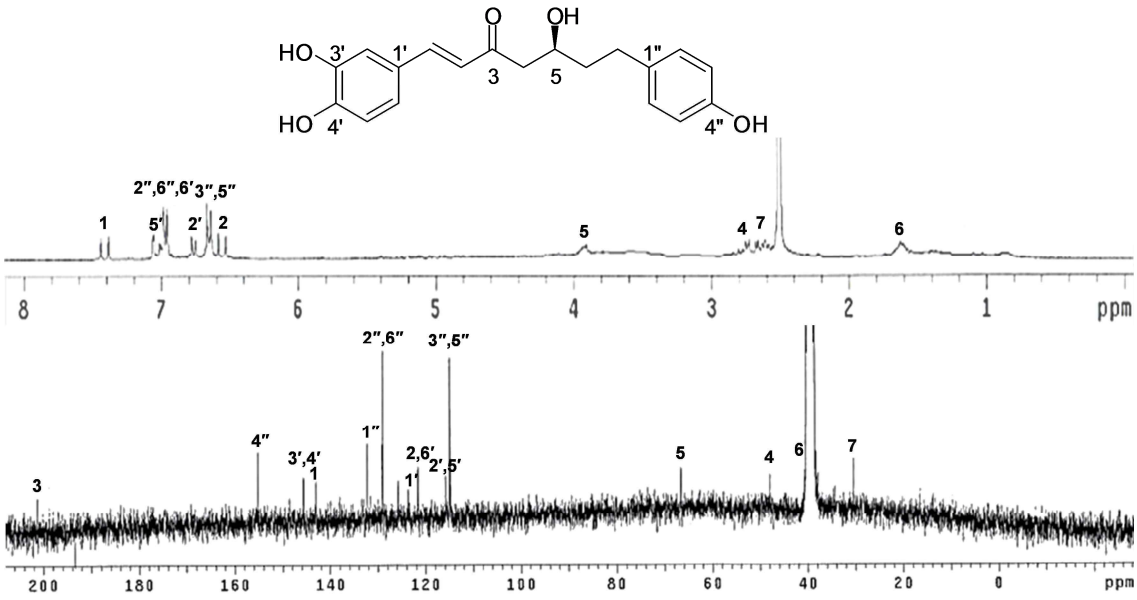

Figure 22. ^{1}H and ^{13}C NMR spectra of compound **AH2**

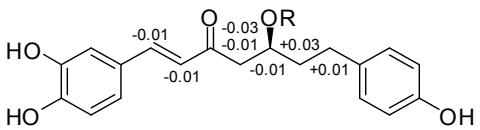

AH2r R = (*R*)-MTPA ester

AH2s R = (*S*)-MTPA ester

Figure 23. $\Delta\delta$ (δ_S-δ_R) (ppm) values obtained from MTPA esters for compound **AH2**

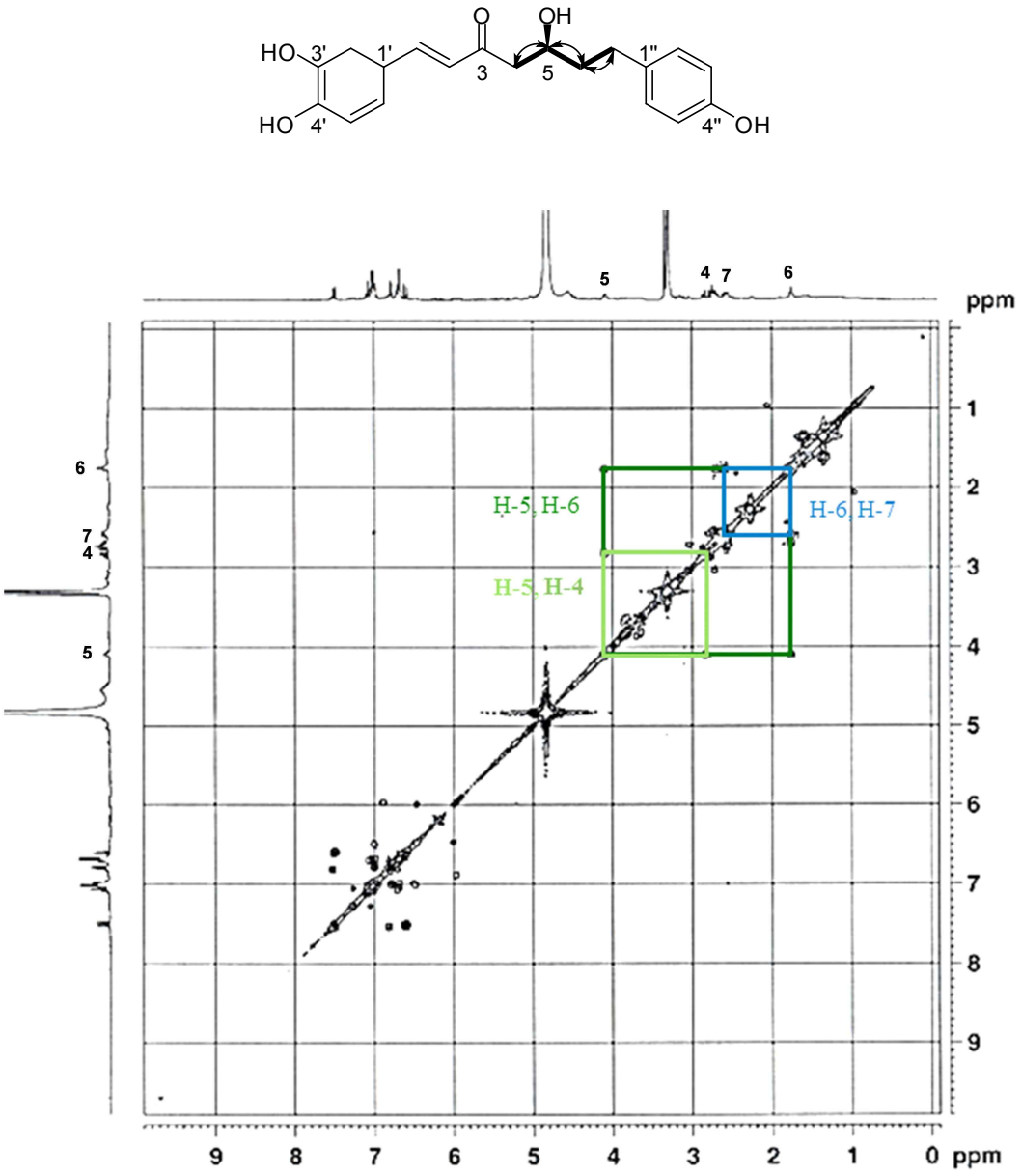

Figure 24. ^{1}H-^{1}H COSY spectrum of compound **AH2**

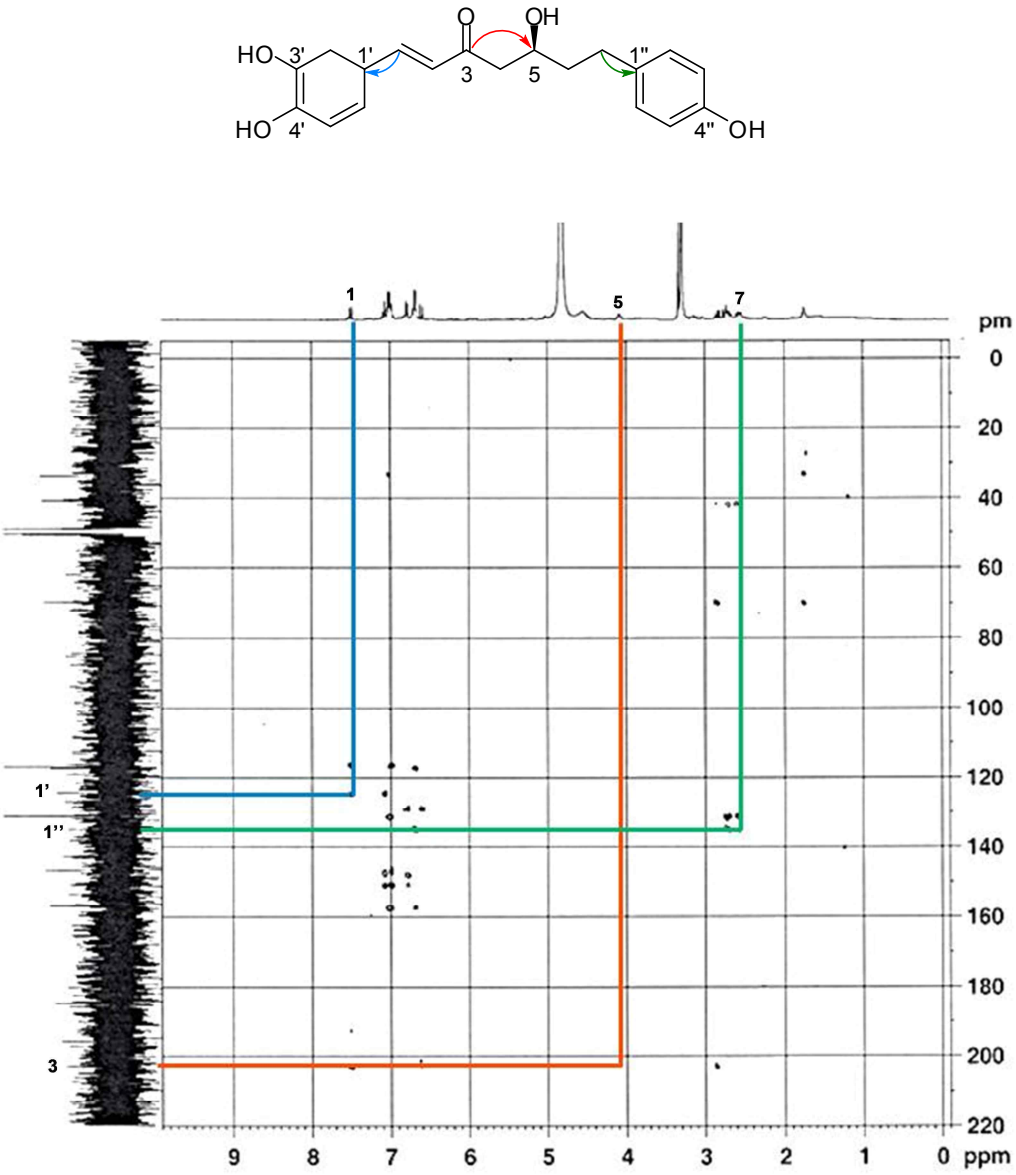

Figure 25. HMBC spectrum of compound **AH2**

1.6. Compound AH3-5

Compound **AH3** was obtained as yellowish syrup and and $[\alpha]_D^{25}$ +3.8 (*c* 1.0 MeOH). Its molecular formula was identified as $C_{19}H_{18}O_5$ by the negative mode ESIMS (*m/z* 327.03 $[M-H]^-$) and the ^{13}C NMR spectrum. The IR spectrum displayed characteristic absorption for hydroxyl (3294 cm^{-1}) and carbonyl (1716 cm^{-1}) functions. The characteristic UV absorption at 274 and 365 nm also suggested the presence of diarylheptanoid skeleton with conjugated double bonds. The ^1H NMR spectroscopic data revealed signals for two 1,3,4-trisubstituted aromatic rings [δ_H 6.63 (1H, d, *J* = 2.2 Hz, H-2'), 6.65 (1H, d, *J* = 8.0 Hz, H-5'), and 6.52 (1H, dd, *J* = 8.0, 2.2 Hz, H-6')] and [δ_H 6.98 (1H, d, *J* = 2.0 Hz, H-2''), 6.68 (1H, d, *J* = 8.2 Hz, H-5''), and 6.87 (1H, dd, *J* = 8.2, 2.0 Hz, H-6'')], signals for an isolated two double bond with *trans* configuration at δ_H 6.23, 7.37 (1H, dd, *J* = 15.3, 10.4 Hz, H-5), 6.89 (1H, d, *J* = 15.3 Hz, H-7), 6.76 (1H, dd, *J* = 15.3, 10.4 Hz, H-6) and 6.23 (1H, d, *J* = 15.3 Hz, H-4), and signals for two methylenes at δ_H 2.85 and 2.77, suggesting the presence of a diarylheptanoid skeleton similar to that of compound **AH1**, except for position of double bond (Figure 26). Therefore, the structure of compound was identified as 1,7-bis(3,4-dihydroxyphenyl)-hepta-4*E*,6*E*-dien-3one (Kikuzaki et al., 2001).

Compound **AH4** was obtained as yellowish syrup and $[\alpha]_D^{25}$ -15.9 (*c* 1.0 5% DMSO in MeOH). Its molecular formula was identified as $C_{19}H_{20}O_3$ by the negative mode ESIMS (*m/z* 295.03 $[M-H]^-$) and the ^{13}C NMR spectrum. The IR spectrum showed absorption for hydroxyl (3414 cm^{-1}) and carbonyl (1715 cm^{-1}) functions. The characteristic UV absorption at 278 nm also suggested that compound has a diarylheptanoid skeleton. The ^1H NMR spectroscopic data revealed signals for two 1,4-disubstituted aromatic rings [δ_H 6.97 (2H, d, *J* = 8.3 Hz, H-2', 6'), 6.67 (2H, d, *J* = 8.4 Hz, H-3', 5'), and δ_H 6.98 (2H, d, *J* = 8.3 Hz, H-2', 6'), 6.68 (2H, d, *J* = 8.3

Hz, H-3', 5'),], signals for double bond at δ_H 6.86 (1H, dt, *J* = 15.9, 7.0 Hz, H-5) and 6.04 (1H, d, *J* = 15.9 Hz, H-4), and signals for two methylenes at δ_H 2.65 and 2.46 (Figure 27). On the basis of above information, compound **AH4** was determined as 1,7-bis-(4-hydroxyphenyl)-5-hepten-3-one by comparison with literatures (Fuchino et al., 1996; Sunnerheimsjoberg and Knutsson, 1995).

Compound **AH5** was obtained as yellow syrup and $[\alpha]_D^{25}$ -6.9 (*c* 0.1 MeOH). Its molecular formula was identified as $C_{19}H_{20}O_5$ by the negative mode ESIMS (*m/z* 327.06 $[M-H]^-$) and the ^{13}C NMR spectrum. The IR spectrum showed the presence of hydroxyl (3365 cm^{-1}) and aromatic ring (1608, 1445 cm^{-1}) functions. The characteristic UV absorption at 282 nm also suggested the presence of diarylheptanoid skeleton. The ^1H and ^{13}C NMR spectra of compound **AH5** were similar to those of compound **AH4** except for the two 1,3,4-trisubstituted aromatic rings [δ_H 6.60 (21H, d, *J* = 2.0 Hz, H-2', 2"), 6.49 (2H, d, *J* = 8.0 Hz, H-5', 5"), and 6.46 (2H, dd, *J* = 8.0, 2.2 Hz, H-6', 6")] (Figure 28). With above observed spectroscopic data, compound **AH5** was confirmed as hirsutenone (Kuroyanagi et al., 2005).

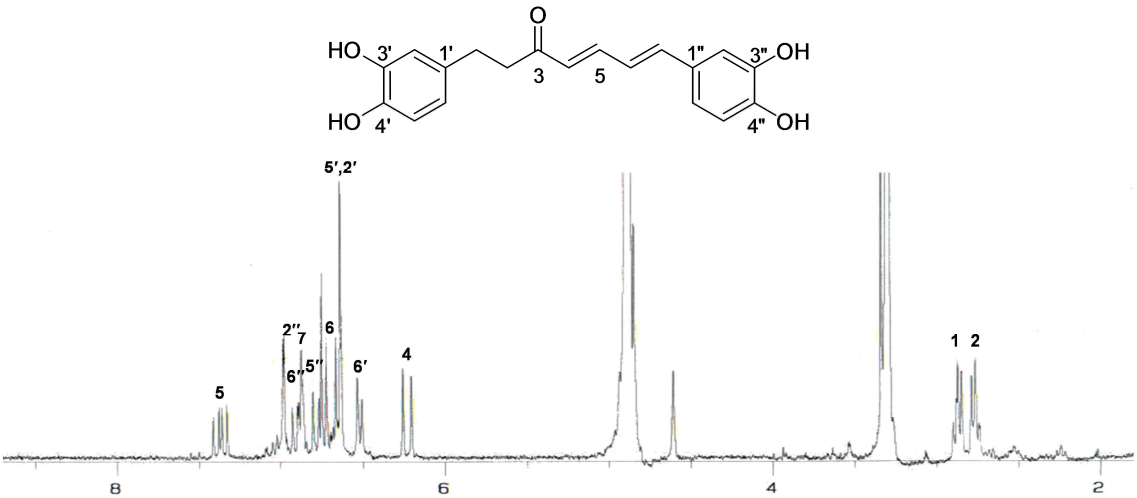

Figure 26. ^1H NMR spectrum of compound **AH3**

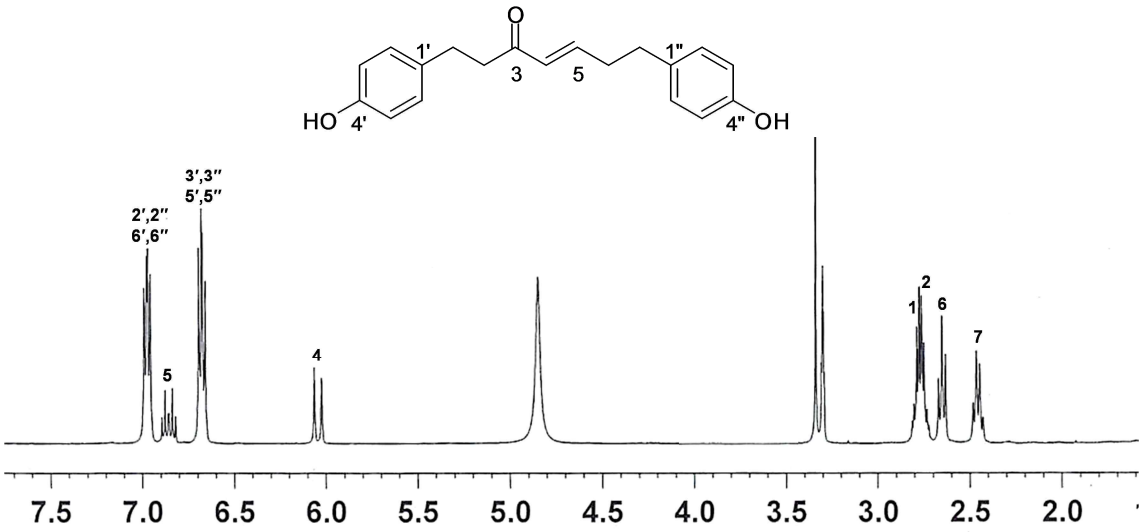

Figure 27. [1]H NMR spectrum of compound **AH4**

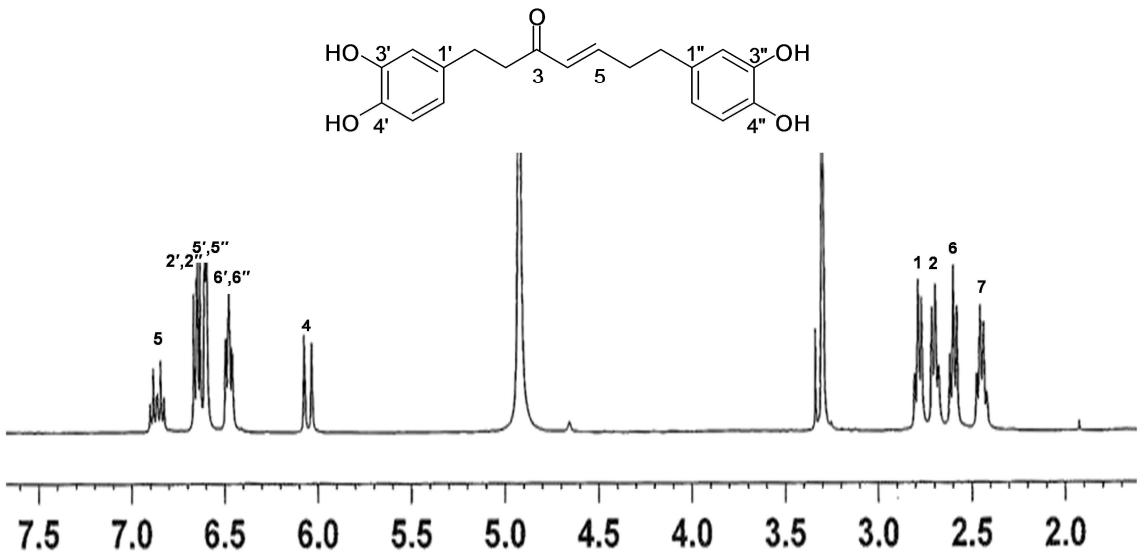

Figure 28. [1]H NMR spectrum of compound **AH5**

1.7. Compounds AH6, AJ9-10, and AF5

Compound **AH6** was obtained as yellowish syrup, and $[\alpha]_D^{25}$ -4.2 (*c* 1.0 MeOH). The negative ESIMS exhibited molecular ion peak at *m/z* 313.06 $[M-H]^-$ indicating $C_{19}H_{22}O_4$ as its molecular formula. The IR spectrum showed the presence of hydroxyl (3348 cm^{-1}), carbonyl (1702 cm^{-1}), and aromatic ring (1445 cm^{-1}) functions. The characteristic UV absorption at 278 nm indicated the presence of diarylheptanoid skeleton. The ^{13}C NMR spectrum showed nineteen carbon signals, indicating two aromatic ring [δ_C 157.5, 157.4, 134.0, 133.8, 131.2 (x 2), 131.1 (x 2), 117.0 (x 4)], five methylene (δ_C 52.0, 47.2, 41.3, 32.7, 30.6), oxygenated methane (δ_C 69.0) and carbonyl (δ_C 212.7) carbons. The ^1H NMR spectroscopic data revealed signals for two 1, 4-disubstituted aromatic ring [δ_H 6.98 (4H, d, *J* = 8.2 Hz, H-2', 6',2",6"), 6.68 (2H, d, *J* = 8.4 Hz, H-3", 5"), 6.67 (2H, d, *J* = 8.4 Hz, H-3', 5')], signals for hydroxy-bearing methane at δ_H 4.03 (Figure 29). Taken together, compound **AH6** was determined as 5-hydroxy-3-platyphyllone (Sunnerheimsjoberg and Knutsson, 1995).

Compound **AJ9** was obtained as yellowish syrup, and $[\alpha]_D^{25}$ -10.3 (*c* 0.5 MeOH). The negative ESIMS exhibited molecular ion peak at *m/z* 444.85 $[M-H]^-$ indicating $C_{24}H_{30}O_8$ as its molecular formula. The ^1H and ^{13}C NMR spectra of compound **AJ9** were similar to those of compound **AH6** except for the signals of xylopyranoside moiety [δ_C 102.6 (C-1'"), 76.7 (C-3'"), 73.4 (C-2'"), 69.6 (C-4'"), 65.8 (C-5'")] (Figure 30). Based on the correlation between δ_H/δ_C 4.11 (H-5)/102.6 (C-1'") in the HMBC analysis, the position of the xylopyranoside moiety was confirmed to be at C-5. Therefore, compound **AJ9** was confirmed as platyphyllonol-5-*O*-*β*-D-xylopyranoside (Chen et al., 2000).

Compound **AJ10** was obtained as brownish syrup, and its molecular formula of $C_{25}H_{32}O_9$ was established by the observed pseudo-molecular ion peak at *m/z* 475.02 $[M-H]^-$ in the negative ESIMS. The ^1H and ^{13}C NMR spectra of compound **AJ10** were similar to those of compound **AH6** except for the signals of glucopyranoside moiety [δ_C 104.2 (C-1‴), 78.8 (C-3‴), 76.0 (C-2‴), 78.6 (C-5‴), 72.4 (C-4‴), 63.5 (C-6‴)] (Figure 31). The HMBC analysis indicated that the sugar moiety was attached at C-5 of aglycone by the correlation from δ_H 4.04 (1H, m, H-5) to δ_C 104.2 (C-1″). On the basis of above information, compound **AJ10** was determined as platyphylloside (Smite et al., 1993).

Compound **AF5** was obtained as brownish syrup, and $[\alpha]_D^{25}$ -55.9 (*c* 0.1 MeOH). The negative ESIMS exhibited molecular ion peak at *m/z* 607.10 $[M-H]^-$ indicating $C_{30}H_{40}O_{13}$ as its molecular formula. The ^1H and ^{13}C NMR spectra of compound **AF5** were similar to those of compound **AH6** except for the signals of apiofuranoside (1⁗→6‴)-glucopyranoside moiety at C-5 [δ_C 104.4 (C-1‴), 78.9 (C-3‴), 77.6 (C-5‴), 76.1 (C-2‴), 72.4 (C-4‴), 69.3 (C-6‴), 111.7 (C-1⁗), 81.3 (C-3⁗), 77.2 (C-2⁗), 75.9 (C-4⁗), 66.6 (C-5⁗)] by the correlation between δ_H/ δ_C 3.90 (1H, m, H-5)/ δ_C 104.4 (C-1‴) and 3.62 (1H, dd, *J* = 8.2 Hz, H-6‴)/ δ_C 104.4 (C-1⁗) in the HMBC spectrum (Figure 32). With above mentioned spectroscopic data, compound **AF5** was determined as (5*S*)-5-hydroxy-1,7-bis-(4-hydroxyphenyl)-3-heptanone-5-*O*-*β*-D-apiofuranosyl-(1→6)-*β*-D-glucopyranoside (Smite et al., 1993).

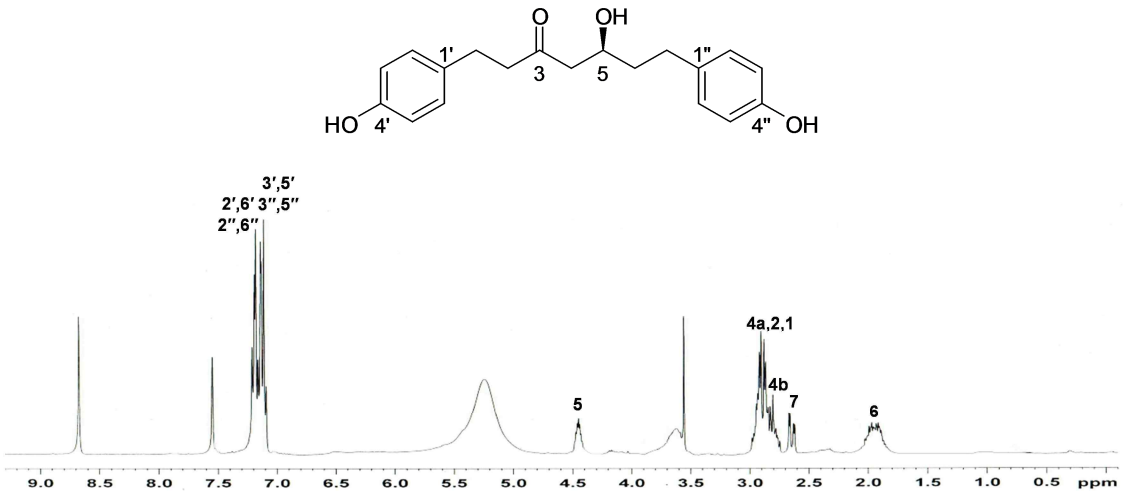

Figure 29. ^{1}H NMR spectrum of compound **AH6**

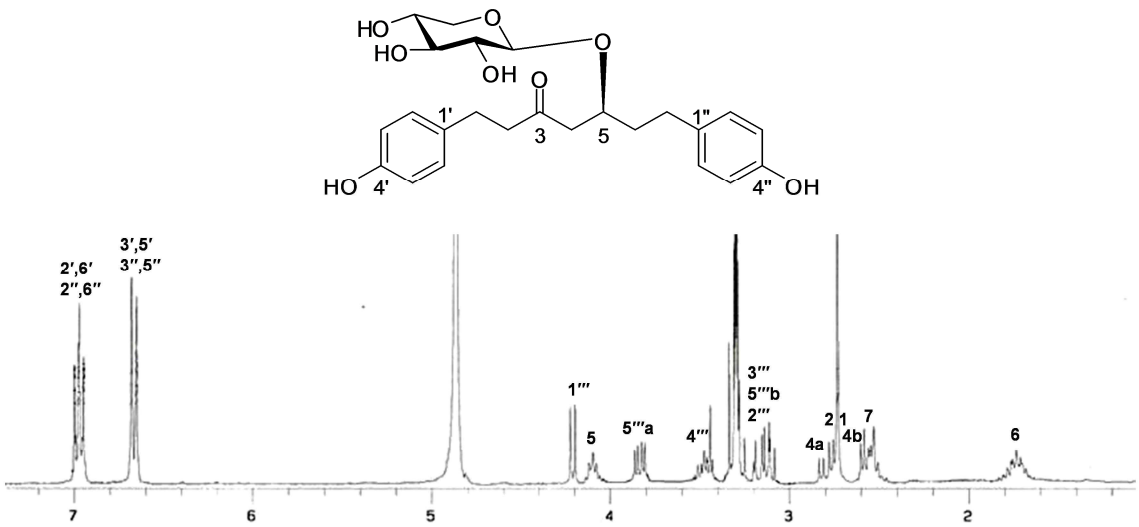

Figure 30. ^{1}H NMR spectrum of compound **AJ9**

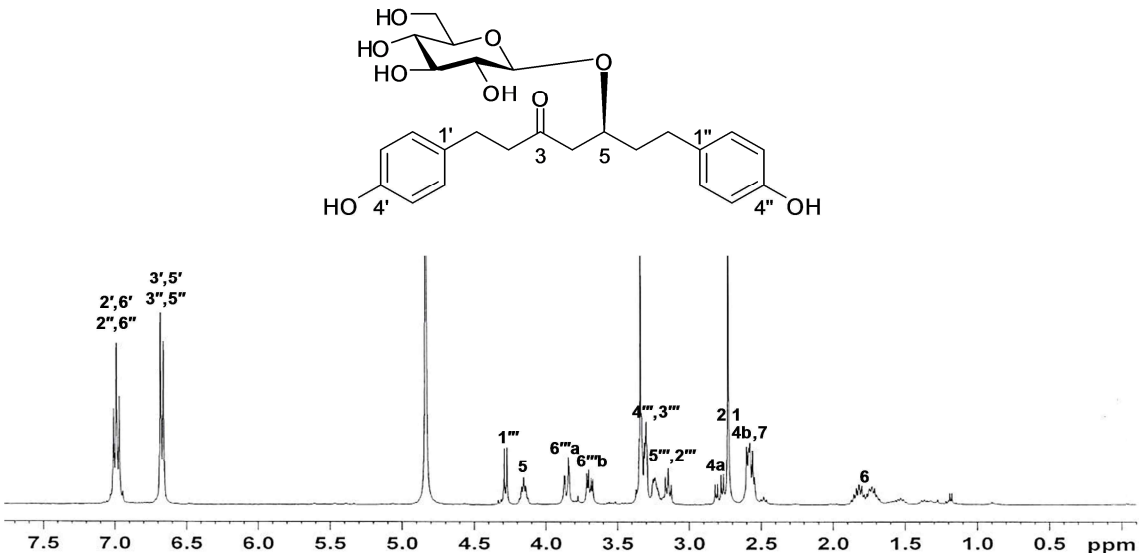

Figure 31. [1]H NMR spectrum of compound **AJ10**

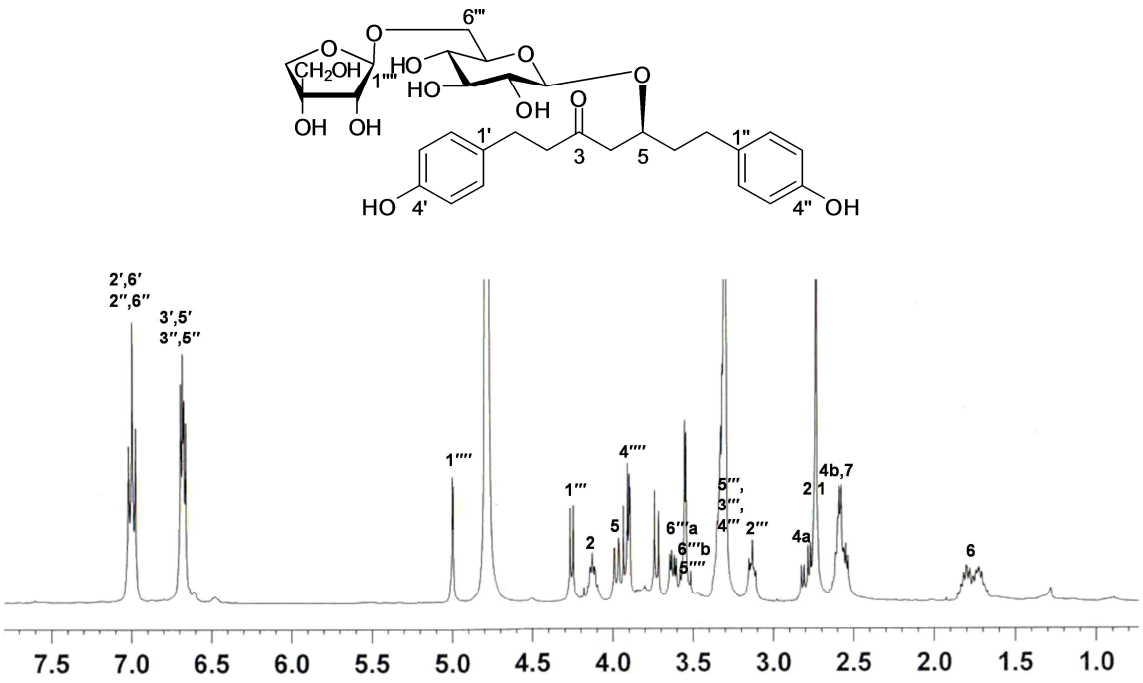

Figure 32. [1]H NMR spectrum of compound **AF5**

1.8. Compounds AH9 and AJ11

Compound **AH9** was obtained as yellowish syrup, and $[\alpha]_D^{25}$ -1.8 (*c* 1.0 MeOH). The negative ESIMS exhibited molecular ion peak at *m/z* 328.95 $[M-H]^-$ indicating $C_{19}H_{22}O_5$ as its molecular formula. The IR spectrum showed the presence of hydroxyl (3345 cm^{-1}) and carbonyl (1710 cm^{-1}) functions. The characteristic UV absorption at 281 nm indicated the presence of diarylheptanoid skeleton. The ^1H NMR spectroscopic data revealed signals for 1, 4-disubstituted aromatic ring [δ_H 6.98 (2H, d, *J* = 8.4 Hz, H-2', 6'), 6.66 (2H, d, *J* = 8.4 Hz, H-3", 5")], and 1, 3, 4-trisubstituted aromatic ring [δ_H 6.59 (1H, d, *J* = 8.0 Hz, H-5'), 6.53 (1H, d, *J* = 2.0 Hz, H-2'), and 6.35 (1H, dd, *J* = 8.0, 2.0 Hz, H-6')] (Figure 33). In addition, the ^{13}C-NMR spectroscopic data showed the presence of seven carbon of the 5-hydroxy-heptan-3-one presence [δ_C 209.5 (C-3), 67.2 (C-5), 51.1 (C-4), 44.9 (C-2), 40.3 (C-6), 31.8 (C-7), 28.4 (C-1)]. Consequently, the structure of compound **AH9** was determined as (5*S*)-5-hydroxy-1-(4-hydroxyphenyl)-7-(3,4-dihydroxyphenyl)-3-heptanone (Li et al., 2011).

Compound **AJ11** was obtained as yellowish syrup, and $[\alpha]_D^{25}$ -14.7 (*c* 1.0 MeOH). The negative ESIMS exhibited molecular ion peak at *m/z* 461.10 $[M-H]^-$ indicating $C_{24}H_{30}O_9$ as its molecular formula. The ^1H and ^{13}C NMR spectra of compound **AJ11** were similar to those of compound **AH9** except for the signal of xylopyranoside moiety [δ_C 102.6 (C-1'"), 76.7 (C-3'), 73.4 (C-2'"), 69.6 (C-4'"), 65.8 (C-5'")] (Figure 34). In the HMBC analysis, the location of the xylopyranoside moiety was at C-5 by the correlation peak from δ_H 3.99 (OCH_3) to δ_C 102.6 (C-1'"). Therefore, compound **AJ11** was confirmed as (5*S*)-5-hydroxy-7-(3,4-dihydroxyphenyl)-1-(4-hydroxyphenyl)-3-heptanone-5-*O*-*β*-D-xylopyranoside (Kuroyanagi et al., 2005)

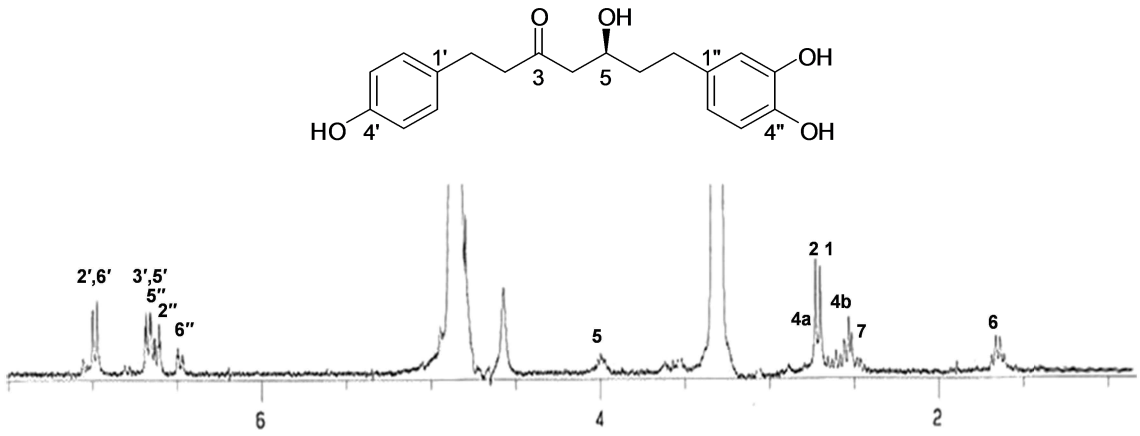

Figure 33. ^{1}H NMR spectrum of compound **AH9**

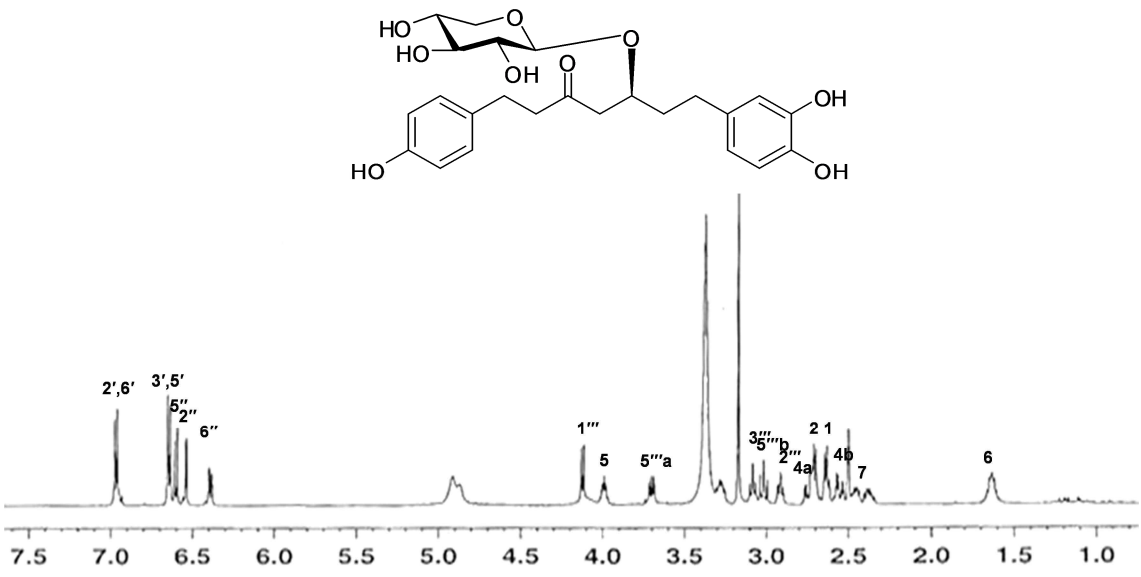

Figure 34. ^{1}H NMR spectrum of compound **AJ11**

1.9. Compound AJ12

Compound **AJ12** was obtained as brownish syrup, $[\alpha]_D^{25}$ -3.5 (*c* 1.0 MeOH) and showed the ion peak at *m/z* 491.1916 $[M-H]^-$ (calcd. for $C_{25}H_{32}O_{10}$ 491.1917) in the negative HRFABMS indicating its molecular formula ($C_{25}H_{32}O_{10}$). The IR spectrum displayed characteristic absorptions for hydroxyl (3373 cm^{-1}) and carbonyl (1715 cm^{-1}) functions. The charctreristic UV absorption at 281 nm suggested that compound has a diarylheptanoid skeleton. The ^1H NMR spectroscopic data revealed signals for 1,4-disubstituted aromatic ring [δ_H 6.98 (2H, d, *J* = 8.4 Hz, H-2', 6'), 6.66 (2H, d, *J* = 8.4 Hz, H-3", 5")], and 1,3,4-trisubstituted aromatic ring [δ_H 6.59 (1H, d, *J* = 8.0 Hz, H-5'), 6.54 (1H, br s, H-2'), and 6.40 (1H, br d, *J* = 8.0 Hz, H-6')], a secondary hydroxyl moiety [δ_H 4.04 (1H, m, H- 5)] (Figure 35). The ^{13}C NMR spectrum showed nineteen carbon signals, indicating two aromatic ring [δ_C 155.0, 145.1, 143.4, 131.9, 131.1, 129.0 (x 2), 118.9, 115.4 (x 2), 115.2 (x 2)], five methylene (δ_C 51.1, 44.9, 40.3, 31.8, 28.4), oxygenated methane (δ_C 67.2) and carbonyl (δ_C 209.5) carbons, similar to those of compound **AH9** except for the signals of glucopyranoside moiety [δ_C 101.9 (C-1'"), 76.8 (C-3'"), 73.5 (C-2'"), 74.2 (C-5'"), 70.1 (C-4'"), 61.0 (C-6'")]. Acid hydrolysis of compound **AJ12** and HILIC-MS analysis afforded D-glucose; the retention times (t_R 6.63 min) and mass spectra (m/z 160.83 $[C_6H_{12}O_6-H_2O-H]^-$, 178.79 $[C_6H_{12}O_6-H]^-$, 224.73 $[C_6H_{12}O_6+HCOOH-H]^-$) of the sugar released on acid hydrolysis were compared with the authentic sample of D-glucose. The coupling constant of doublet at δ_H 4.15 (*J* = 7.7) established the *β*–configuration of the glucose moiety. The HMBC correlations of H-1'" to C-5 indicated that the glucose unit was located at C-5 of the aglycone (Figure 36). On the basis of above information, compound **AJ12** was determined as 5-hydroxy-7-(3,4-dihydroxyphenyl)-1-(4-hydroxyphenyl)-3-heptanone-5-*O*-*β*-D-glucopyranoside

and was first isolated from nature.

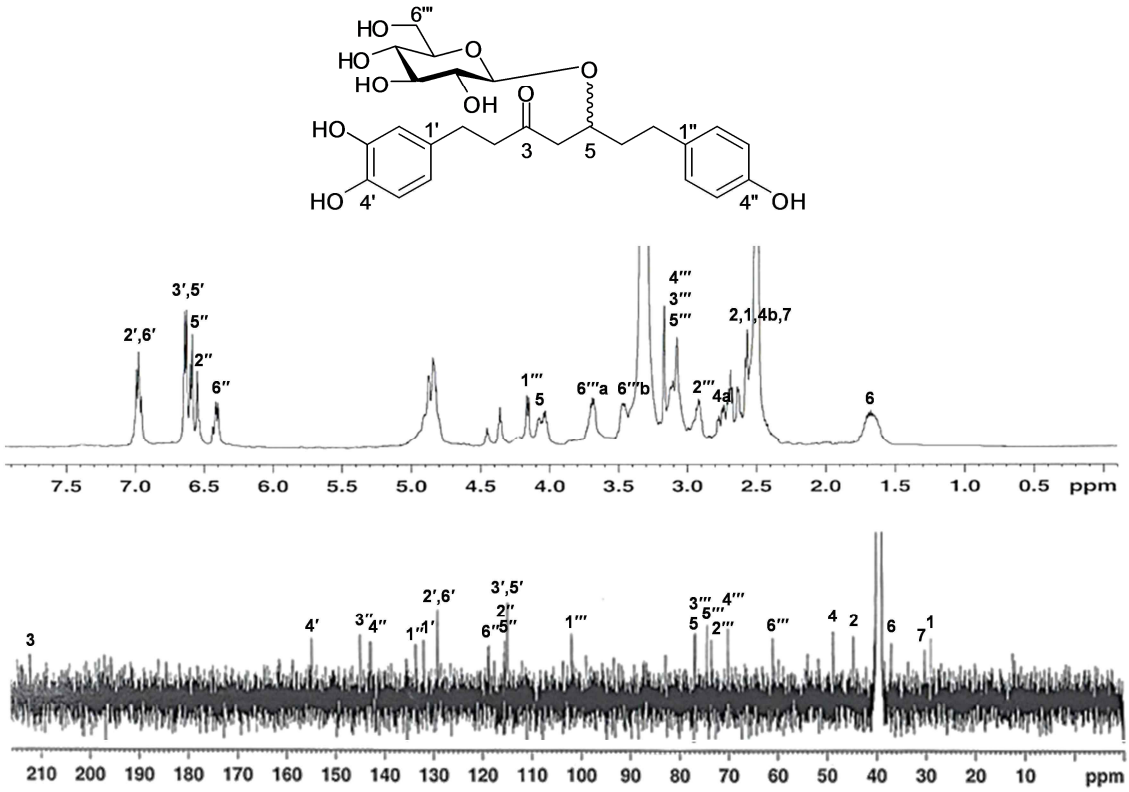

Figure 35. ^{1}H and ^{13}C NMR spectra of compound **AJ12**

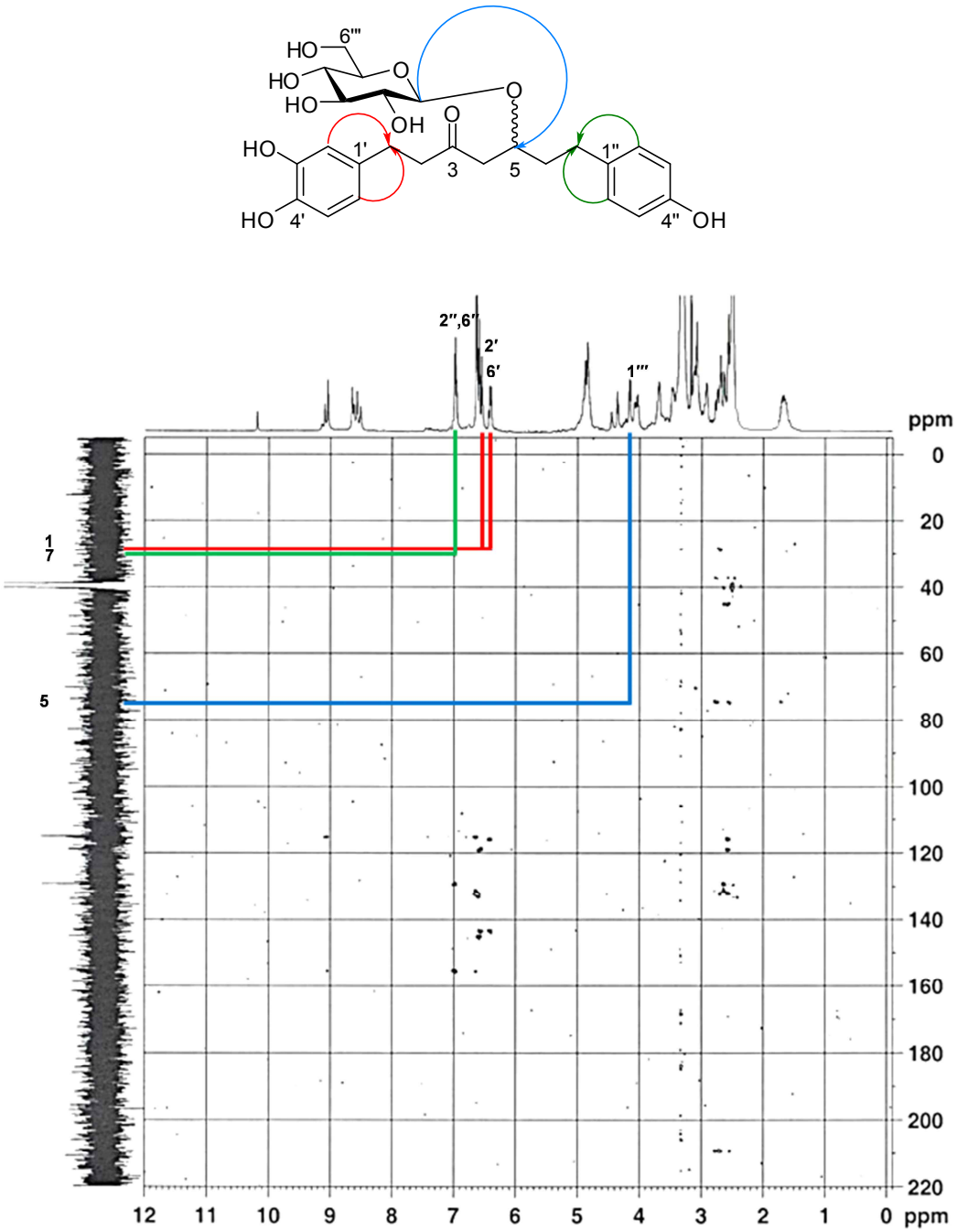

Figure 36. HMBC spectrum of compound **AJ12**

1.10. Compounds AH11, AJ13-15, and AF7

Compound **AH11** was obtained as yellowish syrup, and $[\alpha]_D^{25}$ -2.6 (*c* 1.0 MeOH). The negative ESIMS exhibited molecular ion peak at *m/z* 344.97 $[M-H]^-$ indicating $C_{19}H_{22}O_6$ as its molecular formula. The IR spectrum showed the presence of hydroxyl (3339 cm^{-1}) and carbonyl (1710 cm^{-1}) functions. The characteristic UV absorption at 280 nm indicated the presence of diarylheptanoid skeleton. The ^1H NMR spectroscopic data revealed signals for two 1, 3, 4-trisubstituted aromatic ring [δ_H 6.66 (1H, d, *J* = 8.0 Hz, H-5"), 6.63 (1H, d, *J* = 8.0 Hz, H-5'), 6.60 (2H, d, *J* = 2.2 Hz, H-2',2"), 6.47 (2H, dd, *J* = 8.0, 2.2 Hz, H-6',6")] (Figure 37). In addition, the ^{13}C-NMR spectroscopic data showed the presence of seven carbon of the 5-hydroxy-heptan-3-one presence [δ_C 209.6 (C-3), 67.2 (C-5), 49.2 (C-4), 44.7 (C-2), 40.1 (C-6), 31.8 (C-7), 28.4 (C-1)]. With above observed spectroscopic data, compound **AH11** was determined as hirsutanonol (Gonzalez-Laredo et al., 1998).

Compound **AJ13** was obtained as yellowish syrup, and $[\alpha]_D^{25}$ -21.1 (*c* 0.1 MeOH). The negative ESIMS exhibited molecular ion peak at *m/z* 477.02 $[M-H]^-$ indicating $C_{24}H_{30}O_{10}$ as its molecular formula. The ^1H and ^{13}C NMR spectra of compound **AJ13** were similar to those of compound **AH11** except for the signals of xylopyranoside moiety at C-5 [δ_C 102.7 (C-1'"), 76.8 (C-3'"), 73.5 (C-2'"), 69.7 (C-4'"), 65.9 (C-5'")] (Figure 38). On the basis of the correlated peaks from δ_H 4.08 (1H, m, H-5) to δ_C 102.7 (C-1'") in the HMBC experiment, it was confirmed that the sugar moiety was linked at C-5 of the aglycone. Therefore, compound **AJ13** was confirmed as oregonin (Kuroyanagi et al., 2005).

Compound **AJ14** was obtained as brownish syrup, and its molecular formula of $C_{25}H_{32}O_{11}$

was established by the observed pseudo-molecular ion peak at *m/z* 507.10 $[M-H]^-$ in the negative ESIMS. The ^1H and ^{13}C NMR spectra of compound **AJ14** were similar to those of compound **AH11** except for the signals of glucopyranoside moiety at C-5 [δ_C 101.7 (C-1'''), 77.8 (C-3'''), 73.5 (C-2'''), 73.7 (C-5'''), 70.1 (C-4'''), 61.2 (C-6''')]. In the HMBC spectrum, the signal at δ_H 4.10 (H-5) was correlated with that at δ_C 101.7 (C-1'''). This result indicated that the D-glucose group was attached at C-5 of the aglycone. From obtained spectral data and above analysis, compound **AJ14** was determined as hitsutanonol 5-*O*-*β*-D-glucopyranoside (Park et al., 2010) (Figure 39).

Compound **AJ15** was obtained as a brownish syrup, and $[\alpha]_D^{25}$ +2.1 (*c* 1.0 MeOH). The negative FABMS exhibited molecular ion peak at *m/z* 359 $[M-H]^-$ indicating $C_{20}H_{24}O_6$ as its molecular formula. The ^1H and ^{13}C NMR spectra of compound **AJ15** was similar to those of compound **AH11** except for the substitution of methoxy moiety [δ_C 55.4 (C-OCH_3)]. The HMBC analysis indicated that the methoxy moiety was attached at C-5 by the correlation from δ_H 3.58 (1H, s, H-5) to δ_C 55.4 (C-OCH_3). Taken together, compound **AJ15** was confirmed as (5*S*)-*O*-methylhirsutanonol in comparison with previously reported literature (Park et al., 2010) .

The negative FABMS spectrum of compound **AF7** showed the ion peak at *m/z* 359 $[M-H]^-$ indicating $C_{20}H_{24}O_6$ as its molecular formula. In comparison with the 1D and 2D NMR spectral data of compound **AJ15**, the structure of compound **AF7** was also identified as 5-*O*-methylhirsutanonol. However, the absolute stereochemistry of the methoxy group at C-5 determined to be 5*R* on the basis of the negative sign of the optical rotation, $[\alpha]^{25}_D$ -11.7 (*c* 1.0 MeOH) in comparison with compound **AJ15**. From obtained spectral data and above analysis, compound **AF7** was concluded as (5*R*)-*O*-methylhirsutanonol (Giang et al., 2006) (Figure 39).

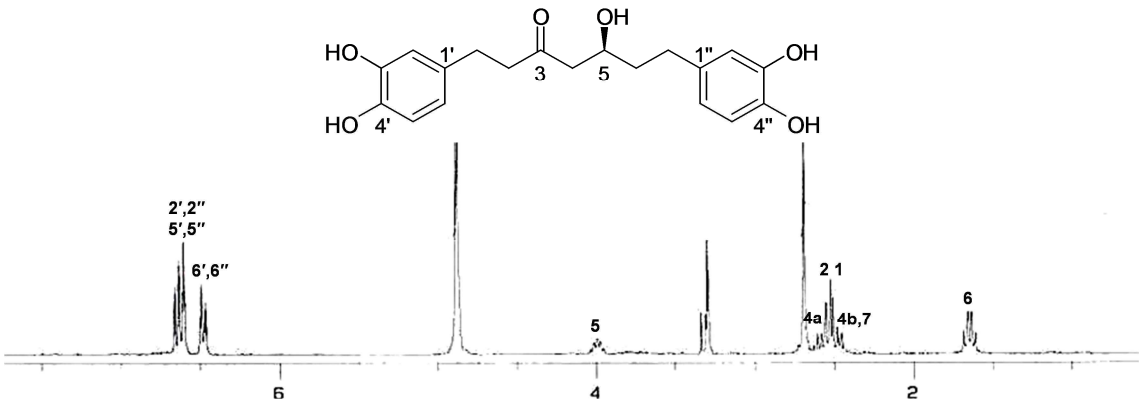

Figure 37. ^{1}H NMR spectrum of compound **AH11**

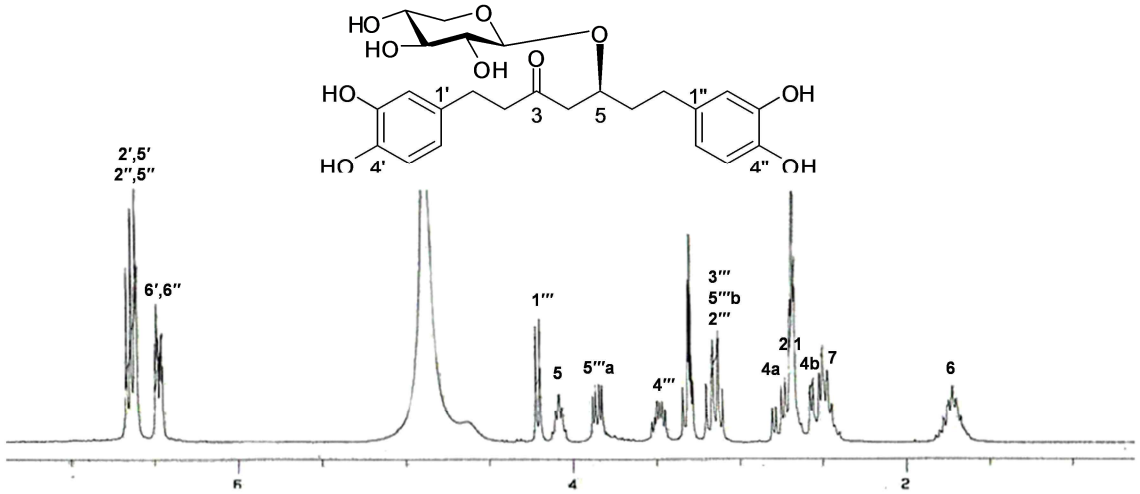

Figure 38. ^{1}H NMR spectrum of compound **AJ13**

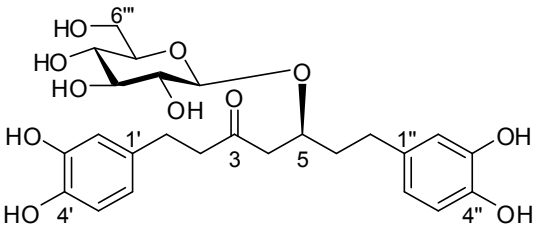

AJ14

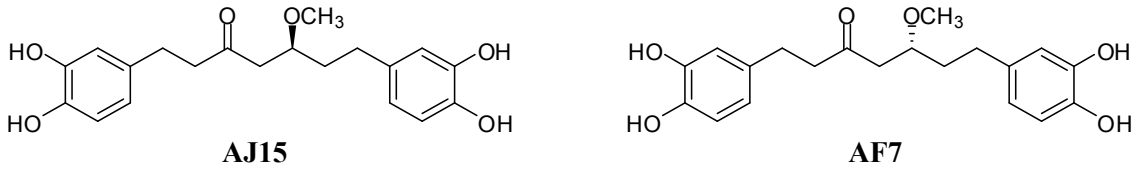

AJ15 **AF7**

Figure 39. The structures of compounds **AJ14**, **AJ15** and **AF7**

1.11. Compounds AJ16-J18

Compound **AJ16** was obtained as brownish syrup and $[\alpha]_D^{25}$ -2.6 (*c* 1.0 MeOH). Its molecular formula was identified as $C_{33}H_{36}O_{11}$ by the negative mode ESIMS (*m/z* 607.08 [M-H]$^-$) and the ^{13}C NMR spectrum. The ^{1}H and ^{13}C NMR spectra of compound **AJ16** were similar to those of compound **AJ13** except for the substitution of cinnamoyl moiety at C-2''' [δ_H 7.68 (1H, d, *J* = 16.0 Hz, H-7''''), 7.52 (2H, m, H-2'''', 6''''), 7.36 (1H, m, H-4''''), 7.35 (2H, m, H-3'''', 5''''), and 6.58 (1H, d, *J* = 16.0 Hz, H-8'''')] by the correlation between δ_H 4.58 (1H, td, *J* = 6.5, 3.8 Hz, H-2''') and δ_C 165.5 (C-9''') in the HMBC spectrum (Figure 40). With above observed spectroscopic data, compound **AJ16** was confirmed as 2'''-cinnamoyloregonin (Lee et al., 2006).

Compound **AJ17** was obtained as brownish syrup and $[\alpha]_D^{25}$ -2.0 (*c* 1.0 MeOH). Its molecular formula was identified as $C_{33}H_{36}O_{12}$ by the negative mode ESIMS (*m/z* 623.10 [M-H]$^-$) and the ^{13}C NMR spectrum. The compound **AJ17** were substituted coumaroyl moiety [δ_H 7.54 (1H, d, *J* = 15.9 Hz, H-7''''), 7.47 (2H, d, *J* = 8.6 Hz, H-2'''', 6''''), 6.77 (2H, d, *J* = 8.6 Hz, H-3'''', 5''''), and 6.39 (1H, d, *J* = 15.9 Hz, H-8'''')] at C-2''' of compound **AJ16**, instead of cinnamoyl moiety (Figure 41). On the basis of above information, compound **AJ17** was determined as oregonyl A by comparison with literatures (Tung et al., 2010b).

Compound **AJ18** was obtained as brownish syrup and $[\alpha]_D^{25}$ -1.6 (*c* 1.0 MeOH). Its

molecular formula was identified as $C_{33}H_{38}O_{13}$ by the negative mode ESIMS (*m/z* 653.08 $[M-H]^-$) and the ^{13}C NMR spectrum. In the same manner, the compound **AJ18** were substituted feruloyl moiety [δ_H 7.54 (1H, d, *J* = 15.9 Hz, H-7""), 7.26 (2H, br s, H-2""), 7.07 (1H, d, *J* = 8.1 Hz, H-5""), 6.77 (1H, dd, *J* = 8.1, 2.0 Hz, H-6""), and 6.37 (1H, d, *J* = 15.9 Hz, H-8"")] at C-2"" of compound **AJ16**, instead of cinnamoyl moiety (Figure 42). Thus, compound **AJ18** was confirmed as oregonyl B by comparison with literatures (Tung et al., 2010b).

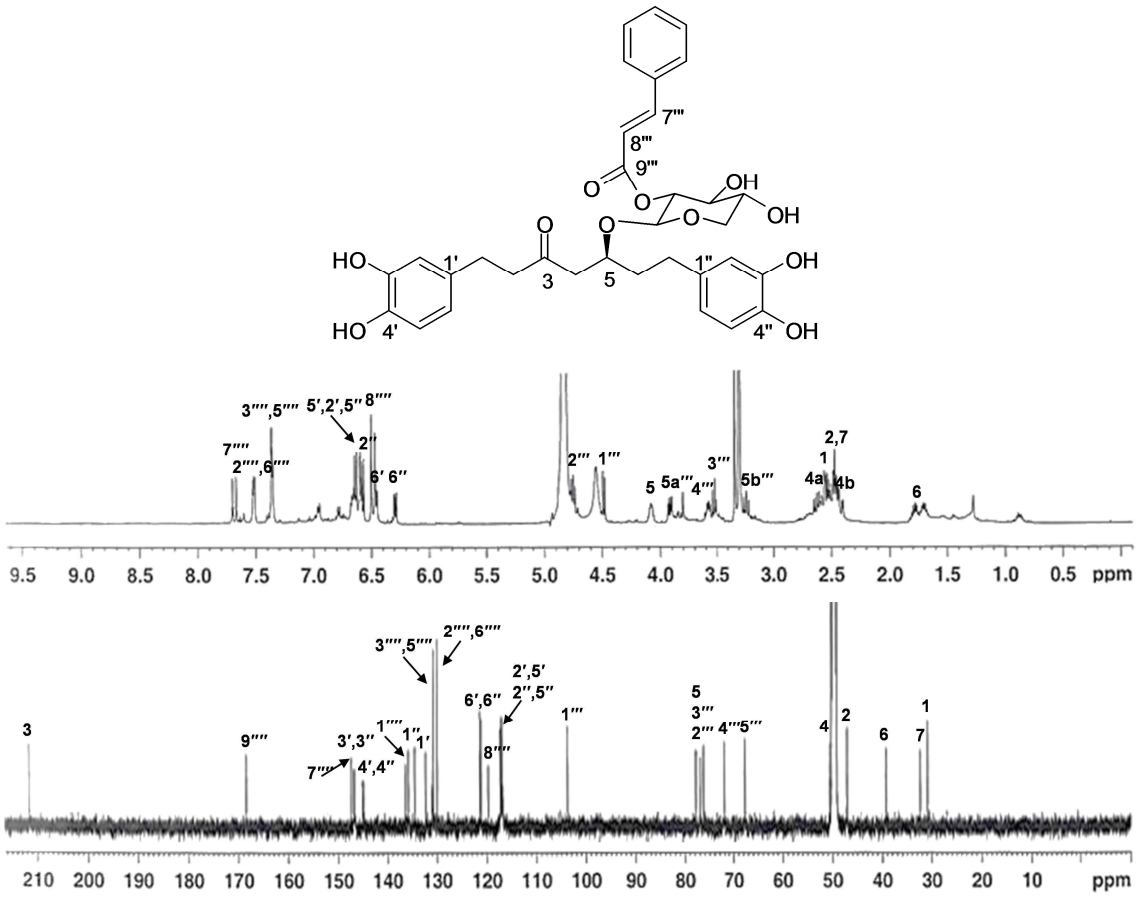

Figure 40. ^1H and ^{13}C NMR spectra of compound **AJ16**

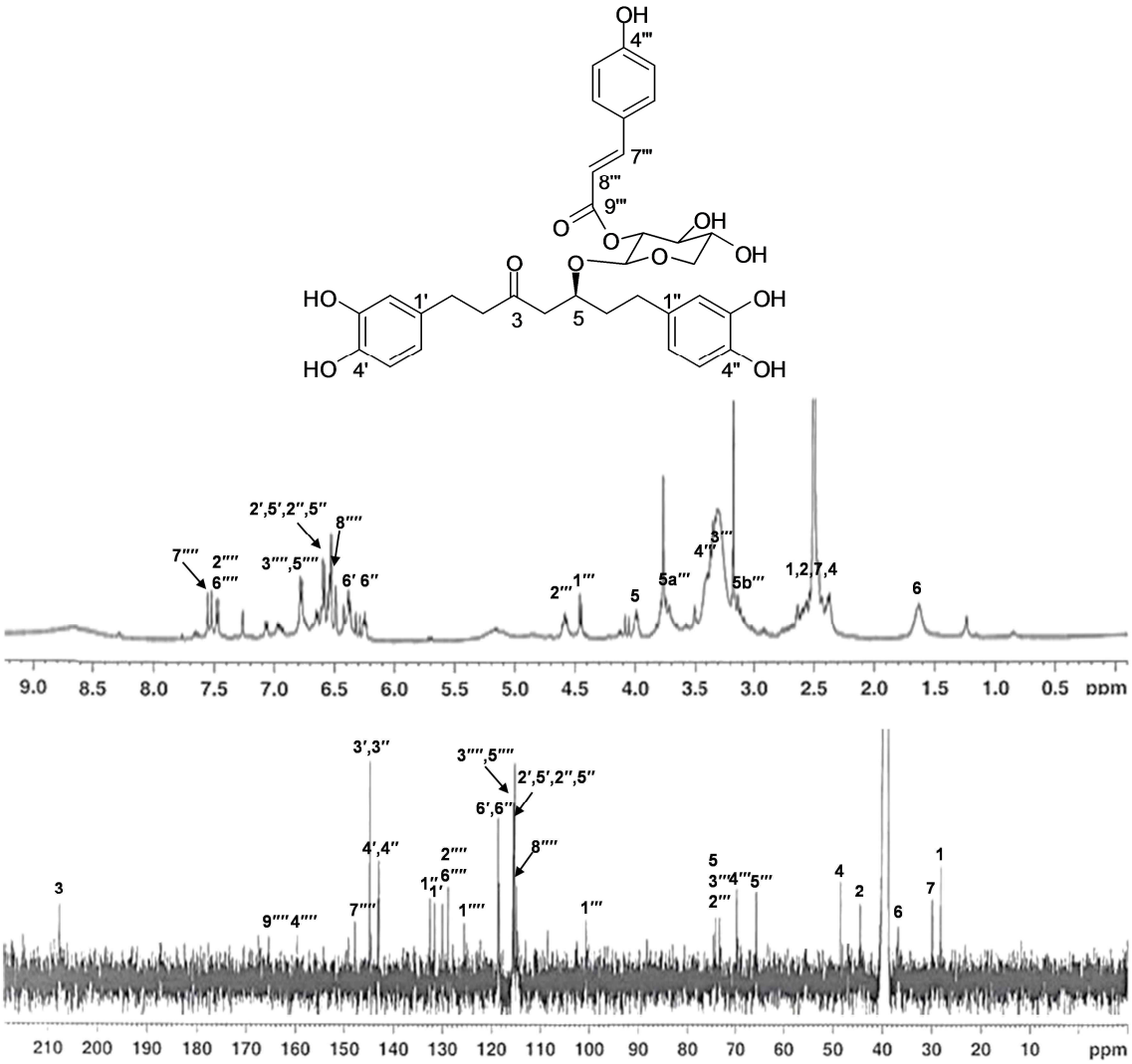

Figure 41. ^{1}H and ^{13}C NMR spectra of compound **AJ17**

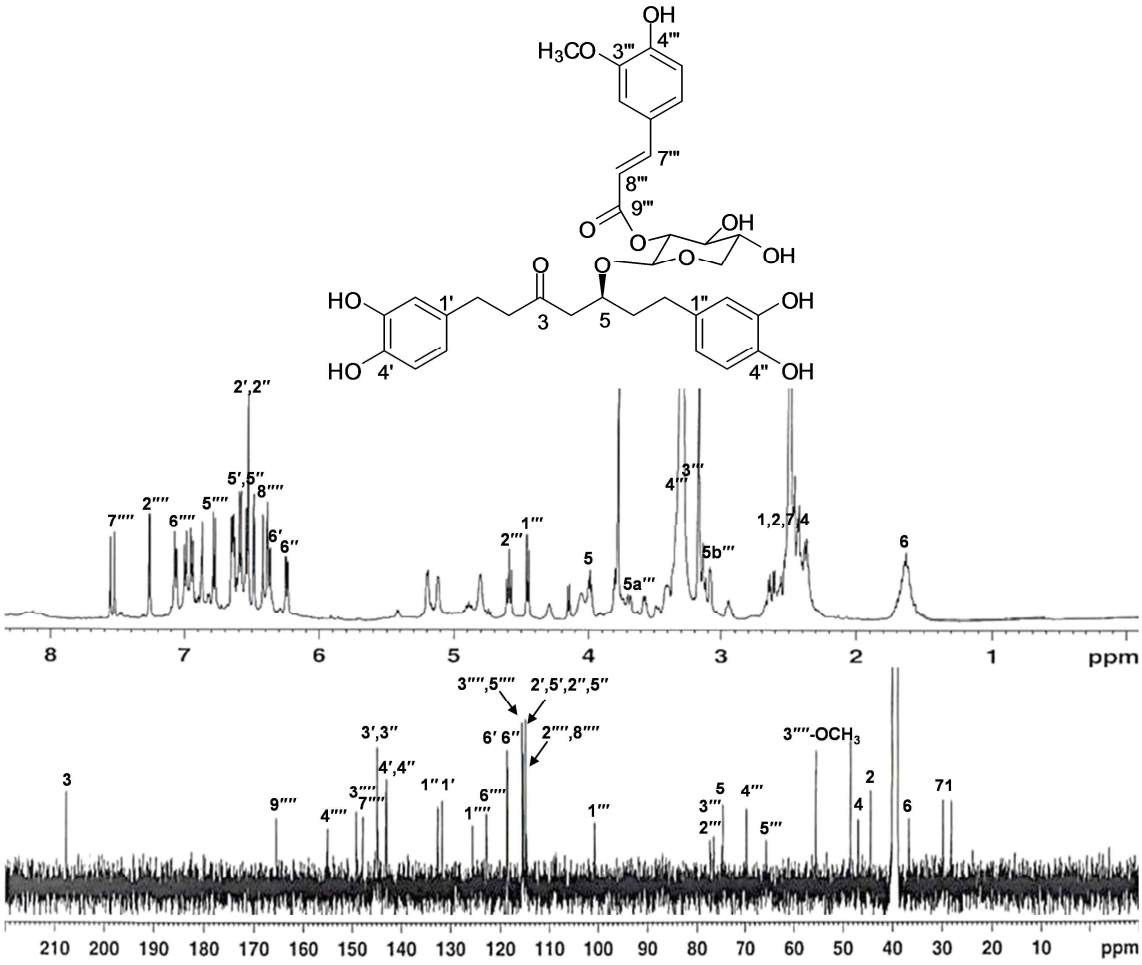

Figure 42. ^{1}H NMR spectrum of compound **AJ18**

1.12. Compounds AH14-16 and AJ19

Compound **AH14** was obtained as yellowish syrup, and $[\alpha]_D^{25}$ -8.3 (*c* 1.0 MeOH) The negative FABMS exhibited molecular ion peak at *m/z* 299 $[M-H]^-$ indicating $C_{19}H_{24}O_3$ as its molecular formula. In IR spectrum, the absorption bands at 3394 cm^{-1} indicated the presence of hydroxyl functions, but absorption band corresponding to carbonyl function was not observed,

dissimilar to other diarylheptanoids. The ^{1}H NMR spectroscopic data revealed signals for two 1, 4-disubstituted aromatic ring [δ_H 6.98 (2H, d, *J* = 8.5 Hz, H-2', 6'), 6.66 (2H, d, *J* = 8.4 Hz, H-3", 5"), 6.96 (1H, d, *J* = 8.5 Hz, H-2", 6"), 6.68 (2H, d, *J* = 8.4 Hz, H-3", 5")], signals for hydroxy-bearing methane at δ_H 3.49 and six methylene at δ_H 2.57, 1.63, 1.46, 1.32, 1.45, 2.35. In addition, the ^{13}C-NMR spectroscopic data showed the presence of seven carbon of the 2-hydroxy-heptanol presence [δ_C 72.5 (C-3), 41.4 (C-2), 39.0 (C-4), 36.8 (C-7), 33.8 (C-6), 32.9 (C-1), 27.1 (C-5)]. Taken together, compound **AH14** was determined as (-)-centrolobol (Nagai et al., 1986) (Figure 43).

Compound **AH15** was obtained as brownish syrup and $[\alpha]_D^{25}$ -25.6 (*c* 1.0 MeOH). Its molecular formula was identified as $C_{24}H_{30}O_8$ by the negative mode FABMS (*m/z* 461 $[M-H]^-$) and the ^{13}C NMR spectrum. The ^{1}H and ^{13}C NMR spectra of compound **AH14** were similar to those of compound **AH14** except for the signals of xylopyranoside moiety [δ_C 104.9 (C-1'"), 78.6 (C-3'"), 75.8 (C-2'"), 72.0 (C-4'"), 67.6 (C-5'")]. The HMBC spectrum showed the location of xylopyranoside moiety was at C-3 due to the correlation peaks from δ_C 78.8 (C-3) to δ_H 4.20 (1H, d, *J* = 7.5 Hz H-1'"). Therefore, compound **AH15** was confirmed as 1,7-bis-(4-hydroxyphenyl)-(3*R*)-*β*-D-xylosyloxyheptane (Lai et al., 2012) (Figure 43).

Compound **AJ19** was obtained as yellowish syrup, and its molecular formula of $C_{25}H_{34}O_8$ was established by the observed pseudo-molecular ion peak at *m/z* 462.02 $[M-H]^-$ in the negative ESIMS. The ^{1}H and ^{13}C NMR spectra of compound **AJ19** were similar to those of compound **AH14** except for the signals of glucopyranoside moiety [δ_C 101.7 (C-1'"), 77.8 (C-3'"), 73.5 (C-2'"), 73.7 (C-5'"), 70.1 (C-4'"), 61.2 (C-6'")]. In the HMBC spectrum, the positions of glucopyranoside moiety were determined to be at C-3 by the correlation peaks between δ_C

79.0 (C-3) to δ_H 4.29 (1H, d, J = 7.8 Hz, H-1'''). On the basis of above information, compound **AJ19** was determined as aceroside VII (Smite et al., 1993) (Figure 43).

Compound **AH16** was obtained as dark brownish syrup, and $[\alpha]_D^{25}$ -4.9 (*c* 1.0 MeOH). The negative ESIMS exhibited molecular ion peak at *m/z* 593.24 $[M-H]^-$ indicating $C_{30}H_{42}O_{12}$ as its molecular formula. The ^1H and ^{13}C NMR spectra of compound **AH16** were similar to those of compound **AH14** except for the substitution of apiofuranoside (1''''→6''')-glucopyranoside moiety at C-5 [δ_C 102.1 (C-1'''), 76.3 (C-3'''), 75.9 (C-5'''), 73.6 (C-2'''), 70.1 (C-4'''), 67.4 (C-6'''), 109.2 (C-1''''), 78.8 (C-3''''), 75.3 (C-2''''), 73.3 (C-4''''), 63.5 (C-5'''')] by the correlation between δ_H/ δ_C 4.14 (1H, d, J = 7.6 Hz, H-1''')/ δ_C 77.7 (C-3) and 5.00 (1H, d, J = 2.3 Hz, H-1'''')/ δ_C 63.7 (C-1''') in the HMBC spectrum.. Thus, compound **AH16** was determined as (3*R*)-1,7-bis-(4-hydroxyphenyl)-3-heptanol-3-*O*-*β*-D-apiofuranosyl-(1→6)-*β*-D-glucopyranoside (Smite et al., 1993) (Figure 43).

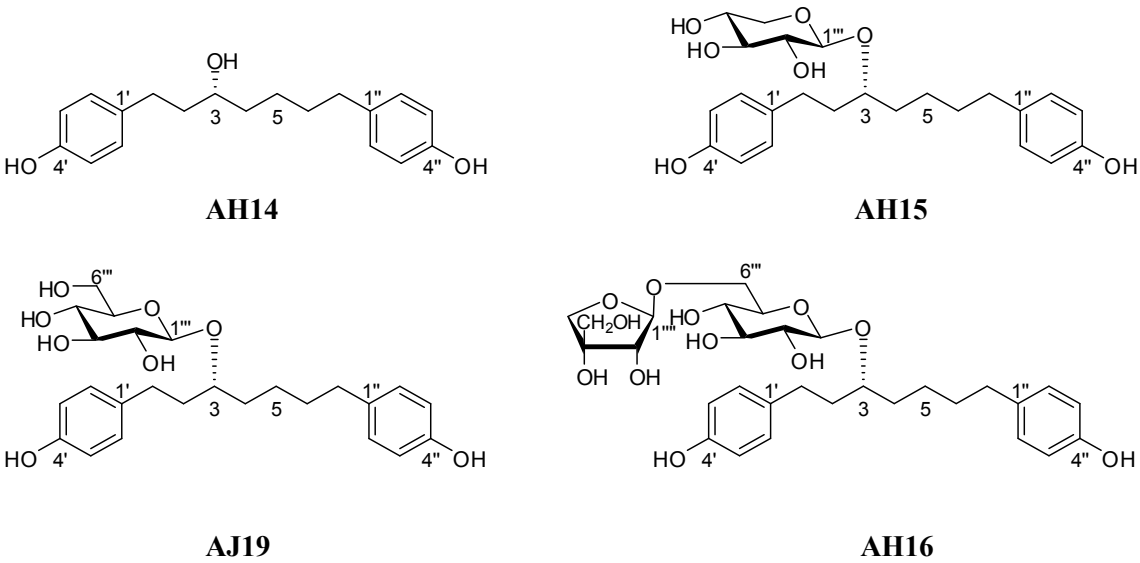

Figure 43. The structures of compounds **AH14**, **AH15**, **AJ19** and **AH16**

1.13. Compounds AH17, AF10-12

Compound **AH17** was obtained as yellowish syrup, and $[\alpha]_D^{25}$ -10.3 (*c* 1.0 MeOH). The negative ESIMS exhibited molecular ion peak at *m/z* 331.18 $[M-H]^-$ indicating $C_{19}H_{24}O_5$ as its molecular formula. In IR spectrum, the absorption bands at 3345 cm^{-1} showed the presence of hydroxyl functions, but absorption band corresponding to carbonyl function was not observed. The characteristic UV absorption at 279 nm indicated the presence of diarylheptanoid skeleton. The ^1H NMR spectroscopic data revealed signals for two 1, 3, 4-trisubstituted aromatic ring [δ_H 6.63 (1H, d, *J* = 8.0 Hz, H-5'), 6.59 (1H, d, *J* = 2.0 Hz, H-2'), and 6.46 (1H, dd, *J* = 8.0, 2.0 Hz, H-6'), 6.63 (1H, d, *J* = 8.0 Hz, H-5''), 6.59 (1H, d, *J* = 2.0 Hz, H-2''), and 6.46 (1H, dd, *J* = 8.0, 2.0 Hz, H-6'')]. In addition, the ^{13}C-NMR spectroscopic data showed the presence of seven carbon of the 3-hydroxyheptanol presence [δ_C 77.9 (C-3), 35.9 (C-6), 33.6 (C-2), 33.2 (C-4), 32.6 (C-1), 30.3 (C-7), 24.1 (C-5)]. With above observed spectral data and previously reported literatures, compound **AH17** was determined as (3*R*)-1,7-bis-(3,4-dihydroxyphenyl)-3-heptanol (Sunnerheimsjoberg and Knutsson, 1995) (Figure 44).

Compound **AF10** was obtained as dark brownish syrup, and $[\alpha]_D^{25}$ -41.5 (*c* 0.1 MeOH). The negative ESIMS exhibited molecular ion peak at *m/z* 463.24 $[M-H]^-$ indicating $C_{24}H_{32}O_9$ as its molecular formula. The ^1H and ^{13}C NMR spectra of compound **AF10** were similar to those of compound **AH17** except for the carbons of xylopyranoside moiety [δ_C 104.3 (C-1'''), 78.1 (C-3'''), 75.2 (C-2'''), 71.4 (C-4'''), 67.0 (C-5''')]. On the basis of the correlated peaks from δ_H 4.21 (1H, d, *J* = 7.7 Hz, H-1''') to δ_C 77.4 (C-3) in the HMBC experiment, it was confirmed that the sugar moiety was linked at C-3 of the aglycone. Taken together, compound **AF10** was

determined as (3*R*)-1,7-bis-(3,4-dihydroxyphenyl)-3-heptanol-3-*O*-*β*-D-xylopyranoside (Gonzalez-Laredo et al., 1999) (Figure 44).

Compound **AF11** was obtained as dark brownish syrup and $[\alpha]_D^{25}$ -14.2 (*c* 0.1 MeOH). Its molecular formula was identified as $C_{25}H_{33}O_{10}$ by the negative mode ESIMS (*m/z* 493.24 $[M-H]^-$) and the ^{13}C NMR spectrum. The ^1H and ^{13}C NMR spectra of compound **AF11** were similar to those of compound **AH17** except for the signals of glucopyranoside moiety [δ_C 101.9 (C-1'''), 76.9 (C-3'''), 76.7 (C-2'''), 73.7 (C-5'''), 70.2 (C-4'''), 61.3 (C-6''')]. In the HMBC analysis, the location of the glucopyranoside moiety was at C-5 by the correlation peak from δ_H 4.14 (1H, d, *J* = 7.5 Hz, H-1''') to δ_C 77.4 (C-3). Therefore, compound **AF11** was confirmed as (3*R*)-1,7-bis-(3,4-dihydroxyphenyl)-3-heptanol-3-*O*-*β*-D-glucoopyranoside (Fuchino et al., 1996) (Figure 44).

Compound **AF12** was obtained as dark brownish syrup, and its molecular formula of $C_{30}H_{42}O_{14}$ was established by the observed pseudo-molecular ion peak at *m/z* 625.24 $[M-H]^-$ in the negative ESIMS. The ^1H and ^{13}C NMR spectra of compound **AF12** were similar to those of compound **AH17** except for the substitution of glucopyranoside (1''''→3''')-xylopyranoside moiety at C-5 [δ_C 103.9 (C-1'''), 87.7 (C-3'''), 72.0 (C-2'''), 68.3 (C-4'''), 64.9 (C-5'''), 102.2 (C-1''''), 76.8 (C-3''''), 76.1 (C-5''''), 73.8 (C-2''''), 70.2 (C-4''''), 61.1 (C-6'''')] by the correlation between δ_H/ δ_C 3.90 (1H, m, H-5)/ δ_C 104.4 (C-1''') and 3.62 (1H, dd, *J* = 8.2 Hz, H-6''')/ δ_C 104.4 (C-1'''') in the HMBC spectrum. On the basis of above information, compound **AF12** was determined as (3*R*)-1,7-bis-(3,4-dihydroxyphenyl)-3-heptanol-3-*O*-*β*-D-glucopyranosyl (1→ 3)-3-*O*-*β*-D-xylopyranoside (Gonzalez-Laredo et al., 1999) (Figure 44).

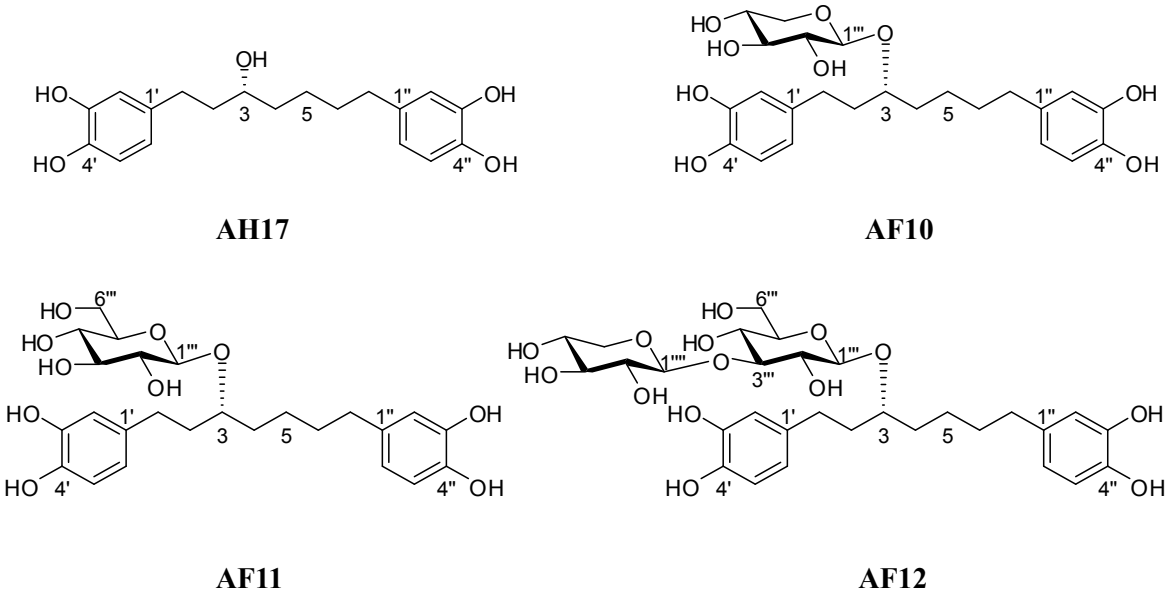

Figure 44. The structures of compounds **AH17** and **AF10-12**

1.14. Compound AH21

Compound **AH21** was obtained as brownish syrup, and $[\alpha]_D^{25}$ +7.4 (*c* 1.0 MeOH). The negative ESIMS exhibited molecular ion peak at *m/z* 315.06 $[M-H]^-$ indicating $C_{19}H_{24}O_4$ as its molecular formula. The absorption bands at 3375 cm^{-1} of IR spectrum, indicated the presence of hydroxyl functions, but absorption band corresponding to carbonyl function was not observed. In the UV spectrum, the characteristic absorption at 277 nm suggested the presence of diarylheptanoid skeleton. The ^1H NMR spectroscopic data revealed signals for two 1, 4-disubstituted aromatic ring [δ_H 6.98 (4H, d, *J* = 8.6 Hz, H-2', 2", 6', 6"), 6.67 (4H, d, *J* = 8.6 Hz, H- H-3', 3", 5', 5")] (Figure 45). In addition, the ^{13}C-NMR spectroscopic data showed the presence of seven carbon of the 3,5-dihydroxy-heptan [δ_C 68.1 (C-3, 5), 44.7 (C-4), 38.9 (C-2, 6), 30.2 (C-1, 7)]. With above mentioned spectroscopic data, the structure of compound **AH21**

was confirmed as (+)-hannokinol (Nomura et al., 1981).

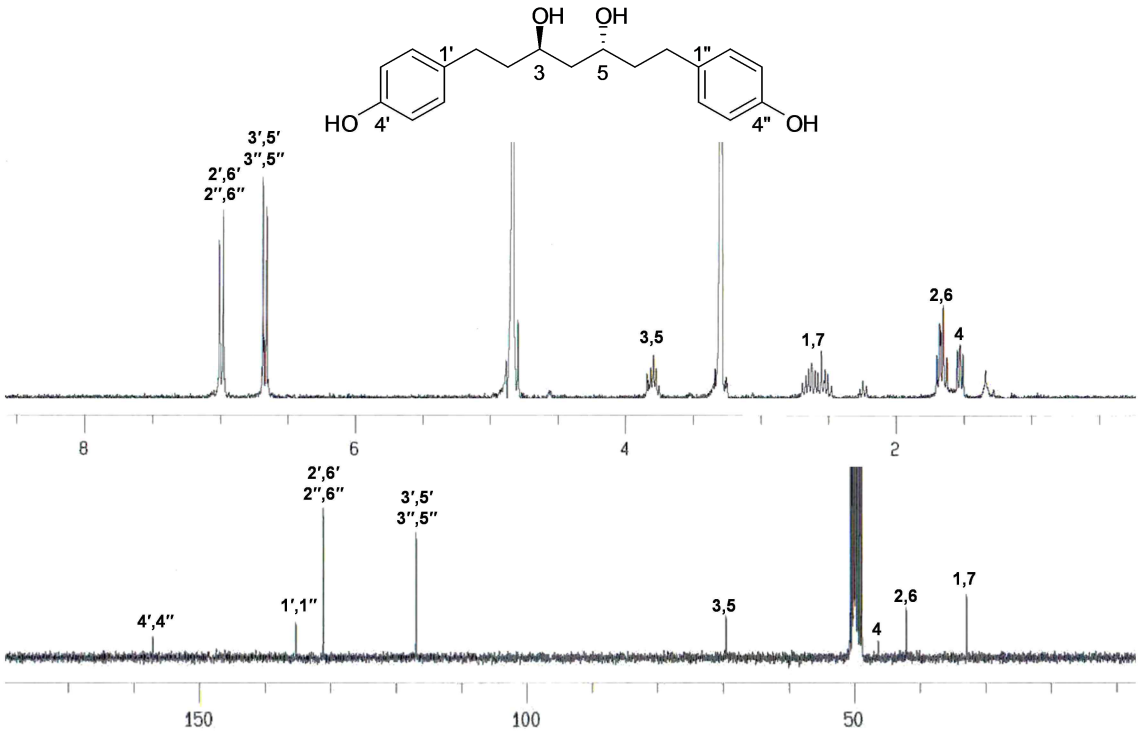

Figure 45. ^{1}H and ^{13}C NMR spectra of compound **AH21**

1.15. Compounds AJ30-36

Compound **AJ30** was obtained as whitish amorphous powder and $[\alpha]_D^{25}$ -1.1 (*c* 1.0 5% DMSO in MeOH) and was confirmed $C_{14}H_6O_8$ by the negative ESIMS (*m/z* 301.17 $[M-H]^-$). The IR spectrum showed absorption for hydroxyl (3270 cm^{-1}), carbonyl (1716 cm^{-1}), and aromatic ring (1606 cm^{-1}) carbons. The charctreristic UV absorption at 254 nm and 368 nm also suggested that compound **AJ30** has a ellagic acid skeleton. The ^{1}H NMR spectra of compound **AJ30** showed only one proton at δ 7.45 (2H, s), similar to ellagic acid moiety of compound

AJ31 (Figure 46). The molecular formula of compound **AJ30** was established as $C_{14}H_6O_8$ by the negative mode ESIMS (*m/z* 301.17 $[M-H]^-$). On the basis of above information, the structure of compound **AJ30** was considered to be symmetrical. Therefore, compound **AJ30** was determined as ellagic acid (Da Silva et al., 2008).

Compound **AJ31** was obtained as whitish amorphous powder and $[\alpha]_D^{25}$ -2.0 (*c* 1.0 5% DMSO in MeOH). Its molecular formula was identified as $C_{15}H_8O_8$ by the negative mode ESIMS (*m/z* 315.04 $[M-H]^-$) and was separated as rectangular plates (mp 290°C). The IR spectrum displayed characteristic absorptions for hydroxyl group at 3247 cm^{-1}, carbonyl group at 1722 cm^{-1}, and aromatic ring at 1606 and 1493 cm^{-1}. The UV spectrum, λ_{max} (5% DMSO in MeOH) (log ε) (nm): 257 (4.41), 368 (4.14), suggested that compound **AJ31** has a ellagic acid skeleton by comparison with literatures (Yan et al., 2004, Khac et al., 1990). The ^1H NMR spectrum of compound **AJ31** showed the presence of two protons as singlets at δ 7.50 and 7.37 assigned to the ellagic acid moiety and one aromatic methoxy group at δ 4.02 (3H, s) (Figure 47). With above observed spectroscopic data, compound **AJ31** was confirmed as 3'-*O*-methyl-ellagic acid (Da Silva et al., 2008).

Compound **AJ32** was obtained as whitish amorphous powder, and $[\alpha]_D^{25}$ -2.9 (*c* 1.0 5% DMSO in MeOH). The negative ESIMS exhibited molecular ion peak at *m/z* 446.99 $[M-H]^-$ indicating $C_{20}H_{16}O_{12}$ as its molecular formula. The IR spectrum showed absorption bands corresponding to hydroxyl (3284 cm^{-1}) and carbonyl (1740 cm^{-1}) functions. In the UV spectrum, absorption at 251 nm and 362 nm indicated the presence of ellagic aicd. The ^1H and ^{13}C NMR spectra of compound **AJ32** were similar to those of compound **AJ31** except for the substitution of xylopyranoside moiety at C-4 [δ_C 102.7 (C-1"), 75.4 (C-3"), 72.9 (C-2"), 69.2 (C-4"), 65.8

(C-5")] (Figure 48). Therefore, compound **AJ32** was confirmed as 3'-*O*-methyl-4-*O*-*β*-D-xylosyl-ellagic acid (Yan et al., 2004).

Compound **AJ33** was isolated as whitish amorphous powder, and its molecular formula was identified as $C_{21}H_{18}O_{13}$ by the negative mode ESIMS (*m/z* 477.00 $[M-H]^-$). The absorption bands of hydroxyl (3361 cm^{-1}) and carbonyl (1747 cm^{-1}) functions in the IR spectrum and the absorption at 251 nm and 362 nm in the UV spectrum suggested that compound **AJ33** has ellagic aicd moiety. The ^1H and ^{13}C NMR spectra of compound **AJ33** were similar to those of compound **AJ31** except for the substitution of glucopyranoside moiety at C-4 [δ_C 106.2 (C-1"), 77.8 (C-5"), 77.2 (C-3"), 73.9 (C-2"), 69.9 (C-4"), 61.2 (C-6")] (Figure 49). These spectral data suggested that compound **AJ33** was 3'-*O*-methyl-4-*O*-*β*-D-glucosyl-ellagic acid (Yan et al., 2004).

Compound **AJ34** was whitish amorphous powder, and demonstrated $C_{15}H_8O_9$ as a moleculat formula by the negative mode ESIMS (*m/z* 328.96 $[M-H]^-$). The IR spectrum revealed the presence of hydroxyl (3297 cm^{-1}) and carbonyl (1715 cm^{-1}) functions. In the UV spectrum, absorption at 246 nm and 375 nm suggested that compound **AJ34** has ellagic aicd. The ^1H and ^{13}C NMR spectra of compound **AJ34** were similar to those of compound **AJ31** except for the substitution of methoxy group at C-3 [δ_C 60.9 (3-OCH_3)] (Figure 50). Therefore, compound **AJ33** was concluded as 3,3'-di-*O*-methyl-ellagic acid (Da Silva et al., 2008).

Compound **AJ35**, $[\alpha]_D^{25}$ -6.4 (*c* 1.0 5% DMSO in MeOH), was fulfilled FABMS (negative mode) and the ^{13}C NMR experiment to assign its molecular formula with $C_{17}H_{12}O_8$. The IR spectrum absorption bands corresponding to hydroxyl (3394 cm^{-1}) and carbonyl (1719 cm^{-1}) functions. In the UV spectrum, absorption at 251 nm and 365 nm suggested that compound

AJ35 has ellagic aicd. The ^{1}H and ^{13}C NMR spectra of compound **AJ35** showed the substitution of three methoxy group at C-3,4,3' [δ_C 61.6 (3-OCH_3), 61.3 (3'-OCH_3), 56.6 (4'-OCH_3)] in compound **AJ30**, ellagic acid (Figure 51). These spectral data indicated that compound was 3,3',4'-tri-*O*-methyl-ellagic acid by comparison with previously reported literature (Da Silva et al., 2008).

The molecular formula of compound **AJ36** which was isolated as whitish amorphous powder and $[\alpha]_D^{25}$ -12.2 (*c* 1.0 5% DMSO in MeOH) was confirmed $C_{22}H_{20}O_{12}$ by the negative FABMS (*m/z* 475 $[M-H]^-$) and ^{13}C NMR experiment. The absorption bands of hydroxyl (3370 cm^{-1}) and carbonyl (1720 cm^{-1}) functions in the IR spectrum and the absorption at 246 nm and 365 nm in the UV spectrum suggested the presence of ellagic aicd. In the ^{1}H and ^{13}C NMR spectra, it was found that compound **AJ36** were similar to those of compound **AJ32** except for the additory substitution of two methoxy group at C-3,4' [δ_C 61.6 (C3-OCH_3), 56.8 (C4'-OCH_3)] (Figure 52). Consequently, compound **AJ36** was determined as 3,3',4'-tri-O-methyl-4-*O*-*β*-xylosyl-ellagic acid (Sinha et al., 1999).

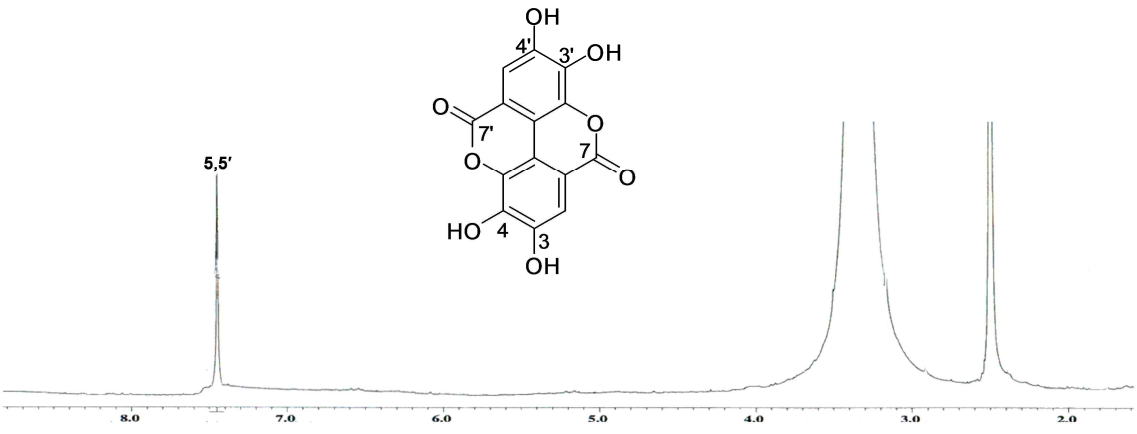

Figure 46. ^{1}H NMR spectra of compound **AJ30**

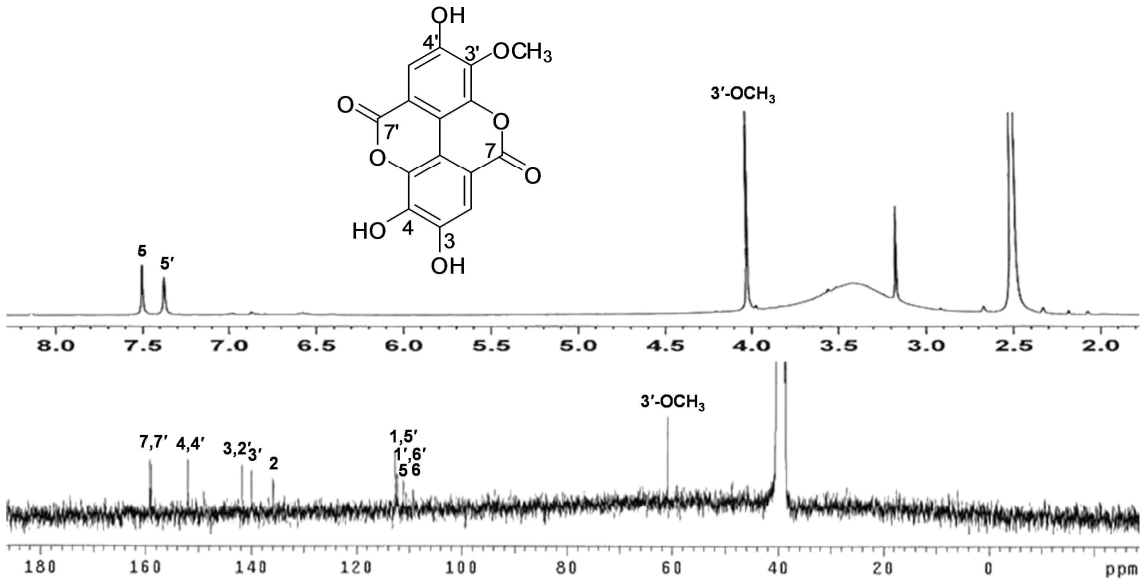

Figure 47. ^{1}H and ^{13}C NMR spectra of compound **AJ31**

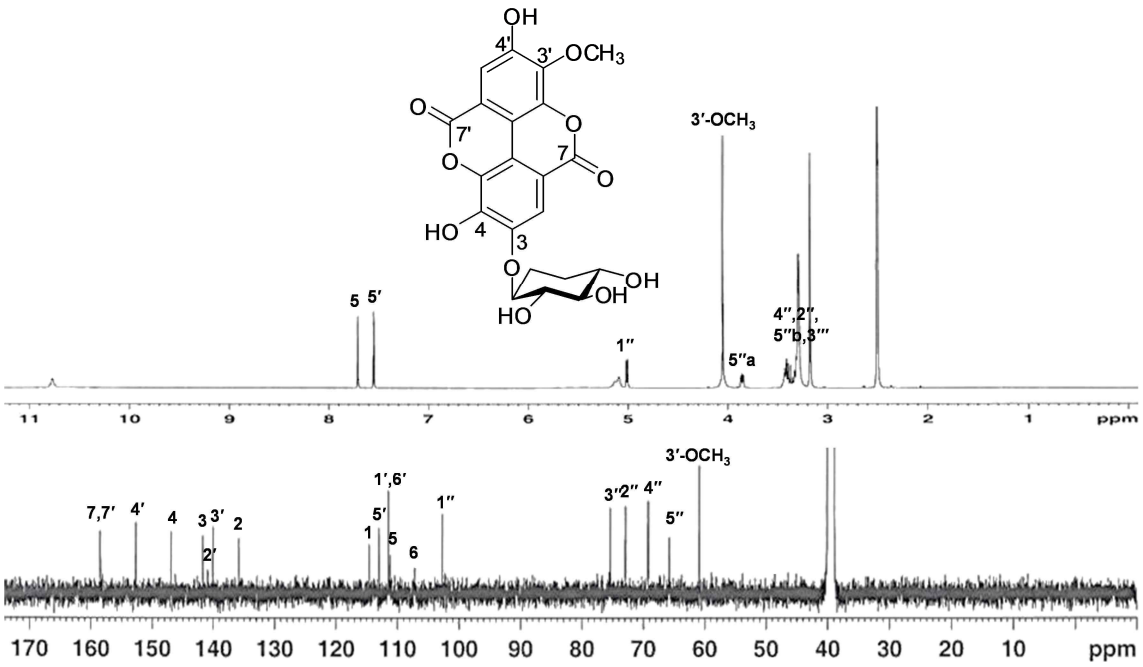

Figure 48. ^{1}H and ^{13}C NMR spectra of compound **AJ32**

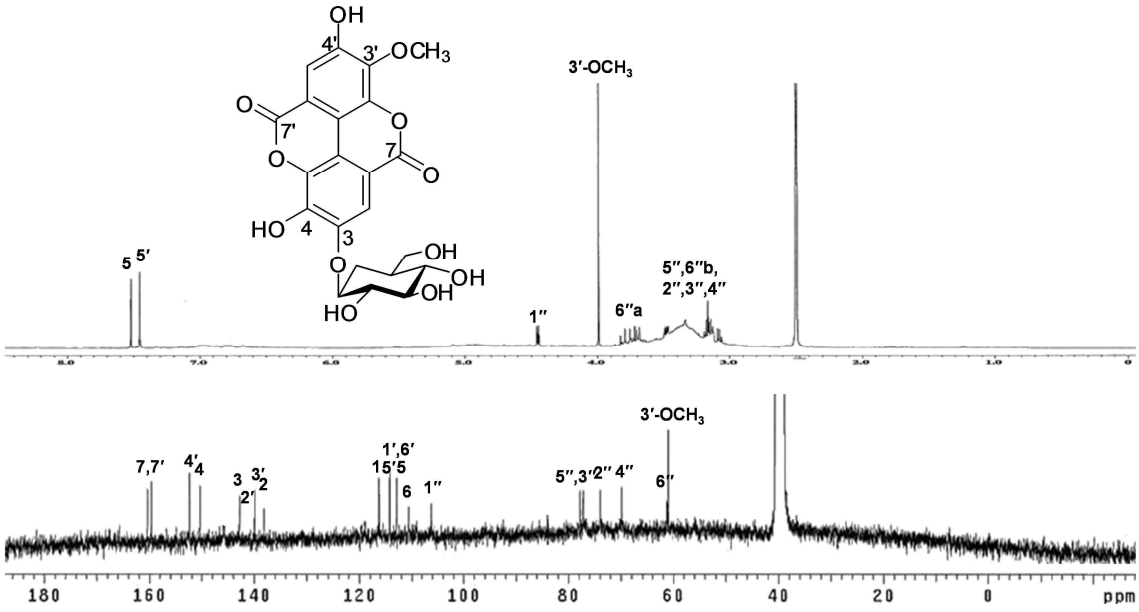

Figure 49. ^{1}H and ^{13}C NMR spectra of compound **AJ33**

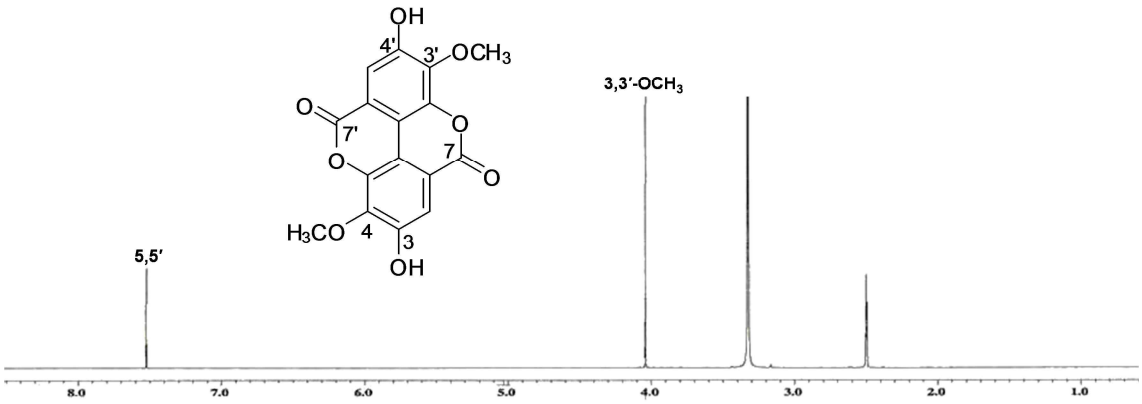

Figure 50. ^{1}H NMR spectrum of compound **AJ34**

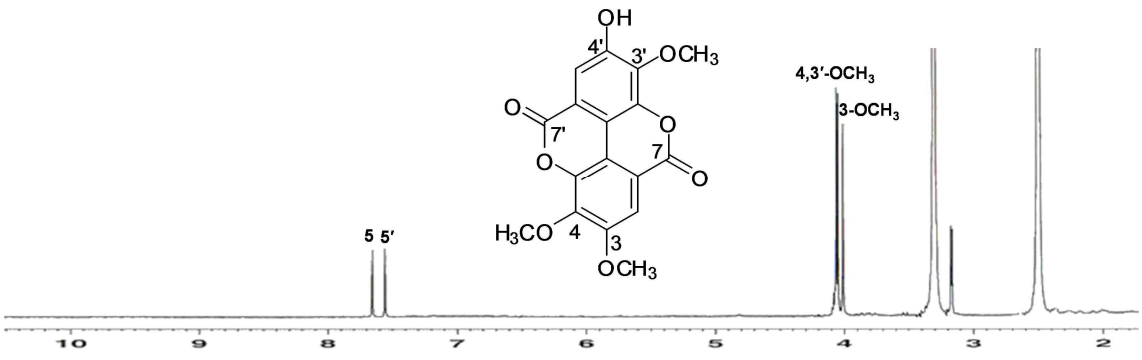

Figure 51. ^{1}H NMR spectrum of compound **AJ35**

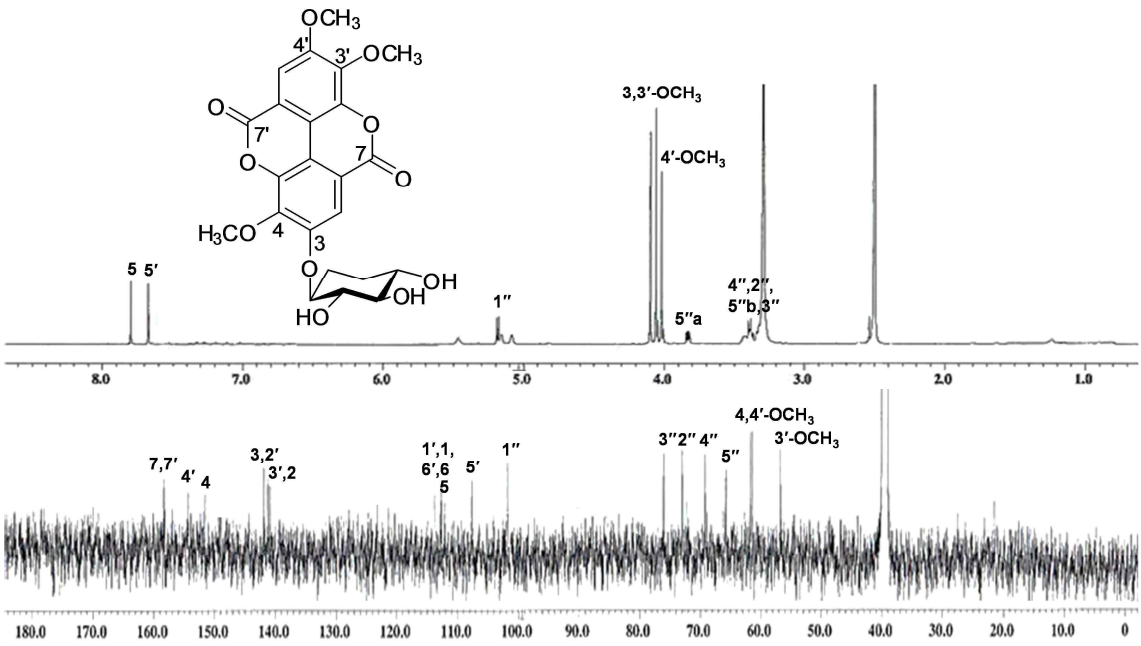

Figure 52. ^{1}H and ^{13}C NMR spectra of compound **AJ36**

1.16. Compound AJ37

Compound **AJ37** was isolated as brownish syrup, and $[\alpha]_D^{25}$ -2.1 (*c* 1.0 CH_3OH). The molecular formula was determined to be $C_{20}H_{20}O_{13}$ from the negative HRFABMS at m/z 467.0828 $[M-H]^-$ (calcd. for $C_{20}H_{19}O_{13}$, 467.0826). The IR spectrum revealed the presence of

hydroxyl (3327 cm^{-1}) and carbonyl (1707 cm^{-1}) functions. The characteristic UV absorption at 277 also suggested the presence of aromatic ring. The ^{1}H NMR spectroscopic data showed signals for 3,4-dihydroxybenzoic acid [δ_H 7.69 (1H, d, *J*= 3.1 Hz, H-2'), 6.89 (1H, dd, *J* = 8.7, 3.1 Hz, H-6'), and 6.61 (1H, d, *J* = 8.7 Hz, H-5')], one galloyl moiety [δ_H 7.24 (2H, s, H-2", 6")], and one glucopyranose unit (Figure 53). Acid hydrolysis of compound **AJ37** and HILIC-MS analysis afforded D-glucose; the retention times (t_R 6.67 min) and mass spectra (m/z 160.86 [$C_6H_{12}O_6$-H_2O-H]$^-$, 178.83 [$C_6H_{12}O_6$-H]$^-$, 224.81 [$C_6H_{12}O_6$+HCOOH-H]$^-$) of the sugar released on acid hydrolysis were compared with the authentic sample of D-glucose. The coupling constant of doublet at δ_H 4.73 (*J* = 7.8) established the *β*–configuration of the glucose moiety. The 3,4-dihydroxybenzoic acid and galloyl group were located at C-1 and C-6, respectively, by the HMBC correlations of C-7" to H-1 and C-3' to H-6a. Based on these spectral data, compound **AJ37** was determined as 3',4'-dihydroxybenzoic acid 3'-*O*-*β*-D-(6-*O*-galloyl)-glucopyranoside.

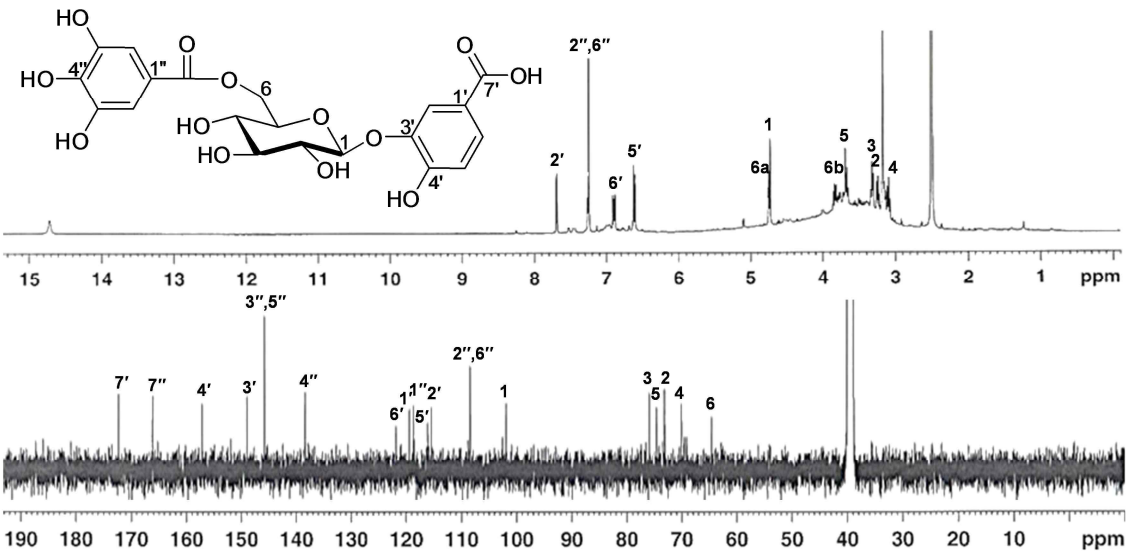

Figure 53. ^{1}H and ^{13}C NMR spectra of compound **AJ37**

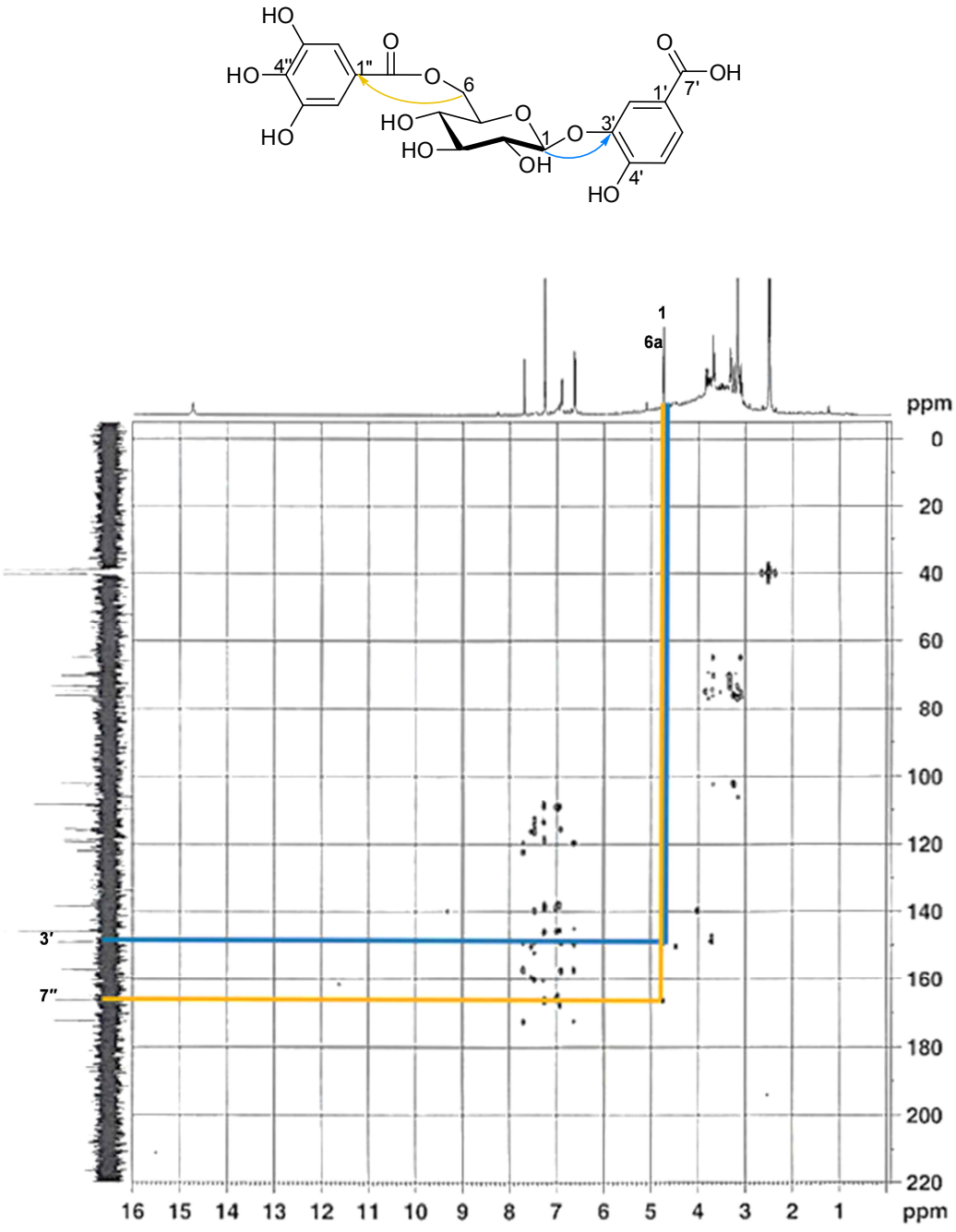

Figure 54. HMBC spectrum of compound **AJ37**

1.17. Compound AJ38

Compound **AJ38** was obtained as whitish amorphous powder, and $[\alpha]_D^{25}$ -22.2 (*c* 1.0 MeOH). Its molecular formula was identified as $C_{27}H_{24}O_{18}$ by the negative mode ESIMS (*m/z* 635.08 $[M-H]^-$) and the ^{13}C NMR spectrum. The IR spectrum of compound xx exhibited strong absorptions due to hydroxyl (3370 cm^{-1}) and estesr carbonyl (1702 cm^{-1}) functions. The ^1H and ^{13}C NMR spectroscopic data showed signals for three galloyl groups [δ_H 6.97, 6.92, 6.88 (each 2H, s, galloyl H, H-2', 2", 2", 6', 6", 6")], and glucose moiety at δ_C 92.1, 74.8, 73.6, 72.7, 69.6, 62.9 (Figure 55). The locations of the three galloyl groups in the glucose moiety were determined to be the C-1, 2 and 6 positions by analysis of the HMBC spectrum of compound **AJ38**. From obtained spectral data and above analysis, compound **AJ38** was characterized as 1,2,6-tri-O-galloyl glucose (Nonaka et al., 1981).

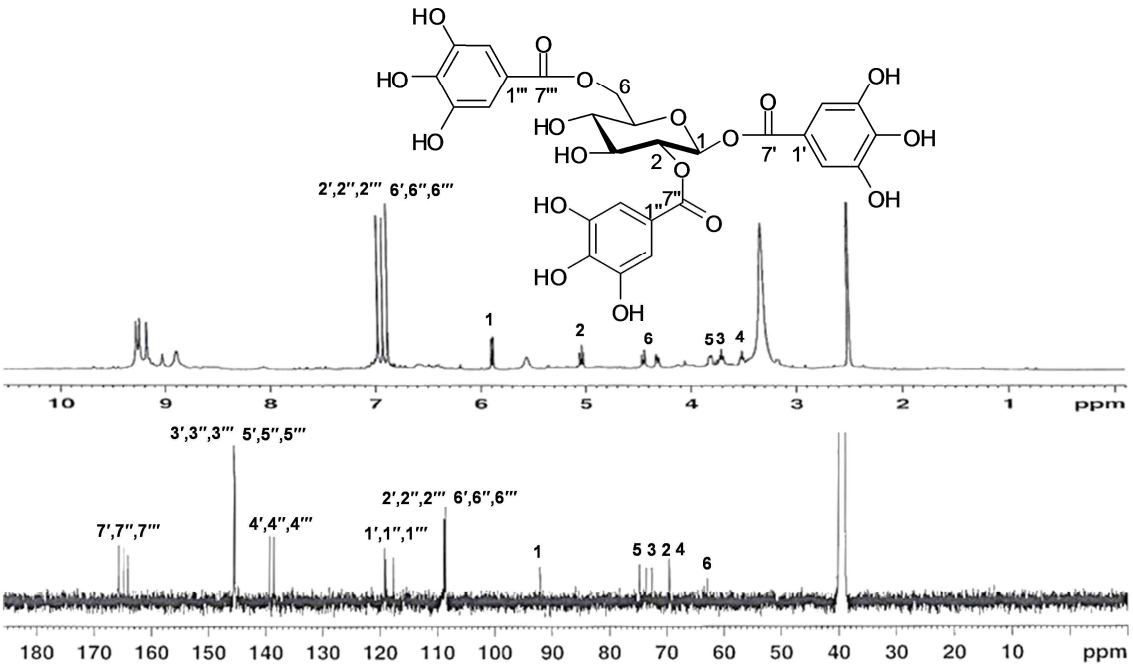

Figure 55. ^1H and ^{13}C NMR spectra of compound **AJ38**

1.18. Compounds AJ39-41

Compound **AJ39** was isolated as whitish amorphous powder, $[\alpha]_D^{25}$ +5.0 (*c* 1.0 $CHCl_3$:MeOH=1:1) and the negative mode FABMS analysis (m/z 455 $[M-H]^-$) indicated that the molecular formula of compound **AJ39** was $C_{30}H_{48}O_3$. The ^1H and ^{13}C NMR spectra of compound **AJ39** were similar to those of compound **AJ41** except for the location of double bond and the oxidation into COOH group at C-26 in side chain at C-17. The ^{13}C NMR spectroscopic data showed the signals for one double bond [δ_C 142.5 (C-24)], one quaternary sp^2-carbon [δ_C 129.0 (C-25)], COOH group [δ_C 170.6 (C-26)] (Figure 56). The locations of these were established by the observed HMBC correlations of H-24 to C-22/C-23/C-25/C-27. Thus, compound **AJ39** was confirmed as 3*β*-hydroxy-lanost-9(11),24(25)-dien-26-oic acid in comparison with previously reported literature (Li et al., 2003).

Compound **AJ40** was isolated as whitish amorphous powder. The molecular formula was determined to be $C_{30}H_{52}O_3$ from the negative HRFABMS at m/z 459 $[M-H]^-$. The ^1H and ^{13}C NMR spectra of compound **AJ40** bears a resemblance to those of compound **AJ41** except for one double bond disappearing and instead one hydroxyl group at C-24, and CH_2OH disappearing and instead CH_3 appearing at C-26 in side chain at C-17 (Figure 57). The location of the oxygenated carbon at C-24 was established by the observed HMBC correlations of H-24 to C-22/C-25/C-27. Therefore, compound **AJ40** was concluded as (24*S*)-lanost-9(11)-ene-3,24,25-triol in comparison with previously reported literature (Ukiya et al., 2001).

Compound **AJ41** was isolated as whitish amorphous powder, $[\alpha]_D^{25}$ +40.3 (*c* 1.0 $CHCl_3$:MeOH=1:1). The molecular formula was determined to be $C_{30}H_{50}O_3$ from the negative HRFABMS at m/z 457.0828 $[M-H]^-$ (calcd. for $C_{30}H_{49}O_3$, 457.0826). The ^1H NMR spectrum of

compound **AJ41** showed evidence for the presence of seven *tert*-CH_3 groups [δ_H 1.65 (3H, s, H-27), 1.29 (3H, s, H-28), 1.12 (3H, s, H-19), 1.07 (3H, s, H-29), 0.77 (3H, s, H-30), 0.69 (3H, s, H-18)], two olefinic double bonds [δ_H 5.27 (1H, br d, *J* = 5.5 Hz, H-11), 6.12 (1H, td, *J* = 15.5, 8.1 Hz, H-23), 6.00 (1H, d, *J* = 15.5 Hz, H-24)], geminal protons [δ_H 3.95 (1H, d, *J* = 10.5, H-26) and 3.90 (1H, d, *J* = 10.5, H-26)] (Figure 59). The ^{13}C NMR spectrum exhibited 30 carbon signals sorted by DEPT experiment as seven *tert*-CH_3 groups [δ_C 28.9 (C-28), 22.6 (C-19), 18.7 (C-21), 18.6 (C-30), 16.5 (C-29), 14.7 (C-18)], nine methylenes including one oxygenated carbon [δ_C 71.2 (C-26), 39.7 (C-22), 37.4 (C-12), 36.8 (C-1), 34.1 (C-15), 28.7 (C-2), 28.5 (C-7), 28.3 (C-16), 21.8 (C-6)], eitht hybridized methines including one oxygenated carbon and three olefinic carbon [δ_C 138.2 (C-24), 127.0 (C-23), 115.0 (C-11), 78.0 (C-3), 53.0 (C-5), 51.5 (C-17), 42.1 (C-8), 36.8 (C-20)], five quaternary sp^3-carbon [δ_C 73.2 (C-25), 47.3 (C-14), 44.6 (C-13), 39.7 (C-4), 25.5 (C-27)], and one quarternary sp^2-carbon [δ_C 149.2 (C-9)], suggesting to be a tetracyclic triterpenoid. The location of hydroxyl groups was evidenced by the relative downfield signals of H-3, H-26 and HMBC correlations; H-3 to C-28/C- 29; H-26 to C-25; H-23/H-24 to C-25 (Figure 60). The ^1H-^1H COSY and HSQC experiments revealed the following key fragments: CH2-CH(OH)-(**A**); C(C)=CH-CH2-(**B**); CH(CH3)-CH-CH2-CH=CH-(**C**) (Figure 59). Taken into account all of the above described spectroscopic data, compound was considered as lanostane type triterpene with hydroxyl and olefinic moieties. In NOESY spectrum, the cross peaks observed between Me-18 and H-8, between Me-19 and H-8 as well as the no cross peak between H-5 and H-8/Me-19 further supported the lanostane-type skeleton (Figure 61). On the basis of these data, compound **AJ41** was determined to be 3*β*-hydroxy-lanost-9(11),23(24)-dien-25,26-diol and was isolated first time from nature.

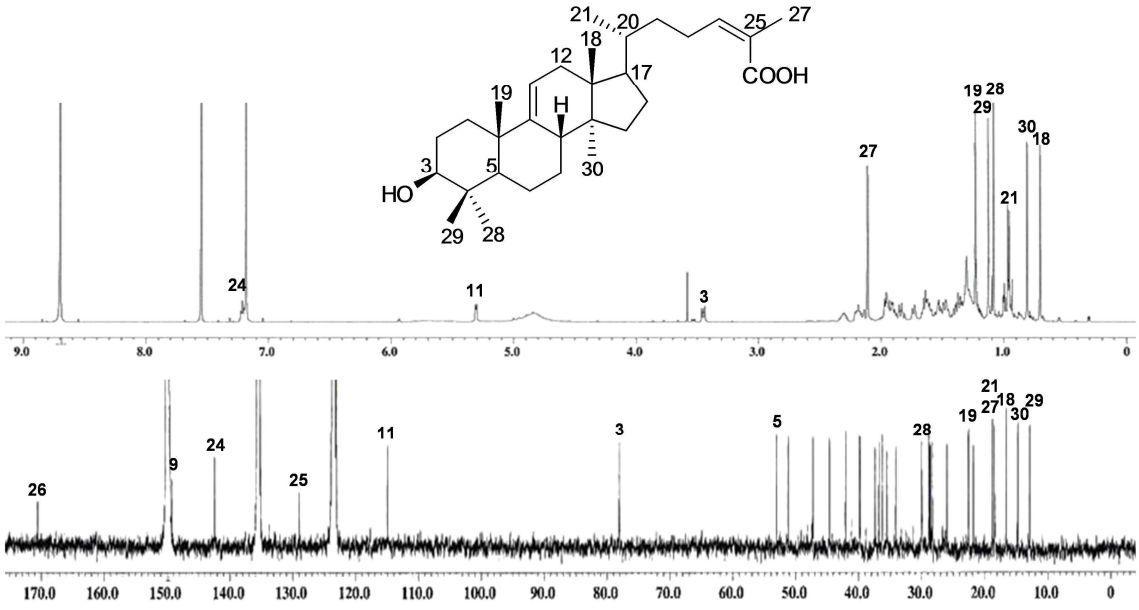

Figure 56. ^{1}H and ^{13}C NMR spectra of compound **AJ39**

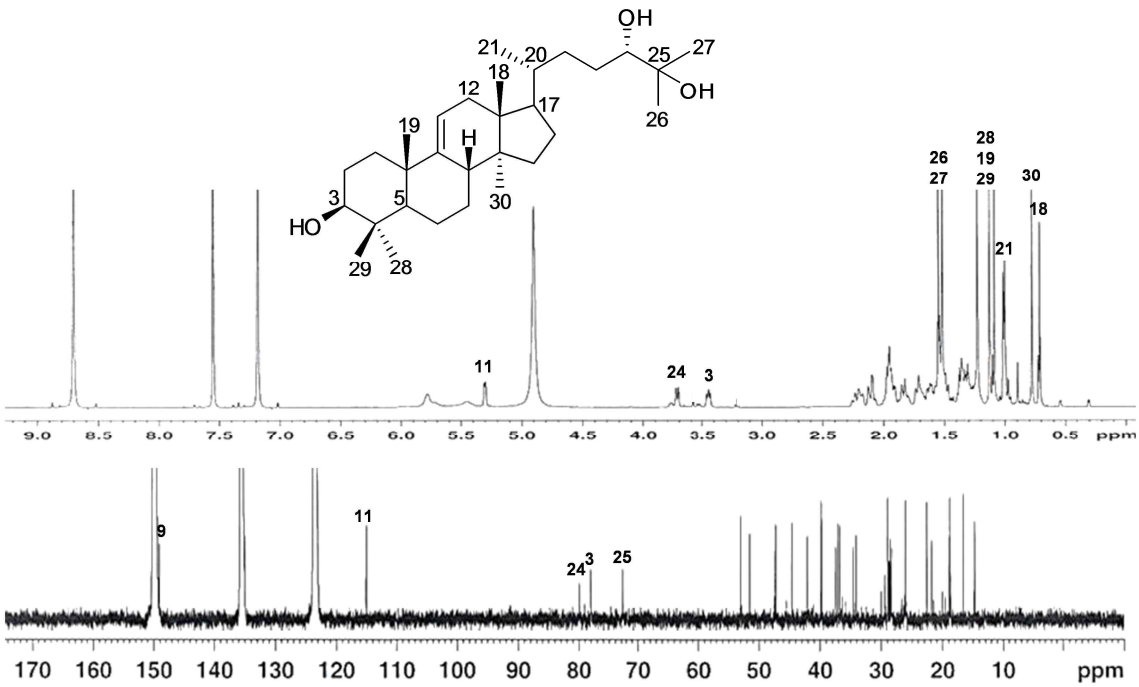

Figure 57. ^{1}H and ^{13}C NMR spectra of compound **AJ40**

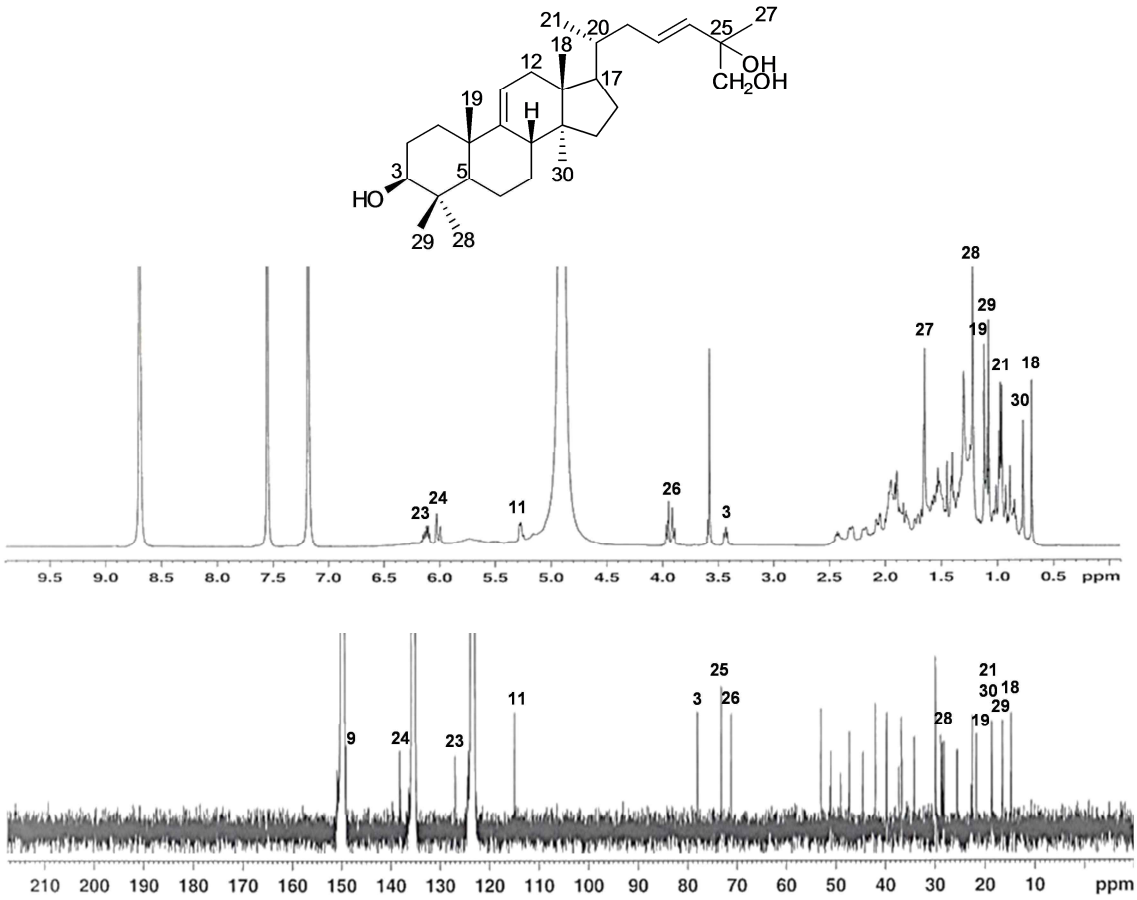

Figure 58. ^{1}H and ^{13}C NMR spectra of compound **AJ41**

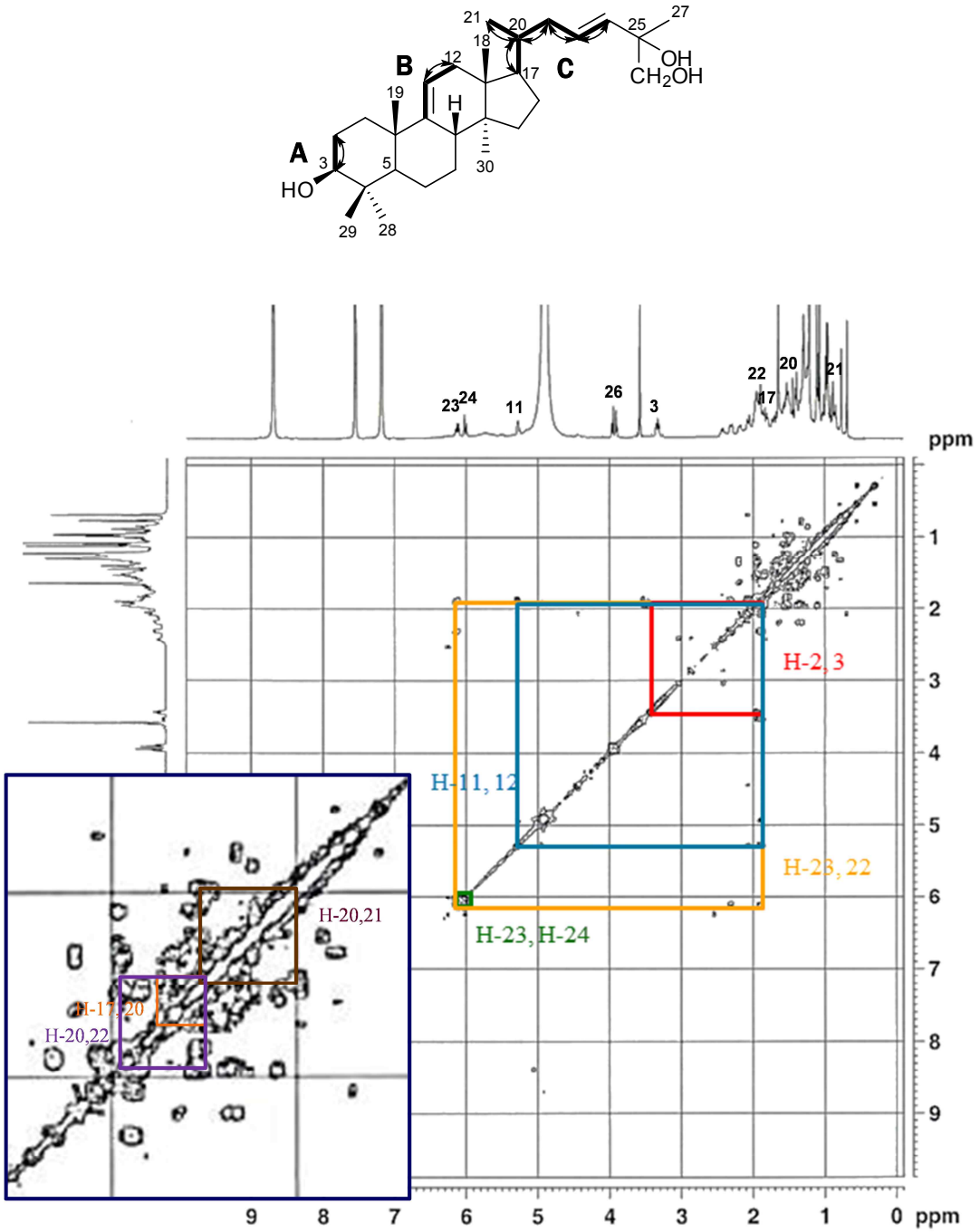

Figure 59. ^{1}H-^{1}H COSY spectrum of compound **AJ41**

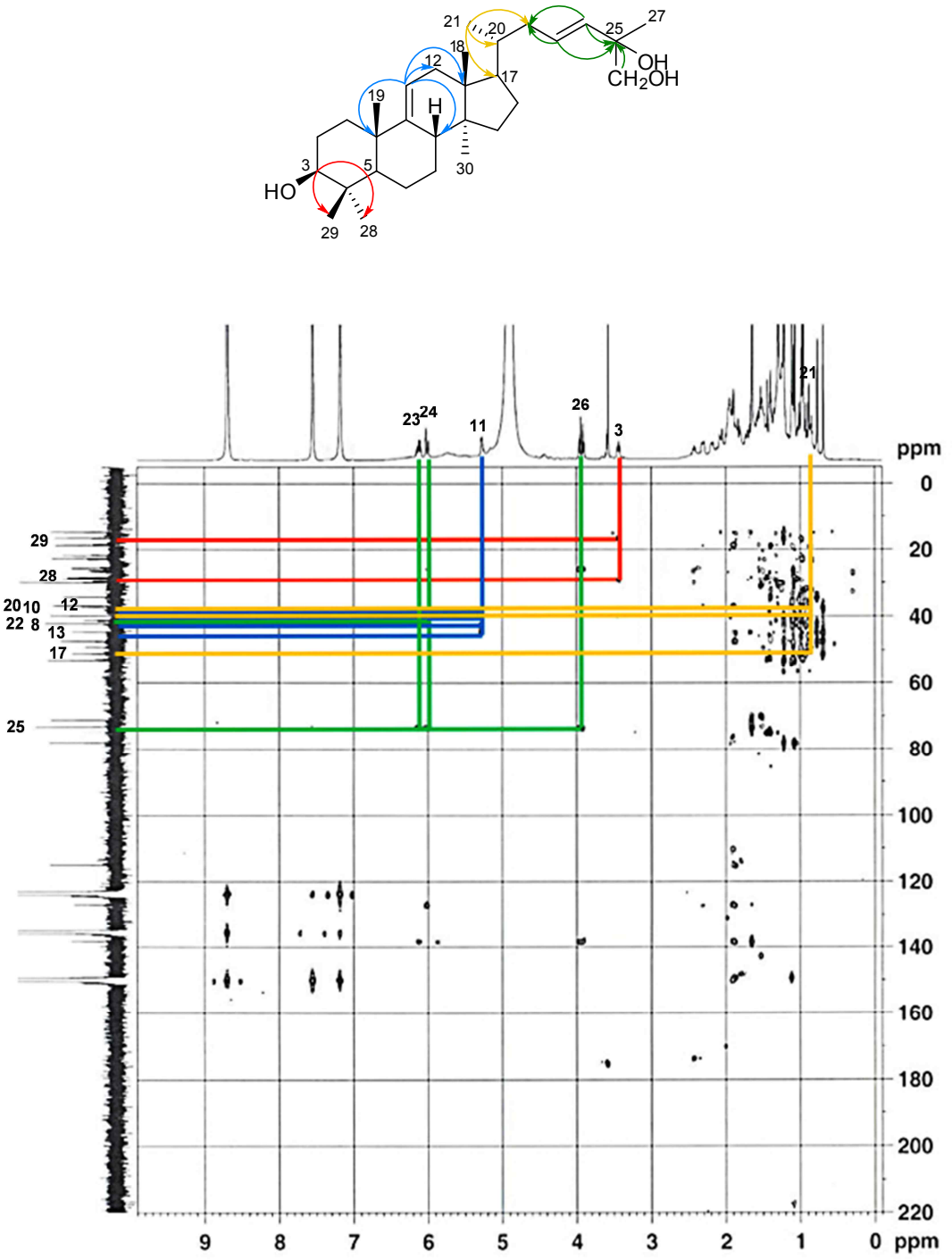

Figure 60. HMBC spectrum of compound **AJ41**

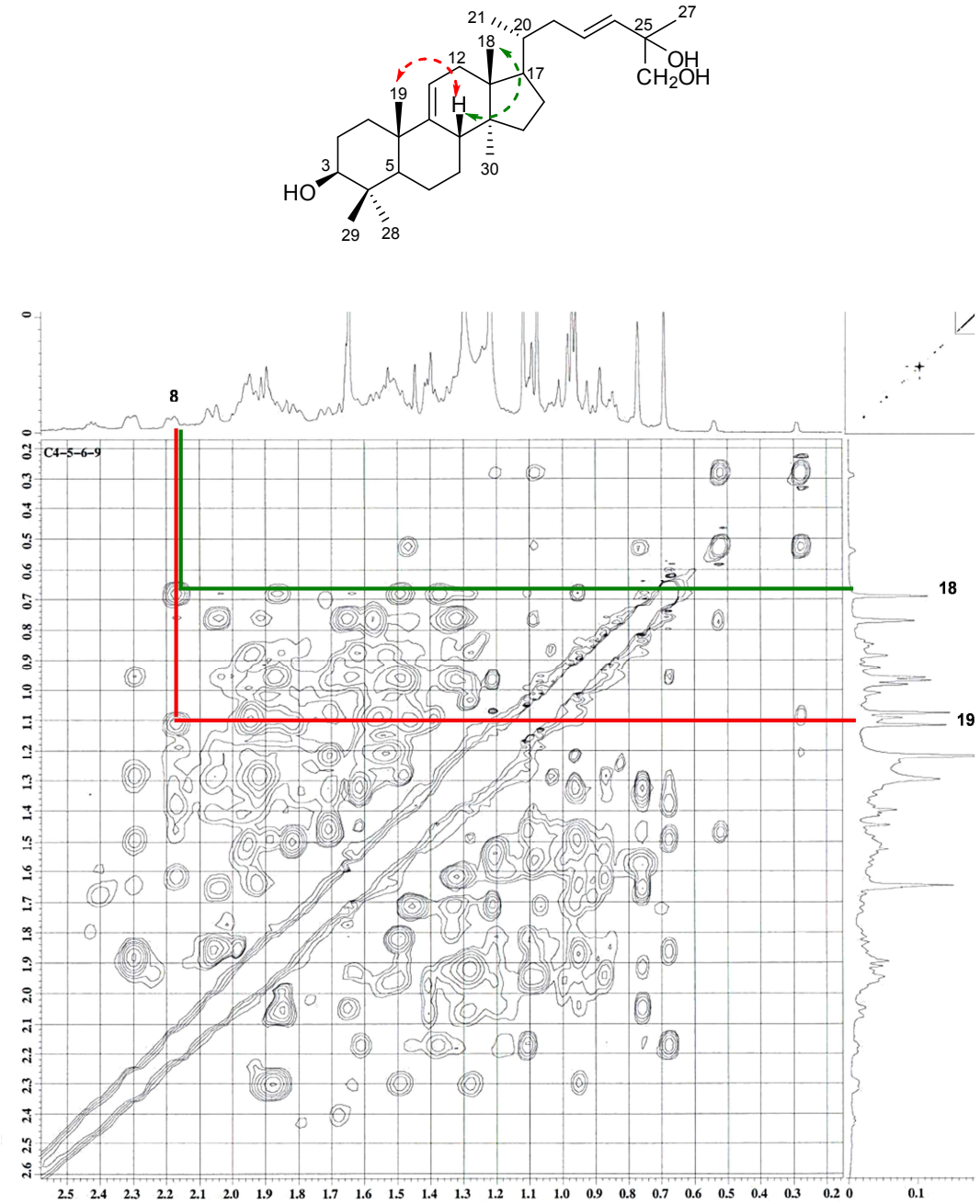

Figure 61. NOESY spectrum of compound **AJ41**

1.19. Compound AJ42

Compound **AJ42** was isolated as whitish amorphous powder, $[\alpha]_D^{25}$ +51.0 (*c* 1.0 $CHCl_3$:MeOH=1:1) and the molecular formula of compound **AJ42** was deduced to be $C_{30}H_{52}O_3$ from the negative mode FABMS analysis (m/z = 459 $[M-H]^-$), ^{13}C-NMR and DEPT spectral data, suggesting compound **AJ42** to be a tetracyclic compound. The ^{1}H NMR spectrum of compound **AJ42** showed evidence for the presence of isopropylene function [δ_H 5.27 (1H, br s, H-26), 4.95 (1H, br s, H-26), 1.90 (3H, s, H-27)], six *tert*-CH_3 groups [δ_H 1.42 (3H, s, H-21), 1.22 (3H, s, H-18), 1.03 (3H, s, H-28), 0.97 (3H, s, H-19), 0.93 (3H, s, H-30), 0.85 (3H, s, H-29)] for the aforesaid triterpenoid skeleton (Figure 62). The ^{13}C NMR spectrum of compound **AJ42** showed signals assignable to seven *tert*-CH_3 groups [δ_C 28.3 (C-28), 28.2 (C-21), 18.3 (C-18), 18.8 (C-19), 16.5 (C-27), 16.3 (C-30), 15.7 (C-29)], ten methylenes [δ_C 35.7 (C-1), 28.7 (C-2), 16.8 (C-6), 37.4 (C-7), 21.9 (C-11), 26.3 (C-12), 31.7 (C-15), 25.4 (C-16), 39.5 (C-22), 30.6 (C-23)], six sp^3-hybridized methines [δ_C 78.1 (C-3), 50.7 (C-5), 50.6 (C-9), 42.6 (C-13), 51.1 (C-17), 76.0 (C-24)], five quaternary sp^3-carbon [δ_C 39.6 (C-4), 40.7 (C-8), 38.1 (C-10), 56.4 (C-14), 74.1 (C-20)], one *exo*-methylene [δ_C 110.0 (C-26)], and one quaternary sp^2-carbon [δ_C 150.0 (C-25)], suggesting to be a tetracyclic triterpenoid. The ^{13}C NMR spectrum of compound **AJ42** also revealed three hydroxyl group [δ_C 78.1 (C-3), 76.0 (C-24), 74.1 (C-20)]. The coupling constant of δ_H 3.43 (1H, dd, *J* = 10.6, 5.4 Hz, H-3) indicated the hydroxyl groups should have 3β-orientation. On the basis of the above data, compound **AJ42** was characterized as leucastrins B in comparison with previously reported literature (Miyaichi et al., 2006).

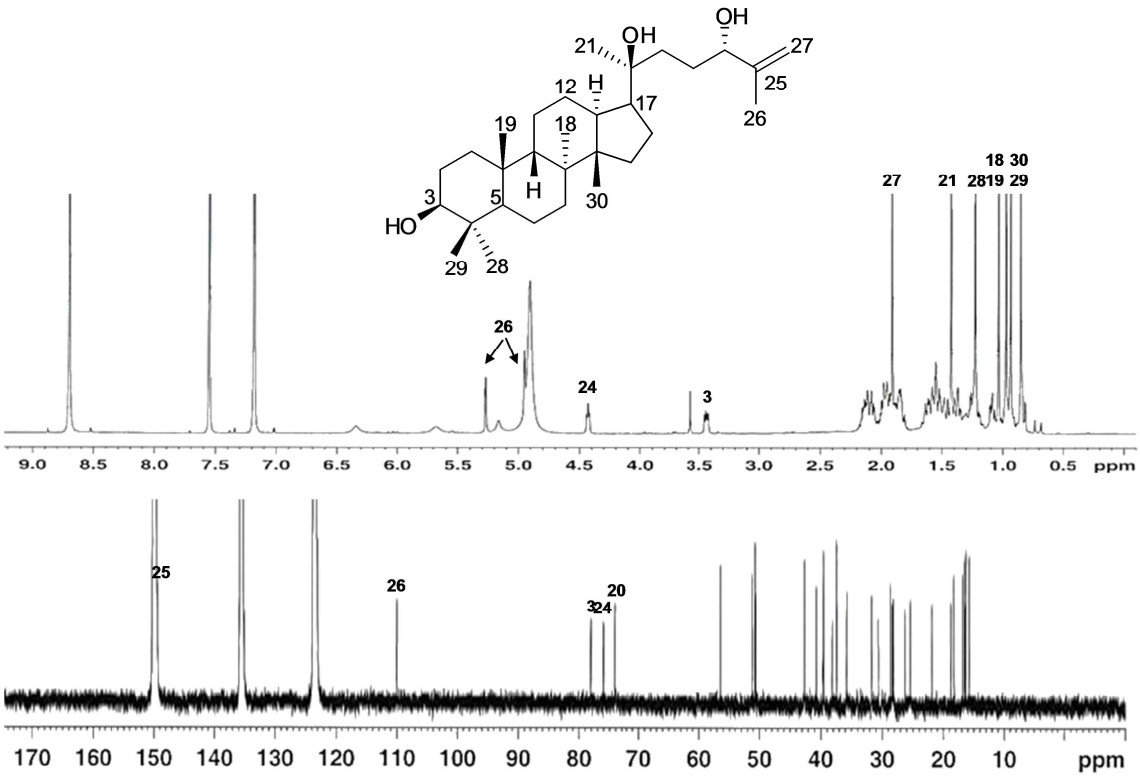

Figure 62. ^{1}H and ^{13}C NMR spectra of compound **AJ42**

1.20. Compounds AF13-16

Compound **AF13** was obtained as pale brownish syrup. The molecular formula was determined to be $C_{23}H_{28}O_{13}$ from the negative FABMS at m/z 511 $[M-H]^-$. The IR spectrum of compound **AF13** showed absorption bands for hydroxy (3376 cm^{-1}), carbonyl (1684 cm^{-1}), and aromatic ring (1610, 1514, 1337 cm^{-1}) functions. ^{1}H- and ^{13}C-NMR data showed evidence for the presence of a symmetric 1,2,4,6-tetrasubstituted benzene ring [δ_H 6.02 (2H, s, H-3, 5); δ_C 156.8 (C-4), 155.8 (C-2, 6), 95.1 (C-3, 5), 130.1 (C-1)], a syringoyl moiety [δ_H 7.24 (2H, s, H"-2, 6); δ_C 168.8 (C-7"), 149.8 (C-3", 5"), 143.1 (C-4"), 122.0 (C-1"), 109.0 (C-2", 6")], and one

glucopyranose moiety. The glucose unit was determined to be attached to C-1 of the phenolic unit by the cross-peak in the HMBC spectrum between H-1' at δ_H 4.68 of the glucose unit and C-1 at δ_C 130.1 of the symmetric benzene ring. ^{1}H-NMR data for the symmetric benzene ring showed the presence of six protons corresponding to two methoxy groups at δ_H 3.66 (6H, s, 2, 6-OCH_3) and HMBCs were observed between the signal at δ_H 3.66 (6H, s, 2, 6-OCH_3) and δ_C 155.8 (C-2, 6). The connection of syringoyl group to the C-6' position was also confirmed by the HMBC correlations between the signals at δ_H 4.55 (1H, H-6'a)/4.38 (1H, H-6'b) and δ_C 168.8 (1H, C-7''). On the basis of the above data, compound **AF13** was characterized as 4-hydroxy-2,6-dimethoxyphenyl 6'-*O*-syringoyl-*β*-D-glucopyranoside (Figure 63).

Compound **AF14** was obtained as pale brownish syrup and shared similar physical and spectroscopic data with compound **AF13**. The molecular formula was determined to be $C_{22}H_{26}O_{12}$ from the negative FABMS at m/z 481 $[M-H]^-$, which suggests the absence of one methoxy group. Compound **AF14** has a vanillic acid moiety instead of syringic acid, which resulted in the different number of methoxy signals in ^{1}H-NMR and ^{13}C-NMR spectra. The position of vanillic acid on glucose was determined by HMBC connection between H-6′ and C-7″. Therefore, compound **AF14** was identified as 4-hydroxy-2,6-dimethoxyphenyl 6'-*O*-vanilloyl-*β*-D-glucopyranoside (Figure 63).

Compound **AF15** was isolated as pale brownish syrup, $[\alpha]_D^{20}$ -35.0 (*c* 1.0 MeOH) and the molecular formula of compound **AF15** was deduced to be $C_{22}H_{26}O_{12}$ from the negative mode ESIMS analysis (*m/z* 481.07 $[M-H]^-$). The ^{1}H and ^{13}C NMR spectra of compound **AF15** bears a resemblance to those of compound **AF13** except for disappearance of methoxy group at C-6. Therefore, compound **AF17** was concluded as 4-hydroxy-2-methoxyphenyl 6'-*O*-syringoyl-*β*-D-

glucopyranoside (Hiltunen et al., 2006) (Figure 63).

Compound **AF16** was obtained as pale brownish syrup, and $[\alpha]_D^{20}$ -19.0 (*c* 0.5 MeOH). The negative ESIMS exhibited molecular ion peak at *m/z* 451.08 $[M-H]^-$ indicating $C_{21}H_{24}O_{11}$ as its molecular formula. The ^1H and ^{13}C NMR spectra of compound **AF16** were similar to those of compound **AF14** except for disappearance of methoxy group at C-6. Thus, compound **AJ13** was confirmed as 6'-*O*-vanilloylisotachioside (Yang et al., 2007) (Figure 63).

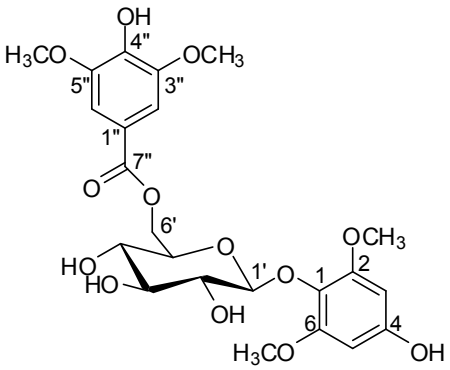

AF13

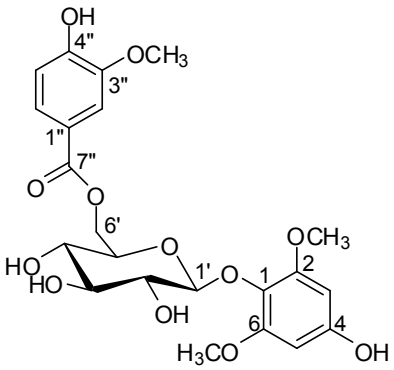

AF14

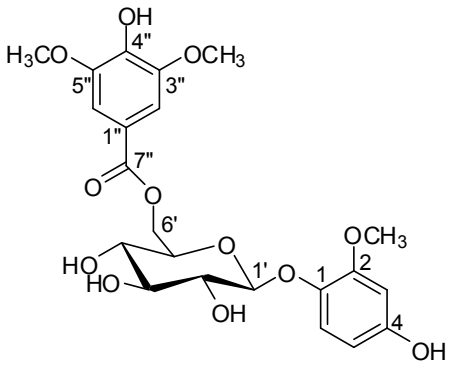

AF15

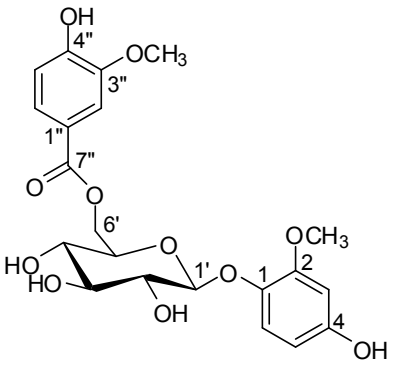

AF16

Figure 63. The structures of compounds **AF13-16**

1.21. Compounds AF17-19

Compound **AF17** was isolated as whitish amorphous powder. The molecular formula was determined to be $C_{30}H_{48}O_3$ from the negative FABMS at m/z 455 $[M-H]^-$. The ^1H and ^{13}C NMR spectra of compound **AF17** bears a resemblance to those of compound **AF19** except for disappearance of both caffeoyl group at C-3 and hydroxyl group at C-2, and carboxyl group appearing at C-28 (Figure 64). Therefore, compound **AF17** was concluded as betulinic acid (Siddiqui et al., 1988).

Compound **AF18** was obtained as whitish amorphous powder and $[\alpha]_D^{25}$ +3.2 (*c* 1.0 $CHCl_3$:MeOH=1:1). Its molecular formula was identified as $C_{39}H_{54}O_7$ by the negative mode ESIMS (*m/z* 633.28 $[M-H]^-$) and the ^{13}C NMR spectrum. The ^1H and ^{13}C NMR spectra of compound **AF18** were similar to those of compound **AF19** except for the connection of caffeoyl group to the C-2 position and carboxyl group to the C-17 position. In the ^1H NMR spectrum, two methane protons (δ 5.59, ddd, *J*=10.6, 10.6, 4.6 Hz, and (δ 3.69, d *J*=9.9 Hz) were assigned to H-2β and H-3α, respectively (Figure 65). With above observed spectroscopic data, compound **AF18** was confirmed as 2-*O*-caffeoylalphitolic acid (Shao et al., 2002).

Compound **AF19** was isolated as whitish amorphous powder. The molecular formula was determined to be $C_{39}H_{56}O_6$ from the negative HR-FAB-MS at m/z 619.3997 $[M-H]^-$ (calcd. for $C_{39}H_{55}O_6$: 619.3999). The ^1H-NMR spectrum of compound **AF19** showed evidence for the presence of isopropylene function [δ 4.76 (1H, br s, H-29), 4.89 (1H, br s, H-29), 1.78 (3H, s, H-30)], five *tert*-CH_3 groups [δ 1.05 (3H, s, H-27), 1.03 (3H, s, H-23), 1.02 (3H, s, H-24), 0.99 (3H, s, H-26), 0.96 (3H, s, H-25)], geminal protons at δ 4.10 (1H, d, *J*=10.8, H-28) and 3.68 (1H, d, *J*=10.8, H-28)], an allylic proton at δ 2.62 (1H, td, *J*=10.8, 6 Hz, H-28) for the aforesaid

triterpenoid skeleton and caffeoyl moiety [δ 8.03 (1H, d, *J*=16.2, H-7'), 7.59 (1H, d, *J*=1.8, H-2'), 7.24 (1H, d, *J*=8, H-5'), 7.15 (1H, dd, *J*=8, 1.8 H-6'), 6.69 (1H, d, *J*=16.2, H-8')] (Figure 66). The coupling constant (9.6 Hz) between proton δ 5.25 (1H, d, *J*=9.6 Hz, H-3) and δ 4.31 (1H, td, *J*=10.8, 4.2 Hz, H-2) indicated the hydroxyl groups should have 2*α*,3*β*-orientation, which was further supported by the NOESY correlations of H-2 with H-1β and H-25 and of H-3 with H-1α (Figure 6668). The connection of caffeoyl group to the C-3 position was also confirmed by the HMBC correlations between the signals at δ_H 5.25 (1H, H-3) and δ_C 168.0 (C-9') (Figure 667). On the basis of the above data, compound **AF19** was characterized as lup-20(29)en-2,28-diol-3-yl caffeate, which has been newly discovered from nature.

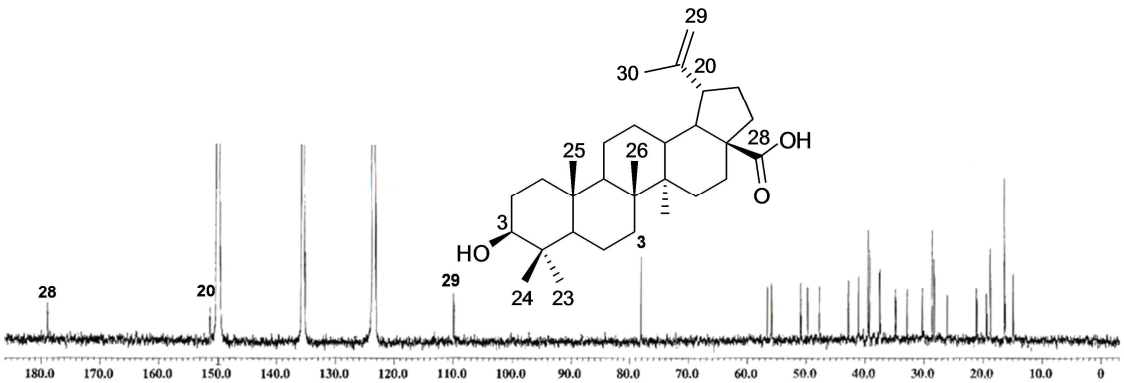

Figure 64. ^{13}C NMR spectrum of compound **AF17**

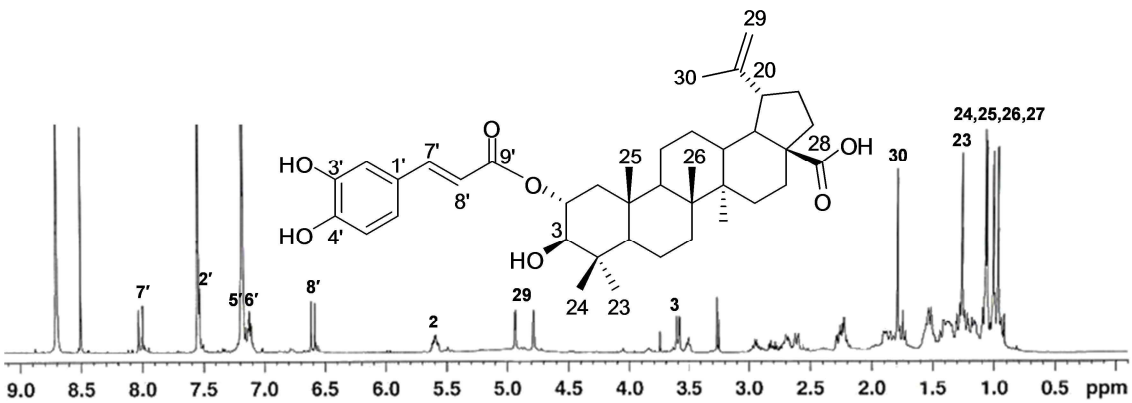

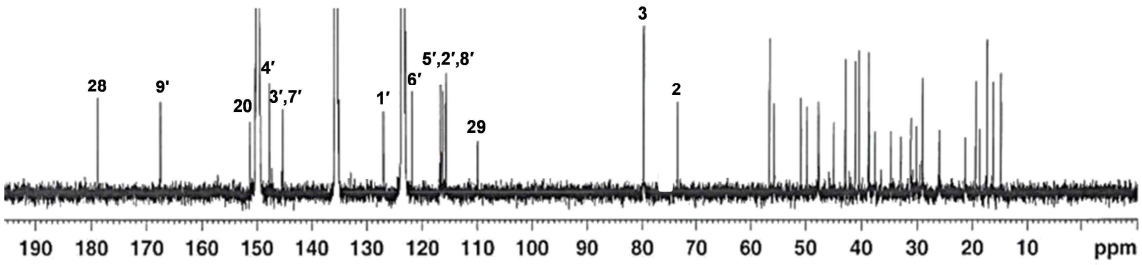

Figure 65. ^{1}H and ^{13}C NMR spectra of compound **AF18**

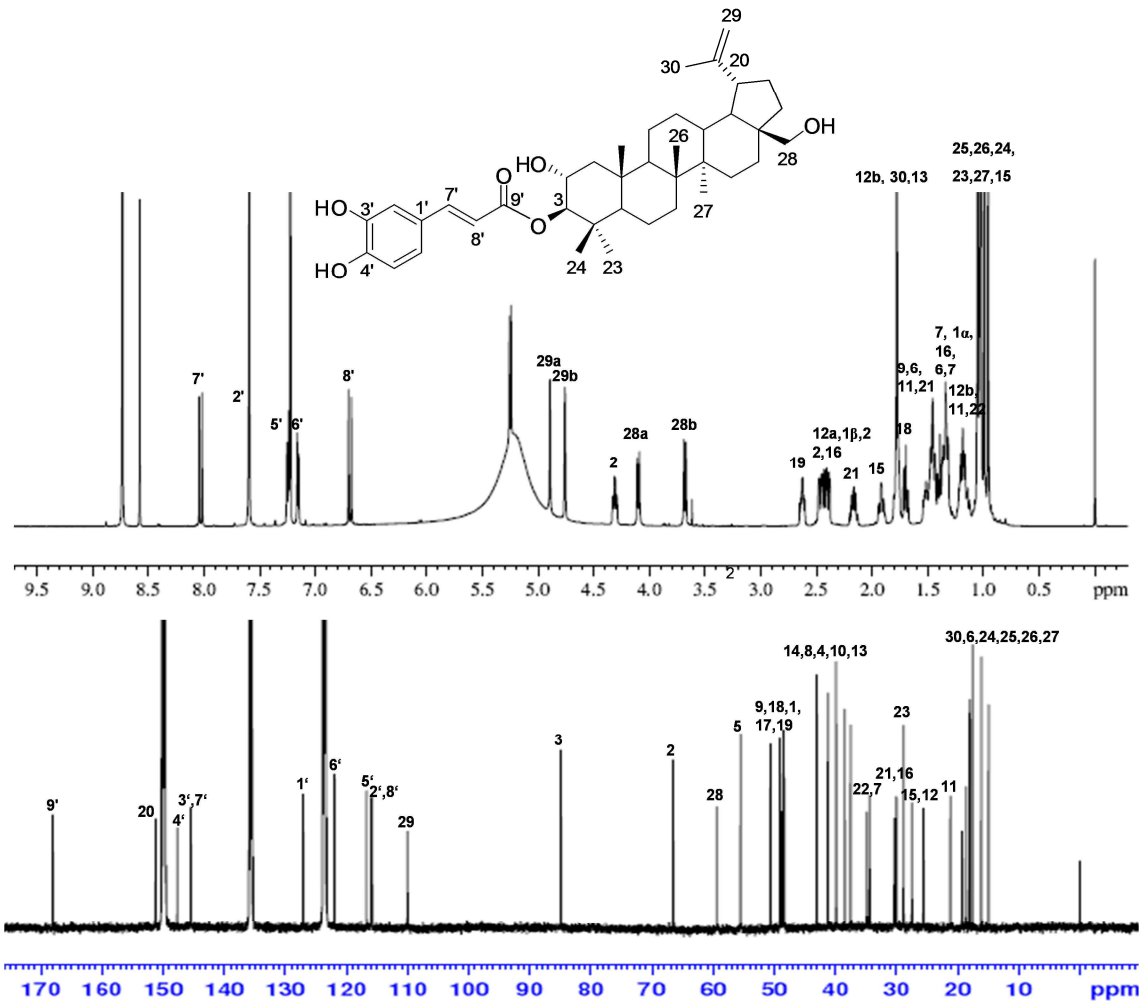

Figure 66. ^{1}H and ^{13}C NMR spectra of compound **AF19**

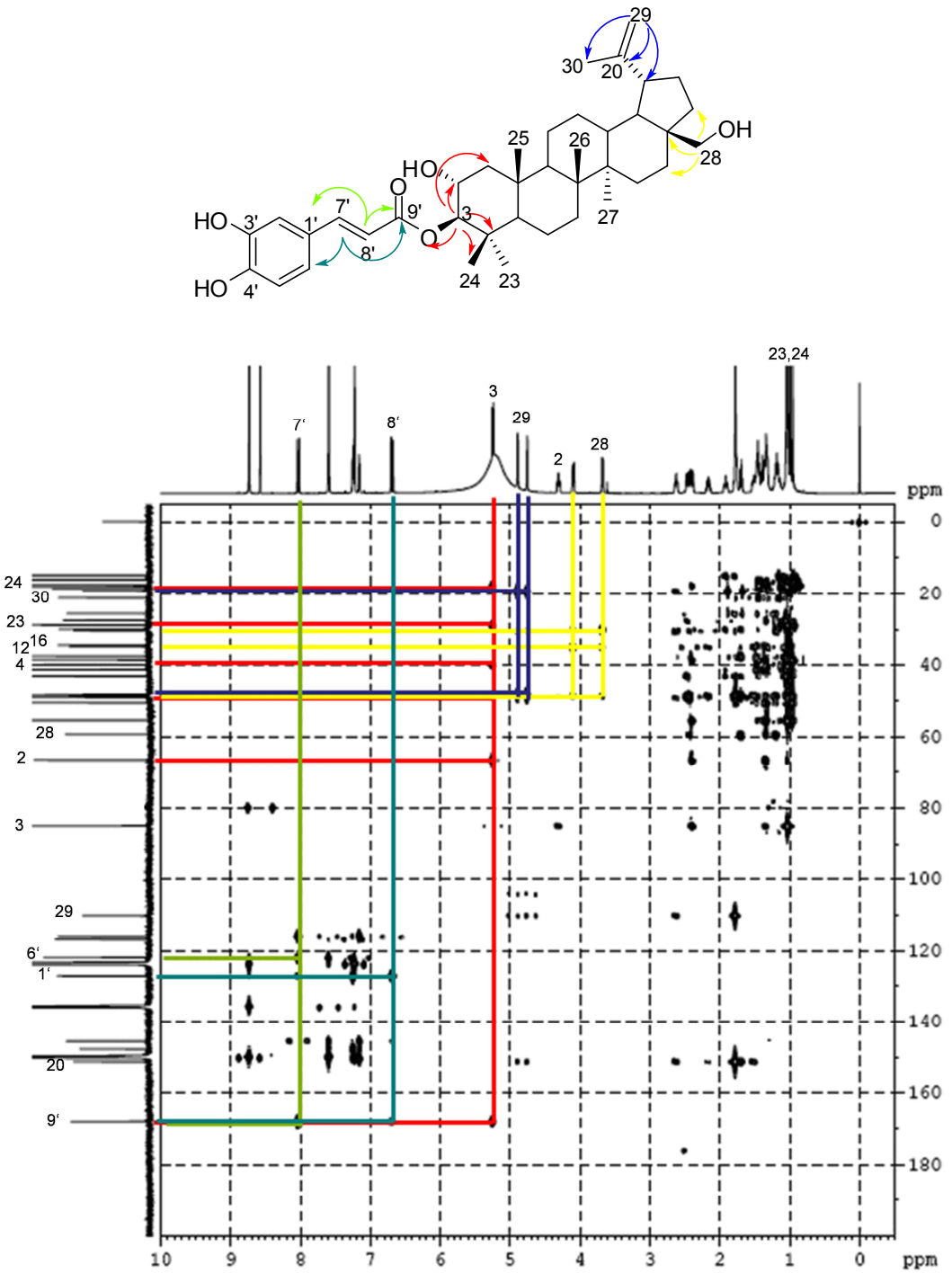

Figure 67. HMBC spectrum of compound **AF19**

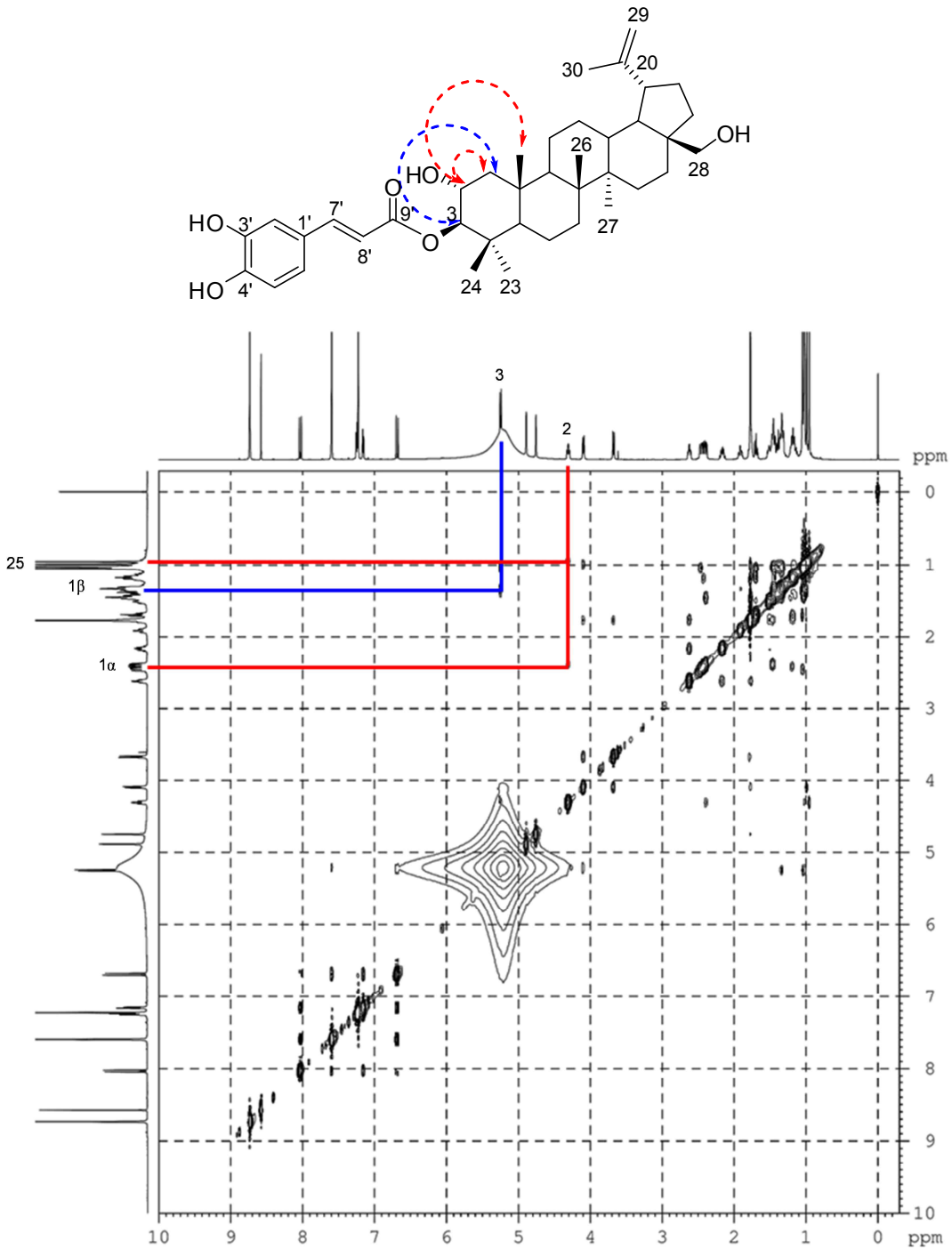

Figure 68. NOESY spectrum of compound **AF19**

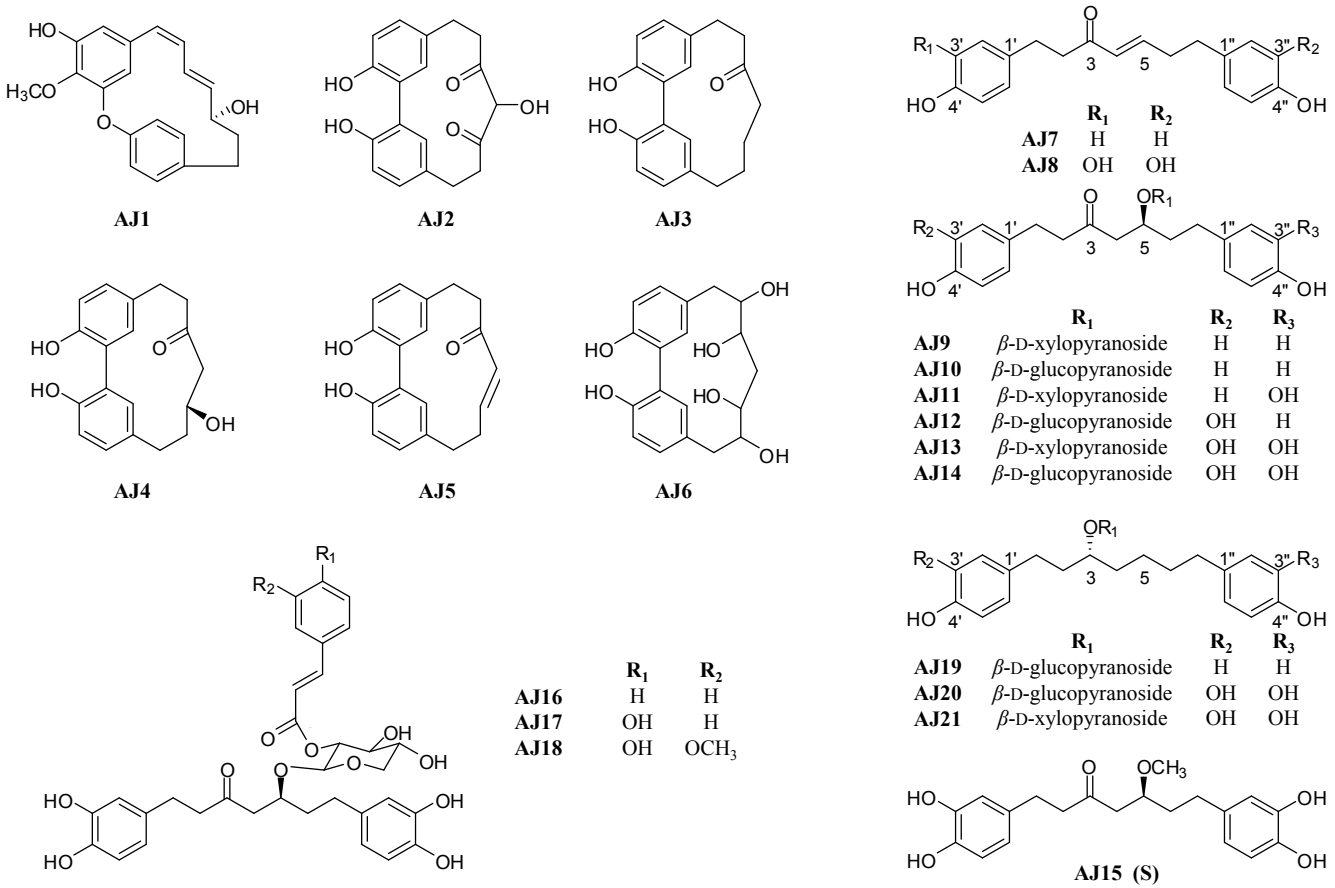

Figure 69. Chemical constituents isolated from *A. japonica* fruits - diarylheptanois

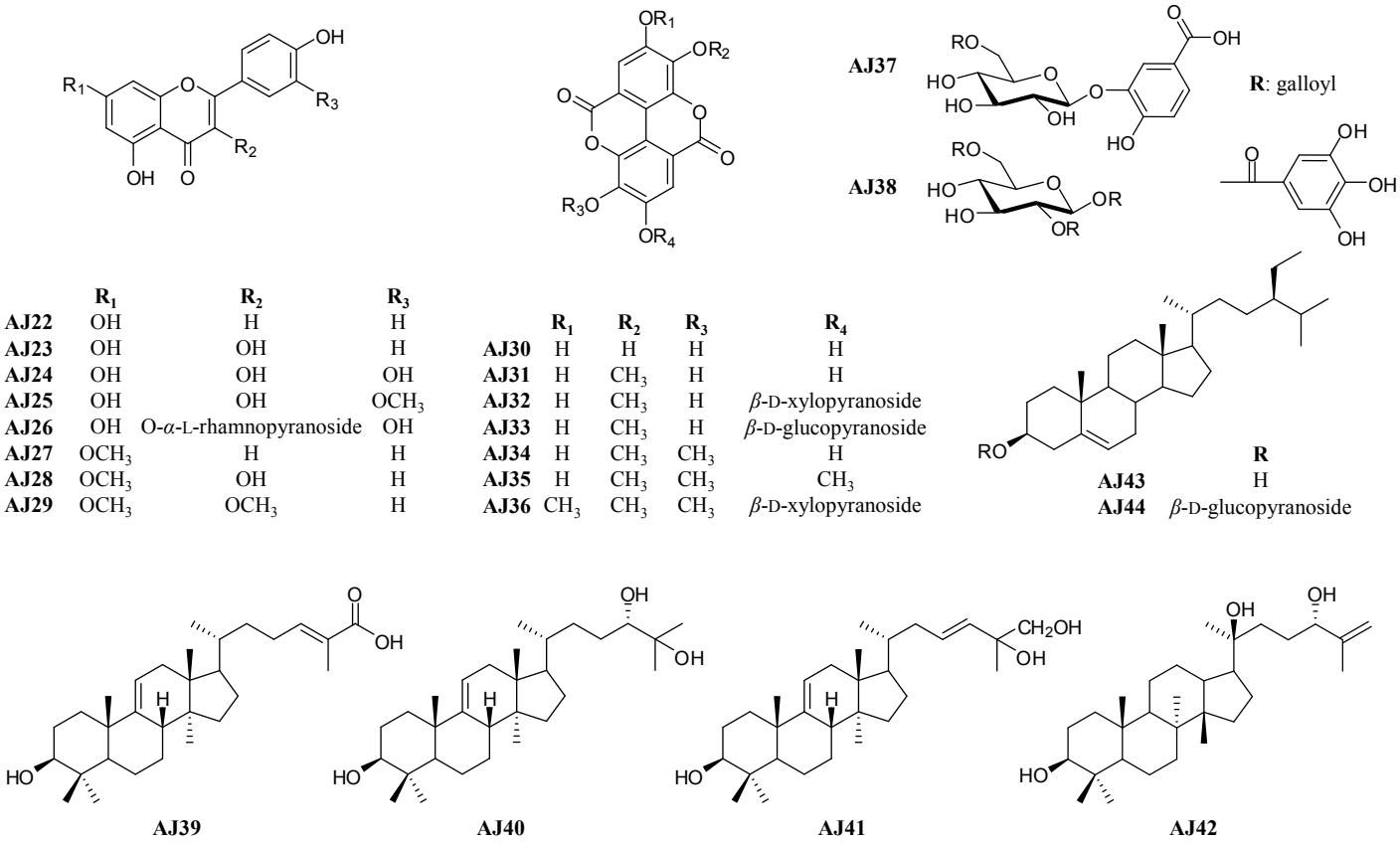

	R_1	R_2	R_3
AJ22	OH	H	H
AJ23	OH	OH	H
AJ24	OH	OH	OH
AJ25	OH	OH	OCH_3
AJ26	OH	O-α-L-rhamnopyranoside	OH
AJ27	OCH_3	H	H
AJ28	OCH_3	OH	H
AJ29	OCH_3	OCH_3	H

	R_1	R_2	R_3	R_4
AJ30	H	H	H	H
AJ31	H	CH_3	H	H
AJ32	H	CH_3	H	β-D-xylopyranoside
AJ33	H	CH_3	H	β-D-glucopyranoside
AJ34	H	CH_3	CH_3	H
AJ35	H	CH_3	CH_3	CH_3
AJ36	CH_3	CH_3	CH_3	β-D-xylopyranoside

	R
AJ43	H
AJ44	β-D-glucopyranoside

Figure 70. Structures of the compounds isolated from *A. japonica* fruits - flavonoids, triterpenoids, tannins, sterols

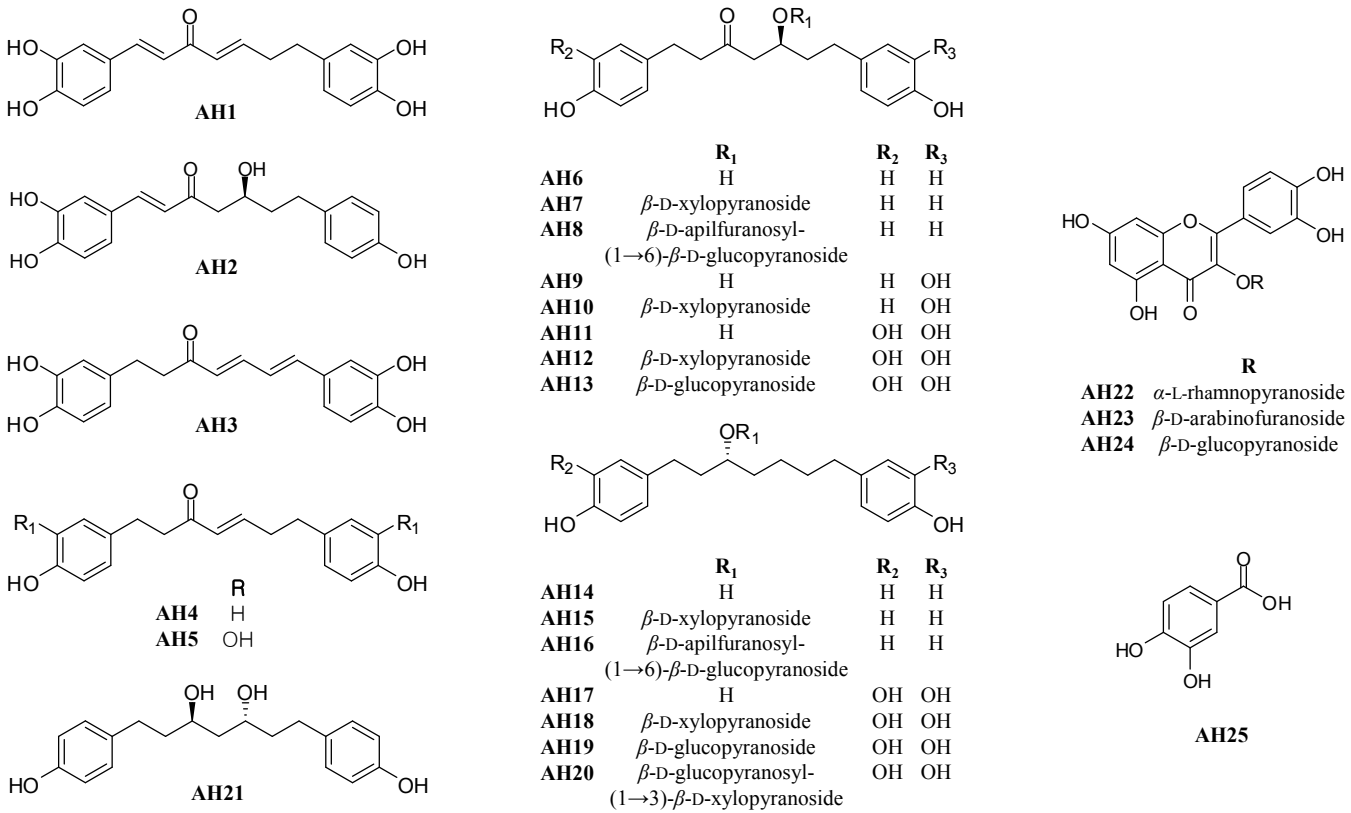

Figure 71. Structures of the compounds isolated from *A. hirsuta* var. *sibirica* leaves

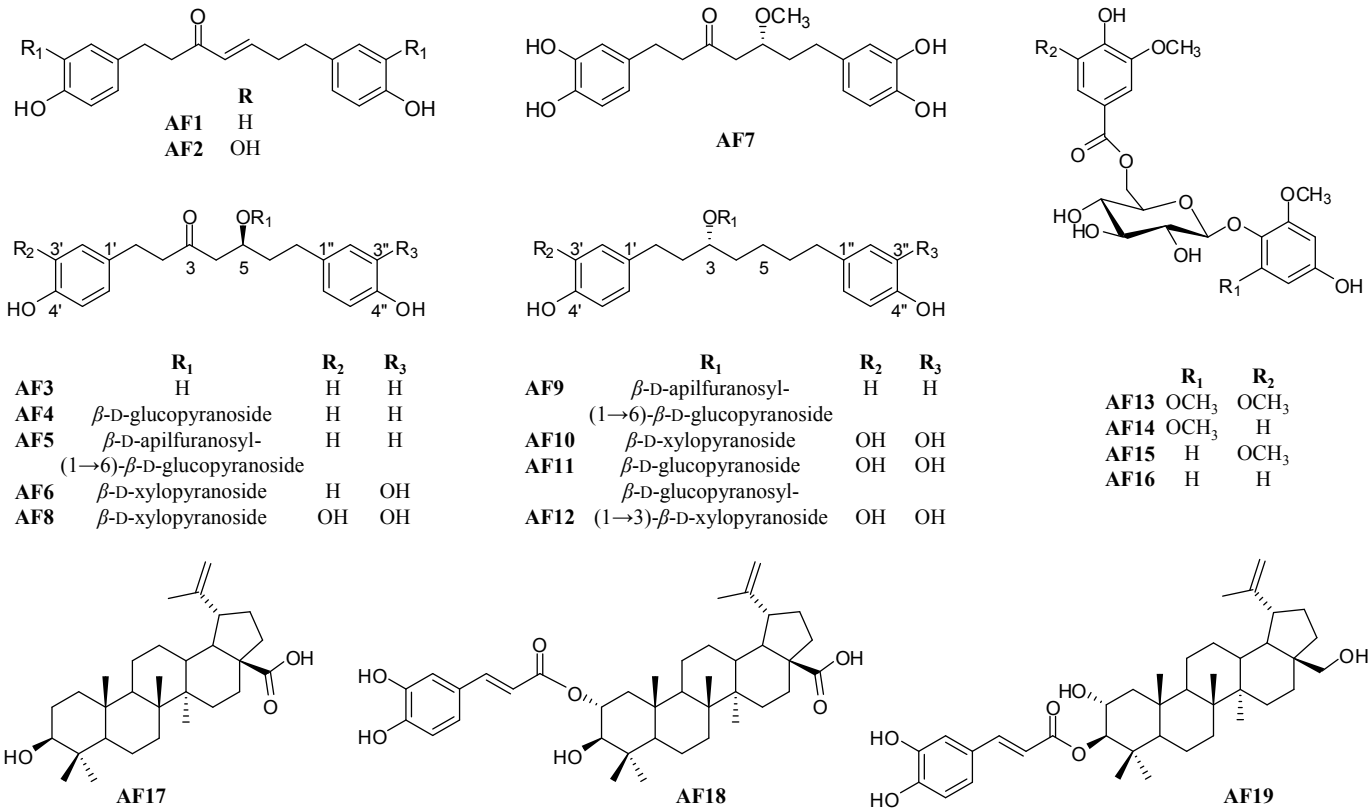

Figure 72. Structures of the compounds isolated from *A. firma* barks

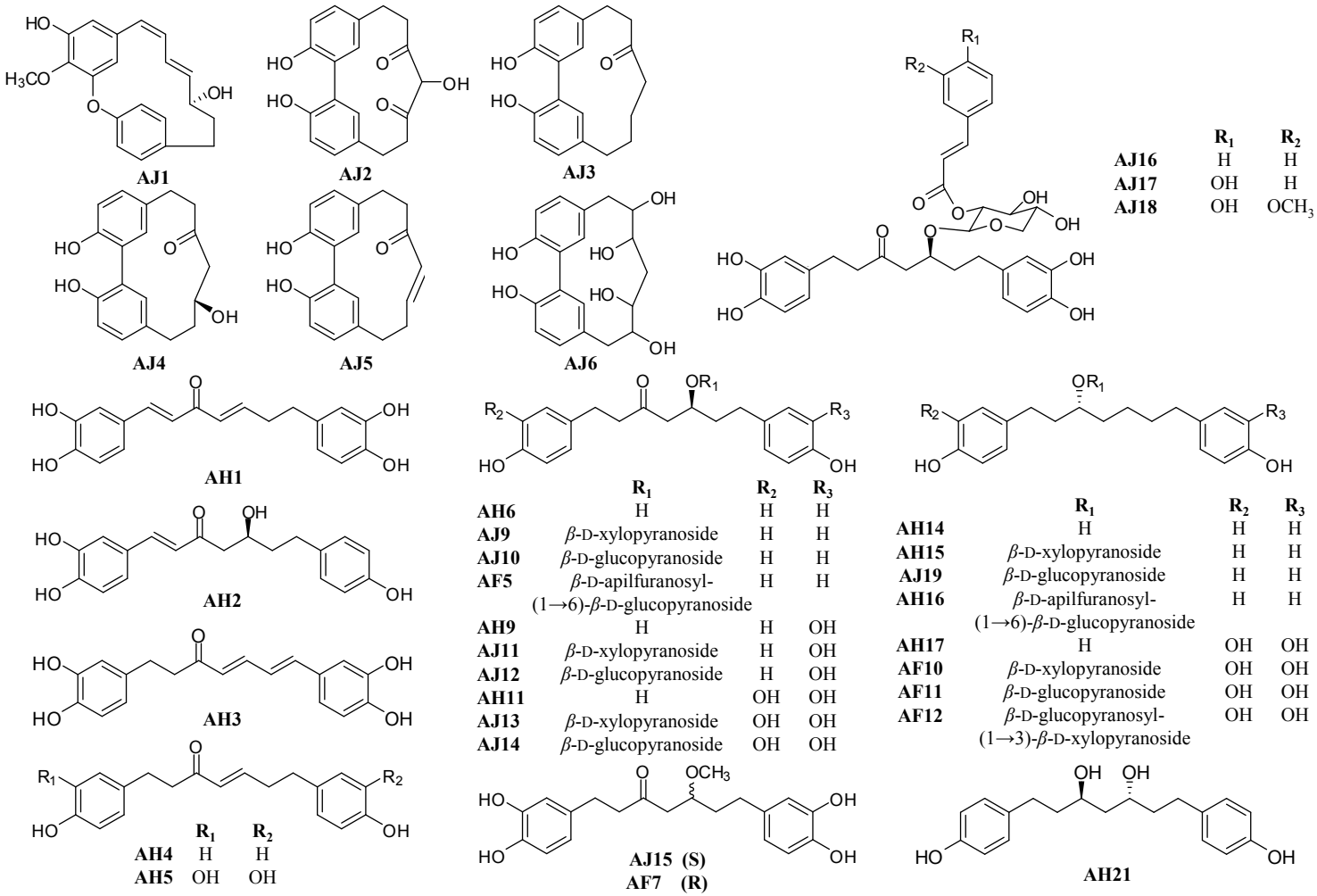

	R_1	R_2
AJ16	H	H
AJ17	OH	H
AJ18	OH	OCH_3

	R_1	R_2	R_3
AH6	H	H	H
AJ9	*β*-D-xylopyranoside	H	H
AJ10	*β*-D-glucopyranoside	H	H
AF5	*β*-D-apilfuranosyl-(1→6)-*β*-D-glucopyranoside	H	H
AH9	H	H	OH
AJ11	*β*-D-xylopyranoside	H	OH
AJ12	*β*-D-glucopyranoside	H	OH
AH11	H	OH	OH
AJ13	*β*-D-xylopyranoside	OH	OH
AJ14	*β*-D-glucopyranoside	OH	OH

	R_1	R_2	R_3
AH14	H	H	H
AH15	*β*-D-xylopyranoside	H	H
AJ19	*β*-D-glucopyranoside	H	H
AH16	*β*-D-apilfuranosyl-(1→6)-*β*-D-glucopyranoside	H	H
AH17	H	OH	OH
AF10	*β*-D-xylopyranoside	OH	OH
AF11	*β*-D-glucopyranoside	OH	OH
AF12	*β*-D-glucopyranosyl-(1→3)-*β*-D-xylopyranoside	OH	OH

	R_1	R_2
AH4	H	H
AH5	OH	OH

Figure 73. Chemical constituents isolated from three *Alnus* species - diarylheptanois

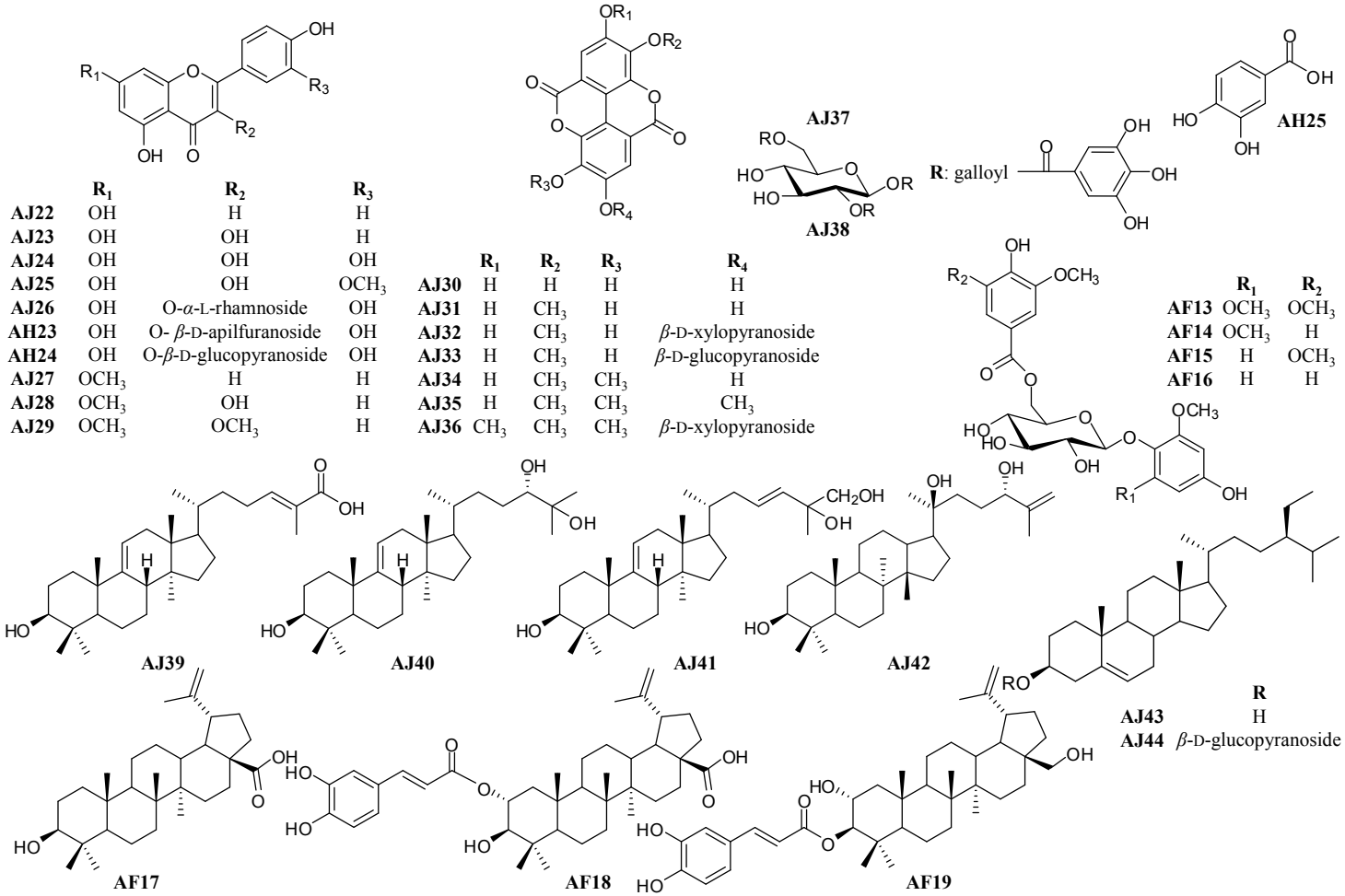

	R_1	R_2	R_3
AJ22	OH	H	H
AJ23	OH	OH	H
AJ24	OH	OH	OH
AJ25	OH	OH	OCH_3
AJ26	OH	O-α-L-rhamnoside	OH
AH23	OH	O- β-D-apilfuranoside	OH
AH24	OH	O-β-D-glucopyranoside	OH
AJ27	OCH_3	H	H
AJ28	OCH_3	OH	H
AJ29	OCH_3	OCH_3	H

	R_1	R_2	R_3	R_4
AJ30	H	H	H	H
AJ31	H	CH_3	H	H
AJ32	H	CH_3	H	β-D-xylopyranoside
AJ33	H	CH_3	H	β-D-glucopyranoside
AJ34	H	CH_3	CH_3	H
AJ35	H	CH_3	CH_3	CH_3
AJ36	CH_3	CH_3	CH_3	β-D-xylopyranoside

	R_1	R_2
AF13	OCH_3	OCH_3
AF14	OCH_3	H
AF15	H	OCH_3
AF16	H	H

	R
AJ43	H
AJ44	β-D-glucopyranoside

Figure 74. Chemical constituents isolated from three *Alnus* species - flavonoids, triterpenoids, tannins, phenolic compounds

Table 29. Compounds isolated from three *Alnus* species

Compound				Name
AJ1			**AJ1**	(5*R*)-3,5'-dihydroxy-4'-methoxy-3',4''-oxo-1,7-diphenyl-1,3-diheptene
AJ2			**AJ2**	4-hydroxy-alnus-3,5-dione
AJ3			**AJ3**	dihydroalnusone
AJ4			**AJ4**	alnusonol
AJ5			**AJ5**	alnusone
AJ6			**AJ6**	betulatetraol
	AH1		**AH1**	1,4-heptadien-3-one-1,7-bis(3,4-dihydroxyphenyl)-(1*E*,4*E*)
	AH2		**AH2**	(5*S*)-hydroxy-1-(3,4-dihydroxyphenyl)-7-(4-hydroxyphenyl)-hepta-1*E*-en-3-one
	AH3		**AH3**	1,7-bis-(3,4-dihydroxyphenyl)-hepta-4*E*,6*E*-dien-3one
AJ7	**AH4**	**AF1**	**AH4**	1,7-bis-(4-hydroxyphenyl)-5-hepten-3-one
AJ8	**AH5**	**AF2**	**AH5**	hirsutenone
	AH6	**AF3**	**AH6**	5-hydroxy-3-platyphyllone
AJ9	**AH7**		**AJ9**	platyphyllonol-5-*O*-*β*-D-xylopyranoside
AJ10		**AF4**	**AJ10**	platyphylloside
	AH8	**AF5**	**AF5**	(5*S*)-5-hydroxy-1,7-bis-(4-hydroxyphenyl)-3-heptanone-5-*O*-*β*-D-apiofuranosyl-(1→6)-*β*-D-glucopyranoside
	AH9		**AH9**	(5*S*)-5-hydroxy-1-(4-hydroxyphenyl)-7-(3,4-dihydroxyphenyl)-3-heptanone
AJ11	**AH10**	**AF6**	**AJ11**	(5*S*)-5-hydroxy-7-(3,4-dihydroxyphenyl)-1-(4-hydroxyphenyl)-3-heptanone-5-*O*-*β*-D-xylopyranoside
AJ12			**AJ12**	5-hydroxy-1-(3,4-dihydroxyphenyl)-7-(4-hydroxyphenyl)-3-heptanone-5-*O*-*β*-D-glucopyranoside
	AH11		**AH11**	hirsutanonol
AJ13	**AH12**	**AF8**	**AJ13**	oregonin
AJ14	**AH13**		**AJ14**	hitsutanonol-5-*O*-*β*-D-glucopyranoside
AJ15			**AJ15**	(5*S*)-*O*-methylhirsutanonol
		AF7	**AF7**	(5*R*)-*O*-methylhirsutanonol
AJ16			**AJ16**	2'''-cinnamoyloregonin
AJ17			**AJ17**	oregonyl A
AJ18			**AJ18**	oregonyl B
	AH14		**AH14**	(-)-centrolobol

	AH15		**AH15**	1,7-di(4-hydroxyphenyl)-3(*R*)-*β*-D-xylosyloxyheptane
AJ19			**AJ19**	aceroside VII
	AH16	**AF9**	**AH16**	(3*R*)-1,7-bis-(4-hydroxyphenyl)-3-heptanol-3-*O*-*β*-D-apiofuranosyl-(1→6)-*β*-D-glucopyranoside
	AH17		**AH17**	(3*R*)-1,7-bis-(3,4-dihydroxyphenyl)-3-heptanol
AJ20	**AH18**	**AF10**	**AF10**	(3*R*)-1,7-bis-(3,4-dihydroxyphenyl)-3-heptanol-3-*O*-*β*-D-xylopyranoside
AJ21	**AH19**	**AF11**	**AF11**	(3*R*)-1,7-bis-(3,4-dihydroxyphenyl)-3-heptanol-3-*O*-*β*-D-glucoopyranoside
	AH20	**AF12**	**AF12**	(3*R*)-1,7-bis-(3,4-dihydroxyphenyl)-3-heptanol-3-*O*-*β*-D-glucopyranosyl (1→3)-3-*O*-*β*-D-xylopyranoside
	AH21		**AH21**	(+)-hannokinol
AJ22			**AJ22**	apigenin
AJ23			**AJ23**	kaempferol
AJ24			**AJ24**	quercetin
AJ25			**AJ25**	isorhamnetin
AJ26	**AH22**		**AJ26**	quercitrin
	AH23		**AH23**	avicularin
	AH24		**AH24**	isoquercitirin
AJ27			**AJ27**	genkwanin
AJ28			**AJ28**	rhamnocitrin
AJ29			**AJ29**	kumatakenin
AJ30			**AJ30**	ellagic acid
AJ31			**AJ31**	3'-*O*-methyl-ellagic acid
AJ32			**AJ32**	3'-*O*-methyl-4-*O*-*β*-D-xylosyl-ellagic acid
AJ33			**AJ33**	3'-*O*-methyl-4-*O*-*β*- D-glucosyl-ellagic acid
AJ34			**AJ34**	3,3'-di-*O*-methyl-ellagic acid
AJ35			**AJ35**	3,3',4'-tri-*O*-methyl-ellagic acid
AJ36			**AJ36**	3,3',4'-tri-*O*-methyl-4-*O*-*β*-xylosyl-ellagic acid
AJ37			**AJ37**	3,4-dihydroxybenzoic acid-3-*O*-*β*-D-(6'-*O*-galloyl)-glucopyranoside
AJ38			**AJ38**	1,2,6-tri-*O*-galloyl glucose
AJ39			**AJ39**	3*β*-hydroxy-lanost-9(11),24(25)-dien-26-oic acid
AJ40			**AJ40**	(24*S*)-lanost-9(11)-ene-3,24,25-triol
AJ41			**AJ41**	3*β*-hydroxy-lanost-9(11),23(24)-dien-25,26-diol
AJ42			**AJ42**	leucastrins B

AJ43		**AJ43**	*β*-sitosterol
AJ44		**AJ44**	daucosterol
	AF13	**AF13**	4-hydroxy-2,6-dimethoxyphenyl-6-*O*-syringoyl-*β*-D-glucopyranoside
	AF14	**AF14**	4-hydroxy-2,6-dimethoxyphenyl-6-*O*-vailloyl-*β*-D-glucopyranoside
	AF15	**AF15**	4-hydroxy-2-methoxyphenyl-6-*O*-syringoyl-*β*-D-glucopyranoside
	AF16	**AF16**	6'-*O*-vanilloylisotachioside
AH25		**AH25**	3,4-dihydroxybenzoic acid
	AF17	**AF17**	betulinic acid
	AF18	**AF18**	2-*O*-caffeoylalphitolic acid
	AF19	**AF19**	lup-20(29)en-2,28-diol-3-yl-caffeate

AJ1-44: forty four compounds isolated from *A. japonica*

AH1-25: twenty five compounds isolated from *A. hirsuta* var. *sibirica*

AF1-19: nineteen compounds isolated from *A. firma*

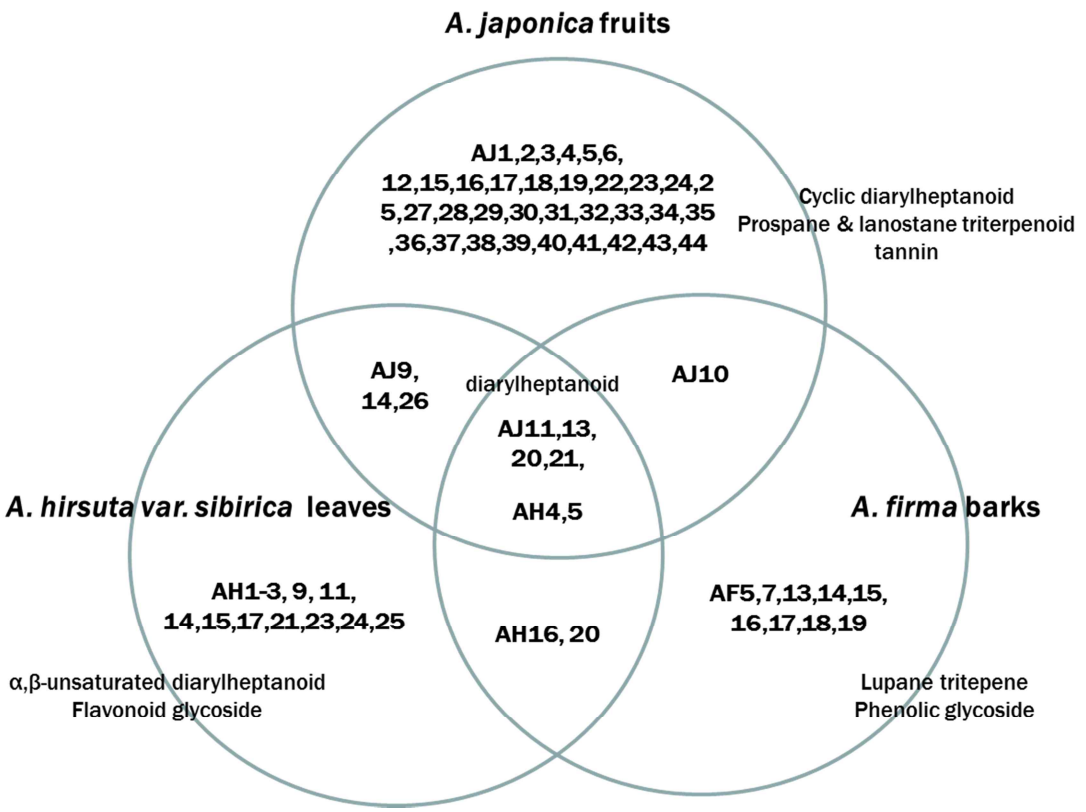

2. Anti-prolieferative activities of total extract, fractions, and compounds isolated from three *Alnus* species on 3T3-L1 cells

2.1. Inhibiory activity of total extract and fractions of *Alnus* species on adipocyte differentiation in 3T3-L1 cells

Adipogenesis is the development of mature fat cells from preadipocytes. The cellular and molecular mechanisms of adipocyte differentiation have been extensively studied using preadipocyte culture systems. Committed preadipocytes undergo alteration of cell shape, growth arrest, clonal expansion, and subsequent terminal differentiation into adipocytes, as well as a complex sequence of changes in gene expression and the storage of lipids (Luong et al., 2000). Therefore, 3T3-L1 cells were used as a screening tool to determine the anti-adipogenic activity of the isolated compounds. Recently, there is growing interest in searching for anti-adipogenic compounds from natural products. In the course of searching for anti-adipogenic molecules from the three *Alnus* species using 3T3-L1 cells, it was found that the total extract of *A. japonica* fruits, *A. hirsuta* var. *sibirica* leaves, and *A. firma* barks, among the respective herbal parts, showed significant inhibitory activity on adipocyte differentiation. In addition, the $CHCl_3$ and *n*-BuOH fractions (67.7±5.9% and 31.4±6.8% at a concentration of 50 μg/ml, respectively) of *A. japonica* fruits, EtOAC and *n*-BuOH fractions (17.7±3.6% and 56.9±7.5% at a concentration of 100 μg/mL, respectively) of *A. hirsuta* var. *sibirica* leaves, 90 % MeOH and EtOAC fractions (49.7±2.6% and 40.8±8.8% at a concentration of 100 μg/mL, respectively) of *A. firma* barks showed the most potent inhibitory activity on adipocyte differentiation in 3T3-L1 cells (Figure 75).

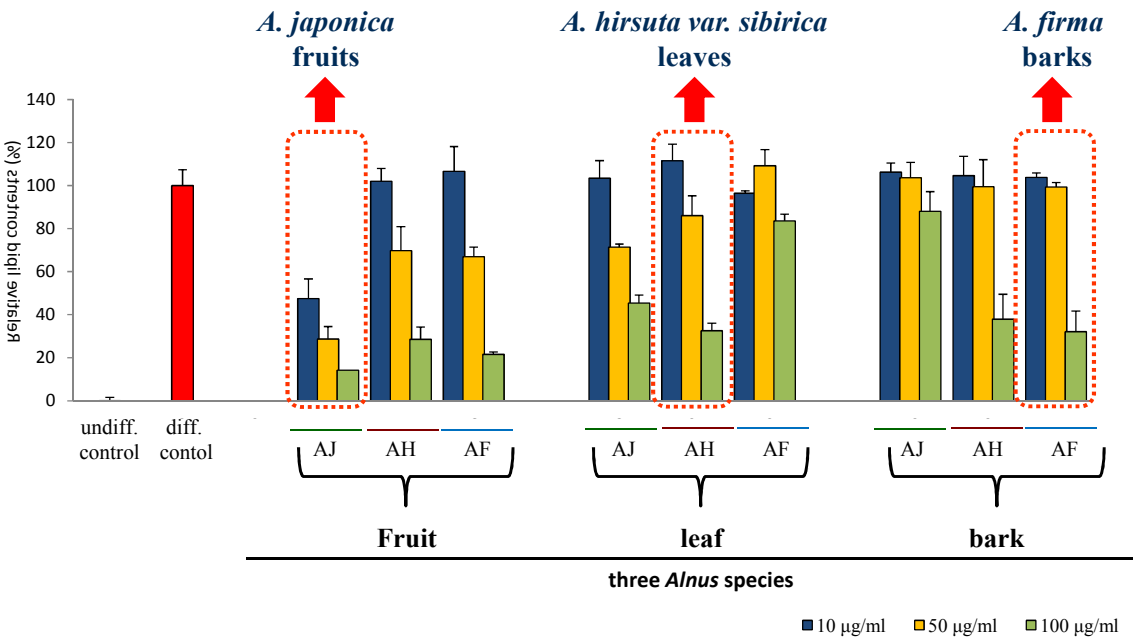

Figure 75. Effects of the total extract and fractions of three *Alnus* species on adipocyte differentiation in 3T3-L1 cells.

Confluent 3T3-L1 preadipocytes were differentiated into a adipocyte with various concentrations (10, 50, and 100 μg/ml) of the total extract of herbal parts of three *Alnus* species during differentiation for 8 days. On day 8, cultures were stained with Oil Red O and lipid contents were quantified. Results represent the mean ± SD of three independent experiments, each performed using triplicate wells. ### $p < 0.001$, compared with untreated control; * $p < 0.05$, ** $p < 0.01$, ***$p < 0.001$, compared with differentiated cells. AJ, *Alnus japonica*; AH, *Alnus hirsuta* var. *sibirica*; AF, *Alnus firma*; undiff, undifferentiated; diff. differentiated.

2.2. Inhibiory activity of compounds isolated from three *Alnus* species on adipocyte differentiation in 3T3-L1 cells

The inhibitory activities of sixty eight compounds on the adipocyte differentiation were evaluated in the established in-house assay system (Table 30). Inhibitory activity of (-)-EGCG, a positive control, was 94.9 % at 10 μM, 81.9 % at 50 μM, and 54.5 % at 100 μM, respectively. Among them, some of diarylheptanoid (**AJ2**, **AJ3**, **AJ6**, **AH1**, **AH2**, **AH4-6**, **AJ9-13**, **AF5**, **AH9**, **AH11**, **AJ15**) showed significant anti-differentiation effects on 3T3-L1 cells. Compounds **AH1**, **AH2**, **AH4-6**, **AJ9-13**, **AF5**, **AH9**, **AH11**, **AJ15** with ketone functionality at C-3 concentration-dependently decreased lipid accumulation of 3T3-L1 preadipocytes except for compounds **AH3** and **AJ15**, while compounds **AH14-17**, **AJ19**, and **AF10-12** seemed to hardly have any antiadipogenic activity (Table 30). Also, compounds **AJ16-18** with substitution of phenylpropanoid, increased differentiation of preadipocytes than compound **AJ13**. Compounds **AH1**, **AH2**, **AH4**, and **AH5**, which are very similar to curcumin with an α,β-unsaturated ketone, significantly inhibited adipocyte differentiation (Ejaz et al., 2009). In compounds **AJ9-13**, **AH6**, **AH9**, **AH11**, **AF5**, with a 5-hydroxy-3-heptanone structure, the substitution of the hydroxyl group in the benzene ring increased adipocyte differentiation at the concentration of 100 μM; **AH6 > AH9 > AH11**; **AJ9 > AJ11 > AJ13**; **AJ10 > AJ12 > AJ14**. In addition, the glycosylation in the hydroxyl group at C-5 affected the inhibitory activity of adipocyte differentiation; **AH6 > AJ9**, **AJ10**, **AF5**; **AH9 > AJ11**, **AJ12**; **AH11 > AJ3**, **AJ14**. For more accurate examination of the structure activity relationship, further study will be required for the investigation of the inhibitory effect of adipocyte differentiation of other diarylheptanoids with more structural variety. Among ten flavonoids (**AJ22-29**, **AH23**, and **AH24**), compound **AJ25** significantly

inhibited adipocyte differentiation on 3T3-L1 cells, on the other hand, compounds **AJ26** and **AH23** and **AH24** increased adipocyte differentiation. To investigate of mechanism associated inducing adipocyte differentiation, it is need to further study. Ellagic acids (**AJ30-36**) did not showed distinctive inhibitory effect of adipocyte differentiation on 3T3-L1 cells. Compound **AJ38** significantly decrease lipid accumulation in concentration-dependent manner in the range of 10 μM to 100 μM, which it is reported that this compound inhibited GPDH activity and triglyceride synthesis. However, compound **AJ37** did not affect the inhibitory activity of adipocyte differentiation. Also, phenolic glycosides (**AF13-16**) and triterpenoids (**AJ39-42** and **AF17-19**) inhibited the lipid accumulation during adipocyte differentiation. Especially, the lupane triperpenoids (**AF17-19**) from *A. firma* showed most potent anti-differentiation at low concentration (10 μM and 25 μM) on 3T3-L1 cells.

Of the compounds tested in the present assay system, compounds **AJ2** and **AJ9** showed the most potent inhibitory activity of adipocyte differentiation at concentration of 100 μM. In the case of compound **AJ10**, it significantly inhibited adipocyte differentiation in dose dependent manners with IC_{50} value of 14.4 μM, which was low concentration among the compounds isolated from genus *Alnus*. Compound **AJ13**, major constituent of three *Alnus* species, was reported its anti-adipogenic activity, but its mechanism have not been investigated yet. Hence, further investigation using compounds **AJ2**, **AJ9**, **AJ10**, and **AJ13** was carried out to reveal any anti-adipogenic activity on 3T3-L1 cells.

Table 30. Effects of compounds from three *Alnus* species on adipocyte differentiation in 3T3-L1 cells.

	Lipid Contents (%)				Lipid Contents (%)		
compound	**10 μM**	**50 μM**	**100 μM**	**compound**	**10 μM**	**50 μM**	**100 μM**
undifferentiated control		0.0±2.8		differentiated control		100±5.0$^{###}$	
AJ1	89.0±1.2	92.8±4.6	73.6±2.7	**AH21**	90.2±6.0	61.2±0.9	−
AJ2	94.5±4.3	78.1±0.6	11.6±1.5***	**AJ22**	86.4±4.2	75.1±4.5	75.0±4.3
AJ3	110.6±3.0	94.1±4.5	54.4±1.7*	**AJ23**	96.1±4.7	108.9±1.2	104.4±2.0
AJ4	87.2±0.9	84.8±2.2	90.3±1.8	**AJ24**	82.8±7.3	85.0±6.6	80.2±6.7
AJ5	86.0±2.7	84.2±1.1	85.0±5.3	**AJ25**	85.4±1.5	81.6±2.7	35.7±2.6***
AJ6	77.8±0.5	65.8±1.1	58.5±0.7*	**AJ26**	127.5±1.4	122.7±6.9	132.8±0.1
AH1	92.6±8.5	81.8±6.7	58.8±26.1	**AH23**	105.1±3.4	99.3±1.5	129.5±10.0
AH2	86.5±5.4	66.5±4.1*	36.5±9.3*	**AH24**	86.9±1.0	89.9±0.7	146.5±1.8
AH3	104.4±0.7	108.9±8.0	103.0±5.2	**AJ27**	98.5±1.2	88.7±2.3	80.9±2.1
AH4	101.7±7.2	82.8±9.0	39.4±6.4**	**AJ28**	90.0±3.2	92.9±0.9	88.0±1.6
AH5	86.1±5.0	45.7±4.1*	38.6±6.7**	**AJ29**	97.1±1.6	97.7±3.6	103.0±2.7
AH6	85.2±4.9	50.7±6.5*	27.5±2.3***	**AJ30**	81.8±2.4	91.8±3.4	91.3±1.4
AJ9	81.7±1.1	28.9±7.0**	14.4±9.1***	**AJ31**	87.8±3.0	91.5±1.5	92.9±1.6
AJ10	58.2±4.9	21.9±2.2**	20.8±4.3***	**AJ32**	87.3±1.4	88.8±4.1	64.1±2.3*
AF5	88.4±11.4	34.6±8.9	24.8±0.5	**AJ33**	103.3±3.4	100.3±3.8	106.5±2.7
AH9	77.3±4.4	70.5±2.1	57.6±1.2*	**AJ34**	98.6±2.2	90.0±3.7	79.8±1.3
AJ11	104.6±8.9	77.2±8.4	34.0±7.3**	**AJ35**	80.3±2.3	91.2±0.5	94.7±3.2
AJ12	98.8±2.1	75.5±2.8	26.2±0.6	**AJ36**	77.4±2.5	74.2±3.2	80.9±1.4
AH11	83.9±6.1	72.6±11.8	59.9±7.9*	**AJ37**	98.7±2.4	94.1±1.6	89.6±1.9

AJ13	89.7±8.7	78.2±3.4	46.2±0.8*	**AJ38**	92.5±0.9	64.1±0.2	26.9±0.4***
AJ14	100.9±1.5	91.8±4.4	90.1±4.2	**AJ39**	105.6±4.9	94.9±1.2	89.3±3.4
AJ15	86.1±1.6	83.8±0.6	36.5±1.0***	**AJ40**	98.7±4.2	96.5±4.2	70.8±0.6
AF7	72.9±0.5	79.6±1.7	95.6±0.5	**AJ41**	102.1±5.7	85.8±1.6	48.8±3.4**
AJ16	99.0±0.6	99.6±0.6	85.6±2.8	**AJ42**	104.9±2.5	89.1±6.6	54.6±4.5*
AJ17	96.8±2.4	93.7±1.2	95.7±2.3	**AF13**	92.6±9.9	86.9±0.7	64.2±0.2*
AJ18	92.6±4.4	103.1±2.8	71.3±2.9	**AF14**	58.9±3.0	55.1±2.1	44.2±1.4**
AH14	103.5±4.0	85.7±5.7	62.9±4.6*	**AF15**	62.6±0.5	61.2±2.2	50.1±2.5**
AH15	85.1±3.7	93.2±5.9	93.6±1.6	**AF16**	90.1±2.0	75.6±8.2	64.2±1.9*
AJ19	80.3±1.6	87.0±0.6	91.9±2.7	**AH25**	122.9±2.2	110.6±9.5	105.8±0.7
AH16	79.6±7.9	92.1±1.9	92.9±8.8	**EGCG**	94.9±1.3	81.9±3.7	54.5±1.8*
AH17	84.6±6.9	86.4±8.1	90.0±4.2		10 μM	25 μM	
AF10	93.2±7.6	110.8±10.6	97.0±4.8	**AF17**	79.0±6.6	58.5±5.6	
AF11	76.0±5.1	103.1±8.5	98.1±5.1	**AF18**	73.2±4.7	41.7±0.8**	
AF12	70.5±8.2	100.7±4.3	107.9±2.7	**AF19**	65.7±1.7	27.5±6.3***	

Confluent 3T3-L1 preadipocytes were differentiated into a adipocyte with various concentrations (10, 50, and 100 μM) of the compounds from three *Alnus* species for 8 days. On day 8, cultures were stained with Oil Red O and lipid contents were quantified. Results represent the mean ± SD of three independent experiments, each performed using triplicate wells. ### $p < 0.001$, compared with untreated control; * $p < 0.05$, ** $p < 0.01$, ***$p < 0.001$, compared with differentiated cells. EGCG was used as a positive control.

2.3. Anti-adipogenic activities of compounds AJ2, AJ9, AJ10, and AJ13 on 3T3-L1 cells

2.3.1. Effects of compounds AJ2, AJ9, AJ10, and AJ13 on adipokine gene expression in 3T3-L1 cells

Adipocyte differentiation causes a series of programmed changes in specific gene expressions. Adipogenesis regulated by transcription factors such as PPARγ, C/EBPα, and SREBP1, which are known to be critical activators for adipogenesis (Xiao et al., 2007). The expression levels of transcription factors for adipogenesis are examined using RT-PCR and quantitative real time PCR (Figure 76). The differentiation of preadipocytes into adipocytes is modulated by a complex network of transcription factors that organize the expression of proteins responsible for establishing the mature adipocyte phenotype. PPARγ and C/EBPα are at the center of this network and oversee the entire terminal differentiation process (Farmer, 2006). Compounds **AJ2**, **AJ9**, **AJ10**, and **AJ13** induced a significant down-regulation of two principal adipogenic factors, compared to the fully differentiated adipocytes. SREBP1c, which is involved in the production of an endogenous PPARγ ligand, regulates the expression of genes related to the metabolism of lipids and cholesterol and the enzymes involved in lipogenesis and fatty acid desaturation, and then, activation of this promotes the expression of FAS (Rosen et al., 2000; Chen et al., 2011). FAS is a critical metabolic enzyme for lipogenesis, and is highly expressed in the liver and adipose tissue. It catalyzes the synthesis of saturated fatty acids in cells (Smith, 1994). Compounds **AJ9** and **AJ10** significanly down-regulated SREBP1c and FAS, while compound **AJ13** did not affect the expression of both genes. In the present study, the cellular deprivation of the product for the enzymatic activity of SCD-1 led to the down-

regulation of SREBP1 and PPARγ, resulting in a decrease in lipogenesis. Leptin, a hormone secreted exclusively in adipose tissue, plays a central role in the regulation of energy expenditure and food intake (Kim et al., 2007). In this study, the decrease in mRNA levels of leptin by Compounds **AJ9**, **AJ10**, and **AJ13** during adipocyte differentiation implies that the inhibition of adipocyte differentiation was mediated by the regulation of leptin. We also found that compounds **AJ9**, **AJ10**, and **AJ13** significantly reduced the mRNA levels of LPL and aP2. Compound **AJ2** which showed the most potent anti-differentiation effect among cyclic diarylheptanoids, induced down-regulation of adipogenic genes at high concentration (100 μM), and had inert activity at low concentration except for PPARγ, C/EBPα, and leptin (Figure 77). PPARγ, C/EBPα, and SREBP1c are induced prior to the transcriptional activation of most adipocyte specific genes in the early stage of adipocyte differentiation, while the aP2 and FAS have been known as terminal markers of adipocyte differentiation (Chen et al., 2011; Ericsson et al., 1997).

To examine the effects of compounds **AJ9**, **AJ10**, and **AJ13** on the initial stage of adipocyte differentiation, mRNA levels of C/EBPβ and δ, which rise early and transiently induced to differentiate in preadipocyte were examined (Figure 78). Compounds **AJ9** and **AJ10** showed a significant down-regulation of C/EBPβ expression. These results suggest that diaryheptanoids isolated from three *Alnus* species might affect adipocyte differentiation through PPARγ, C/EBPα, and SREBP1c induced adipogenesis mechanism, synergistically associated to downstream adipocyte specific gene promoters such as aP2, FAS, SCD-1, LPL, and leptin.

2.3.2. Effects of compounds AJ9, AJ10, and AJ13 on adipocyte differentiation against PPARγ agonist, troglitazone.

To examine whether compounds **AJ9**, **AJ10**, and **AJ13** suppress the transcriptional activity of PPARγ, we performed a competitive inhibition assay using a strong PPARγ agonist, troglitazone, in the adipocyte differentiation process. Compounds **AJ9**, **AJ10**, and **AJ13** suppressed adipocyte differentiation even in the presence of 10 μM troglitazone, as shown by Oil Red O staining, and lipid contents were also noticeably lowered up to 20.8, 23.0, and 56.1 % at a concentration of 100 μM, respectively, when compared to troglitazone-treated differentiated cell (112.7 %), suggesting that compounds **AJ9**, **AJ10**, and **AJ13** prevents adipocyte differentiation through an antagonistic effect on PPARγ transcriptional activity (Figure 79).

2.3.3. Effects of AJ9 on phosphorylation of AMPK and ACC during 3T3-L1 differentiation

AMPK regulates cellular metabolism in glucose regulation and lipid metabolism, and is recognized as a target for metabolic disorders including obesity, diabetes, and cancer (Luo et al., 2005). Therefore, in order to explore whether AMPK activation is involved in the intervention of adipocyte differentiation by compound **AJ9**, we measured the protein levels of phosphorylated AMPK and its substrate, phosphorylated acetyl-CoA carboxylase (pACC), using Western blot analysis (Figure 80). Treatment with four different concentrations (5, 10, 25, and 50 μM) of compound **AJ9** induced the the phosphorylation of AMPK along with its substrate, ACC. These results suggest that the inhibitory effect of compound **AJ9** on adipocyte differentiation might be mediated though the up-regulation of the AMPK pathway (Moon et al.,

2007). Activation of AMPK induces the phosphorylation and regulation of downstream target genes, which are involved in diverse pathways in various tissues such as adipose tissue, liver, muscles, and hypothalamus (Moon et al., 2009). AMPK cascades have emerged as novel targets for the treatment of obesity (Luo et al., 2005). In the present study, we elucidated that treatment with compound **AJ9** induced phosphorylated AMPK along with its substrate, ACC. Moon et al. suggested that several naturally occurring compounds, such as EGCG activate AMPK in a time-dependent manner, leading to the inhibition of adipocyte differentiation. EGCG has been reported to reduce adipose tissue mass and enhance plasma lipid profiles by modulation of the expression of multiple genes involved in adipogenesis, lipolysis, β-oxidation and thermogenesis in the adipose tissue of diet-induced obese mice (Lee et al., 2009). Our study suggests that the activation of AMPK is necessary for the suppression of adipogenesis in 3T3-L1 cells by phytochemicals such as compound **AJ9**, and AMPK as a primary target of adipogenesis modulation.

2.3.4. Determination of glycerol-3-phosphate dehydrogenase (GPDH) activity.

To further characterize the anti-differentiation activities of compounds **AJ9**, **AJ10**, and **AJ13**, the cellular GPDH enzyme activity was measured. Cytosolic GPDH plays an important role in the synthesis of triglyceride. As shown in Figure 81, compounds **AJ9**, **AJ10**, and **AJ13** suppressed the GPDH activity at a concentration of 100 μM. From the result obtained above, the inhibitory activity of compound **AJ9** on adipocyte differentiation were higher than compounds **AJ10** and **AJ13**.

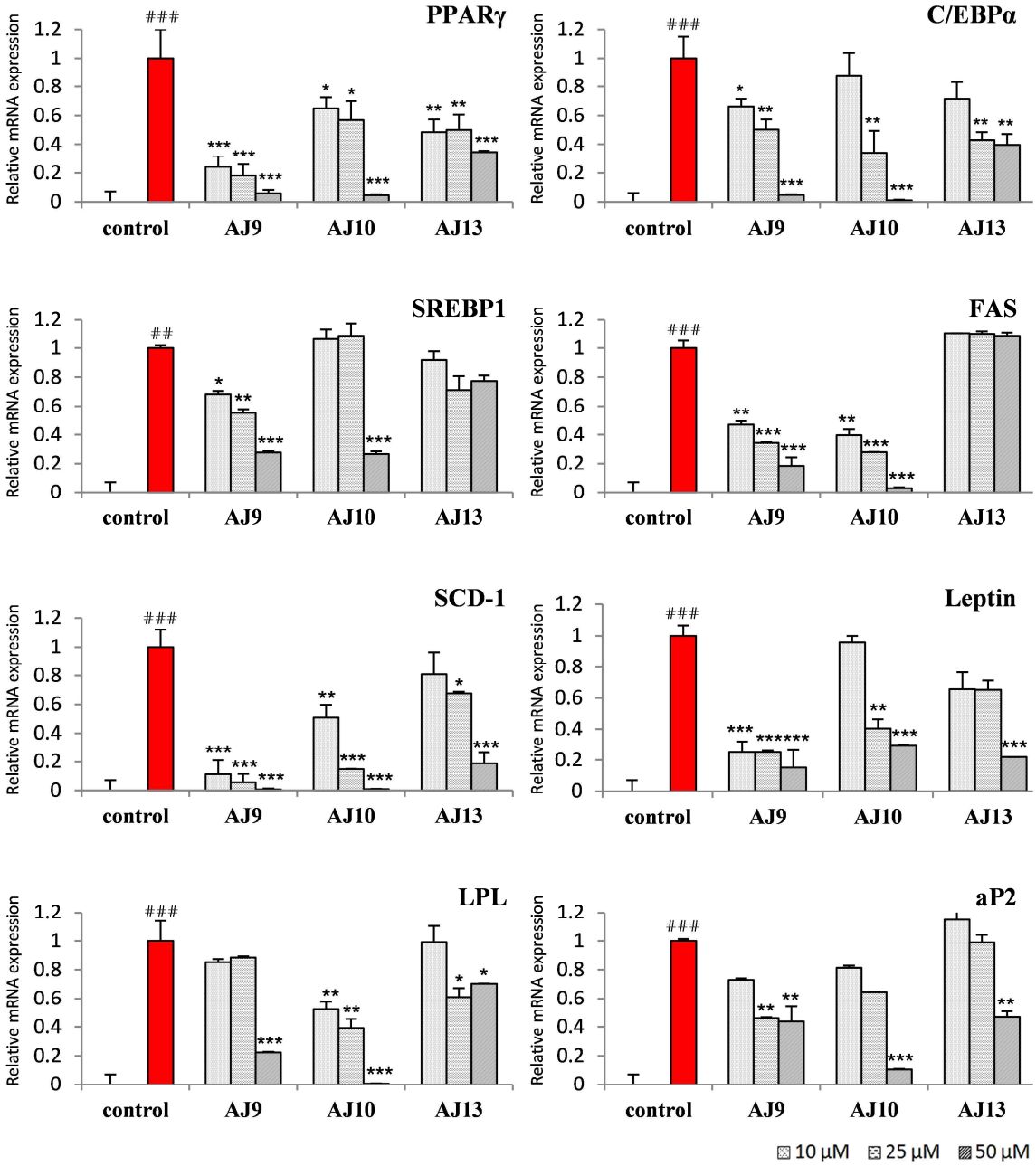
PPARγ
C/EBPα
SREBP1
FAS
SCD-1
Leptin
LPL
aP2
Relative mRNA expression
control
AJ9
AJ10
AJ13
10 μM
25 μM
50 μM

Figure 76. Effects of compounds **AJ9**, **AJ10**, and **AJ13** on PPARγ, C/EBPα, SREBP1, SCD-1, FAS, aP2, LPL, and Leptin gene expression in 3T3-L1 cells by quantitative real-time RT-PCR analysis.

Confluent 3T3-L1 preadipocytes were differentiated into adipocytes in a medium with different concentrations (10, 25, and 50 μM) of compounds **AJ9**, **AJ10**, and **AJ13** for 8 days. On 8 day, the mRNA expression levels of PPARγ, C/EBPα, SREBP1, SCD-1, FAS, aP2, LPL, and Leptin were estimated by quantitative real-time RT-PCR analysis. Each bar represents the mean ± SD of three independent experiments. ## $p < 0.01$, ### $p < 0.001$, compared with untreated control; * $p < 0.05$, ** $p < 0.01$, ***$p < 0.001$, compared with differentiated cells.

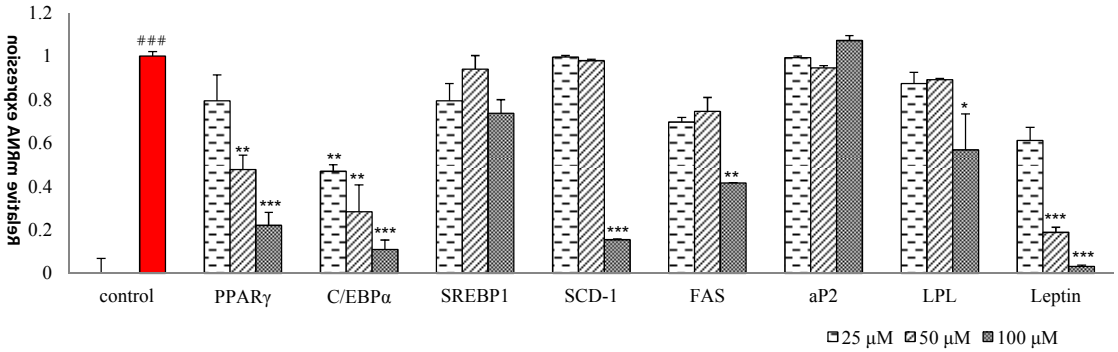

Figure 77. Effects of compound **AJ2** on PPARγ, C/EBPα, SREBP1, SCD-1, FAS, aP2, LPL, and Leptin gene expression in 3T3-L1 cells by quantitative real-time RT-PCR analysis.

Confluent 3T3-L1 preadipocytes were differentiated into adipocytes in a medium with different concentrations (25, 50, and 100 μM) of compound **AJ2** for 8 days. On 8 day, the mRNA expression levels of PPARγ, C/EBPα, SREBP1, SCD-1, FAS, aP2, LPL, and Leptin were estimated by quantitative real-time RT-PCR analysis. Each bar represents the mean ± SD of three independent experiments. ## $p < 0.01$, ### $p < 0.001$, compared with untreated control; * $p < 0.05$, ** $p < 0.01$, ***$p < 0.001$, compared with differentiated cells.

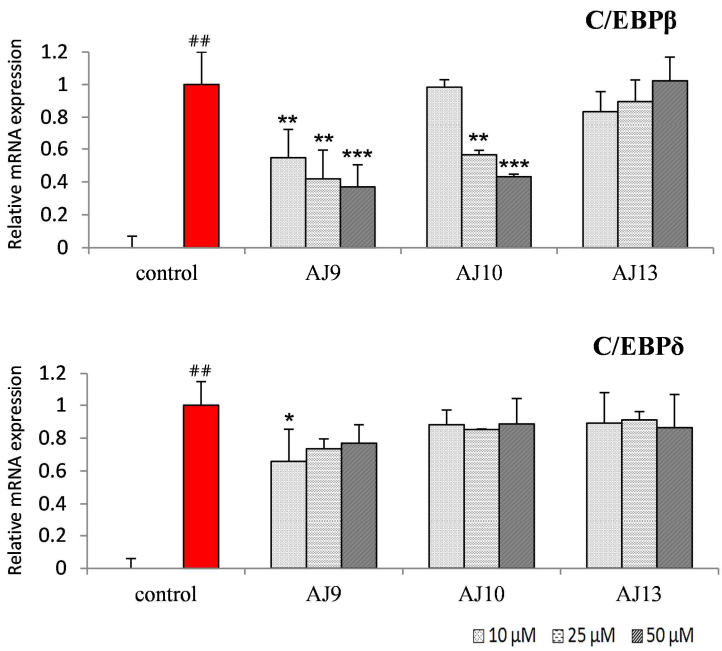

Figure 78. Effects of compounds **AJ9**, **AJ10**, and **AJ13** on C/EBPβ and C/EBPδ gene expression in 3T3-L1 cells by quantitative real-time RT-PCR analysis.

Confluent 3T3-L1 preadipocytes were differentiated into adipocytes in a medium with different concentrations (10, 25, and 50 μM) of compounds **AJ9**, **AJ10**, and **AJ13** for 2 days. On 2 day, the mRNA expression levels of C/EBPβ and C/EBPδ were estimated by quantitative real-time RT-PCR analysis. Each bar represents the mean ± SD of three independent experiments. ## $p <$ 0.01, ### $p < 0.001$, compared with untreated control; * $p < 0.05$, ** $p < 0.01$, ***$p < 0.001$, compared with differentiated cells.

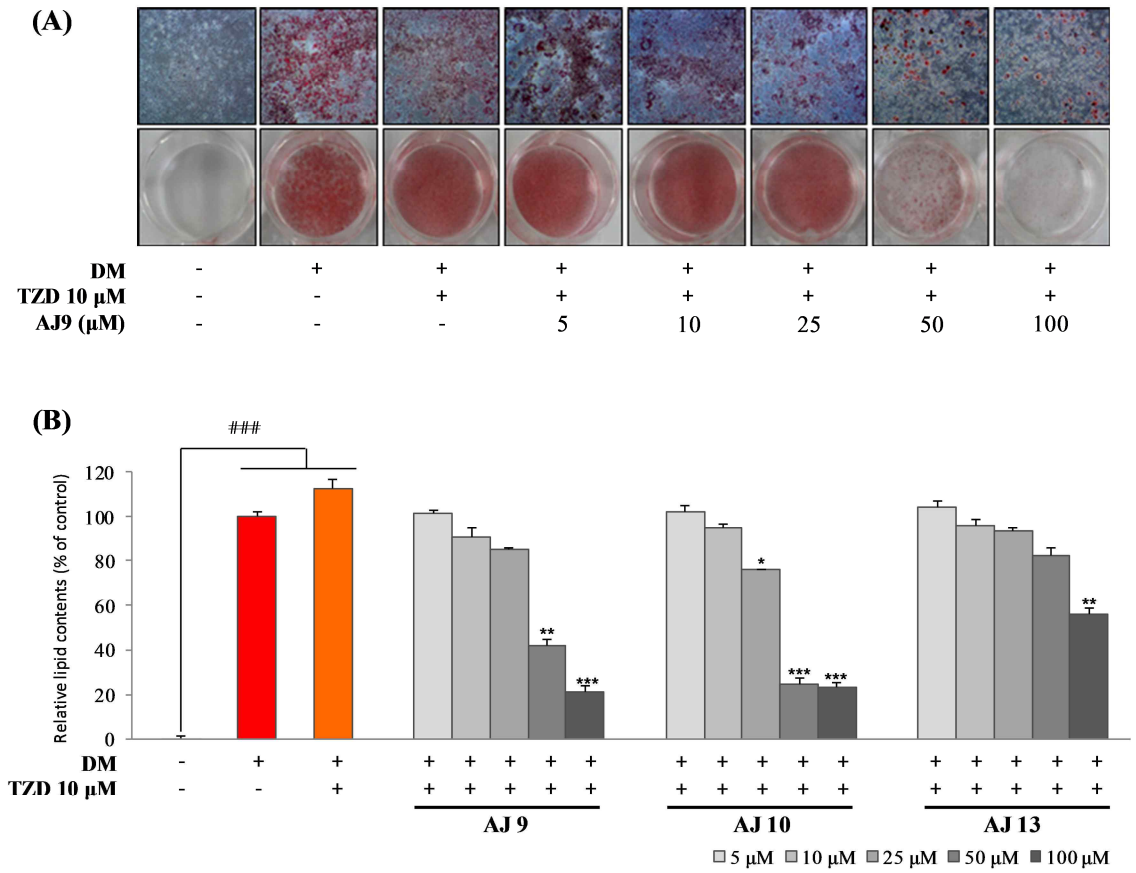

Figure 79. Inhibitory activity of adipogenesis of compounds **AJ9**, **AJ10** and **AJ13** against PPARγ agonist.

Confluent 3T3-L1 preadipocytes were differentiated into adipocytes with compounds **AJ9**, **AJ10**, and **AJ13** (5, 10, 25, 50, and 100 μM) in the presence of troglitazone (10 μM) for 8 days. On day 8, stained cells with Oil Red O were photographed with a phase-contrast microscope (original magnification x 100) (A), and the lipid contents were quantified (B). Results represent the mean ± SD of three independent experiments, each performed using triplicate wells. ### $p <$ 0.001, compared with untreated control; * $p < 0.05$, ** $p < 0.01$, ***$p < 0.001$, compared with differentiated cells. DM, differentiated media; TZD, troglitazone.

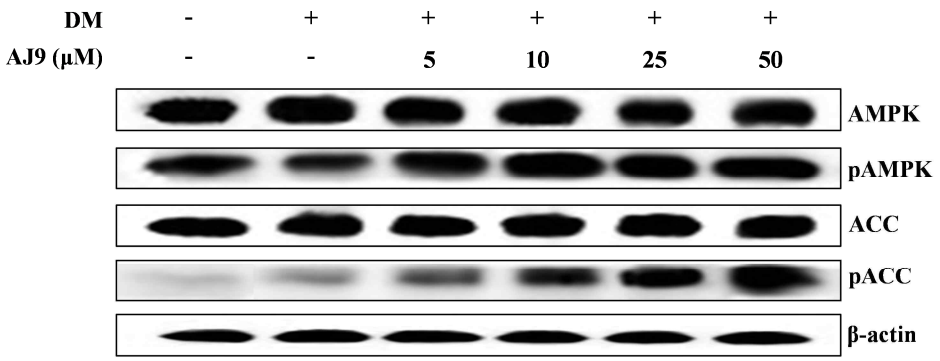

Figure 80. Effects of **AJ9** on phosphorylation of AMPK and ACC during 3T3-L1 differentiation

Confluent 3T3-L1 preadipocytes were differentiated into adipocytes with various concentrations (25, 50, and 100 μM) of compound **AJ9** for 8 days. On 8 day, AMPK activation and its substrate ACC phosphorylation were detected by Western blot analysis.

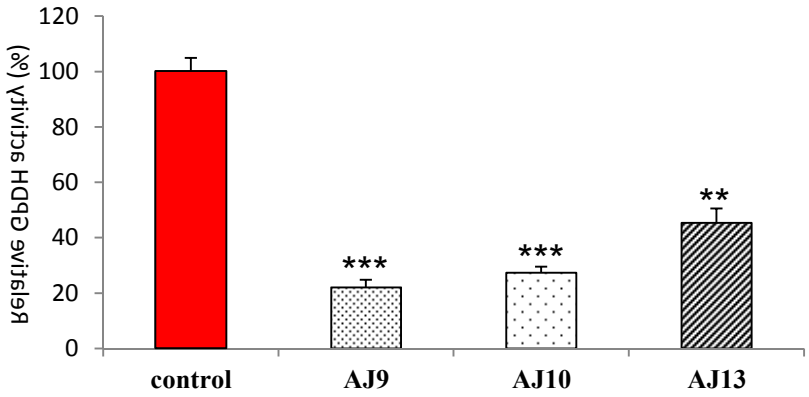

Figure 81. Effects of comounds **AJ9**, **AJ10**, and **AJ13** on adipogenesis in 3T3-L1 preadipocytes.

3T3-L1 preadipocytes were treated with compounds **AJ9**, **AJ10** and **AJ13** at a concentration of 100 μM during differentiation. On day 8, GPDH activity was measured in the same experimental sets. Each bar represents the mean ± SD of three independent experiments. * $p < 0.05$, ** $p < 0.01$, ***$p < 0.001$, compared with differentiated cells.

2.4. Lipolytic activities of compounds on 3T3-L1 cells

Breakdown of triglycerides in adipocytes and the release of glycerol and fatty acids are important for the regulation of energy homeostasis (Frayn et al., 2003). Lipolysis effect of compounds **AJ9**, **AJ10**, and **AJ13** on differentiated adipocytes (8 days) was monitored by Oil Red O staining (Figure 82A). A significant reduction in Oil Red O content was observed in 50 μM to 100 μM of compounds **AJ9**, **AJ10**, and **AJ13.** Effect of compounds **AJ9**, **AJ10**, and **AJ13** on lipolysis was assessed by measuring the expression levels of perilipin, PDE3B, Gia1, HSL, and TNFα upon treatment with compounds **AJ9**, **AJ10**, and **AJ13** of mature adipocytes (post differentiation, 8 days) by real-time PCR. The treatment with compounds **AJ9**, **AJ10**, and **AJ13** down-regulated expression of HSL, perilipin, PPARγ, PDE3B, and Gia1, and up-regulated the expression of TNFα (Figure 82B). The TNFα stimulates adipocyte lipolysis and down-regulates the expression of the lipid droplet-associated protein perilipin which is thought to modulate the accession of HSL to the surface of the fat droplet (Ryden et al., 2004). The phosphorylation of HSL and perilipin is critical processes of lipolysis and the expression levels of perilipin and HSL were determined as the lipolytic response (Ardevol et al., 2000). TNFα can suppress expression and function of PPARγ which is known to promote phosphorylation and down-regulation of perilipin (Xing et al., 1997; Arimura et al., 2004). The TNFα induction and PPARγ repression caused by compounds **AJ9**, **AJ10**, and **AJ13** can indicated that these compounds affect down-regulation of perilipin. TNFα induced lipolysis is also known to downregulate anti-lipolytic genes PDE3B and G*i*α1 (Rahn Landstrom et al., 2000; Gasic et al., 1999). These results suggest that diarylheptanoids from *Alnus* species induced lipolysis in mature adipocyte by regulating lipolysis-associated gene expression.

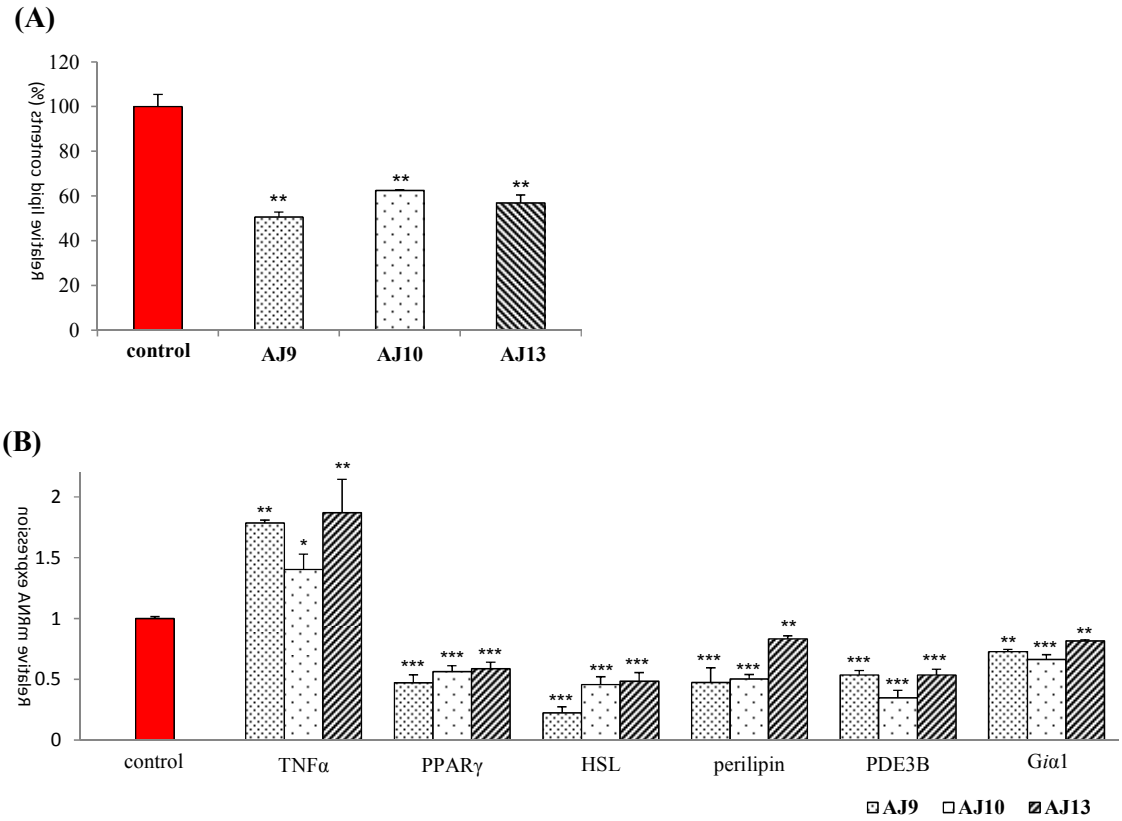

Figure 82. Effects of compounds **AJ9**, **AJ10**, and **AJ13** on lipolysis associated target genes perilipin, HSL, PDE3B, G*i*α1, TNFα, and PPARγ gene expression in 3T3-L1 cells by quantitative real-time RT-PCR analysis.

Compounds **AJ9**, **AJ10**, and **AJ13**-treated (48 h, at 50 μM and 100 μM) mature adipocytes (8 days) were stained for intracellular lipids with Oil Red O. Retention of Oil Red O within cells was quantitated (A). The mRNA expression levels of lipolysis associated target genes perilipin, HSL, PDE3B, G$i\alpha_1$, TNFα, and PPARγ were estimated by quantitative real-time RT-PCR analysis (B). Each bar represents the mean ± SD of three independent experiments. * $p < 0.05$, ** $p < 0.01$, ***$p < 0.001$, compared with differentiated cells.

2.5. Effect of compounds isolated from three *Alnus* species on 3T3-L1 preadipocytes proliferation.

To identify whether compounds isolated from three *Alnus* species inhibited the proliferation of 3T3-L1 cells, preadipocytes were treatead with 10-100 μM for 24, 48, and 72 h and cell proliferation was determined using MTT assay (Table 31). As a result, compounds which showed potent anti-differentiation activity effectively decreased preadipocytes proliferation. Of the compounds tested in the present assay system, compounds **AF18-19**, lupane type triterpenoids, showed the most anti-proliferative activity. We next investigated whether the enhanced reduction in cell viability by compounds **AF17-19** was due to apoptosis. To confirm apoptosis in response to treatment with compounds **AF17-19**, we evaluated Caspase-3/7 activity. The activation of Caspases, especially Caspases 3 and 7, is a biochemical hallmark of apoptosis (Cohen, 1997). Therefore, we measured Caspase-3/7 activity with Apo-ONE Homogenous Caspase-3/7 assay kit using Z-DEVD-rhodamine 110 as a substrate. Caspase-3/7 activity was enhanced with the treatment of these compounds **AF17-19** on 3T3-L1. Especially, compound **AF19** increased the expression of Caspase-3/7 up to 269 % at a concentration of 50 μM. To further investigate whether compound **AF19** affects the intrinsic apoptosis induction, we evaluated the expression of the pro-apoptotic Bax and anti-apoptotic Bcl-2 protein by Western blotting. As shown in Figure 84, the expression of Bax was slightly up-regulated, but the expression of Bcl-2 and Cytochrome *c* was down-regulated in a dose-dependent manner.

Table 31. Effect of compounds from genus *Alnus* on 3T3-L1 preadipocytes proliferation

	24 h			48 h			72 h		
	10 μM	**50 μM**	**100 μM**	**10 μM**	**50 μM**	**100 μM**	**10 μM**	**50 μM**	**100 μM**
control	100±2.6								
AJ1	102.2±5.7	79.4±3.0*	78.7±1.0*	93.6±0.3	65.9±3.4**	53.3±.8.8**	84.9±5.5	57.5±2.0*	52.3±1.8**
AJ2	89.3±1.7	78.9±7.3*	71.2±0.3**	83.8±5.7	60.9±3.8*	57.7±4.5**	73.6±0.7*	53.3±4.1**	37.1±1.1***
AJ3	97.6±9.7	87.8±1.1	61.7±0.3**	90.2±4.3	73.2±1.4*	48.8±3.5**	93.0±6.9	72.0±4.7	47.4±7.1
AJ4	106.4±6.4	98.2±4.8	99.4±6.3	85.4±7.3	80.3±1.6*	76.3±5.3*	83.8±4.6	72.3±7.4*	67.1±5.8*
AJ5	104.6±8.5	103.4±2.8	101.5±3.2	108.3±9.3	106.3±7.0	101.1±8.5	110.9±0.7	106.2±.1	97.5±2.2
AJ6	114.0±0.6	110.3±3.8	109.8±7.7	103.1±2.8	102.0±4.6	90.9±6.0	84.4±5.3	81.6±5.7	70.5±8.7*
AH1	97.0±5.9	90.6±4.9	85.9±4.5	98.9±5.9	82.8±3.5	79.7±4.9	102.3±0.9	83.2±7.1	76.1±4.5*
AH2	105.3±0.8	83.6±3.5	81.8±8.7	101.8±3.1	68.0±1.9*	60.2±1.7**	101.5±4.6	67.7±9.3*	38.2±3.9***
AH3	104.3±2.3	102.9±7.6	93.2±1.0	97.9±2.8	97.4±9.0	92.1±5.4	103.8±1.8	93.0±6.7	87.0±4.2
AH4	95.9±3.4	84.6±3.4	59.6±9.0**	87.8±7.0	46.9±7.0***	43.6±1.2***	101.2±9.5	50.3±6.1***	42.8±3.9***
AH5	93.6±0.1	83.6±6.1	64.7±6.4	81.4±3.9	78.6±2.7*	61.6±6.0**	80.0±6.5	71.6±5.7*	56.5±4.7**
AH6	100.0±3.7	73.4±4.2**	65.7±2.8**	103.6±3.9	50.7±7.4**	43.1±4.5***	82.1±5.7*	48.3±6.3***	38.1±9.2***
AJ9	80.8±6.7	90.5±3.8	87.1±2.3	75.0±6.2**	72.1±1.9**	59.1±7.7***	54.8±2.8***	50.0±1.7***	48.0±3.2***
AJ10	96.6±9.1	56.8±2.3***	51.3±1.4***	73.1±4.8**	45.8±0.7***	45.9±0.4***	57.3±5.6***	35.2±2.6***	34.7±1.0***
AF5	108.4±0.1	97.5±5.6	95.7±5.6	95.7±9.9	76.9±0.5*	73.2±1.3*	96.4±4.7	61.1±1.5*	58.0±1.5**
AH9	101.9±4.5	99.5±3.0	98.6±8.3	92.6±5.4	87.6±4.5	83.1±7.5	92.8±3.7	87.6±1.0	78.8±3.1*
AJ11	81.8±5.4	49.8±3.6***	49.9±2.5***	69.8±1.7**	41.7±3.1***	38.5±2.2***	79.0±2.3*	38.7±2.6***	36.3±0.5***

AJ12	69.0±3.6**	44.8±6.2***	39.9±2.5***	53.4±3.4***	40.7±1.0***	37.5±0.5***	49.8±5.6***	38.3±2.7***	37.5±1.1***
AH11	102.5±8.8	89.0±6.3	82.9±5.9	106.5±8.4	80.9±3.2*	73.0±4.9*	94.5±2.0	76.2±5.1*	64.9±5.8*
AJ13	94.3±5.1	73.1±4.9**	65.0±2.7**	99.1±4.1	75.4±5.4**	43.1±2.9***	97.7±2.9	76.1±5.0**	39.5±1.0***
AJ14	105.6±1.2	98.5±0.7	93.5±3.3	97.3±2.8	96.6±3.8	87.8±7.1	97.3±2.3	91.9±0.9	60.6±3.5
AJ15	77.1±8.0*	62.7±3.2**	59.0±1.8**	75.4±5.4**	55.2±4.0**	47.2±8.5***	76.8±8.5*	56.6±4.6**	47.6±3.4***
AF7	86.5±6.2	70.1±3.2*	69.2±5.2*	103.3±4.2	61.0±4.8***	56.2±4.6***	100.9±2.0	78.4±1.0**	63.0±2.7***
AJ16	81.6±7.8	70.9±3.9**	64.9±1.1*	80.7±3.6*	64.9±4.2*	56.6±8.6***	75.8±5.7*	51.1±2.3***	46.4±4.7***
AJ17	96.4±3.9	83.0±2.9	75.7±1.7*	86.4±7.9	78.0±7.2*	66.8±0.8**	85.6±0.6	56.4±0.9**	51.8±0.2**
AJ18	103.1±9.6	93.4±4.0	81.7±7.6	87.5±7.8	85.0±0.8	71.3±4.1**	88.5±1.7	75.1±7.0	63.9±5.2**
AH14	103.8±6.8	81.6±2.2*	82.1±5.4*	91.8±3.7	59.1±7.3***	61.8±3.3***	82.8±4.5*	61.5±2.9**	53.8±3.8***
AH15	88.1±5.4	107.8±11.5	83.5±7.7	99.8±7.6	139.1±3.0	80.9±4.9	102.7±1.9	126.0±2.0	81.3±0.5
AJ19	90.9±3.9	86.1±7.4	83.4±3.0	83.1±0.9	69.0±0.6*	64.1±1.6*	79.8±4.7*	79.2±7.4*	63.8±6.3**
AH16	117.5±7.9	108.6±7.8	99.9±2.0	105.3±4.1	85.0±2.5	69.0±1.1**	100.6±3.3	88.3±6.9	77.7±2.9*
AH17	90.5±7.0	80.7±1.8	79.9±2.5	94.7±1.8	68.6±9.5*	62.6±3.8**	95.7±2.9	65.8±5.1	55.3±3.2
AF10	111.0±2.7	105.6±6.2	102.4±0.7	95.1±0.8	93.4±9.1	81.0±6.1	93.1±3.2	75.2±4.1*	65.6±6.4*
AF11	117.0±6.9	92.8±8.8	87.7±3.6	86.4±5.5	56.4±2.5***	55.0±4.8***	78.1±4.4	47.0±3.8***	43.7±2.1***
AF12	121.6±3.0	95.0±1.3	69.2±7.1**	109.5±0.2	61.5±2.3**	45.4±6.2***	97.7±2.8	49.2±3.4***	44.7±3.0***
AH21	95.8±6.2	87.5±8.2	85.7±7.7	85.5±0.9	83.3±3.6	36.8±3.3***	97.8±1.4	71.0±0.6*	28.6±3.1***
AJ22	105.3±6.5	86.8±4.4	80.2±2.2*	70.5±4.1**	63.6±1.8***	59.6±2.6***	74.4±7.9*	63.9±3.2***	63.5±3.8***
AJ23	105.0±4.5	67.0±7.7**	62.2±3.8***	100.8±2.0	53.7±3.4***	48.1±0.7***	93.8±5.4	49.7±3.0***	44.2±1.8***
AJ24	99.0±0.6	93.3±4.8	82.8±5.9	105.1±5.6	104.7±0.1	66.8±1.6**	120.2±2.6	122.5±3.0	86.1±8.8

AJ25	112.5±8.7	82.2±5.1	50.7±4.6***	75.2±4.7*	49.9±1.3***	40.8±3.0***	73.1±0.8*	46.0±3.3***	38.8±6.1***
AJ26	100.0±1.2	97.8±7.4	86.6±8.1	101.0±1.9	100.2±6.5	84.6±1.9	97.8±5.4	86.3±5.6	86.3±4.1
AH23	111.0±5.4	101.7±5.5	101.0±5.7	108.7±2.1	97.3±7.6	91.6±5.5	101.1±7.2	96.1±1.6	91.1±4.4
AH24	105.7±7.9	103.8±5.7	99.0±0.4	105.5±4.5	104.4±0.9	97.0±6.1	112.3±1.0	99.9±7.2	90.9±0.8
AJ27	113.8±6.4	89.3±4.4	100.3±4.8	98.0±7.1	84.1±6.9	85.7±5.0	101.0±6.0	61.5±4.6**	83.5±4.0
AJ28	85.5±1.9	81.5±0.3	73.2±5.0	85.1±5.7	68.6±4.2**	83.1±6.7	87.0±5.9	82.0±5.8*	87.8±8.3
AJ29	92.1±6.2	82.1±1.0	73.8±1.6*	74.8±1.0**	57.6±1.8***	54.9±2.6***	69.2±2.1**	54.8±1.4***	52.6±0.2**
AJ30	97.9±.0	97.4±1.8	81.9±5.6	95.6±5.4	90.7±8.1	89.8±4.4	107.5±2.7	92.3±3.6	87.5±9.9
AJ31	102.7±7.2	107.0±7.7	95.7±6.0	100.3±3.2	125.2±8.7	89.1±4.7	89.0±8.4	93.9±0.1	78.2±1.5*
AJ32	107.0±4.3	95.8±5.0	91.5±5.6	102.2±4.3	97.5±0.7	89.5±6.1	102.6±2.9	96.6±3.5	88.6±.0
AJ33	98.6±5.0	83.8±2.7*	82.3±5.8*	97.9±3.2	114.9±0.3	113.5±9.4	88.4±1.9	74.1±4.8	72.2±8.0
AJ34	113.3±8.3	93.7±3.8	102.2±4.7	99.6±4.5	111.0±6.5	90.0±10.1	130.1±7.1	111.9±8.4	94.0±2.7
AJ35	102.4±7.6	92.2±5.5	89.4±2.1	124.7±1.2	122.9±3.2	110.7±4.6	75.4±2.9	73.3±10.8*	67.1±4.0*
AJ36	110.3±4.6	93.6±.0	89.2±1.9	77.7±2.9**	71.2±3.6**	70.6±7.8**	76.7±5.2*	61.7±3.7***	57.7±2.1***
AJ37	105.8±9.8	114.6±9.3	108.9±6.7	96.6±4.6	103.1±2.4	82.8±3.0*	112.8±1.6	112.4±0.3	72.1±4.6*
AJ38	104.4±7.4	77.3±3.7**	71.1±4.3***	98.1±1.5	63.7±6.1***	60.1±3.7***	94.8±6.4	55.9±6.2***	50.5±2.6
AJ39	82.7±5.4	70.6±2.0	77.9±8.5	95.3±5.8	73.1±3.6	86.5±5.7	91.8±4.1	70.4±1.7	77.5±9.1
AJ40	95.8±3.9	90.9±6.3	91.2±6.1	85.4±10.6	97.0±5.9	95.0±5.4	80.2±8.1	79.2±4.5	90.9±7.8
AJ41	87.3±4.8	84.1±0.7	84.8±5.2	67.7±2.8	57.4±8.8	64.0±2.1	89.3±6.0	76.7±5.6	54.2±1.0
AJ42	89.7±6.4	83.7±11.6	77.1±5.5	82.4±7.2	72.0±2.8	84.1±2.6	84.1±6.0	84.2±4.6	82.5±2.9
AF13	116.4±4.7	109.7±0.0	106.9±2.0	90.4±3.4	79.2±4.0*	81.6±1.5	95.2±5.4	85.1±3.3	85.0±5.4

AF14	107.6±4.1	101.9±9.8	94.3±4.5	74.2±1.3*	84.7±5.3	66.9±4.9*	82.5±3.3	80.4±0.2	79.1±4.9
AF15	106.5±8.8	98.2±2.2	84.8±8.3	95.8±5.5	87.8±4.8	67.5±5.8**	104.1±3.3	88.7±6.5	81.6±7.2
AF16	100.3±3.9	88.9±5.9	89.8±8.1	87.3±1.7	84.9±2.3	86.0±2.9	78.4±35	71.9±2.4*	83.5±7.2
AH25	120.6±5.6	103.7±5.8	118.9±4.6	88.2±4.1	85.9±1.7	103.7±0.2	100.9±5.2	107.0±5.7	98.3±3.7
EGCG	82.0±3.7	83.1±3.9	73.2±6.4	62.6±4.0	54.3±4.4	51.0±2.1	72.2±6.4	47.8±5.8	39.3±3.8
	24 h			**48 h**			**72 h**		
	10 μM	**25 μM**	**50 μM**	**10 μM**	**25 μM**	**50 μM**	**10 μM**	**25 μM**	**50 μM**
AF17	89.0±0.9	87.3±7.9	83.0±1.5	86.9±5.3	72.3±1.8**	57.8±3.9***	82.1±3.2	60.3±5.5*	46.1±8.5***
AF18	88.4±7.1	87.9±5.6	75.0±7.5**	74.0±5.0	56.4±7.7	34.9±4.3***	71.3±5.1	50.9±6.8	27.2±5.1***
AF19	84.9±6.2	81.4±4.8	60.8±6.3***	58.0±5.2**	39.6±2.0***	32.3±2.1***	30.1±2.7***	26.2±2.6***	25.7±2.3***

Cells were incubated with different concentration of tested compounds for 24, 48 and 72 h. Cell proliferation was determined by MTT assay. MTT assay were quantified by spectrophotometrically at 540nm. Values are expressed as the means ± S.D. of triplicate experiments. * $p < 0.05$, ** $p < 0.01$, compared with differentiated control.

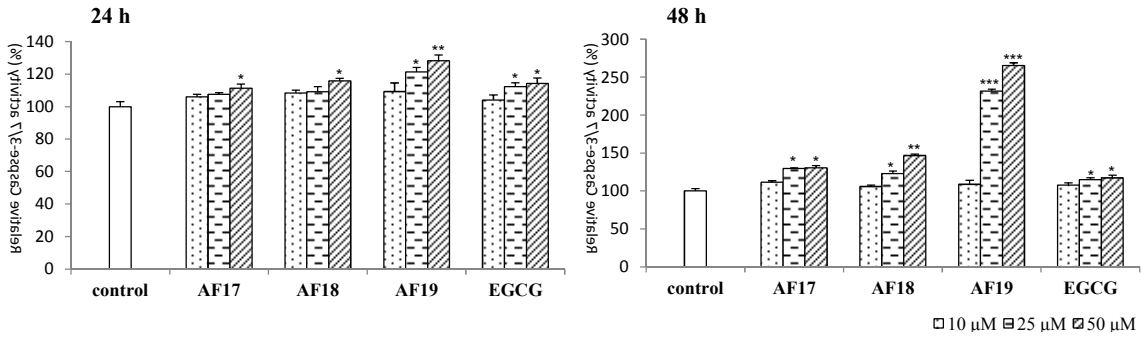

Figure 83. Effects of **AF17-19** on Caspase-3/7 activity in 3T3-L1 preadipocytes

Cells were incubated with different concentration of compounds **AF17-19** for 24 h and 48 h. Cells were analyzed using the Apo-ONE Homogeneous Caspase-3/7 Assay kit. Values are expressed as the means ± S.D. of triplicate experiments. * $p < 0.05$, ** $p < 0.01$, compared with differentiated control.

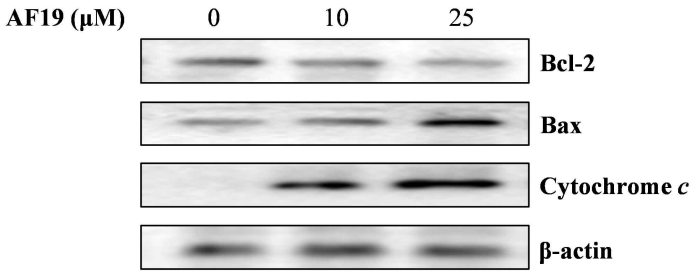

Figure 84. Effects of compound **AF19** on the expression of Bcl-2, Bax, and Cytochrome *c* on 3T3-L1 preadipoctye

3T3-L1 preadipocytes cultured with compound **AF19** (0, 10, and 25 μM) for 48 h. The expression of Bcl-2, Bax, and Cytochrome *c* were detected by Western blot analysis.

IV. Conclusion

Total methanolic extract of *A. japonica* fruits, *A. hirsuta* var. *sibirica* leaves, and *A. firma* barks exhibited significant anti-adipogenic activities in 3T3-L1 cells. Twenty one diarylheptanoids (**AJ1**-**21**), eight flavonoids (**AJ22**-**29**), nine tannin (**AJ30**-**38**), four triterpenes (**AJ39**-**42**), and sterol (**AJ43**-**44**), were isolated by the activity-guided isolation over $CHCl_3$ and *n*-BuOH of *A. japonica*. These forty four compounds were determined as (5*R*)-3,5'-dihydroxy-4'-methoxy-3',4''-oxo-1,7-diphenyl-1,3-diheptene (**AJ1**), 4-hydroxy-3,5-dione (**AJ2**), dihydroalnusone (**AJ3**), alnusol (**AJ4**), alnusonone (**AJ5**), betulatetraol (**AJ6**), 1,7-bis-(4-hydroxyphenyl)-5-hepten-3-one (**AJ7**), hirsutanone (**AJ8**), platyphyllonol-5-*O*-*β*-D-xylopyranoside (**AJ9**), platyphylloside (**AJ10**), (5*S*)-5-hydroxy-7-(3,4-dihydroxyphenyl)-1-(4-hydroxyphenyl)-3-heptanone-5-*O*-*β*-D-xylopyranoside (**AJ11**), 5-hydroxy-1-(3,4-dihydroxyphenyl)-7-(4-hydroxyphenyl)-3-heptanone-5-*O*-*β*-D-glucopyranoside (**AJ12**), oregonin (**AJ13**), hitsutanonol-5-*O*-*β*-D-glucopyranoside (**AJ14**), (5*S*)-*O*-methylhirsutanonol (**AJ15**), 2''''-cinnamoyloregonin (**AJ16**), oregonyl A (**AJ17**), oregonyl B (**AJ18**), aceroside VII (**AJ19**), (3*R*)-1,7-bis-(3,4-dihydroxyphenyl)-3-heptanol-3-*O*-*β*-D-xylopyranoside (**AJ20**), (3*R*)-1,7-bis-(3,4-dihydroxyphenyl)-3-heptanol-3-*O*-*β*-D-glucoopyranoside (**AJ21**), apigenin (**AJ22**), kaempferol (**AJ23**), quercetin (**AJ24**), isorhamnetin (**AJ25**), quercitrin (**AJ26**), genkwanin (**AJ27**), rhamnocitrin (**AJ28**), kumatakenin (**AJ29**), ellagic acid (**AJ30**), 3'-*O*-methyl-ellagic acid (**AJ31**), 3'-*O*-methyl-4-*O*-*β*-xylosyl-ellagic acid (**AJ32**), 3'-*O*-methyl-4-*O*-*β*-glucosyl-ellagic acid (**AJ33**), 3,3'-di-*O*-methyl-ellagic acid (**AJ34**), 3,3',4'-tri-*O*-methyl-ellagic acid (**AJ35**), 3,3',4'-tri-*O*-methyl-4-*O*-*β*-xylosyl-ellagic acid (**AJ36**), 3,4-dihydroxybenzoic acid 3-*O*-

β-D-(6'-*O*-galloyl)-glucopyranoside (**AJ37**), 1,2,6-tri-*O*-galloyl glucose (**AJ38**), 3*β*-hydroxy-lanost-9(11),24(25)-dien-26-oic acid (**AJ39**), (24*S*)-lanost-9(11)-ene-3,24,25-triol (**AJ40**), 3*β*-hydroxy-lanost-9(11),23(24)-dien-25,26-diol (**AJ41**), leucastrins B (**AJ42**), *β*-sitosterol (**AJ43**), daucosterol (**AJ44**). Twenty one diarylheptanoids (**AH1-21**), three flavonoids (**AH22-24**), and a phenolic compound (**AH25**) were isolated by the activity-guided isolation over EtOAc and *n*-BuOH of *A. hirsuta var. sibirica*. These twenty five compounds were elucidated as 1,7-bis(3,4-dihydroxyphenyl)-hepta-1*E*,4*E*-dien-3-one (**AH1**), (5*S*)-hydroxy-1-(3,4-dihydroxyphenyl)-7-(4-hydroxyphenyl)-hepta-1*E*-en-3-one (**AH2**), 1,7-bis(3,4-dihydroxyphenyl)-hepta-4*E*,6*E*-dien-3-one (**AH3**), 1,7-bis-(4-hydroxyphenyl)-5-hepten-3-one (**AH4**), hirsutanone (**AH5**), alnusone (**AH6**), platyphyllonol-5-*O*-*β*-D-xylopyranoside (**AH7**), (5*S*)-5-hydroxy-1,7-bis-(4-hydroxyphenyl)-3-heptanone-5-*O*-*β*-D-apiofuranosyl-(1→6)-*β*-D-glucopyranoside (**AH8**), (5*S*)-5-hydroxy-1-(4-hydroxyphenyl)-7-(3,4-dihydroxyphenyl)-3-heptanone (**AH9**), (5*S*)-5-hydroxy-7-(3,4-dihydroxyphenyl)-1-(4-hydroxyphenyl)-3-heptanone-5-*O*-*β*-D-xylopyranoside (**AH10**), hirsutanonol (**AH11**), oregonin (**AH12**), hitsutanonol 5-*O*-*β*-D-glucopyranoside (**AH13**), (-)-centrolobol (**AH14**), 1,7-di(4-hydroxyphenyl)-3(*R*)-*β*-D-xylosyloxyheptane (**AH15**), (3*R*)-1,7-bis-(4-hydroxyphenyl)-3-heptanol-3-*O*-*β*-D-apiofuranosyl-(1→6)-*β*-D-glucopyranoside (**AH16**), (3*R*)-1,7-bis-(3,4-dihydroxyphenyl)-3-heptanol (**AH17**), (3*R*)-1,7-bis-(3,4-dihydroxyphenyl)-3-heptanol-3-*O*-*β*-D-xylopyranoside (**AH18**), (3*R*)-1,7-bis-(3,4-dihydroxyphenyl)-3-heptanol-3-*O*-*β*-D-glucoopyranoside (**AH19**), (3*R*)-1,7-bis-(3,4-dihydroxyphenyl)-3-heptanol-3-*O*-*β*-D-glucopyranosyl (1→3)-3-*O*-*β*-D-xylopyranoside (**AH20**), (+)-hannokinol (**AH21**), quercitrin (**AH22**), avicularin (**AH23**), isoquercitirin (**AH24**), 3,4-dihydroxybenzoic acid (**AH25**). Twelve diarylheptanoids (**AF1-12**), four phenolic glycoside (**AF13-16**), and three triterpenoids (**AF17-**

19) were isolated by the activity-guided isolation over $CHCl_3$ and EtOAc of *A. firma*. These nineteen compounds were characterized as 1,7-bis-(4-hydroxyphenyl)-5-hepten-3-one (**AF1**), hirsutanone (**AF2**), alnusone (**AF3**), platyphylloside (**AF4**), (5*S*)-5-hydroxy-1,7-bis-(4-hydroxyphenyl)-3-heptanone-5-*O*-*β*-D-apiofuranosyl-(1→6)-*β*-D-glucopyranoside (**AF5**), (5*S*)-5-hydroxy-7-(3,4-dihydroxyphenyl)-1-(4-hydroxyphenyl)-3-heptanone-5-*O*-*β*-D-xylopyranoside (**AF6**), (5*R*)-*O*-methylhirsutanonol (**AF7**), oregonin (**AF8**), (3*R*)-1,7-bis-(4-hydroxyphenyl)-3-heptanol-3-*O*-*β*-D-apiofuranosyl-(1→6)-*β*-D-glucopyranoside (**AF9**), (3*R*)-1,7-bis-(3,4-dihydroxyphenyl)-3-heptanol-3-*O*-*β*-D-xylopyranoside (**AF10**), (3*R*)-1,7-bis-(3,4-dihydroxyphenyl)-3-heptanol-3-*O*-*β*-D-glucoopyranoside (**AF11**), (3*R*)-1,7-bis-(3,4-dihydroxyphenyl)-3-heptanol-3-*O*-*β*-D-glucopyranosyl (1→3)-3-*O*-*β*-D-xylopyranoside (**AF12**), 4-hydroxy-2,6-dimethoxyphenyl-6-*O*-syringoyl-*β*-D-glucopyranoside (**AF13**), 4-hydroxy-2,6-dimethoxyphenyl-6-*O*-vailloyl-*β*-D-glucopyranoside (**AF14**), 4-hydroxy-2-methoxyphenyl-6-*O*-syringoyl-*β*-D-glucopyranoside (**AF15**), 6'-*O*-vanilloylisotachioside (**AF16**), betulinic acid (**AF17**), 2-*O*-caffeoylalphitolic acid (**AF18**), lup-20(29)en-2,28-diol-3-yl caffeate (**AF19**). Among the compounds **AJ1**, **AJ2**, **AJ12**, **AJ37**, **AJ41**, **AH2**, and **AF19** were newly reported from the nature.

Diarylheptanoids showed more siginificant anti-differenetiation effect than other on 3T3-L1 cells. On the structure and activity relationship, the presence of carbonyl group at C-3, additions of hydroxyl group in benzene ring and substitution of glucose moiety, α, β-unsaturated ketone moiety were important for the activity on adipocyte differentiation. Among diarylheptanoids, compounds **AJ2**, **AJ9**, **AJ10**, **AJ13** down-regulated the expression of adipogenic gene in 3T3-L1 cells. Compounds **AJ9**, **AJ10**, and **AJ13** had anti-adipogenic

activity by regulation of PPARγ signaling pathways and promoted lipolysis on differentiated adipocytes. Compounds **AJ9** and **AJ10** inhibited the expression of SREBP1, SCD-1, and FAS, target gene of lipogenesis and affected on initial stage of adipocyte differentiation. Lupane-type triterpenoids **AF17-19** inhibited cell proliferation and induced apoptosis.

V. References

Ardevol, A., Blade, C., Salvado, M. J., Arola, L. 2000. Changes in lipolysis and hormone-sensitive lipase expression caused by procyanidins in 3T3-L1 adipocytes. *Int J Obes* 24, 319-324.

Arimura, N., Horiba, T., Imagawa, M., Shimizu, M., Sato, R. 2004. The peroxisome proliferator-activated receptor gamma regulates expression of the perilipin gene in adipocytes. *J Biol Chem* 279, 10070-10076.

Cha, M. H., Kim, I. C., Lee, B. H., Yoon, Y. 2006. Baicalein inhibits adipocyte differentiation by enhancing COX-2 expression. *J Med Food* 9, 145-153.

Chen, K. H., Li, P. C., Lin, W. H., Chien, C. T., Low, B. H. 2011. Depression by a green tea extract of alcohol-induced oxidative stress and lipogenesis in rat liver. *Biosci Biotechnol Biochem* 75, 1668-1676.

Chen, J., Gonzalez-Laredo, R. F., Karchesy, J. J. 2000. Minor diarylheptanoid glycosides of *Alnus rubra* bark. *Phytochemistry* 53, 971-973.

Choi, S. E., Kim, K. H., Kwon, J. H., Kim, S. B., Kim, H. W., Lee, M. W. 2008. Cytotoxic activities of diarylheptanoids from *Alnus japonica*. *Arch Pharm Res* 31, 1287-1289.

Choi, S. E., Park, K. H., Jeong, M. S., Kim, H. H., Lee, I., Joo, S. S., Lee, C. S., Bang, H., Choi, Y. W., Lee, M. K., Seo, S. J., Lee, M. W. 2011. Effect of *Alnus japonica* extract on a model of atopic dermatitis in NC/Nga mice. *J Ethnopharmacol* 136, 406-413.

Cohen, G. M. 1997. Caspases: the executioners of apoptosis. *Biochemical Journal* 326, 1-16.

Da Silva, S. L., Calgarotto, A. K., Chaar, J. S. 2008. Marangoni S. Isolation and characterization of ellagic acid derivatives isolated from *Casearia sylvestris* SW aqueous extract with anti-PLA(2) activity. *Toxicon* 52, 55-66.

Degerman, E., Belfrage, P., Manganiello, V. C. 1997. Structure, localization, and regulation of cGMP-inhibited phosphodiesterase (PDE3). *J Biol Chem* 272, 6823-6826.

Ejaz, A., Wu, D. Y., Kwan, P., Meydani, M. 2009. Curcumin inhibits adipogenesis in 3T3-L1 adipocytes and angiogenesis and obesity in C57/BL Mice. *J Nutr* 139, 919-925.

Ericsson, J., Jackson, S. M., Kim, J. B., Spiegelman, B. M., Edwards, P. A. 1997. Identification of glycerol-3-phosphate acyltransferase as an adipocyte determination and differentiation factor 1- and sterol regulatory element-binding protein-responsive gene. *J Biol Chem* 272, 7298-7305.

Farmer, S. R. 2006. Transcriptional control of adipocyte formation. *Cell Metabolism* 4, 263-273.

Frayn, K. N., Karpe, F., Fielding, B. A., Macdonald, I. A., Coppack, S. W. 2003. Integrative physiology of human adipose tissue. *Int J Obes Relat Metab Disord* 27, 875-888.

Fuchino, H., Konishi, S., Satoh, T., Yagi, A., Saitsu, K., Tatsumi, T., Tanaka, N. 1996. Chemical evaluation of *Betula* species in Japan .2. Constituents of *Betula platyphylla* var japonica. *Chem Pharm Bull* 44, 1033-1038.

Gasic, S., Tian, B., Green, A. 1999. Tumor necrosis factor alpha stimulates lipolysis in adipocytes by decreasing Gi protein concentrations. *J Biol Chem* 274, 6770-6775.

Gonzalez-Laredo, R. F., Chen, J., Karchesy, Y. M., Karchesy, J. J. 1999. Four new diarylheptanoid glycosides from *Alnus rubra* bark. *Nat Prod Lett* 13, 75-80.

Gonzalez-Laredo, R. F., Helm, R. F., Chen, J., Karchesy, J. J. 1998. Two acylated diarylheptanoid glycosides from red alder bark. *J Nat Prod* 61, 1292-1294.

Green, D. R., Reed, J. C. 1998. Mitochondria and apoptosis. *Science* 281, 1309-1312.

Green, H., Kehinde, O. 1975. Established pre-adipose cell line and its differentiation in culture .2. factors affecting adipose conversion. *Cell* 5, 19-27.

Han, J. M., Lee, W. S., Kim, J. R., Son, J., Kwon, O. H., Lee, H. J., Lee, J. J., Jeong, T. S. 2008. Effect of 5-O-Methylhirsutanonol on nuclear factor-kappaB-dependent production of NO and expression of iNOS in lipopolysaccharide-induced RAW264.7 cells. *J Agric Food Chem* 56, 92-98.

Han, J. M., Lee, W. S., Kim, J. R., Son, J., Nam, K. H., Choi, S. C., Lim, J. S., Jeong, T. S. 2007. Effects of diarylheptanoids on the tumor necrosis factor-alpha-induced expression of adhesion molecules in human umbilical vein endothelial cells. *J Agric Food Chem* 55, 9457-9464.

Hargrave, K. M., Li, C. L., Meyer, B. J., Kachman, S. D., Hartzell, D. L., Della-Fera, M. A., Miner, J. L., Baile, C. A. 2002. Adipose depletion and apoptosis induced by trans-10, cis-12 conjugated linoleic acid in mice. *Obes Res* 10, 1284-1290.

Harmon, A. W., Harp, J. B. 2001. Differential effects of flavonoids on 3T3-L1 adipogenesis and lipolysis. *Am J Physiol Cell Physiol* 280, 807-813.

Holm, C. 2003. Molecular mechanisms regulating hormone-sensitive lipase and lipolysis. *Biochem Soc Trans* 31, 1120-1124.

Hoye, T. R., Jeffrey, C. S., Shao, F. 2007. Mosher ester analysis for the determination of absolute configuration of stereogenic (chiral) carbinol carbons. *Nat Protoc* 2, 2451-2458.

Hsu, C. L., Yen, G. C. 2007. Effects of capsaicin on induction of apoptosis and inhibition of adipogenesis in 3T3-L1 cells. *J Agric Food Chem* 55, 1730-1736.

Huang, C., Zhang, Y., Gong, Z., Sheng, X., Li, Z., Zhang, W., Qin, Y. 2006. Berberine inhibits 3T3-L1 adipocyte differentiation through the PPARgamma pathway. *Biochem Biophys Res Commun* 348, 571-578.

Hwang, J. T., Park, I. J., Shin, J. I., Lee, Y. K., Lee, S. K., Baik, H. W., Ha, J., Park, O. J. 2005. Genistein, EGCG, and capsaicin inhibit adipocyte differentiation process via activating AMP-activated protein kinase. *Biochem Biophys Res Commun* 338, 694-699.

Joo, S. S., Kim, S. G., Choi, S. E., Kim, Y. B., Park, H. Y., Seo, S. J., Choi, Y. W., Lee, M. W., Lee do, I. 2009. Suppression of T cell activation by hirsutenone, isolated from the bark of *Alnus japonica*, and its therapeutic advantages for atopic dermatitis. *Eur J Pharmacol* 614, 98-105.

Kang, H. M., Kim, J. R., Jeong, T. S., Choi, S. G., Ryu, Y. H., Oh, G. T., Baek, N. I., Kwon, B. M. 2006. Cyclic diarylheptanoids inhibit cell-mediated low-density lipoprotein oxidation. *Nat Prod Res* 20, 139-143.

Kang, H. M., Son, K. H., Yang, D. C., Han, D. C., Kim, J. H., Baek, N. I., Kwon, B. M. 2004. Inhibitory activity of diarylheptanoids on farnesyl protein transferase. *Nat Prod Res* 18, 295-299.

Kao, Y., Hiipakka, R. A., Liao, S. 2000. Modulation of obesity by a green tea catechin. *Am J Clin Nutr* 72, 1232-1233.

Kemp, B. E., Stapleton, D., Campbell, D. J., Chen, Z. P., Murthy, S., Walter, M., Gupta, A., Adams, J. J., Katsis, F., van Denderen, B., Jennings, I. G., Iseli, T., Michell, B. J., Witters, L. A. 2003. AMP-activated protein kinase, super metabolic regulator. *Biochem Soc Trans* 31, 162-168.

Kerner, J., Hoppel, C. 2000. Fatty acid import into mitochondria. *Biochim Biophys Acta* 1486, 1-17.

Kessler, R. C., Davis, R. B., Foster, D. F., Van Rompay, M. I., Walters, E. E., Wilkey, S. A., Kaptchuk, T. J., Eisenberg, D. M. 2001. Long-term trends in the use of complementary and alternative medical therapies in the United States. *Ann Intern Med* 135, 262-268.

Khac, D. D., Tran-Van, S., Campos, A. M., Lallemand, J.-Y., Fetizon M. 1990. Ellagic compounds from *Diplopanax stachyanthus*. *Phytochemistry* 29*, 251-256.*

Kikuzaki, H., Kawai, Y., Nakatani, N. 2001. 1,1-diphenyl-2-picrylhydrazyl radical-scavenging active compounds from greater cardamom (*Amomum subulatum* Roxb.). *J Nutr Sci Vitaminol* 47, 167-171.

Kim, H. J., Yeom, S. H., Kim, M. K., Shim, J. G., Paek, I. N., Lee, M. W. 2005. Nitric oxide and prostaglandin E2 synthesis inhibitory activities of diarylheptanoids from the barks of *Alnus japonica* steudel. *Arch Pharm Res* 28, 177-179.

Kim, H. K., Della-Fera, M., Lin, J., Baile, C. A. 2006. Docosahexaenoic acid inhibits adipocyte differentiation and induces apoptosis in 3T3-L1 preadipocytes. *J Nutr* 136, 2965-2969.

Kim, J. B., Sarraf, P., Wright, M., Yao, K. M., Mueller, E., Solanes, G., Lowell, B. B., Spiegelman, B. M. 1998. Nutritional and insulin regulation of fatty acid synthetase and leptin gene expression through ADD1/SREBP1. *J Clin Invest* 101, 1-9.

Kim, J. B., Spiegelman, B. M. 1996. ADD1/SREBP1 promotes adipocyte differentiation and gene expression linked to fatty acid metabolism. *Genes Dev* 10, 1096-1107.

Kim, J. B., Wright, H. M., Wright, M., Spiegelman, B. M. 1998. ADD1/SREBP1 activates PPARgamma through the production of endogenous ligand. *Proc Natl Acad Sci* 95, 4333-4337.

Kim, J. H., Lee, K. W., Lee, M. W., Lee, H. J., Kim, S. H., Surh, Y. J. 2006. Hirsutenone inhibits phorbol ester-induced upregulation of COX-2 and MMP-9 in cultured human mammary epithelial cells: NF-kappaB as a potential molecular target. *FEBS Lett* 580, 385-392.

Kim, J. K., So, H., Youn, M. J., Kim, H. J., Kim, Y., Park, C., Kim, S. J., Ha, Y. A., Chai, K. Y., Kim, S. M., Kim, K. Y., Park, R. 2007. *Hibiscus sabdariffia* L. water extract inhibits the adipocyte differentiation through the P13-K and MAPK pathway. *J Ethnopharmacol* 114, 260-267.

Kim, S. T., Kim, J. D., Ahn, S. H., Ahn, G. S., Lee, Y. I., Jeong, Y. S. 2004. Hepatoprotective and antioxidant effects of *Alnus japonica* extracts on acetaminophen-induced hepatotoxicity in rats. *Phytother Res* 18, 971-975.

Kong, C. S., Kim, J. A., Kim, S. K. 2009. Anti-obesity effect of sulfated glucosamine by AMPK signal pathway in 3T3-L1 adipocytes. *Food Chem Toxicol* 47, 2401-2406.

Kopelman, P. G. 2000. Obesity as a medical problem. *Nature* 404, 635-643.

Kuppusamy, U. R., Das, N. P. 1992. Effects of flavonoids on cyclic-amp phosphodiesterase and lipid mobilization in rat adipocytes. *Biochem Pharmacol* 44, 1307-1315.

Kuroyanagi, M., Shimomae, M., Nagashima, Y., Muto, N., Okuda, T., Kawahara, N., Nakane, T., Sano, T. 2005. New diarylheptanoids from *Alnus japonica* and their antioxidative activity. *Chem Pharm Bull* 53, 1519-1523.

Lafontan, M,, Langin, D. 2009. Lipolysis and lipid mobilization in human adipose tissue. *Prog Lipid Res* 48, 275-297.

Lai, Y. C., Chen, C. K., Lin, W. W., Lee, S. S. 2012. A comprehensive investigation of anti-inflammatory diarylheptanoids from the leaves of *Alnus formosana*. *Phytochemistry* 73, 84-94.

Lee, M., Lee, M. K., Kim, Y. C., Sung, S. H. 2011. Antifibrotic constituents of *Alnus firma* on hepatic stellate cells. *Bioorg Med Chem Lett* 21, 2906-2910.

Lee, M. A., Lee, H. K., Kim, S. H., Kim, Y. C., Sung, S. H. 2010. Chemical constituents of *Alnus firma* and their inhibitory aActivity on lipopolysaccharide-Induced nitric oxide production in BV2 microglia. *Planta Med* 76, 1007-1010.

Lee, M. S., Kim, C. T., Kim, Y. 2009. Green tea (-)-epigallocatechin-3-gallate reduces body weight with regulation of multiple genes expression in adipose tissue of diet-induced obese mice. *Ann Nutr Metab* 54, 151-157.

Lee, M. W., Kim, J. H., Jeong, D. W., Ahn, K. H., Toh, S. H., Surh, Y. J. 2000b. Inhibition of cyclooxygenase-2 expression by diarylheptanoids from the bark of *Alnus hirsuta* var. *sibirica*. *Biol Pharm Bull* 23, 517-518.

Lee, M. W., Tanaka, T., Nonaka, G. I., Hahn, D. R. 1992. Phenolic compounds on the leaves of *Betula platyphylla* var. *latifolia* . *Arch Pharm Res* 15, 211-214.

Lee, S. S., Chen, S. C., Chen, C. K., Chen, C. H., Kuo, C. M. 2006. Chemical constituents from *Alnus formosana* Burk. II. polar constituents from the leaves. *Nat Prod Commun* 1, 461-464.

Lee, W. S., Kim, J. R., Im, K. R., Cho, K. H., Sok, D. E., Jeong, T. S. 2005. Antioxidant effects of diarylheptanoid derivatives from *Alnus japonica* on human LDL oxidation. *Planta Med* 71, 295-299.

Li, J., Liao, C. R., Wei, J. Q., Chen, L. X., Zhao, F., Qiu, F. 2011. Diarylheptanoids from *Curcuma kwangsiensis* and their inhibitory activity on nitric oxide production in lipopolysaccharide-activated macrophages. *Bioorg Med Chem Lett* 21, 5363-5369.

Li, R. T., Han, Q. B., Zhao, A. H., Sun, H. D. 2003. Micranoic acids A and B: two new octanortriterpenoids from *Schisandra micrantha*. *Chem Pharm Bull* 51, 1174-1176.

Lim, S. S., Lee, M. Y., Ahn, H. R., Choi, S. J., Lee, J. Y., Jung, S. H. 2011. Preparative isolation and purification of antioxidative diarylheptanoid derivatives from *Alnus japonica* by high-speed counter-current chromatography. *J Sep Sci* 34, 3344-3352.

Lin, J., Della-Fera, M. A., Baile, C. A. 2005. Green tea polyphenol epigallocatechin gallate inhibits adipogenesis and induces apoptosis in 3T3-L1 adipocytes. *Obes Res* 13, 982-990.

Luo, Z. J., Saha, A. K., Xiang, X. Q., Ruderman, N. B. 2005. AMPK, the metabolic syndrome and cancer. *Trends Pharmacol Sci* 26, 69-76.

Luong, A., Hannah, V. C., Brown, M. S., Goldstein, J. L. 2000. Molecular characterization of human acetyl-CoA synthetase, an enzyme regulated by sterol regulatory element-binding proteins. *J Biol Chem* 275, 26458-26466.

Martinez-Botas, J., Anderson, J. B., Tessier, D., Lapillonne, A., Chang, B. H., Quast, M.J., Gorenstein, D., Chen, K. H., Chan, L. 2000. Absence of perilipin results in leanness and reverses obesity in Lepr(db/db) mice. *Nat Genet* 26, 474-479.

Moon, H. S., Chung, C. S., Lee, H. G., Kim, T.G., Choi, Y. J., Cho, C. S. 2007. Inhibitory effect

of (-)-epigallocatechin-3-gallate on lipid accumulation of 3T3-L1 cells. *Obesity* 15, 2571-2582.

Mitchell, M.J., Driscoll, C. T., Inamdar, S., McGee, G. G., Mbila, M. O., Raynal, D. J. 2003. Nitrogen biogeochemistry in the adirondack mountains of new york: hardwood ecosystems and associated surface waters. *Environ Pollut* 123, 355-364.

Miyaichi, Y., Segawa, A., Tomimori, T. 2006. Studies on Nepalese crude drugs. XXIX. Chemical constituents of Dronapuspi, the whole herb of *Leucas cephalotes* SPRENG. *Chem Pharm Bull* 54, 1370-1379.

Nagai, M., Kenmochi, N., Fujita, M., Furukawa, N., Inoue, T. 1986. Studies on the constituents of aceraceae plants. VI. : Revised stereochemistry of (-)-centrolobol, and new glycosides from *Acer nikoense*. *Chem Pharm Bull* 34, 1056-1060.

Nomura, M., Tokoroyama, T., Kubota, T. 1981. Biarylheptanoids and Other Constituents from Wood of *Alnus japonica*. *Phytochemistry* 20, 1097-1104.

Nonaka, G. I., Nishioka, I., Nagasawa, T., Oura, H. 1981. Tannins and related compoounds. I. Rhubarb (1). *Chem Pharm Bull* 29, 2862-2870.

Popivanova, B. K., Kitamura, K., Wu, Y., Kondo, T., Kagaya, T., Kaneko, S., Oshima, M., Fujii, C., Mukaida, N. 2008. Blocking TNF-alpha in mice reduces colorectal carcinogenesis associated with chronic colitis. *J Clin Invest* 118, 560-570.

Prins, J. B., O'Rahilly, S. 1997. Regulation of adipose cell number in man. *Clin Sci* 92, 3-11.

Rahn Landström, T., Mei, J., Karlsson, M., Manganiello, V., Degerman, E. 2000. Down-regulation of cyclic-nucleotide phosphodiesterase 3B in 3T3-L1 adipocytes induced by tumour necrosis factor alpha and cAMP. *Biochem J* 346, 337-343.

Rayalam, S., Della-Fera, M. A., Baile, C. A. 2008. Phytochemicals and regulation of the adipocyte life cycle. *J Nutr Biochem* 19, 717-726.

Riedl, S. J., Shi, Y. 2004. Molecular mechanisms of caspase regulation during apoptosis. *Nat Rev Mol Cell Biol* 5, 897-907.

Roncari, D. A. K., Lau, D. C. W., Kindler, S. 1981. Exaggerated replication in culture of adipocyte precursors from massively obese persons. *Metabolism* 30, 425-427.

Rosen, E. D., Spiegelman, B. M. 2006. Adipocytes as regulators of energy balance and glucose homeostasis. *Nature,* 444, 847-853.

Rosen, E. D., Hsu, C. H., Wang, X., Sakai, S., Freeman, M. W., Gonzalez, F. J., Spiegelman, B. M. 2002. C/EBPalpha induces adipogenesis through PPARgamma: a unified pathway. *Genes Dev* 16, 22-26.

Rosen, E. D., Walkey, C. J., Puigserver, P., Spiegelman, B. M. 2000. Transcriptional regulation of adipogenesis. *Genes Dev* 14, 1293-1307.

Rydén, M., Arvidsson, E., Blomqvist, L., Perbeck, L., Dicker, A., Arner, P. 2004. Targets for TNF-alpha-induced lipolysis in human adipocytes. *Biochem Biophys Res Commun* 318, 168-175.

Shao, Z. Y., Zhu, D. Y., Guo, Y. W. 2002. Two new triterpene esters from *Daphniphyllum oldhami*. *Chin Chem Lett* 13, 1181-1184.

Siddiqui, S., Hafeez, F., Begum, S., Siddiqui, B. S. 1988. Oleanderol, a new pentacyclic triterpene from the leaves of *Nerium oleander*. *J Nat Prod* 51, 229-233.

Sinha, A., Taylor, W. H., Khan, I. H., McDaniel, S. T., Esko, J. D. 1999. Glycoside primers of *Psittacanthus cucullaris*. *J Nat Prod* 62, 1036-1038.

Smite, E., Lundgren, L. N., Andersson, R. 1993. Arylbutanoid and diarylheptanoid glycosides from inner bark of *Betula pendula*. *Phytochemistry* 32, 365-369.

Smith, S. 1994. The animal fatty-acid synthase - one gene, one polypeptide, 7 Enzymes. *Faseb J*

8, 1248-1259.

Starnes, H. F., Jr., Warren, R. S., Jeevanandam, M., Gabrilove, J. L., Larchian, W., Oettgen, H. F., Brennan, M. F. 1988. Tumor necrosis factor and the acute metabolic response to tissue injury in man. *J Clin Invest* 82, 1321-1325.

Stern, J. S., Hirsch, J., Blair, S. N., Foreyt, J. P., Frank, A., Kumanyika, S. K., Madans, J. H., Marlatt, G. A., St Jeor, S. T., Stunkard, A. J. 1995. Weighing the options: criteria for evaluating weight-management programs. The committee to develop criteria for evaluating the outcomes of approaches to prevent and treat obesity. *Obes Res* 3, 591-604.

Sunnerheimsjoberg, K., Knutsson, P. G. 1995. Platyphylloside - metabolism and digestibility reduction *in vitro*. *J Chem Ecol* 21, 1339-1348.

Tang, Q. Q., Jiang, M. S., Lane, M. D. 1999. Repressive effect of Sp1 on the C/EBPalpha gene promoter: role in adipocyte differentiation. *Mol Cell Biol* 19, 4855-4865.

Tontonoz, P., Hu, E., Spiegelman, B. M. 1995. Regulation of adipocyte gene expression and differentiation by peroxisome proliferator activated receptor gamma. *Curr Opin Genet Dev* 5, 571-576.

Tsuboyama-Kasaoka, N., Takahashi, M., Tanemura, K., Kim, H. J., Tange, T., Okuyama, H., Kasai, M., Ikemoto, S., Ezaki, O. 2000. Conjugated linoleic acid supplementation reduces adipose tissue by apoptosis and develops lipodystrophy in mice. *Diabetes* 49, 1534-1542.

Tung, N. H., Kwon, H. J., Kim, J. H., Ra, J. C., Kim, J. A., Kim, Y. H. 2010a. An anti-influenza component of the bark of *Alnus japonica*. *Arch Pharm Res* 33, 363-367.

Tung, N. H., Kwon, H. J., Kim, J. H., Ra, J. C., Ding, Y., Kim, J. A., Kim, Y. H. 2010b. Anti-influenza diarylheptanoids from the bark of *Alnus japonica*. *Bioorg Med Chem Lett* 20, 1000-1003.

Tung, N. H., Kim, S. K., Ra, J. C., Zhao, Y. Z., Sohn, D. H., Kim, Y. H. 2010c. Antioxidative and hepatoprotective diarylheptanoids from the bark of *Alnus japonica*. *Planta Med* 76, 626-629.

Ukiya, M., Akihisa, T., Yasukawa, K., Kasahara, Y., Kimura, Y., Koike, K., Nikaido, T., Takido, M. 2001. Constituents of compositae plants. 2. Triterpene diols, triols, and their 3-*O*-fatty acid esters from edible chrysanthemum flower extract and their anti-inflammatory effects. *J Agric Food Chem* 49, 3187-3197.

Vazquez-Vela, M. E. F., Torres, N., Tovar, A. R. 2008. White adipose tissue as rndocrine organ and its role in obesity. *Arch Med Res* 39, 715-728.

Vermeulen, K., Van Bockstaele, D. R., Berneman, Z. N. 2005. Apoptosis: mechanisms and relevance in cancer. *Ann Hematol* 84, 627-639.

Wadden, T. A. 1993. Treatment of obesity by moderate and severe caloric restriction. Results of clinical research trials. *Ann Intern Med* 119, 688-693.

Wasan, K. M., Looije, N. A. 2005. Emerging pharmacological approaches to the treatment of obesity. *J Pharm Pharm Sci* 8, 259-271.

Winder, W. W., Hardie, D. G. 1999. AMP-activated protein kinase, a metabolic master switch: possible roles in type 2 diabetes. *Am J Physiol Endocrinol Metab* 277, 1-10.

Woo, K. J., Jeong, Y. J., Park, J. W., Kwon, T. K. 2004. Chrysininduced apoptosis is mediated through caspase activation and Akt inactivation in U937 leukemia cells. *Biochem Biophys Res Commun* 325, 1215-1222.

Xing, H., Northrop, J. P., Grove, J. R., Kilpatrick, K. E., Su, J. L., Ringold, G. M. 1997. TNF alpha-mediated inhibition and reversal of adipocyte differentiation is accompanied by suppressed expression of PPARgamma without effects on Pref-1 expression. *Endocrinology* 138, 2776-2783.

Xiao, B., Heath, R., Saiu, P., Leiper, F. C., Leone, P., Jing, C., Walker, P. A., Haire, L., Eccleston,

J. F., Davis, C. T., Martin, S. R., Carling, D., Gamblin, S. J. 2007. Structural basis for AMP binding to mammalian AMP-activated protein kinase. *Nature* 449, 496-500.

Yan, X. H., Guo, Y. W. 2004. Two new ellagic acid glycosides from leaves of *Diplopanax stachyanthus*. *J Asian Nat Prod Res* 6, 271-276.

Yang, H., Lee, P. J., Jeong, E. J., Kim, H. P., Kim, Y. C. 2011. Selective apoptosis in hepatic stellate cells mediates the antifibrotic effect of phenanthrenes from *Dendrobium nobile*. *Phytother Res* 26, 974-980.

Yang, J. Y., Della-Fera, M. A., Hartzell, D. L., Nelson-Dooley, C., Hausman, D. B., Baile, C. A. 2006. Esculetin induces apoptosis and inhibits adipogenesis in 3T3-L1 cells. *Obesity* 14, 1691-1699.

Yang, J. Y., Della-Fera, M. A., Rayalam, S., Ambati, S., Hartzell, D. L., Park, H. J., Baile, C. A. 2008. Enhanced inhibition of adipogenesis and induction of apoptosis in 3T3-L1 adipocytes with combinations of resveratrol and quercetin. *Life Sciences* 82, 1032-1039.

Yamauchi, T., Kamon, J., Minokoshi, Y., Ito, Y., Waki, H., Uchida, S., Yamashita, S., Noda, M., Kita, S., Ueki, K., Eto, K., Akanuma, Y., Froguel, P., Foufelle, F., Ferre, P., Carling, D., Kimura, S., Nagai, R., Kahn, B. B., Kadowaki, T. 2002. Adiponectin stimulates glucose utilization and fatty-acid oxidation by activating AMP-activated protein kinase. *Nat Med* 8, 1288-1295.

Yao-Borengasser, A., Rassouli, N., Varma, V., Bodles, A. M., Rasouli, N., Unal, R., Phanavanh, B., Ranganathan, G., McGehee, R. E., Kern, P. A. 2008. Stearoyl-coenzyme A desaturase 1 gene expression increases after pioglitazone treatment and is associated with peroxisomal proliferator-activated receptor-gamma responsiveness. *J Clin Endocrinol Metab* 93, 4431-4439.

Yin, X. M. Signal transduction mediated by Bid, a pro-death Bcl-2 family proteins, connects the death receptor and mitochondria apoptosis pathways. *Cell Res* 10, 161-167.

Yu, Y. B., Miyashiro, H., Nakamura, N., Hattori, M., Park, J. C. 2007. Effects of triterpenoids

and flavonoids isolated from *Alnus firma* on HIV-1 viral enzymes. *Arch Pharm Res* 30, 820-826.

Zhang, F., Lavan, B., Gregoire, F. M. 2004. Peroxisome proliferator-activated receptors as attractive antiobesity targets. *Drug News Perspect* 17, 661-669.

국 문 초 록

전세계적으로 문제가 되고 있는 비만은 체내에 과잉된 에너지가 지방으로 축적됨으로써 야기되는 지방 조직의 이상 비대화에 기인한다. 지방 조직의 비대화는 지방세포의 크기가 커지거나, 그 수가 증가하는 현상으로 비만 치료를 위해서는 지방전구세포에서 지방세포로 분화하는 과정인 adipogenesis를 조절하는 것이 중요하다. 본 연구에서는 마우스의 지방전구세포로부터 유래한 3T3-L1 세포주를 검색계로 사용하여 지방형성을 억제하는 물질을 천연물에서 찾고자 하였고, 이를 검색하는 과정에서 국내에 자생하는 오리나무 열매, 물갬나무 잎과 사방오리나무 줄기껍질의 메탄올 추출물이 유의적인 지방세포로의 분화 억제활성을 나타내는 것을 확인하였다.

오리나무속 식물은 예로부터 간염, 위장병, 설사, 만성기관지염, 외상출혈, 위장병, 알코올 해독의 목적으로 널리 사용하였고 주요 성분으로 diarylheptanoid, triterpenoid, flavonoid, tannin 등의 다양한 성분들이 분리 보고되었다. 최근의 연구에 따르면 오리나무속 식물의 추출물 및 단일 성분이 기존의 항산화, 항염, 항암, 간보호활성 외에도 지방세포로의 분화 억제활성이 보고되어 천연물 유래 비만치료약물 개발 대상으로서의 기대 역시 증가하고 있으나 구체적이고 체계적인 활성 기전 연구는 여전히 미흡한 실정이다. 따라서 본 연구에서는 활성지향적인 기법을 활용하여 오리나무 열매, 물갬나무 잎과 사방오리나무 줄기껍질의 메탄올 추출물에서 3T3-L1 세포주의 지방형성을 억제하는 활성성분을 분리하여 그 화학구조를 동정하고 작용기전을 규명하고자 하였다. 이에 오리나무 열매, 물갬나무 잎과 사방오리나무 줄기껍질의 80% 메탄올 추출물에서 활성

지향적 분리기법에 따라 분리를 수행하여, 35종의 diarylheptanoids, 10 종의 flavonoids, 9종의 tannin, 7종의 triterpenoids, 5종의 phenolic compounds 및 2종의 sterols을 분리하였다. 이 중 화합물 **AJ1**, **AJ2**, **AH2**, **AJ12**, **AJ37**, **AJ41**, 및 **AF19**는 천연에서 처음으로 분리보고 되는 물질로 (5*R*)-3,5'-dihydroxy-4'-methoxy-3',4''-oxo-1,7-diphenyl-1,3-diheptene (**AJ1**), 4-hydroxy-alnus-3,5-dione (**AJ2**), (5*S*)-hydroxy-1-(3,4-dihydroxyphenyl)-7-(4-hydroxyphenyl)-hepta-1*E*-en-3-one (**AH2**), 5-hydroxy-1-(3,4-dihydroxyphenyl)-7-(4-hydroxyphenyl)-3-heptanone-5-*O*-*β*-D-glucopyranoside (**AJ12**), 3,4-dihydroxybenzoic acid 3-*O*-*β*-D-(6'-*O*-galloyl)-glucopyranoside (**AJ37**), 3*β*-hydroxy-lanost-9(11),23(24)-dien-25,26-diol (**AJ41**) lup-20(29)en-2,28-diol-3-yl-caffeate (**AF19**)로 결정하였다.

오리나무 열매, 물갬나무 잎 및 사방오리나무 줄기껍질에서 분리한 68 종의 화합물에 대하여 Oil Red O 염색법을 이용하여 3T3-L1 지방 전구세포의 분화 억제활성을 측정한 결과, diarylheptanoids 계열 화합물들이 다른 성분 군에 비하여 뛰어난 억제활성을 보였다. Diarylheptanoids 계열의 화합물의 구조와 활성관계 연구를 통하여 3번 탄소 위치에서 carbonyl 그룹의 존재, benzene ring에서 hydroxyl 그룹의 치환, heptane chain에서 당의 치환, *α*,*β*-unsaturated ketone 그룹의 존재가 지방세포로의 분화 억제활성에 중요한 영향을 끼치는 것을 확인할 수 있었다. 이 중에서 100 μM에서 다른 diarylheptanois계 화합물에 비하여 강한 활성을 보였던 화합물 **AJ2**, **AJ9**, **AJ10**과 지방분화 억제활성이 보고된 화합물 **AJ13**에서 real-time PCR을 통하여 각종 adipokine을 측정한 결과, 화합물 **AJ9**, **AJ10**와 **AJ13**이 지방형성에 중요한 역할을 하는 PPARγ와 C/EBPα 뿐만 아니라 지방세포로 분화 시 증가하는 aP2 LPL, 및 leptin을 감소시키는 것으로 확인하였다. 화합물 **AJ9**과 **AJ10**은 SREBP1, SCD-1 및FAS의 유전자 발현을 감소시켜 지방생합성을 억제하고, 또한 분화 초

기에도 영향을 미치나, 화합물 **AJ13**은 지방생합성 및 분화 초기에 영향을 적게 미치는 것으로 확인하였다. 한편, 화합물 **AJ2**는 100 μM의 고농도에서만 adipokine에 영향을 미치는 것으로 확인하였다. 또한, 이들 화합물 **AJ9**, **AJ10**와 **AJ13** 모두 분화된 지방세포에서 lipolysis를 일으켜 지방의 함량이 감소하는 것을 확인하였다. 오리나무속 식물에서 분리한 화합물의 지방전구세포의 증식과 사멸에 대한 영향을 알아보기 위하여 지방전구세포에서 세포증식을 평가한 결과, lupane triterpenoid 계열 물질인 화합물 **AF17-19**가 농도 및 시간 의존적으로 세포생존율을 감소시켰으며 Caspase-3/7를 활성화시켜 apoptosis를 유도함으로써 지방세포형성이 억제되는 것을 확인할 수 있었다.

이상의 결과로 오리나무 열매, 물갬나무 잎 및 사방오리나무 줄기껍질에서 3T3-L1 세포주의 지방형성을 억제하는 활성 분획에서 총 68 종의 화합물을 분리하여 구 구조를 규명하였고, 이 중에서 diarylheptanoids계열 성분은 지방세포로의 분화에 영향을 미치는 adipokine의 발현을 감소하고 지방생합성을 억제하고 지방산산화를 증가시키며, lupan triterpenoids 계열 성분은 지방전구세포의 증식을 억제하고 사멸을 유도하여 지방세포 주기의 여러 과정에 영향을 미쳐 지방형성을 억제하는 것으로 확인하여, 오리나무속 식물들이 비만의 예방 또는 치료를 위한 천연물 후보물질로서 가능성을 제시하였다.

주요어: *Alnus japonica* Steud., *Alnus hirsuta* Turcz. var. *sibirica* (Spach) H. Ohba, *Alnus firma* Sieb. et Zucc., 자작나무과, 지방전구세포주, 비만, 지방분화 억제 활성

학번: 2009-30470